CHARACTERIZATION OF POSSIBLE ARRHYTHMIA MECHANISMS:

THE IMPORTANCE OF ATTENUATED REPOLARIZATION RESERVE

Ph.D. dissertation

Leila Topal, PharmD

Szeged

2023

CHARACTERIZATION OF POSSIBLE ARRHYTHMIA MECHANISMS:

THE IMPORTANCE OF ATTENUATED REPOLARIZATION RESERVE

Ph.D. dissertation

Supervisors:
Professor András Varró, MD, Ph.D., DSc
Professor Norbert Jost, Ph.D., DSc

Department of Pharmacology and Pharmacotherapy,
Albert Szent-Györgyi Medical School,
Doctoral School of Multidisciplinary Medical Sciences,
University of Szeged

Szeged, Hungary

2023

TABLE OF CONTENTS

LIST OF PUBLICATIONS

The publications related to the subject of the Ph.D. thesis

I. ***Leila Topal****, Alexandra Polyák*, Noémi Tóth, Gergely Ágoston, Péter Bencsik, Zsófia Kohajda, János Prorok, Szilvia Déri, Norbert Nagy, Norbert Jost, László Virág, Attila S. Farkas, András Varró, István Baczkó (2022). Endurance training-induced cardiac remodeling in a guinea pig athlete's heart model.
CANADIAN JOURNAL OF PHYSIOLOGY AND PHARMACOLOGY, 100 (10) pp 993- 1004. doi: 10.1139/cjpp-2022-0073.
IF: 2.245, Q2

II. Péter Orvos*, Bence Pászti*, ***Leila Topal***, Péter Gazdag, János Prorok, Alexandra Polyák, Tivadar Kiss, Edit Tóth-Molnár, Boglárka Csupor-Löffler, Ákos Bajtel, András Varró, Judit Hohmann, László Virág, Dezső Csupor (2020). The electrophysiological effect of cannabidiol on hERG current and in guinea-pig and rabbit cardiac preparations
SCIENTIFIC REPORTS, 10 1 Paper 16079. 9 p. doi: 10.1038/s41598-020-73165-2.
IF: 4.38, D1

III. ***Leila Topal****, Muhammad Naveed*, Péter Orvos, Bence Pászti, János Prorok, Ákos Bajtel, Tivadar Kiss, Boglárka Csupor-Löffler, Dezső Csupor, István Baczkó, András Varró, László Virág László, Norbert Jost (2021). The electrophysiological effects of cannabidiol on action potentials and transmembrane potassium currents in rabbit and dog cardiac ventricular preparations
ARCHIVES OF TOXICOLOGY, 95 7 pp 2497-2505. doi: 10.1007/s00204-021-03086-0.
IF: 6.168, D1

IV. Bence J. Pászti*, János Prorok*, Tibor Magyar, Tamás Árpádffy-Lovas, Balázs Györe Balázs**,** ***Leila Topál***, Péter Gazdag, Jozefina Szlovák, Muhammad Naveed, Norbert Jost, Norbert Nagy, András Varró, László Virág, István Koncz. (2021). Cardiac electrophysiological effects of ibuprofen in dog and rabbit ventricular preparations: Possible implication to enhanced proarrhythmic risk
CANADIAN JOURNAL OF PHYSIOLOGY AND PHARMACOLOGY, 99 1 pp 102-109**.** doi: 10.1139/cjpp-2020-0386
IF: 2.245, Q2

*Shared First Authorship

Impact factor of publications related to the subject of the Ph.D. thesis: **15.038**

Other publications published under Ph.D. scholarship

I. Alexandra Polyák*, ***Leila Topal****, Noémi Zombori-Tóth, János Prorok, Zsófia Kohajda, Szilvia Déri, Vivien Demeter-Haludka, Péter Hegyi, Viktória Venglovecz, Gergely Ágoston, Zoltán Husti, Péter Gazdag, Jozefina Szlovák, Tamás Árpádffy-Lovas, Muhammad Naveed, Annamária Sarusi, Norbert Jost, László Virág, Norbert Nagy, István Baczkó, Attila S. Farkas, András Varró (2023). Cardiac electrophysiological remodeling associated with enhanced arrhythmia susceptibility in a canine model of elite exercise
eLIFE, 12 Paper e80710. 27 p. doi: 10.7554/eLife.80710.
IF: 8.713, D1

II. Zsófia Kohajda*, László Virág*, Tibor Hornyik, Zoltán Husti, Anita Sztojkov-Ivanov, Norbert Nagy, András Horváth, Richárd Varga, János Prorok, Jozefina Szlovák, Noémi Tóth, Péter Gazdag, ***Leila Topal***, Muhammad Naveed, Tamás Árpádffy-Lovas, Bence J. Pászti, Tibor Magyar, István Koncz, Szilvia Déri, Vivien Demeter-Haludka, Zoltán Aigner, Balázs Ördög, Márta Patfalusi, László Tálosi, László Tiszlavicz, Imre Földesi, Norbert Jost, István Baczkó, András Varró (2022). In vivo and cellular antiarrhythmic and cardiac electrophysiological effects of desethylamiodarone in dog cardiac preparations
BRITISH JOURNAL OF PHARMACOLOGY, 179 13 pp 3382-3402.
doi: 10.1111/bph.15812
IF: 9.473, D1

III. Dénes Kiss*, Balázs Horvát*, Tamás Hézső, Csaba Dienes, Zsigmond Kovács, ***Leila Topal***, Norbert Szentandrássy, János Almássy, János Prorok, László Virág, Tamás Bányász, András Varró, Péter Nánási, János Magyar (2021). Late Na^+ Current Is $[Ca^{2+}]$i-Dependent in Canine Ventricular Myocytes
PHARMACEUTICALS, 14 11 Paper 1142. 16 p. doi: 10.3390/ph14111142.
IF: 6.36, Q1

IV. Tamás Hézső*, Muhammad Naveed, Dienes Csaba, Dénes Kiss, János Prorok, Tamás Árpádffy-Lovas, Richárd Varga, Erika Fujii, Tanju Mercan, ***Leila Topal***, Kornél Kistamás, Norbert Szentandrássy, János Almássy, Norbert Jost, János Magyar, Tamás Bányász, István Baczkó, András Varró, Péter Nánási, László Virág, Balázs Horváth, (2021). Mexiletine-like cellular electrophysiological effects of GS967 in canine ventricular myocardium
SCIENTIFIC REPORTS, 11 1 Paper 9565. 11 p. doi: 10.1038/s41598-021-88903-3.
IF: 4.996, D1

V. Khadija Belasri, ***Leila Topal***, Matthias Heydenreich, Andres Koch, Erich Kleinpeter, Ferenc Fülöp, István Szatmári (2020). Synthesis and Conformational Analysis of Naphthoxazine-Fused Phenanthrene Derivatives

MOLECULES, 25 11 Paper 2524. 15 p. doi: 10.3390/molecules25112524.

IF: 4.411, Q1

*Shared First Authorship

Impact factor of all publications: 48.991

ABBREVIATIONS

AP(s): action potential(s)

APD: action potential duration

APD_{90}: action potential duration at 90% of repolarization

BW: body weight

CBD: cannabidiol

C_{max}: the highest concentration of a drug in the blood, cerebrospinal fluid, or target organ after a dose is given

DMSO: dimethyl sulfoxide

ECG: electrocardiogram

EC_{50}: half-maximal effective concentration value

EF: ejection fraction

EXE: exercised

FS: fractional shortening

I: instability

I-QT: instability of QT interval

IC_{50}: half-maximal inhibitory concentration

I_{CaL}: L-type calcium current

I_{Na}: fast sodium current

I_{NaL}: late sodium current

I_{NCX}: sodium-calcium exchanger

I_{Kr}: rapid component of delayed rectifier potassium current

I_{Ks}: slow component of delayed rectifier potassium current

I_{K1}: inward rectifier potassium current

I_{to}: transient outward potassium current

IVS: thickness of the interventricular septum

IVSd: thickness of the interventricular septum during diastole

LTI: long-term instability

LTI-QT: long-term instability of QT interval

LTV: long-term variability

LTV-QT: long-term variability of QT interval

LVIDd: left ventricular internal diameter during diastole

LVIDs: left ventricular internal diameter during systole

LVPWs: thickness of the left ventricular posterior wall in systole

NSAID(s): Non-steroidal anti-inflammatory drug(s)

OTC: over-the-counter

rmsSD: root mean square of successive differences

sdSD: standard deviation of the successive differences

STV: short-term variability

STV-APD: short-term variability of action potential duration

STV-QT: short-term variability of the QT interval

SCD: sudden cardiac death

SED: sedentary

TdP: Torsades de Pointes

THC: tetrahydrocannabinol

TTX: tetrodotoxin

QTc: heart rate corrected QT interval

ABSTRACT

Besides the health benefits of regular exercise, high-level training, above an optimal level, may have adverse effects. In this study, we investigated the long-term vigorous training evoked structural–functional changes in a small animal model of athlete's heart. Thirty-eight 4- month- old male guinea pigs were randomized into sedentary and exercised groups. The latter group underwent a 15-week-long endurance-training program. To investigate the effects of the intense long-term exercise, *in vivo* (echocardiography, electrocardiography), *ex vivo* and *in vitro* (histopathology, patch clamp) measurements were performed. Following the training protocol, the exercised animals exhibited structural left ventricular enlargement and a significantly higher degree of myocardial fibrosis. Furthermore, resting bradycardia accompanied by elevated heart rate variability occurred. The observed bradycardia, prolonged QTc intervals and increased repolarization variability parameters may raise the risk of electrical instability in exercised animals. Complex arrhythmias did not occur in either group, and there were no differences between the groups in *ex vivo* or cellular electrophysiological experiments. The detected structural–functional changes share similarities with the human athlete's heart; therefore, this model might be useful for investigations on cardiac remodeling.
Athletes often seek various avenues to achieve their goals in sport career. The consumption of cannabis, cannabidiol, a non–psychoactive cannabinoid, and non-steroidal anti-inflammatory drugs is not rare among athletes to reach greater sporting achievements. However, the use of cannabis or ibuprofen is associated with known cardiovascular side effects such as cardiac arrhythmias or cardiac arrest. The mechanisms behind these adverse effects are poorly understood yet. In the present studies, we investigated the cellular electrophysiological effects of cannabidiol and ibuprofen with whole-cell configuration of patch clamp technique in native left ventricular myocytes on several potassium currents with major roles in the repolarization reserve, and on inward currents. Since both drugs significantly influenced the amplitude of various transmembrane ionic currents, they can evoke prolonged action potential duration and, consequently, prolonged QT interval under certain circumstances. Therefore, these agents should be consumed with caution by athletes, as they can attenuate the repolarization reserve and, together with the cardiac structural-electrophysiological changes that can result from long- term vigorous training, may lead to life-threatening arrhythmias.

1. INTRODUCTION

1.1 Athletic training-induced functional and structural cardiac remodeling

Regular physical activity and competitive sports have undeniable benefits in improving quality of life and life expectancy, hence regular exercise should be encouraged in all individuals (Mahindru et al., 2023; Ruegsegger & Booth, 2018; Wang & Ashokan, 2021). It should be emphasized that participating in sporting activities and the corresponding training have profound effects on the cardiovascular system, including the size, mass, function, and structure of the heart. Repetitive high-intensity exercise over a long period of time requires increased demand. The enhanced demand due to increased physical activity leads to the adaptation of the heart to the elevated workload, this type of cardiac condition is often referred to as the "athlete's heart" (Beaudry et al., 2016). Namely, the term "athlete's heart" describes the reversible physiological structural and functional cardiac changes following long-term training. Besides the positive impacts, recent decades have witnessed a growing number of athletes who constantly push their limits to achieve greater athletic performance. Those who perform high- level training beyond an optimal level may be more prone to unpleasant cardiac events such as atrial and ventricular arrhythmias, and even sudden cardiac death (SCD) in certain circumstances (Eijsvogels et al., 2018; Merghani et al., 2016). Therefore, it is important to be familiar with the U-shaped relationship between exercise intensity and the risk of cardiovascular events (Merghani et al., 2016; Polyak et al., 2023). Long-term high-level exercise or sometimes overexertion may act as a trigger for arrhythmogenesis especially in pre-existing cardiac conditions (e.g., hypertrophic cardiomyopathy, long-QT syndrome) or in the presence of silent attenuated repolarization reserve due to various causes, including electrolyte imbalance, doping or seemingly harmless drugs (Polyak et al., 2023; Varro & Baczko, 2010).

A growing body of literature indicates the enhanced incidence of various sports-related arrhythmias, including bradyarrhythmias, supraventricular arrhythmias, ventricular arrhythmias, and even SCD (Link & Estes, 2010; Palatini et al., 1985; Zorzi et al., 2020). As Maron previously pointed out, SCD occurs more often among athletes who engage in low isometric and high dynamic intensity sporting activities, such as soccer and basketball players (Maron, 2007). Fortunately, the prevalence of SCD among athletes is low, approximately 1:50 000 – 1:100 000 (Maron, 2007; Pigozzi & Rizzo, 2008); however, this ratio is presumably underestimated by these statistics.

In many cases; however, the underlying causes of malignant cardiac arrhythmias and even SCD cannot be satisfactorily verified. In some cases, autopsy findings remain negative (Asif et al., 2013), raising suspicions of other unknown mechanisms behind these tragic events.

Up to now, the presence of fibrosis in endurance racers has been reported in several studies (Malek & Bucciarelli-Ducci, 2020; Rajanayagam & Alsabri, 2021; Zhang et al., 2020), and also several animal studies confirmed this issue in detail (Benito et al., 2011; Kui et al., 2021; Polyak et al., 2023; Topal et al., 2022). The enhanced level of myocardial fibrosis may contribute to the development of cardiac arrhythmias, as a potential arrhythmia substrate by decreasing the impulse conduction and interfering with the propagation of the impulse.

Several studies have described changes in the different intervals of the electrocardiogram (ECG) following athletic training, such as increased RR intervals, prolonged QT, and heart rate corrected QT interval (QTc) (Holly et al., 1998; Lengyel et al., 2011; Pelliccia et al., 2002). Presumably, the coexistence of altered cardiac structure and attenuated repolarization reserve may enhance the susceptibility to arrhythmogenicity among athletes. It is important to emphasize that the prolonged repolarization-induced repolarization inhomogeneity, which is also an important contributor to an arrhythmia substrate, alone is not sufficient to elicit cardiac arrhythmias but it may establish a potential substrate (Roden, 2008; Varro & Baczko, 2010, 2011). In this case, a "trigger" like an extrasystole in a vulnerable period with unfortunate timing can traverse the ventricle where the repolarization inhomogeneity was augmented, so it can form a reentry pathway (see detail in Chapter 1.4) (Varro & Baczko, 2010). The research community continues to show a great interest in studying the underlying cellular electrophysiological drivers of different arrhythmias associated with chronic high-intensity exercise.

1.2 The association between the QT interval and the cellular electrical cycle of ventricular myocytes

Sound and reliable electrical function are indispensable for the proper mechanical function of the heart. Each myocardial cell generates a special electrical signal, called action potential (AP) (Nerbonne & Kass, 2005). It is well known that action potentials (APs) originating from different regions of the heart have a unique pattern. These differences contribute to the normal unidirectional propagation of excitation through the myocardium and the generation of normal cardiac rhythms (Nerbonne & Guo, 2002; Zicha et al., 2003). The summary of local potential changes, for instance, action potentials results in an easily measurable composite record from the body surface, known as an electrocardiogram (ECG). Therefore, ECG is a non-invasive

diagnostic tool that provides valuable information about the current electrical status of the heart, including rhythm or conduction, and even cardiac remodeling due to various conditions, such as long-term extreme exercise, agents, or drug-induced alterations (Joukar, 2021).

The ECG is composed of several sections, among which the QRS interval represents the time needed for the depolarization of the ventricles. Similarly, the QT interval represents the full depolarization and subsequent repolarization of the ventricles, with the duration of repolarization playing a major role in the duration of the QT interval. During this period, firing and recharging of ventricular myocytes are produced by the finely tuned balance between the consecutive activation (opening) and inactivation (closing) of various transmembrane ion channels that conduct depolarizing, inward (Na^+, Ca^{2+}) and repolarizing, outward (K^+) currents (Fig. 1).

The cellular electrical cycle of the left ventricular myocardial cell can generally be divided into five distinct phases. The initial phase (phase 0) reflects the rapid depolarization of the myocytes when the negative resting membrane potential (approximately – 90 mV) rapidly shifts into a positive voltage range. It refers to the function of the fast sodium current (I_{Na}) which is the main contributor to the rapid propagation of the electrical cycle. During the overshoot, the short-lived fast sodium current begins to inactivate while the transient outward potassium current (I_{to}) simultaneously activates. The interplay of these ionic currents mainly supports the development of the rapid repolarization phase (phase 1) which sets the potential for the next phase (Grant, 2009). The magnitude of this phase has a key role in creating the spike-and-dome configuration of the AP, which is a specific marker for identifying the ventricular origin of the cell. Phase 2, also known as the "plateau phase", is maintained by balanced interactions of several inward and outward currents. Throughout this phase, the membrane permeability to calcium increases (via L-type calcium current; I_{CaL}), maintaining and prolonging the action potential duration (APD) which is crucial for myocyte contraction. Besides that, the additional contributors to phase 2 are the window/late sodium current (I_{NaL}) and the sodium-calcium exchanger (I_{NCX}). As I_{CaL} slowly decays towards the end of phase 2, outward potassium currents namely the slow (I_{Ks}) and fast (I_{Kr}) components of delayed rectifier potassium current start to activate. After the inward current decayed, during the initial part of phase 3, I_{Kr} and I_{Ks} start restoring the membrane potential to its resting level, and lastly and primarily the inward rectifier potassium current (I_{K1}) completes the repolarization. Finally, phase 4, or resting membrane potential during diastole, is generated in part by I_{K1} and presumably the sodium-potassium ATPase pump.

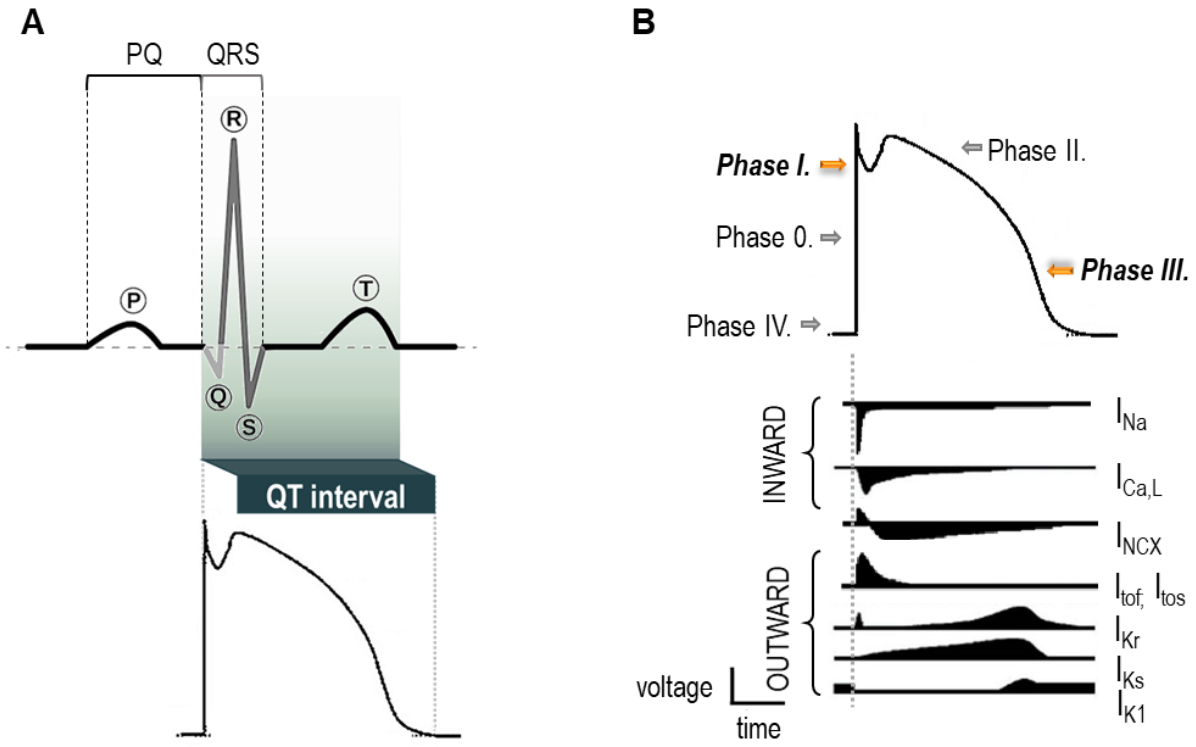

Figure 1. Schematic illustration of ventricular cardiac electrical processes
Fig. 1A indicates a schematic illustration of ECG and its QRS and QT intervals with the underlying action potential characteristic of a midmyocardial left ventricular myocyte. The upper panel of Fig. 1B. shows a representative ventricular action potential waveform and the five distinct phases of the action potential kinetics. The yellow arrows indicate the two repolarization phases (phase 1 and phase 3, respectively). On the lower panel of Fig. 1B., the inward currents are depicted as downward, and outward currents are depicted as upward deflections. The amplitudes of the illustrated currents are not proportional to each other.

1.3 The importance of repolarization reserve

As described above, the repolarization phase of the AP depends on the critical balance of several inward and outward transmembrane ionic currents that forms a strong repolarization reserve. In recent times, it has become evident that the repolarization is adequately over-secured to protect the heart against extremely lengthened APD and consequently prolonged QT interval, which can provide a potential substrate for the development of different arrhythmias. The concept of repolarization reserve is originally proposed by Roden (Roden, 2004, 2006, 2008) and later this concept has been proven experimentally (Jost et al., 2005; Varro et al., 2000). Based on this concept and strongly evidenced experimental data, the loss of one repolarization component (i.e., I_{Kr}) does not lead to a marked lengthening of APD and, therefore, excessively prolonged QT interval. In other words, repolarizing currents, until a certain level, can compensate for the function of each other. The underlying mechanism behind this observation is that other transmembrane ion channels can partly compensate for the function of the missing link,

therefore, the repolarization remains seemingly intact. Consequently, the properly functioning heart is defended by the orchestrated cooperation between the different repolarizing ionic currents against malignant cardiac arrhythmias.

The different outward potassium currents during the repolarization phases have important roles in the repolarization reserve. It is widely accepted that the control of the repolarization process is mainly governed by I_{Kr}, while I_{Ks}, because of its slow activation and fast deactivation kinetic, presumably has little impact on normal repolarization. But when the APD is lengthened and its plateau is shifted into a more positive voltage range, it may provide the opportunity for the development of greater I_{Ks}, which successfully limits further APD lengthening. This potency highlights the significance of I_{Ks} as an important player of the repolarization reserve (Varro et al., 2000).

Additionally, recent studies about the repolarization reserve highlighted that I_{to} is an essential contributor of the initial phase 1 repolarization, and greatly influences the amplitude of the plateau phase and consequently the kinetics of other transmembrane currents (Dong et al., 2006; Niwa & Nerbonne, 2010). However, I_{to} also can be a part of the repolarization phase, since it has a slowly decaying and "window current" components (Virag et al., 2011). Therefore, it may also have an impact on repolarization together with other repolarizing currents. It has been shown that I_{to} varies between the layers of the heart, therefore it may contribute to the spatial heterogeneity as well (Antzelevitch et al., 1991).

1.4 The dispersion of repolarization, as a potential underlying mechanism for cardiac arrhythmias

Cardiac arrhythmia is an umbrella term that involves several conditions characterized by alterations in the physiological rhythm of the heart. Among the many potential cellular electrophysiological mechanisms, cardiac arrhythmias can develop by abnormal impulse conduction as a result of fibrosis and/or enhanced repolarization inhomogeneity. The characteristics of phase 1 and phase 3 repolarization differ in the epicardial, midmyocardial, and endocardial cells of the left ventricle (Johnson et al., 2018). Despite these differences, the neighboring myocytes are electrotonically well-coupled, resulting in a relatively small dispersion of repolarization. According to the well-established and experimentally proved hypothesis, the incidence of cardiac arrhythmias can be augmented if the repolarization is lengthened thereby increasing spatial repolarization heterogeneity (Akar et al., 2005; Varro & Baczko, 2011; Varro et al., 2021). The explanation for this mechanism is that a significantly prolonged effective refractory period, coupled with increased repolarization heterogeneity,

favors the development of re-entry arrhythmias, especially after an extrasystole acts as a trigger (Varro & Baczko, 2010; Varro et al., 2021) (Fig. 2).

The repolarization reserve can be attenuated by drug exposures (i.e., cardioactive or typically non-cardioactive agents), cardiac remodeling due to various conditions (i.e., diseases, heart failure, extreme training), hypokalemia, or genetic disorders like long-QT syndromes. In these conditions, even a moderate potassium current inhibition may lead to potentially proarrhythmic prolongation of the ventricular APD. Consequently, it is important to keep in mind that the inhibition of multiple potassium channels or the failure of these channels can cause excessive impairment of repolarization, associated with enhanced proarrhythmic risk (Varro & Baczko, 2010, 2011).

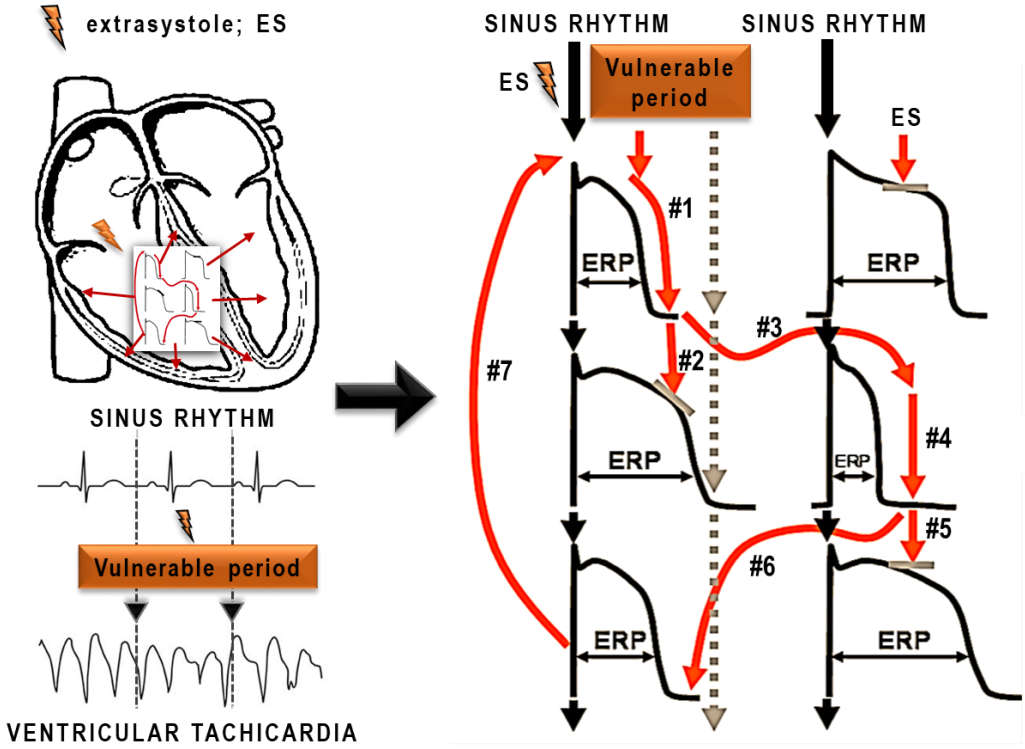

Figure 2. Schematic illustration of the mechanism of inhomogeneous repolarization provoked cardiac arrhythmias

Sinus impulses (grey arrows) travel via physiological pathways in normal conditions. An extrasystole during a vulnerable period can only propagate via myocytes which are not in an effective refractory period (#1, #3, #4, #6). The abnormal impulse can travel towards myocytes which are in an effective refractory period (#2 and #5). Re-entry pathways can occur as a result of inhomogeneous repolarization (#7). As the lower representative ECG illustration on the left side indicates, this mechanism can facilitate different types of arrhythmias, like ventricular tachycardia. ERP, effective refractory period; ECG, electrocardiogram. Modified from Varro and Baczko (2011), with permission.

1.5 The impact of seemingly harmless drugs among athletes

To achieve higher levels of physical strength, high work performance over time, increased period of exhaustion, and more supportive psychological functions are essential for also "elite" and "amateur" athletes, therefore, they often seek different avenues to reach greater achievements. A lot of products in the market, for instance, various dietary supplements (e.g., cannabidiol; CBD) and even some medicines (e.g., non-steroidal anti-inflammatory drugs; NSAIDs) offer several benefits for athletes to accomplish their goals (Docter et al., 2020; Lima et al., 2016; Lundberg & Howatson, 2018; McCartney et al., 2020). Surprisingly, the cardiovascular safety profile of some compounds found in these products, like the impact on the duration of the QT interval and/or different transmembrane ionic currents, has not been properly investigated yet. Therefore, the interplay between these compounds and other factors, such as chronic high-intensity exercise evoked cardiac structural and electrophysiological remodeling, may attenuate the repolarization reserve, thus increasing the potential arrhythmogenic substrate in athletes. Accurate characterization of the effects of some seemingly harmless compounds on ventricular repolarization would be necessary, regardless of their seemingly marginal effects.

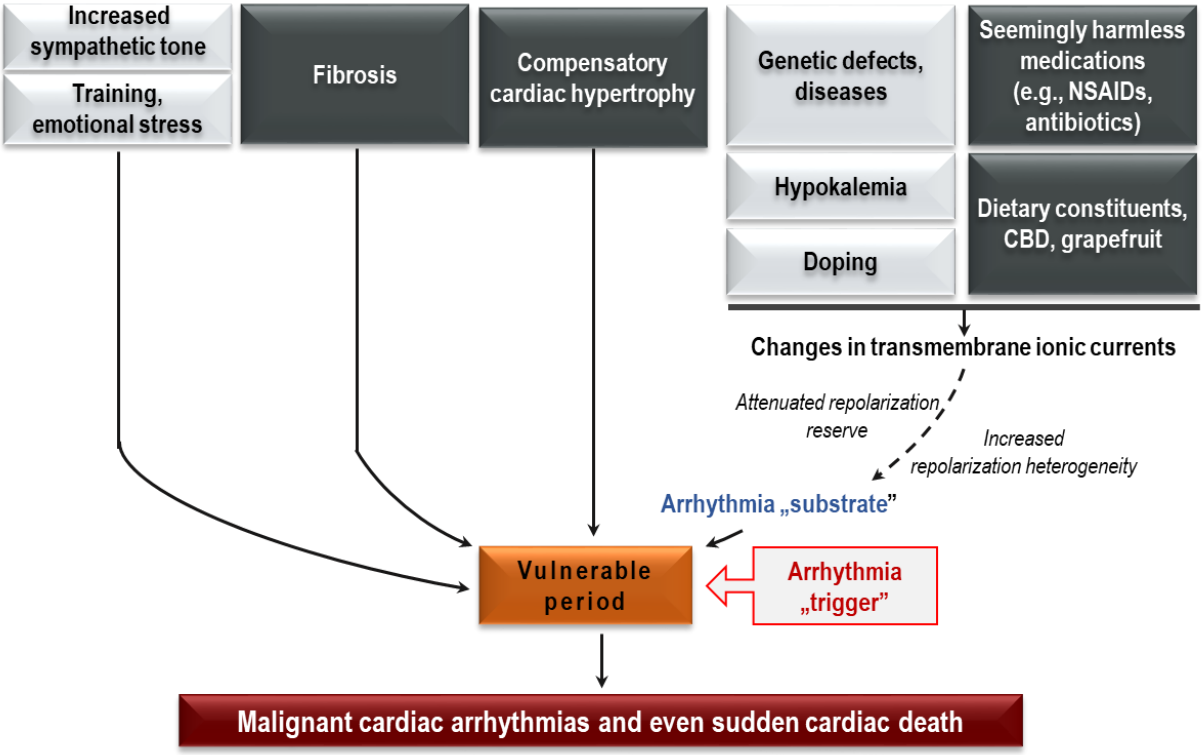

Figure 3. Hypothetical mechanism and summary of risk factors most likely involved in malignant arrhythmias and sudden cardiac death of competitive athletes
Modified from Varro and Baczko (2011), with permission.

1.6 Arrhythmogenic potency of cannabidiol consumption

While being illegal in many jurisdictions, according to surveys, cannabis (marijuana) is one of the most commonly used drugs with hallucinogenic side effects, and the number of users is increasing worldwide (Kalla et al., 2018). Nowadays, it is becoming fashionable, not only for its pleasurable effects but also for its potential beneficial impacts on athletic performance and recovery (Docter et al., 2020; McCartney et al., 2020). Cannabis consists of several compounds, of which tetrahydrocannabinol (THC) is a psychoactive compound, while cannabidiol (CBD) gained pharmacological interest due to its lack of psychotropic activity (Fraguas-Sanchez & Torres-Suarez, 2018; Rapin et al., 2021). Following the discovery of the endocannabinoid system, healthcare professionals have been closely monitoring the intensive research into their potential effects. Cannabis-based medicines contain known amounts of CBD and/or THC levels with well-defined medical indications (Adel, 2017; Fraguas-Sanchez & Torres-Suarez, 2018; Stampanoni Bassi et al., 2017). Interestingly, CBD consumption has increased dramatically over the last few years thanks to readily available products, for example, CBD oil, which can contain up to 20 % CBD and a significant amount is absorbed (Czegeny et al., 2021; Topal et al., 2021). Moreover, CBD is widely used among athletes for its claimed effects, such as decreased anxiety, fear memory extinction, anti-inflammatory properties, relief of pain, and post-exercise recovery (Rojas-Valverde, 2021). It is important to note that these dietary supplements usually do not meet quality standards and the exact CDB content is unknown, nevertheless, the efficacy and indications of these products are mainly unsupported in clinical settings.

Some recent studies raised concerns about cannabinoid-related adverse cardiovascular events, such as significant QT prolongation, the development of multiform cardiac arrhythmias, myocardial infarction, and even SCD; however, the mechanism of these cardiac arrhythmias is poorly understood (Manolis et al., 2019; Ozturk et al., 2019). Possible impacts of CBD on various voltage-gated outward and inward transmembrane ion channels with key roles in the repolarization reserve are not negligible, therefore may contribute to arrhythmogenic potential.

1.7 Potential arrhythmogenic effects of a widely used non-steroidal anti-inflammatory drug, called ibuprofen

Non-steroidal anti-inflammatory drugs (NSAIDs) are widely used for the treatment of fever, inflammatory processes, and to provide pain relief (Panchal & Prince Sabina, 2023). A large number of over-the-counter (OTC) NSAID products are available on the market. Furthermore, over the last years, a robust and extensive product portfolio of NSAIDs, product approvals, and launches have been raised extremely making them easily available. Ibuprofen is a common OTC and prescribed NSAID for the treatment of mild to moderate pain (i.e., menstrual cramps, toothache, migraine), to control fever, for easing pain and inflammation related to joints, bones, and muscles (i.e., rheumatoid arthritis), and for easing pain and swelling caused by sprains and strains such as sports injuries (Bushra & Aslam, 2010; Rainsford, 2009; Warden, 2010). Different NSAIDs (i.e., ibuprofen, diclofenac, naproxen, etc.) are commonplace among athletes, including elite, recreational, and college-athletes as well (Lippi et al., 2006; Ziltener et al., 2010). The NSAID-containing OTC products are not on the drug prohibited list of the World Anti-Doping Agency, therefore, they are favored for possible prevention of exercise-induced fatigue, to increase pain tolerance, and to reduce inflammation from injuries (Warden, 2010; Warner et al., 2002).

In a recent report, it was shown that diclofenac enhanced cardiovascular risk and caused SCD in some soccer players (Gillon D., 2006). In an experimental study, it was shown that diclofenac decreased repolarization reserve by inhibiting I_{Kr} and I_{Ks} which is associated with enhanced proarrhythmic susceptibility (Kristof et al., 2012).

While ibuprofen has a relatively safe drug profile, some studies raised awareness of its contribution to the development of various cardiovascular events, including cardiac arrest, palpitation, and a higher rate of arrhythmic events (Pratt et al., 1994; Sondergaard et al., 2017). Interestingly, only a few studies have experimentally investigated the link between the therapeutically relevant and supratherapeutic concentrations of ibuprofen and its cardiac electrophysiological effects experimentally (Wolfes et al., 2022; Yang et al., 2008; Yarishkin et al., 2009). However, our knowledge of the impact of ibuprofen on different transmembrane ionic currents, with significant relevance on repolarization reserve, remains incomplete.

2 AIMS

Since the different changes occurring during repolarization present a very complex issue affected by several factors, such as structural and functional cardiac remodeling associated with long-term endurance training, as well as drug-induced alternations of repolarization reserve, the aims of the present study were the following:

1. To develop a small animal model that was relevant to the human athlete's heart.
2. To assess the underlying mechanism of structural–electrical cardiac changes due to long-term endurance training.
3. To investigate the cardiac electrophysiological effects of cannabidiol and ibuprofen at the cellular level in native left ventricular myocytes obtained from larger animals that closely mimic human basic cellular electrophysiology (rabbit and canine). To elucidate their proarrhythmic side effects, their attenuating impacts were studied on various transmembrane ionic currents, which play a key role in the repolarization reserve.

3 MATERIALS AND METHODS

3.1 Ethical issues of animal studies

All experiments were carried out in compliance with the *Guide for the Care and Use of Laboratory Animals* (USA NIH publication No. 85-23, revised 1996) and conformed to Directive 2010/63/EU of the European Parliament. The protocols have been approved by the Ethics Committee for the Protection of Animals in Research of the University of Szeged, Szeged, Hungary (authority approval number: I-74-24-2017) and by the Department of Animal Health and Food Control of the Ministry of Agriculture and Rural Development (following authority approval numbers related to all studies: XIII/2163/2019, XIII/3331/2017, XIII/3330/2017 and XIII/1211/2012).

3.2 Various experimental settings for the examination of endurance training-induced structural and electrophysiological cardiac remodeling in a guinea pig athlete's heart model

To examine the profound impacts of long-term endurance training, we developed a small animal athlete's heart model. To understand this issue in depth, several investigation techniques were applied.

3.2.1 Experimental protocol

Male albino Dunkin-Hartley guinea pigs were used for the evaluation of potential structural and electrophysiological changes due to long-term endurance training. Four-month-old animals with initial weighing between 300–350 g were randomized into exercised ("EXE" n = 19) and sedentary ("SED", n = 19) groups.

Training sessions were performed on a special rodent treadmill system with four separated glass-wall corridors for the animals and adjustable gradient and speed intensity (Treadmill for rats, Elunit Group/Elunit Medical Equipment, Belgrade, Serbia). The "EXE" group was involved in the 15-week-long running training program, while the "SED" group did not participate. The latter group received the same handling (i.e., placement on the treadmill) to avoid differences originating from different handling procedures.

The training protocol was initiated with a 2-week-long warm-up period, to familiarize the animals with handling and the laboratory environment. Subsequently, the "EXE" group underwent a progressive endurance-training program combined with interval running sessions for 60–90 minutes daily, 5 times a week. Speed and inclination of the treadmills were increased

progressively each week until reaching a range of 0.6–1.92 km/h and 14 % inclination. Based on the related literature and preliminary studies, the animals achieved high-level performance with a lack of distress.

3.2.2 Echocardiography measurements

Transthoracic echocardiographic examination was performed in the 15th week of the training protocol in conscious animals. M-mode parasternal long-axis view was applied using an 11.5 MHz transducer (GE10S-RS, GE Healthcare, Chicago, IL, USA), connected to an echocardiographic imaging unit (VividS5, GE Healthcare, Chicago, IL, USA). All parameters were analyzed by an expert cardiologist in a randomized and blinded manner. The mean values of three distinct measurements were calculated and used for statistical evaluation.

Left ventricular internal diameter during systole (LVIDs) and diastole (LVIDd), the thickness of the left ventricular posterior wall at systole (LVPWs), interventricular septum (IVS), and end ejection fraction (EF) were measured in M-mode images. The wall thickness and diameter parameters were corrected with the animal's body weight (BW). The BW of the animals was measured immediately before the echocardiography study. Fractional shortening (FS) was calculated as FS = (LVIDd− LVIDs)/LVIDd×100.

3.2.3 Electrocardiography measurements

In conscious guinea pigs, ECG recordings were performed using pericardial leads before (0th week) and at the end (15th week) of the training protocol without any pain or stress. The ECGs were recorded with National Instruments data acquisition hardware (PC card, National Instruments, Austin, TX., USA) and SPEL Advanced Haemosys software (version 3.26, MDE Heidelberg GmbH, Heidelberg, Germany). Various ECG parameters, including heart rate (HR), RR, PQ, QRS, and QT intervals, were analyzed manually by positioning screen markers at 40 consecutive sinus beats, starting 10 minutes into the ECG recording. As the QT interval is influenced by the heart rate, based on a recently published paper (Polyak et al., 2018), the relationship between the RR interval and the consecutive QT interval in sinus rhythm was examined. Briefly, 40 consecutive QT intervals were measured together with the corresponding RR intervals. Simple linear regression revealed a positive correlation between QT and RR obtained from 38 guinea pigs (QT = 0.55 x RR + 9.31). The equation was rearranged to allow the calculation of the heart rate –corrected QT interval in guinea pigs at an RR interval of 182 ms using the formula $QT_{CX} = QT_X – 0.55$ x $(RR_{(X-1)} – 182)$. With these equations, plotting QTc against the corresponding RR interval procedures a regression line with a slope of zero, indicating that these corrections remove the influence of the heart rate.

3.2.4 Evaluation of beat-to-beat variability and instability of ECG intervals

Beat-to-beat variability and instability parameters of the RR and QT intervals, including the "root mean square of successive differences", the "standard deviation of the successive differences", the "short-term variability", the "long-term variability", the "long-term instability", and "instability" of the ECG intervals were derived and calculated from 60 consecutive sinus beats as described previously (Polyak et al., 2018).

3.2.5 *Ex vivo* electrophysiological study in isolated Langendorff perfused guinea pig hearts and histopathological studies

Out of 38 guinea pigs, 12 were used for *ex vivo* Langendorff measurements ("EXE" n = 6, "SED" n = 6). The applied method of Langendorff perfusion was described in detail (Kui et al., 2016). The animals were anticoagulated with sodium heparin (1000 international units) injected intraperitoneally and were over-anesthetized with thiopental-sodium (80 mg/kg intraperitoneally), then their hearts were excised and attached to a vertical Langendorff apparatus. Throughout the experiments, Krebs–Henseleit buffer solution was used containing (in mM): NaCl 118.5, glucose11.1, $MgSO_4$ 0.5, NaH_2PO 1.2, KCl 4.3, NaHCO 25.0, and $CaCl_2$ 1.8. The experimental protocol started with a 20-minute equilibration period followed by a 30-minute period when the ECG recordings were performed.

After these experiments, the hearts were removed from the apparatus, and cardiac tissue samples were fixed using a formaldehyde solution. Samples were taken from the subendocardial region of the atria, septal region, and free-wall region of the ventricular for histological studies. Paraffin sections of the hearts were stained with Crossmon's trichrome staining (Crossmon, 1937) to identify collagen deposition. An independent pathologist performed a semi-quantitative analysis in a blinded manner to evaluate the degree of interstitial fibrosis as follows: 0 = no fibrosis, 1 = moderate fibrosis, and 2 = severe fibrosis.

3.3 Cell preparations

Enzymatic isolation of the left ventricular segment is a crucial step in whole-cell patch-clamp experiments. The termination protocols of each experimental species (guinea pig, rabbit, and canine) strictly followed the corresponding animal ethical regulations. In all cases, a general isolation method was followed. A general isolation method was followed across all species, with only the Ca^{2+} concentration of the isolation solution, and the types and quantities of enzymes used throughout the enzymatic isolation differing per species. The general Ca^{2+}-free isolation solution was always composed of (in mM) NaCl 135, KCl 4.7, KH_2PO_4 1.2,

$MgSO_4$ 1.2, HEPES 10 glucose 10, Taurine 35, Na-pyruvate 5, with the pH adjusted to 7.4 using NaOH.

3.3.1 Enzymatic isolation of guinea pig left ventricular myocytes

Left ventricular tissue was enzymatically isolated to study the endurance training-induced electrophysiological changes at the cellular level. The termination of the animals is described in detail above. Hearts were rapidly excised and immersed in a cold (4 °C) isolation solution containing 0.75 mM Ca^{2+}. Thereafter, each heart was cannulated via the aorta onto a Langendorff apparatus. The blood from the heart was washed out retrogradely with oxygenated and pre-warmed (37 °C) isolation solution containing 0.75 mM Ca^{2+}. After the washout period (10 to 12 minutes), the hearts were perfused with Ca^{2+}-free isolation solution for 8–10 minutes, until the hearts stopped beating. Finally, the process was completed with enzymatic isolation: for 10–15 minutes the hearts were perfused with the general isolation solution containing 0.8 g/L collagenase (type II, Worthington), 0.1 g/L proteinase (type XIV, Sigma–Aldrich), 100 μm Ca^{2+}. At the end of the enzymatic isolation process, the left ventricular myocardium was minced and cut into small strips. For approximately 10 minutes, the strips were placed into a storage solution with a high concentration of potassium, containing (in mM): L-glutamic acid monohydrate 203.2, Taurine 125.15, KCl 74.55, KH_2PO 136.09, HEPES 238.3, $MgCl_2$ 203.31, glucose 180.16, EGTA 380.35, pH adjusted to 7.3 with KOH. After gentle agitation, the cells were separated by filtering through a nylon mesh and they were stored at room temperature in the high-concentrated K^+-solution (Topal et al., 2022).

3.3.2 Enzymatic isolation of rabbit left ventricular myocytes

To examine the effects of different cardioactive drugs on transmembrane ion channels, New Zealand white rabbits of either sex (weighing 1.5–2.0 kg) were used. The rabbits initially received iv. injection of 400 IU/kg heparin into the marginal vein of the ear vein, then they were sacrificed by a concussion to avoid the possible cardio-depressant effects of anesthetics. After the quick removal of the heart, it was placed into cold (4 °C) isolation solution containing 1mM Ca^{2+} The blood was washed out over a period of approximately 3–5 minutes, then enzymatic isolation was performed using the general isolation solution supplemented with 1.8 mg/ml collagenase (type II, Worthington) and 33 μM Ca^{2+} for 12–15 minutes. Subsequently, the left ventricular region was excised and cut into small strips, then they were placed in an enzyme-free solution containing 1 mM Ca^{2+} for 10 minutes. It was followed by gentle agitation and

filtering through a nylon mesh. The cells were stored at room temperature in 1 mM Ca^{2+}- contained isolation solution.

3.3.3 Enzymatic isolation of canine left ventricular myocytes

To study different cardioactive drugs, Beagle canines of either sex (weighing 10–12 kg) were used. The animals were anesthetized and sacrificed with iv. injection of pentobarbital (60 mg/kg), then the heart was rapidly removed through a right lateral thoracotomy. Thereafter, the left ventricular segment was gently excised. Subsequently, it was cannulated via a coronary artery and placed on a modified Langendorff perfusion system. After the previously describes processes (see detail in Chapter 3.3.2) the segment was enzymatically isolated with an isolation solution containing 0.66 mg/mL collagenase (type II, Worthington) and 33 μM Ca^{2+}. In the 15^{th} minute of the enzymatic isolation, 0.12 mg/mL protease (type XIV, Sigma-Aldrich) was added to the solution. The remaining steps were the same as mentioned in the previous chapter.

3.4 Whole-cell patch-clamp experiments of various transmembrane ionic currents in left ventricular myocytes

The full methodology of transmembrane ionic current measurements using the whole-cell configuration of the patch clamp technique was described in detail in recent studies (Kohajda et al., 2022; Polyak et al., 2023). Briefly, the experiments were carried out at 37 °C. HEPES- buffered Tyrode's solution served as the normal superfusate (composition in mM: NaCl 144, NaH_2PO_4 0.4, KCl 4.0, $CaCl_2$ 1.8, $MgSO_4$ 0.53, glucose 5.5, and HEPES 5.0, at a pH of 7.4). One drop of cell suspension was placed in a transparent chamber mounted on the stage of an inverted microscope (Olympus IX51, Tokyo, Japan), and individual myocytes were allowed to settle and adhere to the bottom of the chamber before the suspension was initiated and maintained by gravity. Micropipettes were fabricated from borosilicate glass capillaries (Science Products GmbH, Hofheim, Germany), using a P-79 Flaming/Brown micropipette puller (Sutter Co, Novato CA, USA), and had a resistance of 1.5 to 2.5 Mohm when filled with pipette solution. The membrane currents were recorded with Axopatch-200B amplifiers (Molecular Devices, Sunnyvale, CA, USA) by applying the whole-cell configuration of the patch-clamp technique. The membrane currents were digitized with 250 kHz analog to digital converters (Digidata 1440A, Molecular Devices, Sunnyvale, CA, USA) under software control (pClamp 10, Molecular Devices, Sunnyvale, CA, USA). The same software was used for offline analysis.

3.4.1 Measurements of various potassium currents

Under rectangular command pulses, the inward rectifier (I_{K1}), the transient outward (I_{to}), the rapid (I_{Kr}), and the slow (I_{Ks}) delayed rectifier potassium currents were recorded in HEPES-buffered Tyrode's solution. The composition of the pipette solution (mM) was: KOH 110, KCl 40, K_2ATP 5, $MgCl_2$ 5, EGTA 5, and HEPES 10 (the pH was adjusted to 7.2 using aspartic acid). 1 μM nisoldipine was added to the bath solution to block I_{CaL}. When I_{to} and I_{K1} were recorded, both I_{Ks} and I_{Kr} were inhibited by using their selective blockers, 0.5 μM HMR-1556, and 0.1 μM dofetilide, respectively. When I_{Kr} was recorded, I_{Ks} was inhibited by using the selective I_{Ks} blocker HMR-1556 (0.5 μM). For I_{Ks} measurements, I_{Kr} was blocked by 0.1 μM dofetilide, and the bath solution contained 0.1 μM forskolin.

3.4.2 Measurement of L-type calcium current

The L-type calcium current (I_{CaL}) was recorded in HEPES-buffered Tyrode's solution supplemented with 3 mM 4-aminopyridine. The pipette solution contained (in mM): $CsCl_2$ 125, TEACl 20, MgATP 5, EGTA 10, and HEPES 10. The pH was adjusted to 7.2 with CsOH.

3.4.3 Measurement of late sodium current

The late sodium current (I_{NaL}) was activated by depolarizing voltage pulses of 2 s at –20 mV from a holding potential of –120 mV, with pulsing cycle lengths of 5 s. After incubation with the drug for 5–7 minutes, the external solution was replaced with a solution containing 20 μM tetrodotoxin (TTX), which completely blocked the I_{NaL}. The external solution was HEPES-buffered Tyrode's solution supplemented with 1 μM nisoldipine, 0.5 μM HMR-1 556, and 0.1 μM dofetilide to block I_{CaL}, I_{Ks}, and I_{Kr} currents. The composition of the pipette solution is described above (lásd ICal).

3.4.4 Measurement of NCX current

For the measurement of the Na^+/Ca^{2+} exchanger current (I_{NCX}), the method of Hobai et al. was applied (Hobai et al., 1997). Accordingly, the NCX current is defined as a Ni^{2+}- sensitive current and measured in a special K^+-free solution (composition in mM: NaCl 135, $CsCl_2$ 10, $CaCl_2$ 1, $MgCl_2$ 1, $BaCl_2$ 0.2, NaH_2PO_4 0.33, TEACl 10, HEPES 10, glucose 10, ouabain 20 μM, nisoldipine 1 μM, and lidocaine 50 μM at pH 7.4) as described earlier in detail (Jost, Nagy, et al., 2013). The pipette solution used for recording I_{NCX} contained (in mM) CsOH 140, aspartic acid 75, TEACl 20, MgATP 5, HEPES 10, NaCl 20, EGTA 20, and $CaCl_2$ 10. The pH was adjusted to 7.2 by CsOH.

3.5 Measurements of single-cell action potentials

The perforated patch-clamp technique was used to measure action potentials from isolated left ventricular myocytes. The membrane potential was recorded in the current-clamp configuration. The myocytes were paced with a rapid rectangular pulse (from 0 to 180 mV, 5 ms) at a frequency of 1 Hz to elicit the action potential. A HEPES- Tyrode solution was used as the extracellular solution. The patch pipette solution contained (in mM): 120 K-gluconate, 2.5 NaCl, 2.5 MgATP, 2.5 Na2ATP, 5 HEPES, 20 KCl, titrated to a pH of 7.2 with KOH. 50 μM β-escin was added to the pipette solution to achieve the membrane patch perforation. Membrane voltage was obtained by using an Axoclamp 1-D amplifier (Molecular Devices, Sunnyvale, CA, USA) connected to a Digidata 1440A (Molecular Devices, Sunnyvale, CA, USA) analog-digital converter. The membrane voltage was recorded by Clampex 10.0 (Molecular Devices, Sunnyvale, CA, USA). At least 60 beats were recorded, and the action potential duration was measured at 90% of repolarization (APD_{90}). The short-term variability of action potential duration (STV-APD) was calculated by analyzing 30 consecutive action potentials.

3.6 Statistical analysis

IBM SPSS Statistics V25 software package was used for statistical analysis. Continuous data were expressed as mean ± standard error of the mean (SEM). The normality of distributions was verified using the Shapiro-Wilk test and the homogeneity of variances was verified using Bartlett's test. Unpaired and paired Student's t-tests were applied to assess whether there was a statistically significant difference between the means in independent and paired groups, respectively. Variance analysis (ANOVA) for repeated measurements with Bonferroni post hoc test. Data were considered statistically significant when $p < 0.05$.

4 RESULTS

4.2 Examination of long-term endurance training-induced cardiac remodeling in a small animal model

4.2.1 Echocardiographic changes after long-term endurance training

The 15-week-long training program led to significant changes in diastolic parameters in the „EXE" group: greater internal dimension of the left ventricle (LVIDd) and increased interventricular septum thickness (IVSd) (Fig. 4A; 4B). Additionally, the thickness of the left ventricular posterior wall in systole (LVPWs) was significantly increased in the „EXE" group (Fig. 4C). It is important to highlight that „EXE" animals showed an increasing tendency in the left-ventricular end-diastolic dimension (LVIDs) („EXE vs. „SED": 5.1 ± 0.4 vs. 4.3 ± 0.3, $p > 0.05$). The ejection fraction (EF) and fractional shortening (FS) did not differ significantly between the groups (EF: „EXE" vs. „SED": 86.1 ± 1.9 vs. 87.4 ± 2.2, $p > 0.05$, FS: „EXE" vs. „SED" 52.9 ± 2.5 vs. 54.9 ± 2.7, $p > 0.05$). The structural changes after long-term endurance training detected by echocardiography are shown in Fig. 4.

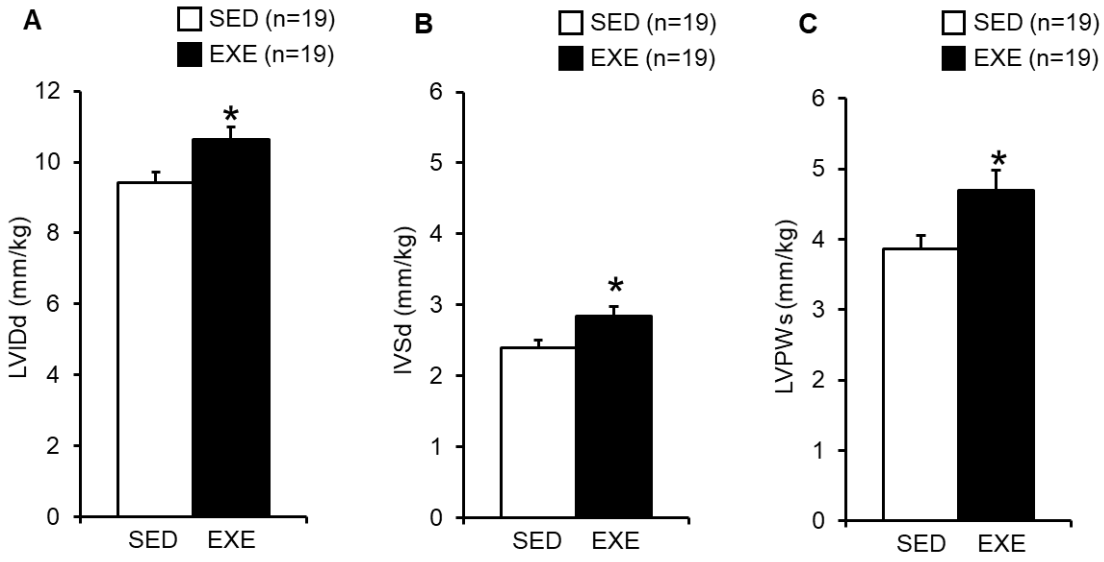

Figure 4. Echocardiographic cardiac parameters in conscious guinea pigs following a 15- week-long endurance training program
The wall thicknesses and diameter parameters were corrected with the BW of the animals. LVIDd, end-diastolic left ventricular internal diameter (A); IVSd, end-diastolic interventricular septal wall thickness (B); LVPWs, end-systolic left ventricular posterior wall thickness (C); BW, body weight; EXE, exercised group; SED, sedentary group. All values are means ± SEM. *$p < 0.05$, unpaired t-test, „EXE" vs. „SED" groups.

4.2.2 Long-term endurance training-induced cardiac fibrosis in guinea pig athlete's heart model

The histopathological study identified a significantly greater degree of fibrosis in the subendocardial region of the right atria, the right ventricle, and the septal wall of the hearts in the „EXE" group (Fig. 5D). In addition, enhanced fibrosis was also presented in the left ventricle in the „EXE" animals. The long-term endurance training indicated greater fibrosis scores and the greater presence of scarring tissue in „EXE" animals compared to their sedentary counterparts (Fig. 5E).

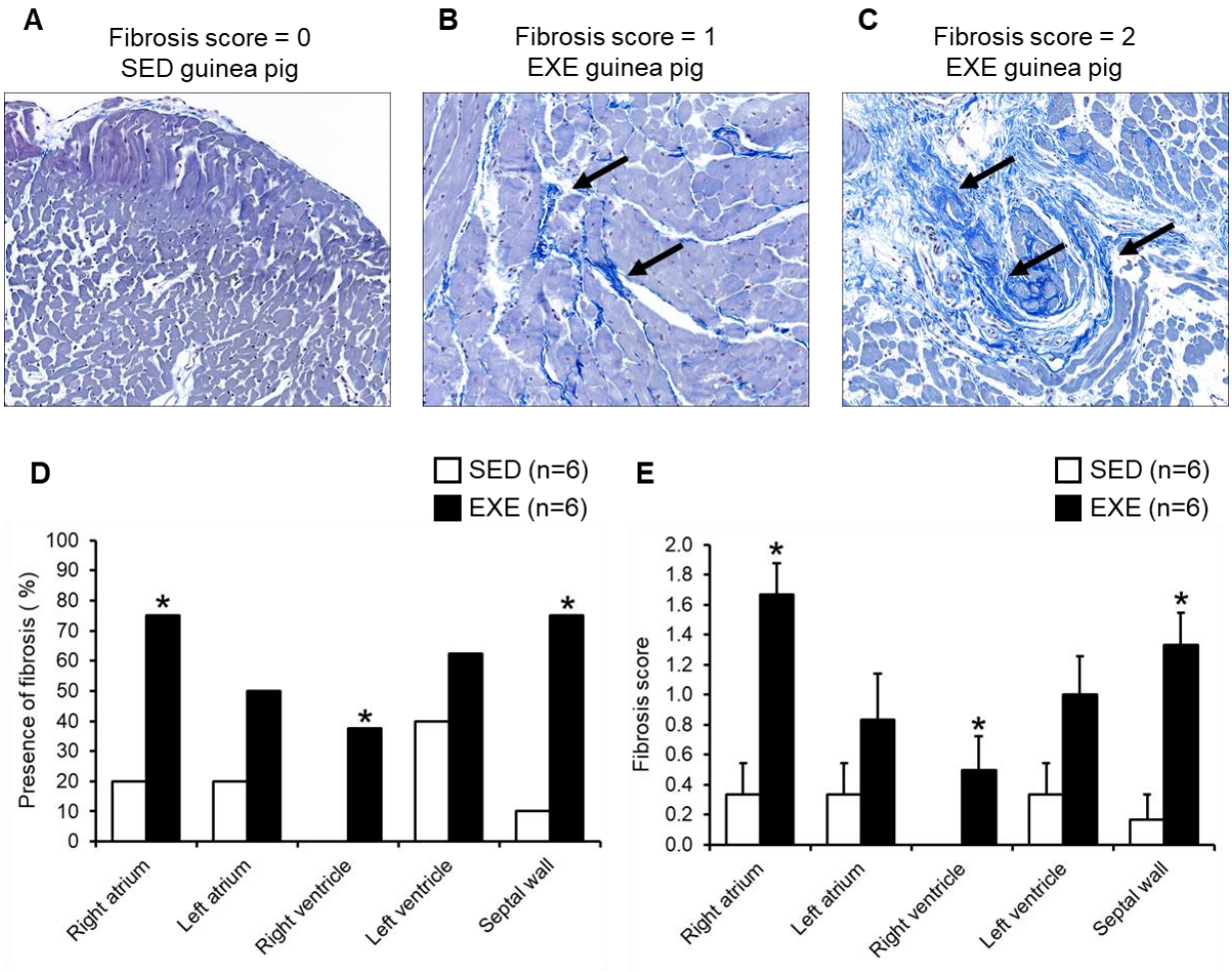

Figure 5. Enhanced myocardial fibrosis in the exercised guinea pig hearts
Upper panels (A, B, C), display representative histological images using Crossmon's trichrome staining taken from sedentary control (A, fibrosis score = 0) and exercised guinea pigs (B, fibrosis score = 1 and C, fibrosis score = 2). Bar charts show the presence of fibrosis within the groups, expressed as the percentage of the total number of animals, irrespective of the degree of fibrosis (D), and the estimation of the amount of scarring via fibrosis scoring (E) in sedentary and exercised guinea pigs. Semi-quantitative analysis was performed to score the degree of interstitial fibrosis with the following criteria: 0 = no fibrosis; 1 = moderate fibrosis; 2 = severe fibrosis. EXE, exercised group; SED, sedentary group. *$p < 0.05$, unpaired t-test; "EXE" vs. "SED" guinea pigs.

4.2.3 The effect of long-term endurance training on heart rate in conscious animals and in *ex vivo* isolated Langendorff perfused guinea pig hearts

In conscious "EXE" animals the endurance training program resulted in significantly lengthened RR intervals indicating training-induced bradycardia (Fig. 6A). However, in contrast with the *in vivo* data, after the denervation of the autonomic nervous system during *ex vivo* Langendorff experiments, the RR intervals did not differ significantly between the groups (Fig. 6B). These outcomes together support the impact of increased vagal tone on training-induced resting bradycardia in conscious "EXE" guinea pigs.

Various beat-to-beat variability parameters, including the root mean square of the successive differences (rmsSD) and the standard deviation of successive differences (sdSD) of the RR intervals, significantly increased by the end of the training protocol in conscious "EXE" guinea pigs compared to the "SED" animals (Fig. 6C and 6D, respectively). These outcomes further support the hypothesis of a notable increase in parasympathetic tone due to long-term endurance training in this model.

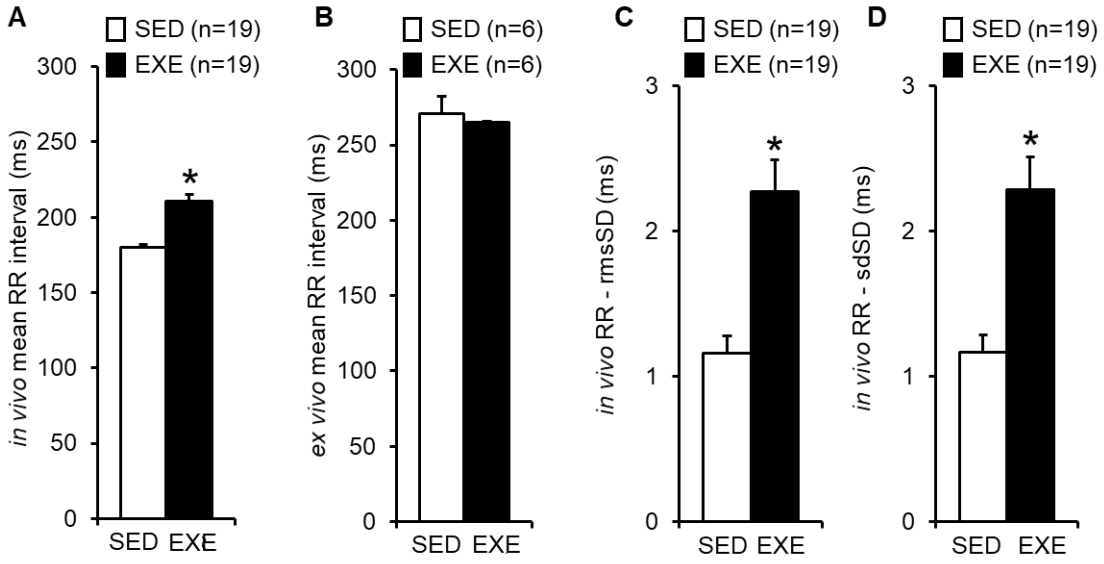

Figure 6. The impact of long-term endurance training on RR intervals and its variability parameters in *in vivo* and in *ex vivo* studies

The RR intervals in conscious guinea pigs at the end of the training program (A) and in *ex vivo* Langendorff experiments (B). The *in vivo* RR variability parameters in conscious guinea pigs: rmsSD, root mean square of successive differences (C); sdSD, the standard deviation of successive differences (D). All values were derived and calculated from 60 consecutive ventricular complexes during sinus rhythm by the end of the training protocol. EXE, exercised group; SED, sedentary group. All values are means ± SEM. *$p < 0.05$, unpaired t-test; "EXE" vs. "SED" guinea pigs.

4.2.4 The effect of long-term endurance training on ECG parameters and their variability parameters

The ECG recordings at the 15th week in conscious animals revealed no significant difference in the PQ interval between the examined groups ("EXE" vs. "SED": 55.0 ± 1.5 vs 51. 9 ± 1.2 ms, $p > 0.05$); however, the QRS interval significantly widened in the "EXE" group ("EXE" vs. "SED": 51.8 ± 1.5 vs. 45.6 ± 1.0 ms*, $p < 0.05$). Contrarily, the lengths of PQ and QRS intervals did not differ significantly between the groups in *ex vivo* Langendorff experiments. (PQ: "EXE" vs. "SED": 54.0 ± 2.0 vs. 59.4 ± 2.3 ms, $p > 0.05$, QRS: "EXE" vs. "SED": 30.9 ± 1.02 vs. 29.7 ± 1.2 ms, $p > 0.05$).

The 15-week-long training program led to several changes in the repolarization and its variability parameters in conscious animals. At the end of the training protocol, the QT interval was significantly prolonged in the "EXE" group compared to the "SED" group (Fig. 7A). Since the heart rate influences the length of the QT interval, the heart rate corrected QT interval (QTc) was calculated as described above (see detail in Chapter 3.2.3). The QTc of conscious "EXE" animals was significantly longer compared to the untrained animals at the end of the training protocol (Fig. 7B). The short-term variability of the QT intervals (STV-QT) seemed elevated in the "EXE" group; however, it did not reach statistical significance (Fig. 7C).

Additionally, an increased tendency was observed in other beat-to-beat variability parameters of repolarization in "EXE" animals (including long-term variability (LTV), long-term instability (LTI), instability (I)), but none reached a statistically significant difference (LTV- QT: "EXE" vs. "SED": 3.2 ± 0.2 vs. 2.7 ± 0.2 ms, $p > 0.05$, LTI-QT: "EXE" vs. "SED": 2.8 ± 0.2 vs. 2.4 ± 0.2 ms, $p > 0.05$, I-QT: "EXE" vs. "SED": 4.8 ± 0.3 vs. 4.3 ± 0.3 ms, $p > 0.05$).

Similar to the unchanged RR intervals, the duration of QT intervals did not differ between the groups in *ex vivo* Langendorff experiments ("EXE" vs. "SED" 133.1 ± 2.2 vs. 131.7 ± 2.6 ms, $p > 0.05$).

Cardiac arrhythmias were not detected during in *in vivo* ECG studies in either group. Although a few cardiac arrhythmias developed in both groups during *ex vivo* Langendorff experiments, there were no differences in the number and complexity of these arrhythmias between the groups (data not shown).

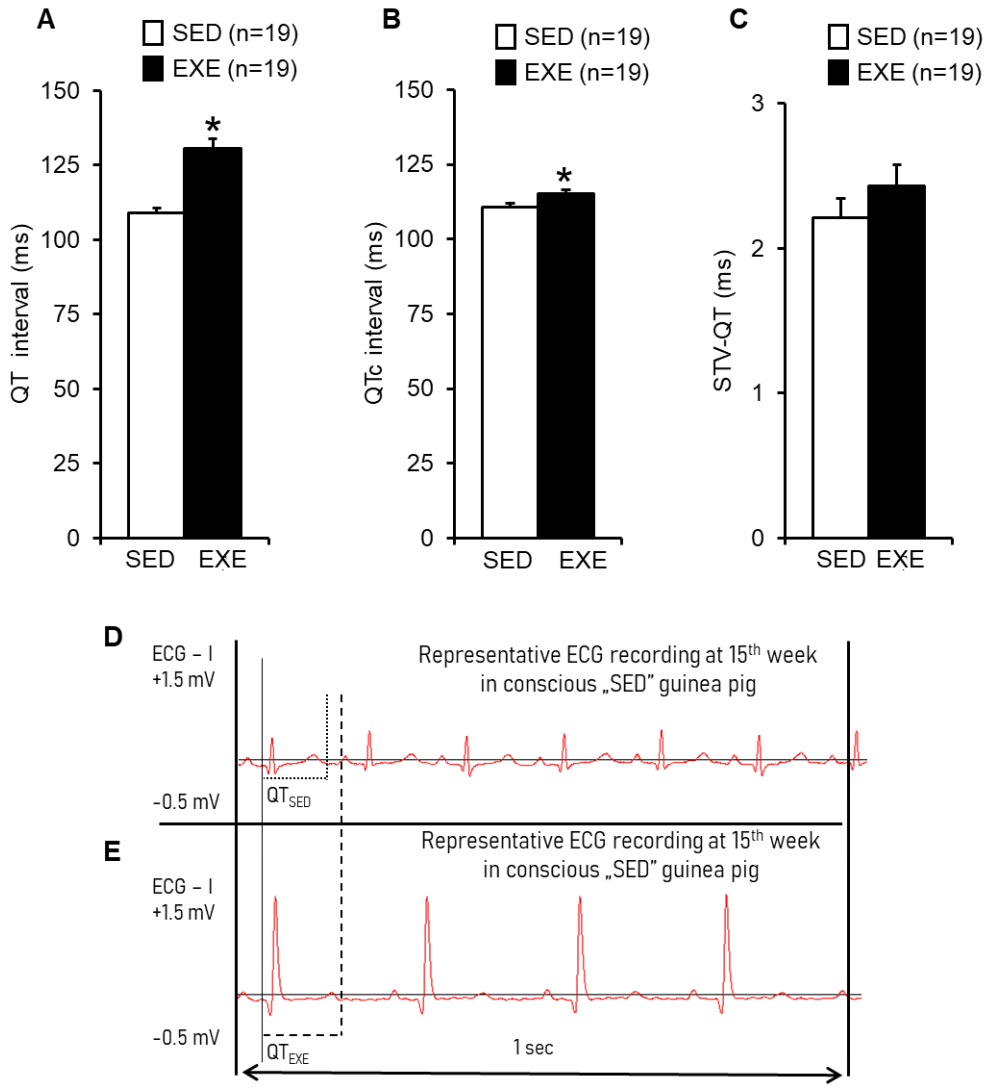

Figure 7. Effect of long-term endurance training on the ECG QT interval and its beat-to-beat variability parameters as markers of repolarization inhomogeneity
The QT interval (A), the heart rate corrected QT interval (QTc) (B), and the short-term variability of QT interval (STV-QT) (C) of the ECG in conscious guinea pigs at the end of the training protocol. All values were derived and calculated from 40 consecutive ventricular complexes during sinus rhythm. Representative images illustrate the length of the QT interval in conscious sedentary (D) and exercised (E) guinea pigs at the end of the several-week-long training program. EXE, exercised group; SED, sedentary group. All values are means ± SEM. *$p < 0.05$, unpaired t-test; "EXE" vs. "SED" guinea pigs.

4.2.5 Electrophysiological findings at the cellular level following long-term endurance training

Under the current exercise training protocol and experimental measuring conditions, magnitudes of the slow component of delayed rectifier potassium current (I_{Ks}) (Fig. 8D), the late sodium current (I_{NaL}) (Fig. 8E), and the sodium-calcium exchanger (I_{NCX}) (Fig. 8F) in native guinea pig left ventricular myocytes showed no significant differences between the groups.

In agreement with the patch clamp data, there was no significant difference in the length of action potential duration measured at 90% repolarization (APD_{90}) in myocytes isolated from the left ventricle of the exercised group compared to the sedentary group (Fig. 8B). The short-term variability of action potential duration (STV-APD) did not differ significantly between the groups (Fig. 8C).

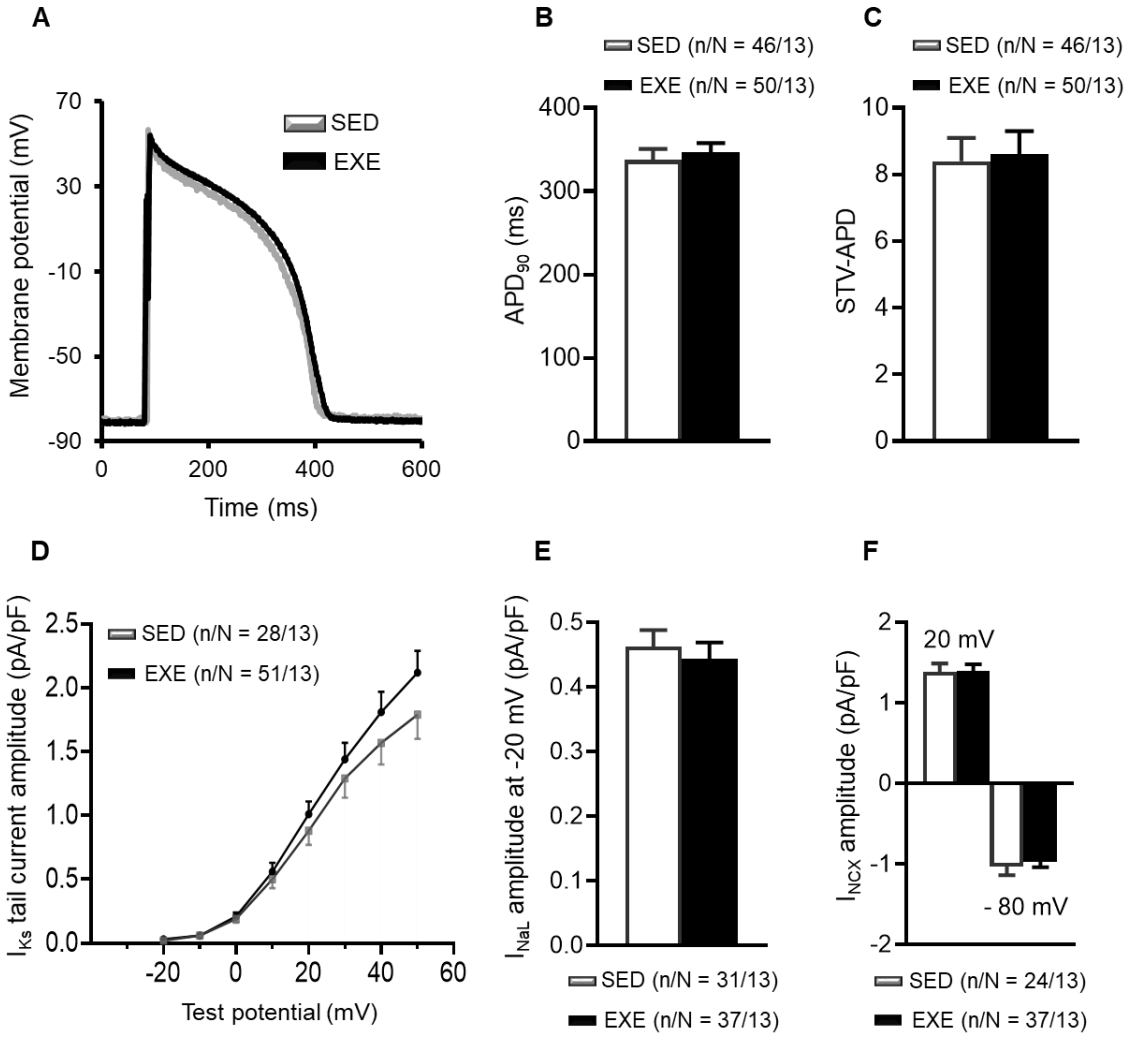

Figure 8. Effects of long-term sustained training on cardiac action potential duration, its short-term variability, and transmembrane ionic currents in left ventricular myocytes
Fig. 8A illustrates the representative action potential curves recorded from isolated left ventricular myocytes of sedentary and exercised guinea pigs. Fig. 8B shows the action potential duration (APD) measured at 90% repolarization (APD_{90}) in enzymatically isolated left ventricular single myocytes of sedentary and exercised animals. Fig. 8C shows the short-term variability of action potential duration (STV-APD) of a single left ventricular myocyte of sedentary and exercised guinea pigs. The lower panels demonstrate the effects of long-term endurance training on different transmembrane ionic currents: the current-voltage curve shows the amplitude of I_{Ks} (D), bar charts indicate the late Na^+ current (I_{NaL}) (E), and the Na^+/Ca^{2+} exchange current (I_{NCX}) (F). The term "n" represents the number of experiments and the term "N" refers to the number of animals. EXE, exercised group; SED, sedentary group. All values are means ± SEM. *$p < 0.05$, unpaired t-test; "EXE" vs. "SED" guinea pigs.

4.3 Investigating the electrophysiological effects of cannabidiol on repolarizing transmembrane potassium currents

4.3.1 Effects of cannabidiol on rapid delayed rectifier potassium current in native rabbit left ventricular myocytes

The possible effect of CBD on the rapid delayed rectifier potassium current (I_{Kr}) was examined in enzymatically isolated left ventricular myocytes from a rabbit heart at 37 °C. The following rectangular voltage pulse protocol was used for whole-cell patch clamp measurements: the holding potential at – 80 mV was followed by a 25 ms long pre-pulse at – 40 mV for inactivating the fast sodium current. The I_{Kr} was activated by one-second-long depolarizing voltage pulses with 0.05 Hz pulse frequency. The depolarizing test potentials ranged from – 30 mV to + 50 mV, after which, the cell was repolarized to – 40 mV. The deactivating tail current at – 40 mV was evaluated as I_{Kr} tail current. To understand the drug response in detail, different concentrations of CBD were used.

The whole-cell patch clamp studies showed significant inhibition of I_{Kr} after 3–5 minutes of acute drug superfusion. As Fig. 9A indicates, already the experiments with 1 μM CBD clearly show an inhibition of I_{Kr} in native rabbit left ventricular myocytes. The subsequent current- voltage curves show that greater inhibitions were observed after applying higher concentrations of CBD, namely 2.5, 5, and 10 μM CBD (Fig. 9B, C, D). While there was a slighter inhibition of I_{Kr} following the application of 1 μM CBD (Fig. 9A), the I_{Kr} tail was significantly depressed by the acute superfusion of the highest CBD concentration (10 μM) (Fig. 9D). These results support the concentration-dependent inhibition on I_{Kr} by CBD.

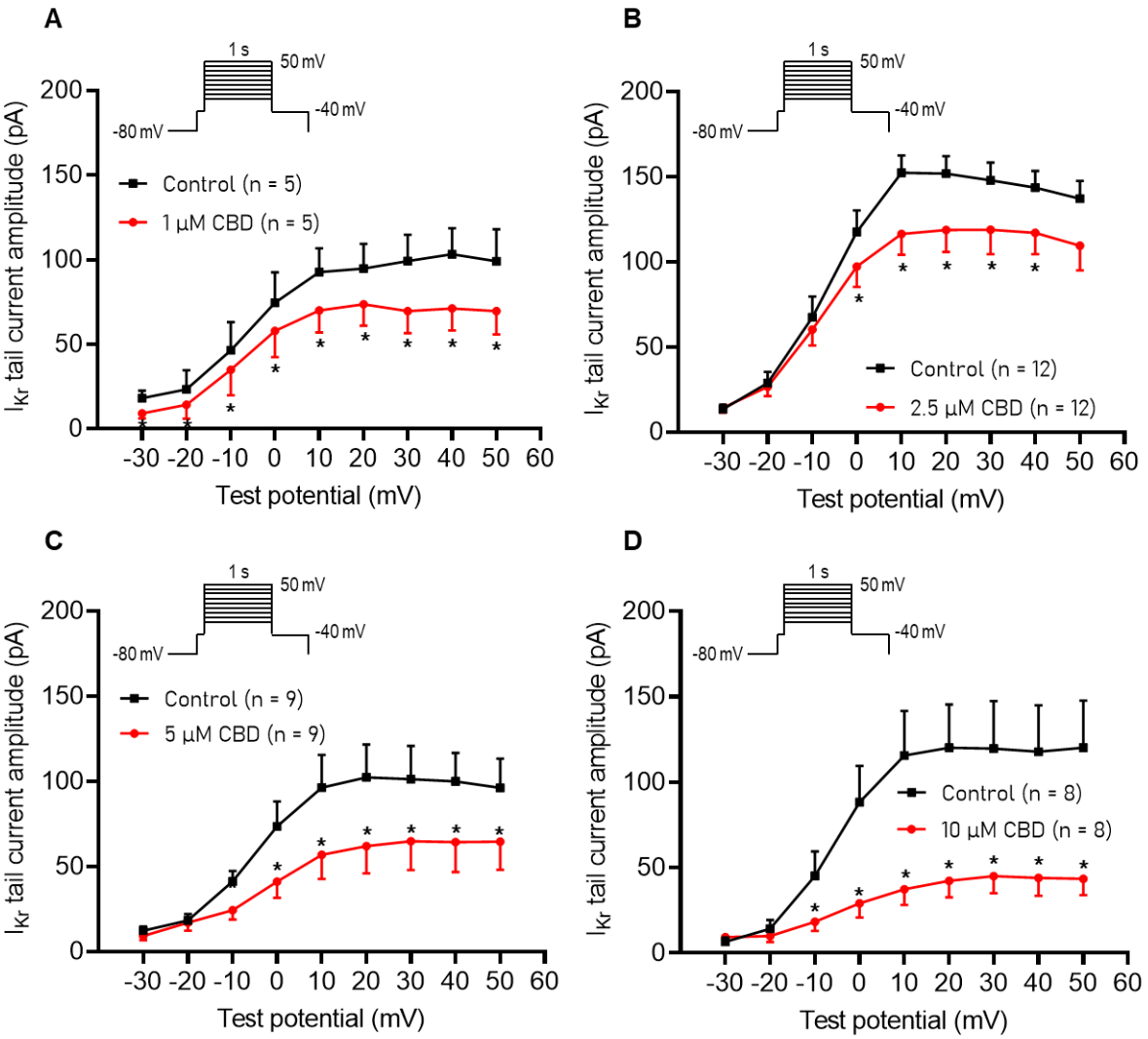

Figure 9. Effect of CBD on the rapid delayed rectifier potassium current (I_{Kr}) in native rabbit ventricular myocytes at 37 °C
Current-voltage curves show the inhibition of I_{Kr} under control conditions and after the application of 1 µM (A), 2.5 µM (B), 5 µM (C), and 10 µM (D) CBD. Insets indicate the used voltage rectangular protocols. The I_{Kr} deactivating tail current was measured at -40 mV. The term "n" represents the number of experiments. All values are means ± SEM. *p < 0.05, ANOVA for repeated measurements.

After the experiments were conducted with several different concentrations, the half-maximal effective concentration (EC_{50}) was estimated to promote greater understanding. To determine this value, enzymatically isolated left ventricular myocytes were depolarized to + 20 mV for one-second-long followed by a test pulse at – 40 mV, during which the I_{Kr} deactivating tail current was measured. The cycle length was 20 s. The concentration-dependent patch clamp studies revealed an estimated EC_{50} value of 4.9 µM (Fig. 10).

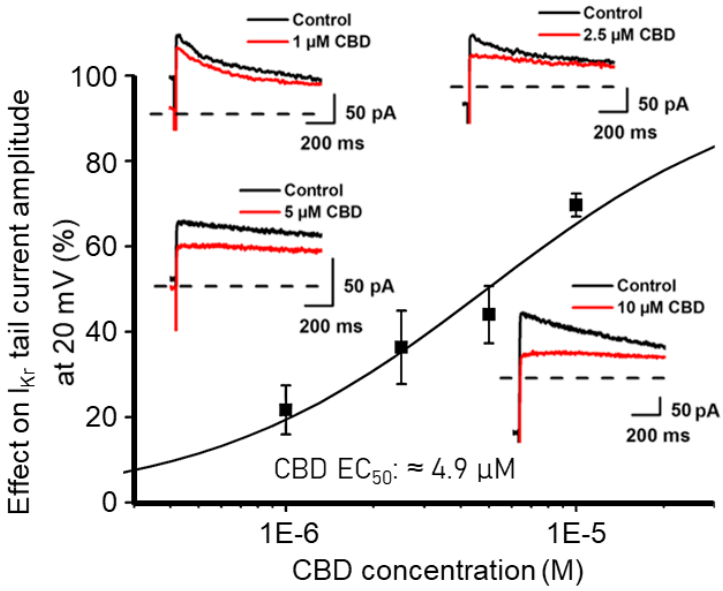

Figure 10. Examination of the inhibitory effect of CBD on the rapid delayed rectifier potassium current (I_{Kr}) in native rabbit left ventricular myocytes
The concentration-response curve indicates an estimated half-maximal effective concentration value (EC_{50}) of 4.9 μM CBD for I_{Kr}. Insets indicate the tail current section of the original I_{Kr} current under control conditions and in the presence of 1 μM, 2.5 μM, 5 μM, and 10 μM CBD. The dashed lines of the inset representative images refer to the baseline for the I_{Kr} tail current level after the test pulse at -40 mV. All values are means ± SEM.

4.3.2 Investigating the inhibitory effect of cannabidiol on slow delayed rectifier potassium current in native rabbit left ventricular myocytes

The inhibitory effect of CBD on the slow component of delayed rectifier potassium current (I_{Ks}) was examined under rectangular voltage pulse command: the holding potential at – 80 mV, with a short pre-pulse at – 40 mV for eliminating the fast sodium current which was followed by five- second-long depolarizing voltage pulses ranging from – 30 mV to + 50 mV, with a pulse frequency of 0.1 Hz. Thereafter the I_{Ks} tail current amplitude was measured at – 40 mV. The patch clamp studies revealed that CBD depressed the amplitude of I_{Ks} in native rabbit left ventricular myocytes. As shown by the inset representative section of the original I_{Ks} tail current in Fig. 12 and the current-voltage curve in Fig. 11A, acute superfusion of 1 μM CBD resulted in a significantly decreased tail current amplitude. The subsequent current-voltage curves illustrate that the inhibition increased with higher CBD concentrations. A significant reduction was observed after the acute superfusion of 2.5 μM CBD (Fig. 11B), which concentration is close to the estimated EC_{50} value (Fig. 12). The current amplitude decreased further after acute superfusion of 5 μM CBD (Fig. 11C), additionally, the I_{Ks} tail current seemingly vanished after

application of 10 µM CBD (Fig. 11D). On this basis, CBD depressed the I_{Ks} tail current amplitude in a concentration-dependent manner.

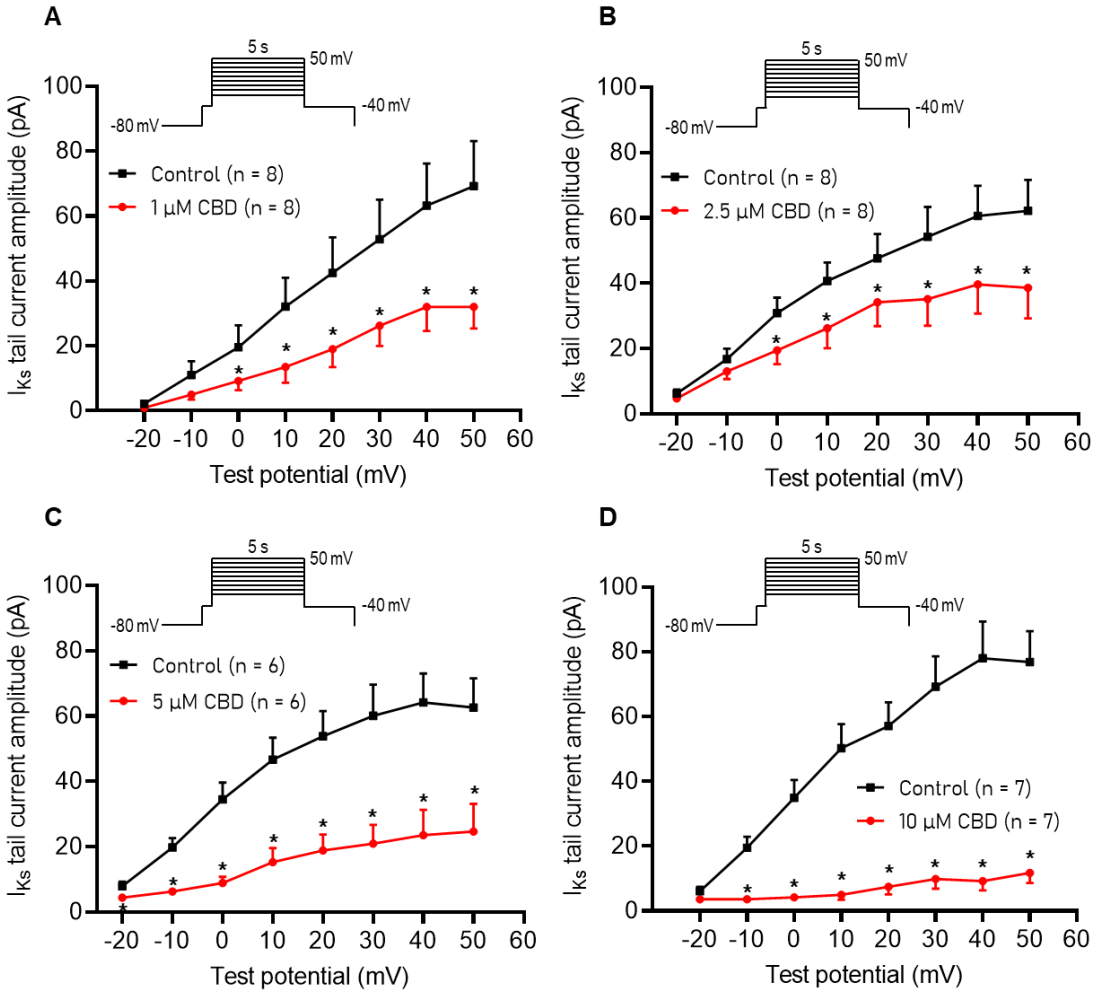

Figure 11. Effect of CBD on the slow delayed rectifier potassium current (I_{Ks}) in native rabbit ventricular myocytes at 37 °C
Current-voltage curves show the inhibition of I_{Ks} under control conditions and after the application of 1 µM (A), 2.5 µM (B), 5 µM (C), and 10 µM (D) CBD. Insets indicate the used voltage rectangular protocols. I_{Ks} tail current amplitude was measured at – 40 mV. The term "n" refers to the number of experiments. All values are means ± SEM. *p < 0.05, ANOVA for repeated measurements.

Following the determination of the inhibitory effects of various CBD concentrations, the EC_{50} value was estimated. As shown in Fig. 12, the concentration-response curve indicated an estimated EC_{50} value of 3.1 µM, after a five-second-long + 20 mV depolarizing test pulse measured at – 40 mV with a pulsing cycle length of 10 s. The inserted original I_{Ks} tail current records clearly illustrate the inhibitory potential of each CBD concentration used.

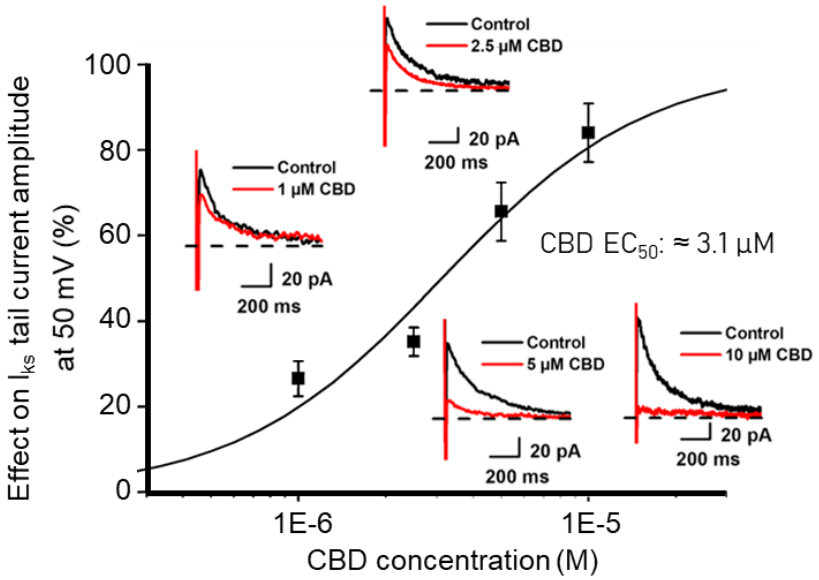

Figure 12. Examination of the inhibitory effect of CBD on the slow delayed rectifier potassium current (I_{Ks}) in native rabbit left ventricular myocytes
The concentration-response curve indicates an estimated half-maximal effective concentration value (EC_{50}) of 3.1 µM CBD for I_{Ks}. Insets indicate the tail current section of the original I_{Ks} current under control conditions and in the presence of 1 µM, 2.5 µM, 5 µM, and 10 µM CBD. The dashed lines of the inset representative images refer to the baseline for the I_{Ks} tail current level after the test pulse at -40 mV. All values are means ± SEM.

4.3.3 Examination of the cannabidiol-induced changes on transient outward potassium current and inward rectifier potassium current in native canine and rabbit left ventricular myocytes

The impact of CBD on the transient outward potassium current (I_{to}) was studied under the following rectangular voltage pulse command: the – 90 mV holding potential was followed by a 300 ms long depolarizing test pulse where the I_{to} sharply activated. The depolarizing voltage pulses raised from the holding potential to – 20 mV, gradually increasing by 10 mV up to + 50 mV with a pulsing cycle length of 3 s.

The whole-cell patch clamp experiments revealed that the I_{to} amplitude in enzymatically isolated canine left ventricular myocytes was significantly reduced by CBD (Fig. 13A). However, no change in the current amplitude of native rabbit left ventricular myocytes was detected even in the presence of 10 µM CBD (Fig. 13B). As shown in Fig. 13C, various CBD concentrations were applied in isolated canine left ventricular myocytes to estimate the EC_{50} value, including 1 µM, 2.5 µM, 5 µM, and 10 µM. As shown by the inset representative section of the original I_{to} record in Fig. 13C and the current-voltage curve in Fig. 13A, the I_{to} current amplitude was significantly depressed by 5 µM CBD, aligning closely with the

estimated EC_{50} value. To exclude the influence of DMSO, a solvent control experiment was performed. As the inset representative image shows in Fig. 13C, the latter experiment design revealed that 0.01 % DMSO had no effect on I_{to}.

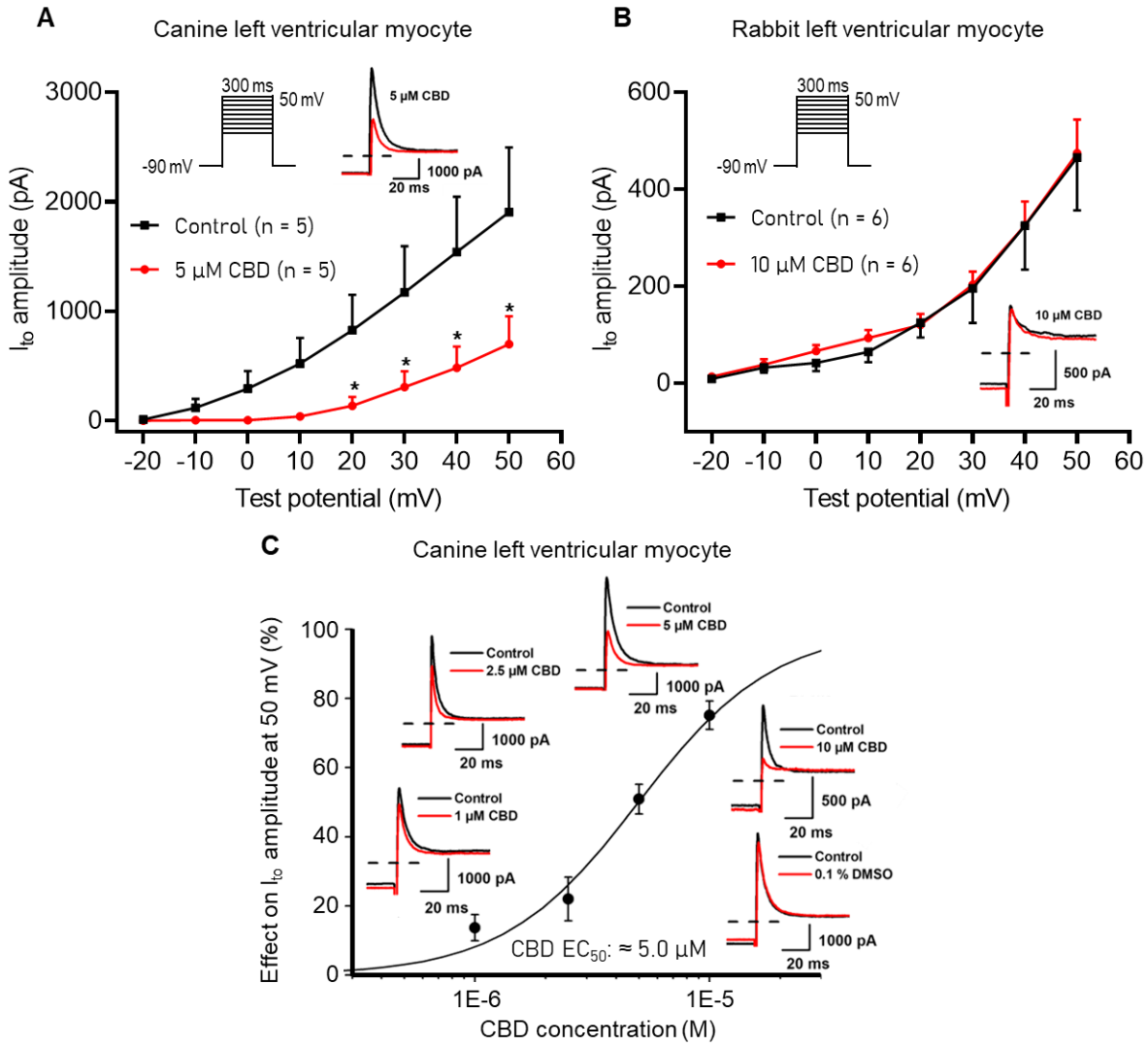

Figure 13. Effect of CBD on transient outward potassium current (I_{to}) in native canine and rabbit left ventricular myocytes at 37 °C

Current-voltage curves show the inhibition of I_{to} under control conditions and after the application of 5 µM and 10 µM CBD in canine (A) and rabbit (B) left ventricular myocytes, respectively. Insets indicate the voltage protocols and sections of original I_{to} records in control and in the presence of CBD. The concentration-response curves indicate an estimated half-maximal effective concentration value (EC_{50}) of 5.0 µM CBD (C). In Fig. 12C, insets indicate sections of the original I_{to} current under control conditions and in the presence of 1 µM, 2.5 µM, 5 µM, 10 µM CBD, and 0.01 % DMSO. These representative images were recorded from canine left ventricular myocytes after a 300 ms long pulse to 50 mV test potential with a pulsing cycle length of 3 s. The term "n" refers to the number of experiments. All values are means ± SEM. *$p < 0.05$, ANOVA for repeated measurements.

As Fig. 14 presents, CBD had no impact on the inward rectifier potassium current (I_{K1}): for instance, even the highest applied concentration (10 μM) did not show a significant change on I_{K1} in native rabbit left ventricular myocytes. I_{K1} was measured as a steady-state current at the end of the 400 ms pulses from - 90 mV to 0 mV with a pulse frequency of 0.33 Hz. The holding potential was – 90 mV.

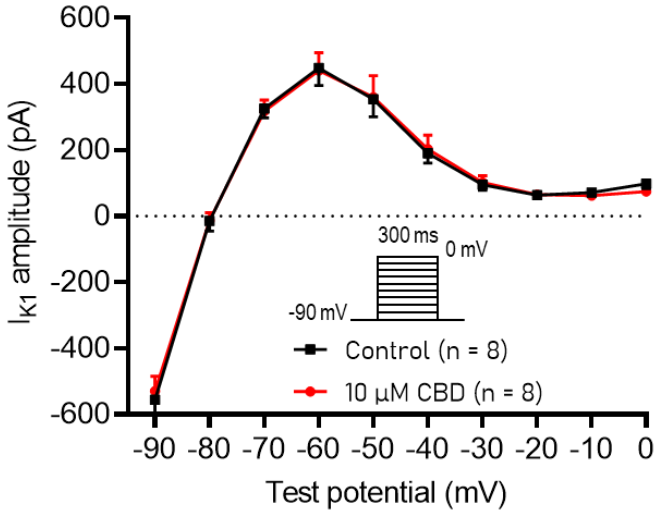

Figure 14. Lack of CBD effect on inward rectifier potassium current (I_{K1}) in native rabbit ventricular myocytes at 37 °C
The steady-state current of voltage curves of I_{K1} in control conditions and after the application of 10 μM CBD. Inset indicates the used rectangular voltage protocols. Data expressed as means ± SEM. $p > 0.05$, ANOVA for repeated measurements.

4.4 Investigating the electrophysiological effects of cannabidiol on different inward transmembrane ionic currents

4.4.1 Effects of cannabidiol on L-type calcium current in native rabbit left ventricular myocytes

The potential effects of CBD were also studied on the L-type calcium current (I_{CaL}) in enzymatically isolated left ventricular myocytes. For the imitation of slower and faster heart rates at the cellular level, two voltage protocols with different cycle lengths were used to measure the I_{CaL}: 1) after – 80 mV holding potential and short prepulse at – 40 mV, serving the inactivation of I_{Na}, the I_{CaL} was evoked by 400 ms long depolarizing voltage pulse to various test pulses ranging from – 35 mV to + 55 mV with a 5000 ms long cycle length, 2) another voltage protocol was similar to the latter one but with 300 ms long depolarizing voltage pulse and 500 ms long cycle length.

As current-voltage curves indicate, 10 µM CBD markedly reduced the amplitude of I_{CaL} in a frequency-dependent manner (Fig. 15A, 15C). The current amplitude was significantly depressed under both longer and shorter cycle lengths as well. As the representative original I_{CaL} traces indicate, 10 µM CBD markedly reduced the amplitude of the current at 0 mV test potential (Fig. 15B, 15D).

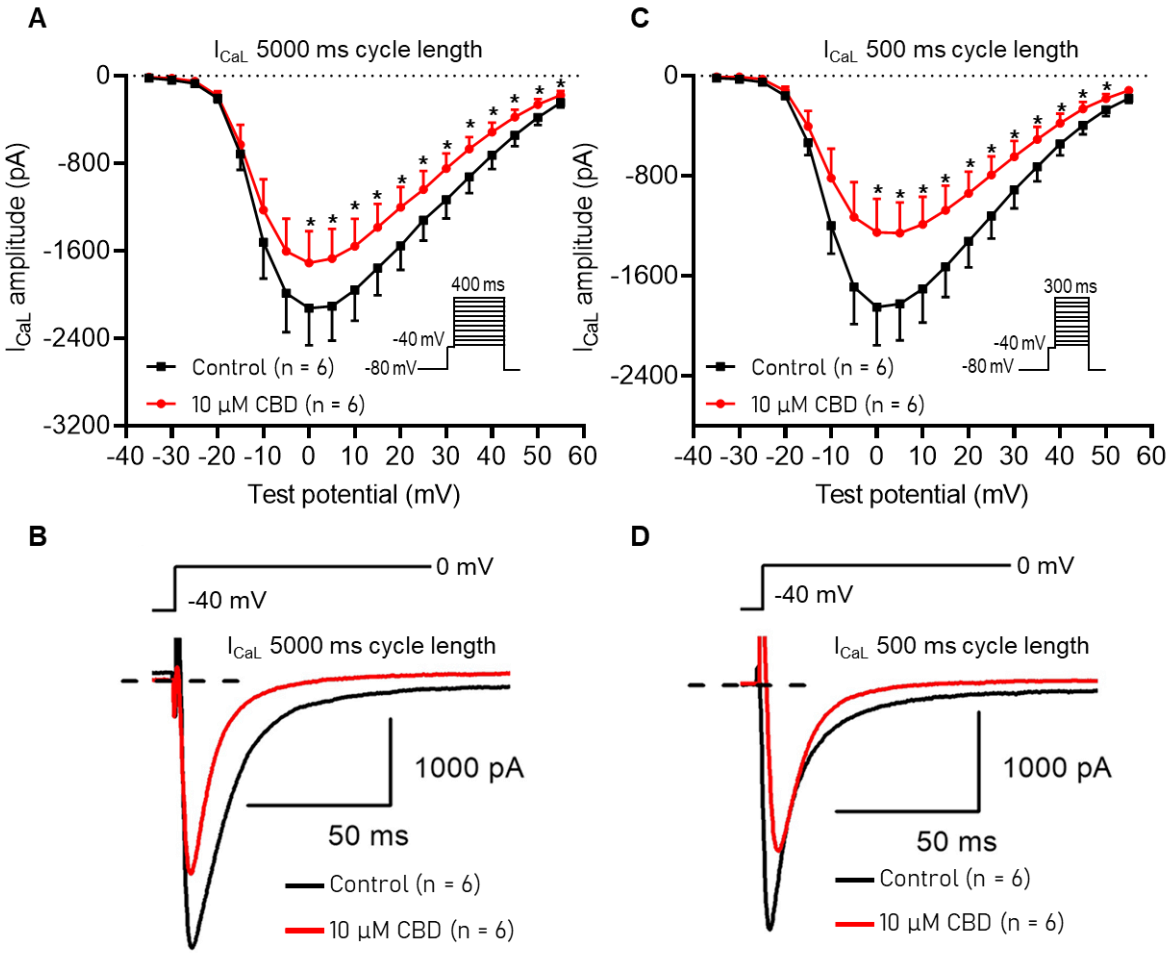

Figure 15. Effect of CBD on the L-type calcium current (I_{CaL}) in native rabbit ventricular myocytes at 37 °C

The current-voltage curves indicate the inhibition of 10 µM CBD on I_{CaL} at 5000 ms (A) and 500 ms (C) cycle lengths. Insets indicate the used voltage rectangular protocols. Representative I_{CaL} current traces were recorded under control conditions and in the presence of 10 µM CBD at 5000 ms (B) and 500 ms (D) cycle lengths at 0 mV test potential. The "n" refers to the number of experiments. All values are means ± SEM. *$p < 0.05$, ANOVA for repeated measurements.

4.4.2 Effects of cannabidiol on late sodium current in native rabbit left ventricular myocytes

The potential effect of CBD was studied on late sodium current (I_{NaL}) in native rabbit left ventricular myocytes as well. The current was activated by raising the depolarizing pulses to – 20 mV from a holding potential of – 120 mV, and the current amplitude was measured at 50 ms.

The application of 10 µM CBD led to a significant reduction of the I_{NaL} at – 20 mV. I_{NaL} was defined as a TTX-sensitive current by subtracting current traces recorded in the presence of 20 µM TTX from traces of control and 10 µM CBD recordings (Fig. 16A).

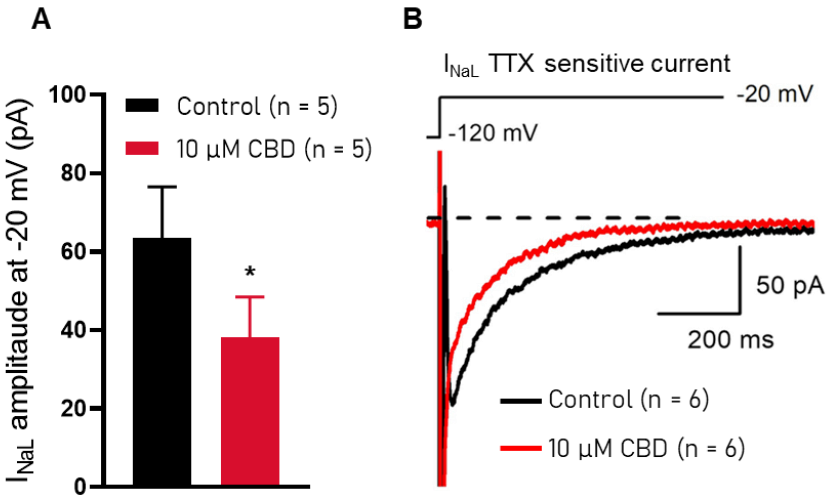

Figure 16. Effect of CBD on the late sodium current (I_{NaL}) in native rabbit ventricular myocytes at 37 °C

The bar diagram of 10 µM CBD induced inhibition on I_{NaL} (A) and representative original record of TTX-sensitive current (I_{NaL}) traces at - 20 mV (B). The "n" refers to the number of experiments. All values are means ± SEM. *$p < 0.05$, ANOVA for repeated measurements.

4.5 Investigating the electrophysiological effects of ibuprofen on transmembrane ionic currents

4.5.1 Effects of ibuprofen on transient outward potassium current and inward rectifier potassium current in native canine left ventricular myocytes

Previously described rectangular voltage protocols and experimental settings were used to study the impacts of ibuprofen on I_{to} and I_{K1} in enzymatically isolated left ventricular myocytes of the canine heart. As voltage-current curves show, the amplitude of I_{to} slightly but significantly reduced after the acute superfusion of 250 µM ibuprofen. To exclude the influence of DMSO,

a solvent control experiment was performed. Based on our findings, 0.01 % DMSO did not affect I_{to} (Fig. 17A).

As the steady-state current-voltage curves indicate, the I_{K1} remained unchanged after the application of both the solvent and 250 µM ibuprofen (Fig. 17B).

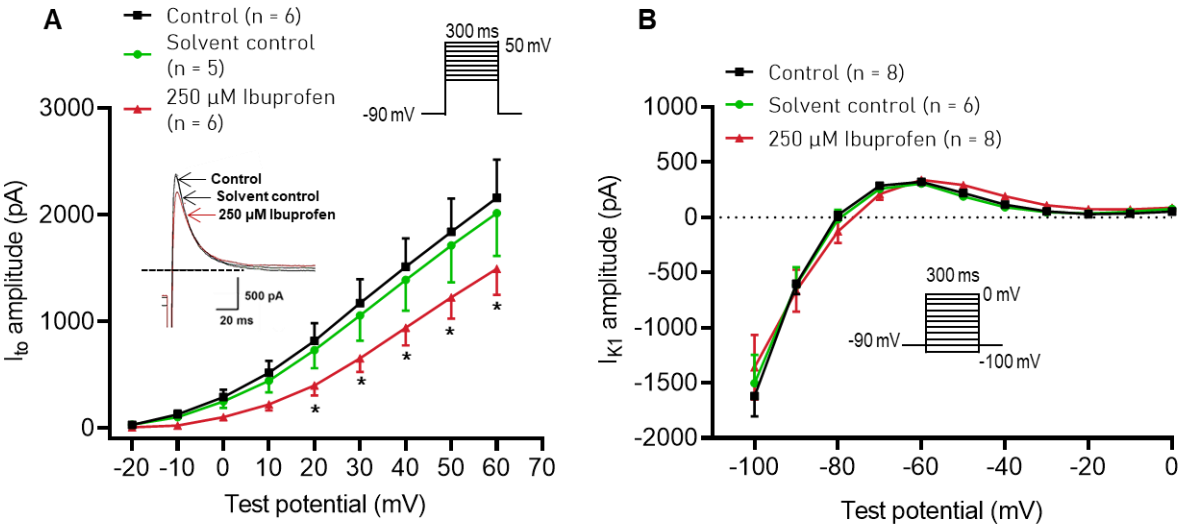

Figure 17. Effect of ibuprofen on the transient outward potassium current (I_{to}) and the inward rectifier potassium current (I_{K1}) in native canine left ventricular myocytes at 37 C
Current-voltage curves show the inhibition of I_{to} under control conditions and after the application of 0.01 % DMSO and 250 µM ibuprofen (A). In Fig. 16A, the inset shows the inhibitory effect of 250 µM ibuprofen in the section of the original I_{to} current record. In Fig. 16B, the steady-state current of voltage curves of I_{K1} in control conditions and after the application of 0.01 % DMSO and 250 µM ibuprofen. Insets indicate the used voltage rectangular protocols. The "n" refers to the number of experiments. All values are means ± SEM. *p < 0.05, ANOVA for repeated measurements.

4.5.2 Effects of ibuprofen on the L-type calcium current and the late sodium current in native canine left ventricular myocytes

The previously detailed voltage protocol with a cycle length of 5000 ms was used to measure I_{CaL} in enzymatically isolated canine left ventricular myocytes. As shown by the voltage-current curve, the 0.01 % DMSO did not change the amplitude of the current. However, 250 µM ibuprofen reduced the I_{CaL} moderately but significantly (Fig. 18A). As the representative original I_{CaL} traces show, the amplitude of I_{CaL} returned to baseline levels after an approximately ten-minute-long drug washout period (Fig. 18B).

In addition, I_{NaL} was also affected by 250 µM ibuprofen under the rectangular protocol described above. The current amplitude was moderately but significantly reduced at – 20 mV (Fig. 18C). No effect of the 0.01 % DMSO application was observed on I_{NaL} (Fig. 18C).

As previously mentioned, the current was defined as TTX-sensitive current by subtracting current traces recorded in the presence of 20 µM TTX from traces of control, DMSO, and ibuprofen recordings.

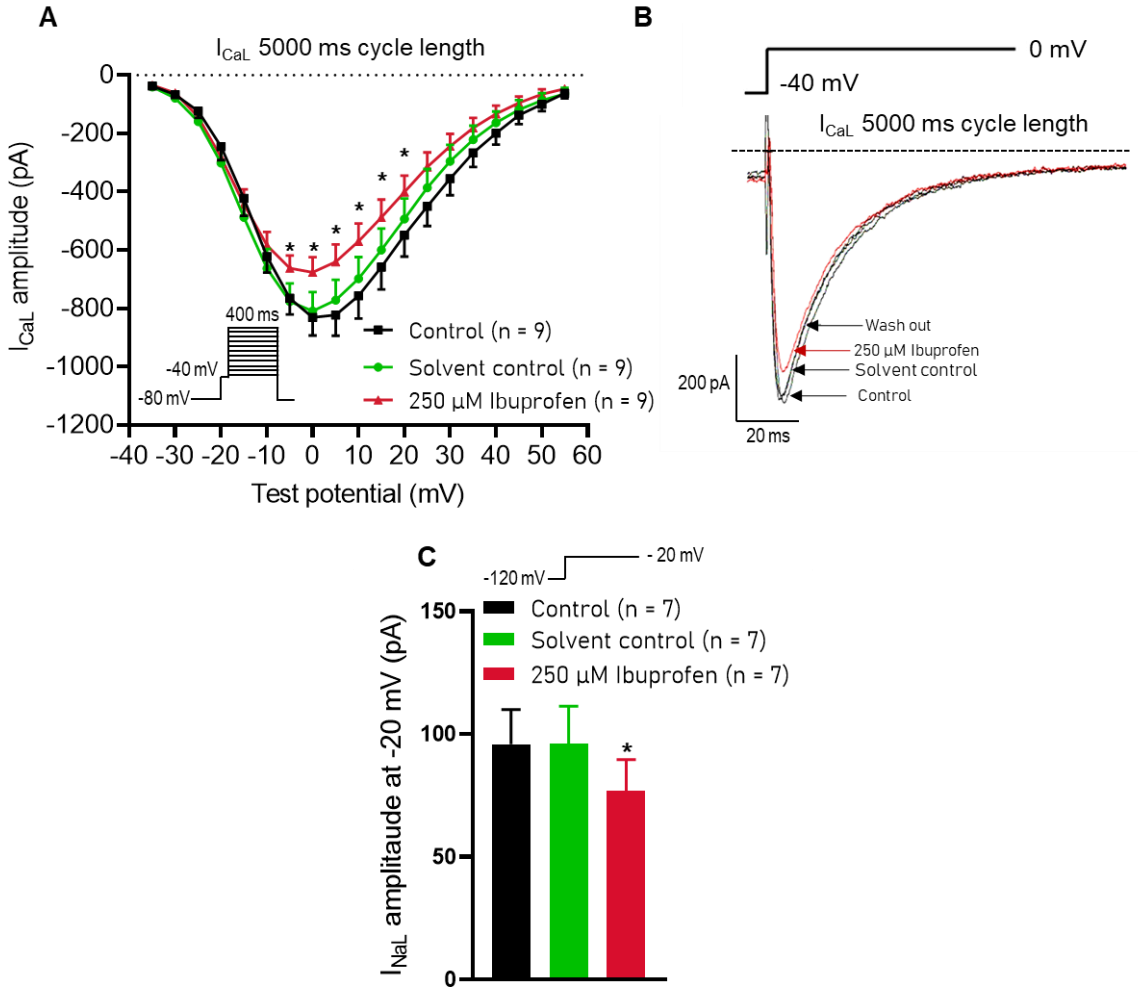

Figure 18. Effect of ibuprofen on L-type calcium current (I_{CaL}) and late sodium current (I_{NaL}) in native canine ventricular myocytes at 37 °C

The current-voltage curve indicates the inhibitory effects of 250 µM ibuprofen and 0.01 % solvent DMSO on I_{CaL} with a cycle length of 5000 ms (A). The representative I_{CaL} current traces were recorded under control conditions and in the presence of 0.01 % DMSO and 250 µM ibuprofen, as well as after the washout period, at 5000 ms cycle length at 0 mV test potential (B). The bar chart in Fig. 17C illustrates the absence of effect from 0.01 % DMSO and the inhibitory effect of 250 µM ibuprofen on I_{NaL}. The I_{NaL} was defined as TTX-sensitive current by subtracting current traces recorded in the presence of 20 µM TTX from traces of control, DMSO, and ibuprofen recordings. Insets indicate the used voltage protocols. Values are measured at - 20 mV. The "n" refers to the number of experiments. All values are means ± SEM. *p < 0.05, ANOVA for repeated measurements.

5 DISCUSSION

The main goals of my thesis were the attempt to investigate possible changes of the repolarization reserve in certain situations like chronic endurance training-induced cardiac remodeling and to identify the cannabidiol (CBD) and ibuprofen treatment-evoked cellular cardiac electrophysiological alterations, since these certain situations may be associated with a higher risk of the development of cardiac arrhythmias.

5.1 Considerations for the appropriate choice of experimental animal models for the human heart

Cardiac arrhythmias continue to be a major health burden worldwide, as they are one of the leading causes of mortality and morbidity, especially in patients with pre-existing cardiovascular diseases such as atherosclerosis, heart failure, or myocardial infarction. In particular, sudden cardiac death (SCD) secondary to cardiac arrhythmias is a leading cause of death in the Western World, accounting for up to 20 % of all natural deaths and up to 50 % of all cardiovascular deaths (Deo & Albert, 2012). Therefore, research into the underlying mechanisms is important for the development of novel preventive and therapeutic strategies. While human-induced pluripotent stem cell-derived cardiomyocytes offer several advantages, their use is limited due to their distinct cellular electrophysiological properties compared to mature adult myocytes (Karbassi et al., 2020; Lundy et al., 2013) Therefore, animal studies remain prominent in understanding the mechanisms of cardiac arrhythmias, developing and testing drugs, and exploring various treatment strategies in cardiac electrophysiology at both the atrial and ventricular levels (Odening et al., 2021).

The proper choice of an animal model depends mainly on the investigated research question and the nature of arrhythmia. Rodents are widely used laboratory animals for their advantages, such as low maintenance costs, ease of housing, breeding, and handling (Milani-Nejad & Janssen, 2014). However, rodents present substantial differences from the cardiac electrophysiological features of the human heart, including heart rate, transmembrane ionic currents, and autonomic regulation. The high heart rate, especially of small rodents, leads to faster systolic and diastolic phases of the heart muscle to maintain proper cardiac output (Janssen & Periasamy, 2007). Consequently, the ventricular action potential duration (APD), a short repolarization phase, and the absence of a distinct plateau phase are present at the cellular level (Farraj et al., 2011). Not surprisingly, many of the potassium currents during repolarization in mice and rats differ markedly from those in humans.

The heart rate of larger laboratory animals and humans is considerably lower than that of small rodents, such as mice and rats. Noteworthy, some electrophysiological characteristics of other laboratory animals, like dogs, rabbits, and guinea pigs, share similarities with the human heart. The left ventricular region of the canine heart has similar cellular electrophysiological properties to human hearts, with a similar transmembrane ionic profile, therefore, the canine model is an important platform in cardiac arrhythmia research (Odening et al., 2021). Consequently, it serves as a useful tool for determining the relevance of the arrhythmogenic mechanism of different drugs (Piktel & Wilson, 2019). It is important to note that in the field of cardiovascular research, the guinea pig and rabbit animal models offer the same economic benefits and large sample sizes similar to rats and mice but provide additional advantages. Besides the heart rate is lower than in mice and rats, the characteristic of QT interval and action potential (AP) are similar to larger laboratory animals such as dogs (Baczko et al., 2016; Nanasi et al., 2021). Therefore, comparable to the canine model, rabbits and guinea pigs are often employed as 'drug-induced long-QT' models in safety pharmacology and toxicology research (Odening et al., 2021). Although, it should be noted that the transient outward potassium current (I_{to}) in native left ventricular myocytes of guinea pig and rabbit hearts is distinct from those of dogs and humans (Odening et al., 2021).

Overall, the cardiac electrophysiological characteristics of canine, rabbit, and guinea pig animal models enable a more relevant approximation of human cardiac electrophysiology in experimental arrhythmia research.

5.2 The impact of endurance training-induced cardiac remodeling in a small animal athlete's heart model

5.2.1 Long-term endurance training-induced structural changes

In our small animal training model, we aimed to characterize the chronic endurance training- induced structural cardiac changes. The main structural change involved the dilation and enlargement of the left ventricular myocardium following long-term endurance training, this finding is consistent with the results of Polyak et al. in larger animal models (Polyak et al., 2018). However, similar to elite athletes, ejection fraction and fractional shortening remained unchanged in the exercised group compared to the sedentary animals (Pluim et al., 2000). Our structural and hemodynamic echocardiographic results correspond to the high dynamic demand training-induced cardiac adaptations among endurance athletes. Even though some of our measurements turned out to be not statistically significant, the observed overall trends could be valuable to understand the structural adaptations in the athlete's heart model and can facilitate

further investigations. The specific nature and frequency of each sporting activity fundamentally affect the exercise-induced physiological cardiac response and adaptation (Morganroth et al., 1975), therefore the validation of cardiac morphological changes through echocardiography was essential. Some investigators have reported that regular isotonic exercises related to endurance training (i.e., swimming, long-distance running, road cycling) commonly lead to cardiac enlargement (increased left ventricular cavity dimension), albeit obvious cardiac hypertrophy (increased left ventricular wall thickness) is not present in every case (D'Andrea et al., 2010; Mitchell et al., 2005; Morganroth et al., 1975).

Recently many studies have focused on the incidence and prevalence of myocardial fibrosis and its arrhythmogenic potency among athletes who engaged in intense endurance training. Since the development of cardiac fibrosis is not rare, our study attempted to assess the degree of fibrosis in exercised guinea pigs. Myocardial fibrosis, as a potential arrhythmia substrate, can contribute to the development of re-entry arrhythmias since the structural integrity of the heart is damaged (Nguyen et al., 2014). In a multicenter study, a higher prevalence of left ventricular scars were observed via high-sensitivity cardiac magnetic resonance imaging among 251 enrolled athletes with otherwise unremarkable clinical findings (Crescenzi et al., 2021). They raised the concern of a possible association between the presence of left ventricular fibrosis and apparently idiopathic ventricular arrhythmias in seemingly healthy athletes. Based on the “extreme exercise hypothesis”, repetitive and uninterrupted exposure to long-term vigorous exercise may increase the risk for the development of cardiac fibrosis (Eijsvogels et al., 2018). Since this type of structural alteration is strongly linked to the cumulative exercise dose, clinical follow-up of active veteran athletes is essential to reduce the risk of adverse cardiovascular outcomes (Eijsvogels et al., 2018; Wilson et al., 2011). Although we focused on the prolonged endurance training-induced left ventricular remodeling in our study, it is noteworthy that highly trained endurance athletes are prone to atrial fibrillation. Fibrotic changes within the atria may contribute to the occurrence of supraventricular arrhythmias (Peritz et al., 2020). Besides the human data, several training models conducted on large and small animals clearly documented the increased level of myocardial fibrosis after several weeks of training (Benito et al., 2011; Kui et al., 2021; Polyak et al., 2023).

Our histopathological findings align with the aforementioned studies: higher levels of cardiac fibrosis developed after chronic endurance training in the hearts of exercised guinea pigs compared to their sedentary counterparts. A significantly increased level of fibrosis was documented in the left and right atrial, septal, and right ventricular regions of the heart, additionally, a similar nearly significant trend was observed in the left ventricle. Since our

working hypothesis focused on electrophysiological alteration due to long-term vigorous training, we did not determine the biological markers or underlying causes of cardiac fibrosis. However, some studies have investigated this issue in depth among highly trained humans and in animals (Aschar-Sobbi et al., 2015; Benito et al., 2011; Kui et al., 2021; Lindsay & Dunn, 2007; Oh et al., 2020). Although this type of structural abnormality is undetectable in most cases under the generally used non-invasive methods, like echocardiography or electrocardiography, it may impact the development of re-entry cardiac arrhythmias. Therefore, myocardial fibrosis may predispose to potentially life-threatening cardiac arrhythmias, as an arrhythmia substrate.

5.2.2 Investigation of chronic endurance training-induced resting bradycardia and beat-to-beat heart rate variability parameters

Sinus resting bradycardia is considered to be a characteristic and well-recognizable electrophysiological hallmark of long-term high-intensity aerobic training among humans (Azevedo et al., 2014; Chapman, 1982; Jensen-Urstad et al., 1997), as well as in animal models of athlete's heart (D'Souza et al., 2014; Kui et al., 2021; Polyak et al., 2023). Our results well correlate with the literature, since the exercised guinea pigs developed significant resting bradycardia compared to the sedentary animals at the end of the training protocol.

Although resting bradycardia is a general finding, there is considerable debate about the underlying mechanism of training-induced resting bradycardia in recent years. Earlier studies suggested that resting bradycardia is a consequence of increased vagal activity (Jensen-Urstad et al., 1997; Macor et al., 1996). While other studies took a critical look at the exclusive role of enhanced parasympathetic tone in the development of training-induced resting bradycardia. They proposed that intense exercise induces morphological and electrical intrinsic remodeling of the sino-atrial node (SAN), which plays a crucial role in the development of resting bradycardia. According to this hypothesis, the role of vagal tone is most probably secondary, or non-existent (Boyett et al., 2013; Katona et al., 1982). In our previous study, we demonstrated that SAN remodeling occurred in the large animal model of the athlete's heart and presumably it has an important role in the observed decreased resting heart rate in conscious trained dogs (Polyak et al., 2023). However, our results in guinea pigs seem inconsistent with the latter perspective since no statistically significant difference was detected in spontaneous heart rate between the groups during *ex vivo* Langendorff experiments. Although we do not know the appropriate reason of the observed differences between our results and other studies, there are some possibilities that can account for this observation. Firstly, species-dependent

differences cannot be ruled out. Also, the SAN region *in vivo* is mainly perfused by extracardiac vessels rather than the coronary vasculature. During *ex vivo* isolated heart perfusion a relative bradycardia can be observed, which may not accurately reflect the *in vivo* SAN activity. Moreover, potential alterations of the calcium homeostasis could also occur (Bell et al., 2011; Sutherland & Hearse, 2000). In addition, it cannot be ruled out that this training protocol at the applied frequency and intensity may not have induced intrinsic remodeling of the SAN. Therefore, all these factors must be considered prior to interpreting the outcomes of our study.

To summarize, our findings suggest that an enhanced vagal tone played an important role in the development of resting bradycardia and the observed increased heart rate variability parameters in conscious exercised guinea pigs. However, a more diverse methodology, including the isolation of the right atrial region and the SAN, might have provided a better insight into the SAN remodeling. Additionally, a more intense and prolonged endurance training program, resulting in more pronounced resting bradycardia, might have made possible the detection of the intrinsic remodeling of the SAN.

The enhanced beat-to-beat heart rate variability parameters are intrinsically linked to the previously described sinus bradycardia. The present study revealed that exercised guinea pigs, with significant resting bradycardia, developed significantly enhanced heart rate variability parameters, suggesting the effectiveness of the applied training protocol. Athletes usually have greater heart rate variability than untrained counterparts: an increased heart rate variability, accompanied by decreased resting heart rate, typically indicates an individual's ability to cope well with the training. Therefore, these parameters correlate well with physical fitness levels in elite athletes (Buchheit, 2014) and provide insight into the function and responsiveness of the heart. Heart rate variability parameters are often considered surrogate markers of parasympathetic tone (Thomas & Viljoen, 2019). Consequently, our findings support the idea that resting bradycardia accompanied by the increased heart rate variability parameters in conscious exercised guinea pigs may result from higher parasympathetic activity induced by endurance training.

5.2.3 The effect of long-term endurance training on ventricular depolarization and repolarization under *in vivo* and *in vitro* circumstances

Experimental and human data have shown that long-term intense training can produce prolonged QT interval in healthy athletes compared to sedentary subjects. Supposedly, prolonged QT interval may act as a potential arrhythmia substrate, as may favor life-threatening arrhythmias and even SCD in apparently healthy individuals (Schouten et al., 1991). Some

studies pointed out that different QT interval variability parameters, like heart rate corrected QT (QTc) and short-term variability of QT interval (STV-QT) can be considered as potential cost- effective arrhythmia predictors in different conditions with prolonged QT interval, such as in patients with long QT syndrome or patients with dilatated cardiomyopathy and also in athletes (Hinterseer et al., 2009; Hinterseer et al., 2010; La Fountaine et al., 2011; Lengyel et al., 2011)

Our *in vivo* ECG results correlate with the human data since profound QT interval prolongation was presented in the exercised group by the end of the training protocol. Since the QT interval is greatly affected by the heart rate, to minimize the influence, it is essential to implement a frequency correction. Although there are many correction formulas in the literature, universal QT correction formulas can be problematic in QTc comparisons at different heart rates and in different species as well. A simple linear regression was used to calculate QTc which resulted in plotting QTc against the corresponding RR interval procedures a regression line with a slope of zero, indicating that these corrections remove the influence of the heart rate. Presumably, this methodology could offer a reliable tool for examining the QTc in guinea pigs. The QTc of conscious exercised animals was slightly but significantly enhanced and a seemingly greater STV-QT variability parameter was observed in conscious exercised guinea pigs at the end of the training protocol.

Interestingly, the imprint of QT interval prolongation detected in conscious exercised guinea pigs was not observed in *in vitro* experiments. The duration of the QT interval did not differ between the groups in *ex vivo* Langendorff studies. Therefore, the detected *in vivo* QT interval prolongation most likely can be attributed to exercise-induced resting bradycardia resulting from increased parasympathetic tone. A further support of this statement, neither the action potential duration (APD) nor the short- term variability of action potential duration (STV-APD) was altered in enzymatically isolated left ventricular myocytes of exercised guinea pigs compared to sedentary animals. Our recently published study of a large animal model of the athlete's heart showed that besides significantly lengthened QT and QTc intervals, prolonged APD and STV-APD developed in exercised dogs. In this study, it was pointed out that decreased amplitude of the transient outward potassium current ($_{Ito}$) may contribute to the observed prolongation in *in vivo* and *in vitro* experiments as well (Polyak et al., 2023). Since the I_{to} lacks in the native left ventricular myocytes of the guinea pig's heart, it can limit the electrophysiological translational value to the human hearts. In guinea pig left ventricular myocytes the major repolarizing rate-dependent current is the slow component of the delayed rectifier potassium current (I_{Ks}), which may have a more prominent role than I_{Kr} in

repolarization of the guinea pig heart (Bartos et al., 2015; O'Hara & Rudy, 2012; Zicha et al., 2003). Based on our cellular electrophysiological data, the amplitude of I_{Ks} did not differ between the examined groups. However, similar to the results of our previous study, the amplitude of I_{Ks}, late sodium current (I_{NaL}), and sodium-calcium exchanger (I_{NCX}) did not differ significantly between the exercised and sedentary groups (Polyak et al., 2023). Although it cannot be excluded the control of other uninvestigated currents, like the rapid component of delayed rectifier potassium (I_{Kr}) current and/or the L-type calcium current (I_{CaL}), may have an impact on the altered QT interval and its variability parameters in conscious exercised guinea pigs. Presumably, the electrophysiological differences among the species strongly limit the correlation between the human heart and our small animal model from the perspective of repolarization.

The PQ interval in conscious exercised guinea pigs although showed some tendency to increase but did not reach the level of statistical significance. This may be attributed to the enhanced vagal tone after endurance training; however, further investigations are needed. Widened QRS complex on the ECG suggests an electrical conduction abnormality (Crescenzi et al., 2021), and it is associated with a higher risk of arrhythmias (Robyns et al., 2016). Similar to our previous study conducted on dogs (Polyak et al., 2023), long-term training evoked a significantly widened QRS complex in conscious exercised guinea pigs. Interestingly, this finding diminished in *ex vivo* Langendorff experiments. Since the observed broad QRS complex of the conscious exercised guinea pigs and the absence of this phenomenon in *ex vivo* Langendorff experiments are not entirely understood, it would be essential to examine this issue in more depth.

5.3 Investigating the cannabidiol evoked cellular electrophysiological alterations and its possible consequences

5.3.1 Effects of cannabidiol on cardiac transmembrane ionic channels

CBD has become widely used and a fashionable compound because of its potential benefits. However, its detailed electrophysiological features on cardiac ionic currents are poorly investigated. Therefore, we aimed to investigate the effects of CBD on various transmembrane ionic currents. Our studies pointed out that CBD has multiple inhibitory effects on various transmembrane ionic currents which play a key role in ventricular repolarization. Application of lower (1 2.5, 5 μM) and higher (10 μM) concentrations resulted in significant depression of I_{Kr} in native rabbit left ventricular myocytes. In a recent study, QT prolongation was reported in anesthetized rats by a synthetic cannabinoid compound, namely JWH-030 (Yun et al., 2016).

However, the chemical structure of this compound is different from CBD and it inhibited hERG channels with a relatively high EC_{50} value (88.36 μM). However, it is important to highlight that in the rat ventricle the role of I_{Kr} seems not as prominent for controlling repolarization as in other laboratory animals with greater translational value to the human heart (Arpadffy-Lovas et al., 2022). Based on this, the observed synthetic cannabinoid compound evoked QT alternations attributed to Kv1.5 and Kv4.2 rather than hERG channel inhibition. Besides the I_{Kr} inhibition, our study showed that I_{Ks} was also inhibited significantly by CBD at lower (1, 2,5, 5 μM) and highest (10 μM) concentrations as well. This current has an essential role in the repolarization reserve. As described thoroughly in the introduction section (see detail in Chapter 1.3), I_{Ks} can partially replace the role of other poorly operating outward potassium currents during the repolarization phase (Jost et al., 2005; Varro et al., 2000; Varro et al., 2021). If I_{Ks} is suppressed, the repolarization reserve is attenuated, therefore it potentially increases the risk of the development of cardiac arrhythmias under certain circumstances.

Moreover, our experimental design revealed that CBD significantly inhibited I_{to} in isolated canine left ventricular cells at every concentration used (1, 2.5, 5, 10 μM). But even the highest applied concentration of CBD (10 μM) did not show any effect in isolated rabbit myocytes. This difference can be attributed to the marked species-dependent expression of the pore- forming protein subunits. The I_{to} is conducted by Kv4.3 in the canine heart (Han et al., 2002), whereas in rabbits I_{to} is conducted by Kv1.4 channels in the left ventricle (Wang et al., 1999). In this scenario, the canine model is believed to show a greater level of translational value to humans. In the left ventricle of the human heart, similar to dogs, two distinct subtypes form the I_{to}, namely $I_{to,fast,}$ and $I_{to,slow}$, determined by Kv3.4 and Kv1.4, respectively (Odening et al., 2021). As pointed out in several studies, I_{to} is critical in regulating myocardial electrical properties during the very early phase of the AP (Dong et al., 2006; Niwa & Nerbonne, 2010; Virag et al., 2011; Zicha et al., 2004). Given the multiple outward potassium channel inhibition by CBD, the use of this cannabinoid may result in APD prolongation and consequent QT lengthening (Orvos et al., 2020; Topal et al., 2021).

Other major findings of our study were that I_{CaL} and I_{NaL} were inhibited by 10 μM CBD. These observations are in line with the study of Isaev et al., which also pointed out that CBD inhibits the I_{CaL} in isolated rabbit left ventricular myocytes (Isaev et al., 2022). Therefore, the suppression of these inward currents with 10 μM CBD can counterbalance the inhibited multiple potassium channel-induced repolarization lengthening.

Summarizing the electrophysiological results of the previously described experiments, lower concentrations of CBD can lead to a lengthened APD, and consequently, prolonged QT and

QTc intervals, due to multiple potassium channel inhibition. However, higher concentrations (≥ 10 μM) may result in an unchanged or even shorter duration of left ventricular AP due to the coinhibition of inward transmembrane ionic currents. It is worth noting that the effect of CBD on the repolarization duration is controversial in the literature. For instance, based on a computational model of rabbit ventricular AP, Isaev et al. hypothesized that I_{Ks} and I_{Kr} inhibition alone at low (≤ 2 μM) concentrations of CBD, causes significantly lengthened APD (29 %), whereas integration of I_{NaL} and I_{CaL} inhibition at higher CBD concentrations (≥ 5 μM) results in significantly shortened APD (27 %) (Isaev et al., 2022).

5.3.2 Potential adverse cardiovascular events associated with cannabidiol consumption

Nowadays, CBD is widely used as a popular dietary supplement in various formats; however, the exact CBD content of these products usually remains unclear and may contain significant levels of other unknown substances. Since CBD is not prohibited by the World Anti-Doping Agency, CBD consumption is getting fashionable among amateur and elite athletes because of its alleged or real positive effects (Lachenmeier & Diel, 2019). Despite its growing popularity spreading, some studies warn athletes to avoid the use of CBD until further research into the efficacy and safety of supplementation is available (McCartney et al., 2020). A recent systematic review showed that 23.4 % of athletes reported using cannabis in 2019 (Docter et al., 2020). Although this seems to be a lower rate of use than in the general population, it is important to highlight that this number is presumably underreported since the surveys about cannabis use were reliant on self-reporting. Since several routes of administration exist, it is important to be familiar with the pharmacokinetics of CBD. At high temperatures, the majority of CBD is broken down (Czegeny et al., 2021), whilst from CBD oils containing up to 20 % CBD, a significant amount of CBD is absorbed (Zgair et al., 2016). According to human pharmacokinetic data, the mean maximal plasma concentration (C_{max}) values for CBD can reach 0.58 μM and 0.7 μM (at 3 hours) after oral administration of 400 and 800 mg of CBD, respectively (Millar et al., 2018). On the other hand, cigarette smoking containing 19.2 mg CBD led to a C_{max} value of 0.35 μM (Millar et al., 2018). In the present experiments, CBD had inhibitory potential on the activity of several outward transmembrane potassium currents during the repolarization phases. Taking into account our experiments, the EC_{50} values for I_{Kr}, $I_{Ks,}$ and I_{to} inhibition were 4.9, 3.1, and 5 μM, respectively. These EC_{50} values are higher than the C_{max} values observed in enrolled individuals in the aforementioned studies. Redfern et al. have attempted to investigate the risk of Torsades de Pointes ventricular tachyarrhythmia (TdP) development based on the comparison of hERG activity, APD, and QT prolongation with the

observed QT alterations and reports of TdP in humans for 100 different drugs. They suggested that at least a margin of 30-fold between hERG EC_{50} and C_{max} is an acceptable degree of safety to avoid arrhythmogenic events (Redfern et al., 2003). The ratios of IC_{50} and C_{max} values in our study are in the range of 2.96–18.57, which may refer to moderately increased pro-arrhythmic risks in clinical settings.

Our findings suggest a small or negligible pro-arrhythmic risk in physiological conditions in healthy individuals. Our results align with a clinical report showing that CBD oromucosal spray did not lead to alterations of different ECG parameters, including QTc (Sellers et al., 2013). Another clinical study reported that long-term Sativex (THC + CBD) treatment evoked T-wave alteration in only one out of 146 patients (Serpell et al., 2013). Therefore, it is likely that in the case of inhalation or oral use of cannabis-derived products, CBD itself may not represent a significant pro-arrhythmic risk. Nevertheless, higher C_{max} values may occur in certain individuals with markedly slower drug elimination due to concomitant diseases or with concomitant use of other drugs that inhibit the metabolism of CBD, therefore cautions should be advised (Iffland & Grotenhermen, 2017). As CBD can affect cardiac electrophysiology, it may further increase the risk of developing cardiac arrhythmias. When the intake of CBD is combined with pharmacological agents that affect cardiac repolarization, as well as in certain pathophysiological situations in which cardiac repolarization reserve is attenuated (Varro & Baczko, 2011; Varro et al., 2021) or drug metabolism is impaired, CBD may have an additive effect, further increasing the proarrhythmic risk and the possible incidence of SCD. Such additive interactions have been reported in both experimental (Lengyel et al., 2007) and clinical settings (Wisniowska et al., 2016). Evidence from several clinical studies suggests that athletes who engage in chronic high-intensity exercise appear to experience irregular heart rhythm, which in rare and sudden cases can be fatal (Dello Russo et al., 2022; Link & Estes, 2010; Maron, 2007; Zorzi et al., 2020). Considering the literature reports presented previously and the experiments in guinea pigs presented in my thesis, as well as our results in trained dogs in our previous work, it is important to note that the effects of electrophysiological cardiac remodeling induced by long-term heavy endurance exercise and the use of CBD can be additive, and may result in life-threatening cardiac arrhythmias. Therefore, it needs particular attention in the future. Although the underlying causes of malignant arrhythmias can be diverse, it cannot be excluded that CBD intake may contribute to their development, therefore, CBD-containing preparations should be used with appropriate caution.

The cardiovascular effects of CBD may only be partially due to its impacts on transmembrane ion channels. The cardiovascular safety of this agent may be influenced by its interaction with

other targets, and by the presence of myocardial ischemia (Ferdinandy et al., 2019) as well. Therefore, further studies are needed to evaluate the adverse cardiovascular effects of CBD and other cannabinoids both *in vivo* and *in vitro* studies, with a particular focus on the benefit-risk assessment of products with different cannabinoid content.

5.4 Investigating the ibuprofen evoked cellular electrophysiological changes and its possible consequences

5.4.1 Investigating the alterations in transmembrane ionic current magnitude induced by therapeutic concentrations of ibuprofen

Although ibuprofen has long been one of the most commonly used non-steroidal anti-inflammatory drug (NSAID) on the market, its electrophysiological effects are poorly investigated. A recent nationwide case-time-control study reported that the use of two NSAIDs, namely diclofenac and ibuprofen, is associated with an increased risk of out-of-hospital cardiac arrest and consequent sudden cardiac death (Sondergaard & Gislason, 2017). Although the mechanism of these tragic events is unclear and can be diverse, the possible direct modulation of these drugs on the transmembrane ionic channels should also be considered.

In our study, 250 μM (51.5 μg/mL) ibuprofen affected the amplitude of various transmembrane ionic currents in isolated canine left ventricular myocytes. Neither the kinetic nor the measured amplitude of the inward rectifier potassium current (I_{K1}) was affected by the applied concentration of ibuprofen. However, it moderately but significantly decreased the amplitude of I_{to}. In our previous study, it was found that 250 μM ibuprofen significantly inhibited the I_{Kr} in canine left ventricular myocytes (Paszti et al., 2021). This argument is further strengthened by the previous experimental study (Kristof et al., 2012), which indicated that diclofenac decreased repolarization reserve by inhibiting I_{Ks} and I_{Kr} in the canine heart. In this paper it has also been shown that diclofenac during the attenuation of the repolarization reserve with dofetilide also facilitated TdP-like arrhythmia in *in vivo* rabbit experiments (Kristof et al., 2012). Our previous study pointed out (Paszti et al., 2021), identically to the study of Kristof et al., that in normal situations and at therapeutically relevant concentrations, ibuprofen exerted no or only a moderate prolongation of repolarization in ventricular muscle preparations, but in situations where the repolarization reserve was attenuated, the degree of repolarization lengthening was further increased.

Since cardiac repolarization is determined not only by outward potassium currents, the effect of ibuprofen was also studied on I_{NaL} and I_{CaL} in isolated canine left ventricular myocytes. At a concentration of 250 μM, ibuprofen moderately, but in a statistically significant manner

decreased the amplitude of both inward transmembrane ionic currents. Similar to our study, Kristof et al. found that 30 μM diclofenac slightly inhibited the I_{CaL}. (Kristof et al., 2012).

A previous study has hitherto investigated the electrophysiological effects of ibuprofen experimentally (Yang et al., 2008). They pointed out that ibuprofen dose-dependently shortened the APD and the effective refractory period on fast and slow response action potentials in guinea pig ventricular papillary muscle preparations. It might be speculated that sodium and calcium transmembrane ionic channels are dose-dependently suppressed by ibuprofen. In our present study, we could confirm the hypothesized inhibition of I_{CaL} and I_{NaL}. However, Yarishkin et al. found that diclofenac, but not ibuprofen inhibited I_{NaL} and I_{CaL} in a dose-dependent manner in rat ventricular myocytes (Yarishkin et al., 2009).

To sum up our cellular electrophysiological results, 250 μM ibuprofen induced moderate but significant inhibition of several transmembrane ionic currents, including I_{NaL}, I_{CaL}, I_{Kr}, and I_{to}, which can lead to unchanged or moderately prolonged repolarization (Paszti et al., 2021). These dissimilarities can be attributed to the different baseline electrophysiological features of the used species in respective studies (i.e., rabbit, neonatal rat, or dog), and differences in the experimental conditions (room temperature vs 37 °C). Unlike dogs, left ventricular guinea pig myocytes are unique due not only to their total lack of native I_{to} but the very strong expression of I_{Ks} as well (Bartos et al., 2015; Zicha et al., 2003). Consequently, inhibition of I_{to} and I_{Kr} in the left ventricular region of the guinea pig heart has a lesser impact on repolarization compared to dogs. Therefore, ibuprofen-induced inhibition of I_{CaL} and I_{NaL} in the guinea pig ventricle would alter the balance of outward and inward currents, and favor a relative enhancement of outward currents, resulting in shortened repolarization. The opposite effect is expected in the mid-myocardial region of the left ventricle of rabbit and canine hearts, where the density of I_{Ks} is weaker than in guinea pigs, therefore, I_{Kr} should make a stronger contribution to the repolarization (Jost, Virag, et al., 2013). Additionally, it is well-established that I_{to} is a key regulator in shaping the morphology of broad, plateau-possessing cardiac AP and in repolarization (Dong et al., 2006; Virag et al., 2011). Consequently, the co-inhibition of I_{Kr} and I_{to} can lead to attenuated repolarization reserve. Since ibuprofen is commonly prescribed for the symptomatic treatment of fever, it would be useful to investigate its electrophysiological effects under hyperthermic conditions as well.

5.4.2 Increased risk of arrhythmic events associated with ibuprofen intake

Ibuprofen is a common over-the-counter (OTC) and prescribed NSAID (Bushra & Aslam, 2010; Rainsford, 2009; Warden, 2010). Athletes are also frequent consumers since they often

seek new ways to enhance their athletic performance, therefore different NSAIDs provide opportunities to amateur and professional athletes not just for pain relief but also increased pain tolerance and faster recovery. Many athletes take pre-emptive NSAIDs in the hope of preventing exercise-induced soreness and pain (Harle et al., 2018; Lima et al., 2016; Warden, 2010; Warner et al., 2002). Some studies reported that NSAIDs, especially ibuprofen, are common among endurance athletes (i.e., marathon runners, and soccer players) who usually take them daily to achieve the desired effect. For instance, based on a recently published survey, nearly 90 % of the runners who participated in Parkrun UK used NSAIDs, usually in the form of over-the-counter ibuprofen. Moreover, most of them used NSAIDs directly before, during, and after the race to relieve pain and to compete more effectively (Rosenbloom et al., 2020) According to the literature, athletes frequently use higher doses of ibuprofen than the recommended therapeutic dose. Despite valuable studies joining the growing evidence that ibuprofen and other NSAID consumption before workout does not offer any benefit and causes disagreeable damage, particularly to the intestines (Da Silva et al., 2015; Manoukian et al., 2017; Nieman et al., 2006; Van Wijck et al., 2012), the adverse cardiovascular events are poorly highlighted. Despite that, some studies have drawn attention to the greater risk of adverse cardiovascular events, such as myocardial infarction, and sudden cardiac arrest, associated with larger doses and/or chronic use of these drugs (Bohm et al., 2013; Lundberg & Howatson, 2018; Pratt et al., 1994; Ratliff et al., 2002). The applied concentration of ibuprofen in our experiments was relatively well-fitted to the therapeutic range in patients (10 μg/mL to 50 μg/mL; 48.5 μM to 242.4 μM, respectively) (Holubek et al., 2007; Mazaleuskaya et al., 2015). Although ibuprofen counts as a relatively safe drug among other NSAIDs, it is also worth noting that in certain situations, such as old age, altered metabolism due to disease (e.g., liver or kidney failure), or drug interactions, plasma levels may rise above the therapeutic range.

Based on our cellular electrophysiological findings, ibuprofen seems a relatively safe drug under normal circumstances. However, under certain conditions characterized by attenuated repolarization reserve, like the athlete's heart presented also in this thesis, ibuprofen may enhance proarrhythmic risk and may even contribute to the incidence of adverse cardiovascular events, such as arrhythmias and even sudden cardiac arrest. This possibility should be considered and addressed in clinical practice, given that ibuprofen is a commonly used OTC drug taken daily by millions of people without any medical supervision.

6 CONCLUSION

The most important new results in this Ph.D. thesis are the followings:

1. In exercised guinea pigs, long-term endurance training decreases the repolarization reserve, but unlike other experimental animal models of the athlete's heart, it is mainly attributed to the chronic endurance training-induced enhanced vagal tone, not to the electrophysiological remodeling.
2. Similar to other animal models of athlete's heart and human data, long-term heavy endurance training evoked a significant level of cardiac fibrosis in the exercised guinea pigs, which may enhance proarrhythmic risk.
3. Cannabidiol (CBD) depresses the amplitude of several transmembrane ionic currents, such as I_{to}, I_{Kr}, I_{Ks}, I_{CaL}, and I_{NaL}, which can attenuate the repolarization reserve in the ventricle.
4. Ibuprofen decreases different transmembrane ionic currents, such as I_{to}, I_{CaL}, and I_{NaL} which can lead to decreased repolarization reserve in the ventricle.

The present study introduced a novel guinea pig exercise-induced athlete's heart model. In our model, similar to the endurance-trained human athlete's heart, long-term endurance training led to increased left ventricular end-diastolic diameter and moderate enlargement of cardiac muscle due to increased volume load. In addition, mild fibrosis was also present that may also occur in human athlete's hearts according to recently published studies. The several-week-long endurance training program also led to electrophysiological changes in conscious exercised guinea pigs. The *in vivo* resting bradycardia and increased heart rate variability parameters together with unchanged *ex vivo* results indicated a higher resting vagal tone in exercised animals. The widened QRS interval in conscious exercised animals may be associated with structural and functional remodeling of the heart. The significantly prolonged QT interval due to decreased resting heart rate can be related to the increased vagal tone in exercised animals. Besides the observed QT interval prolongation, conscious exercised guinea pigs developed slightly increased QT variability parameters, which may indicate impaired repolarization and higher repolarization instability.

These observations do not necessarily indicate that at a competitive level, endurance exercise is harmful since the evidence regarding the beneficial effect of exercise is overwhelming. However, in certain individuals or in situations where the repolarization reserve is impaired due to hidden diseases, such as hypertrophic cardiomyopathy, long QT-syndromes, diabetes or electrolyte imbalances, doping substances, or any seemingly harmless drugs, the observed significant resting bradycardia, alterations of *in vivo* depolarization and repolarization, and mild

fibrosis induced by endurance training in our study may present additional potential risk factors to be considered in the prevention of possible adverse events in competitive sport.

Athletes often seek different avenues to reach greater sporting achievements. Therefore, they often use different agents, for instance, CBD or NSAIDs, like ibuprofen to accomplish their goals.

CBD has a prominent impact on the cellular level of the heart. It decreases the amplitude of various potassium currents each of which plays a prominent role in left ventricular repolarization. CBD significantly depressed the amplitude of I_{to}, I_{Kr}, and I_{Ks} of enzymatically isolated left ventricular myocytes at lower (1, 2.5, 5 μM) and higher (10 μM) concentrations. The inhibition of multiple potassium currents can evoke prolonged action potential duration and consequently prolonged QT interval. It is worth noting that the proper selection of the animal model for investigating the effects of a drug is important since the incorrect choice can lead to poor translational value to human hearts. As our study indicates, the applied highest concentration (10 μM) of CBD caused significantly decreased I_{to} of the left ventricular myocytes of the canine heart; however, the amplitude of the current remained unchanged in native rabbit left ventricular myocytes. Our study suggests that potential prolongation of the repolarization can be counterbalanced by the 10 μM CBD evoked inhibition of I_{CaL} and I_{NaL}.

The alterations of transmembrane ionic currents at lower concentrations of CBD could decrease the repolarization reserve of the cardiac action potentials contributing to the proarrhythmic risks of CBD resulting in cardiac arrhythmias or even sudden cardiac death.

Based on our study, ibuprofen has a slight impact on different transmembrane ionic currents, including I_{to}, I_{NaL}, and I_{CaL} in the therapeutic concentration. Consequently, at least regarding its cardiac electrophysiological properties, ibuprofen is a relatively safe drug in normal situations. Despite that, because of the easy availability of different over-the-counter products, ibuprofen can be easily administered above the therapeutic range. However, in certain conditions characterized by attenuated repolarization reserve, ibuprofen may enhance proarrhythmic risk, and may even contribute to the incidence of sudden cardiac death observed in clinical studies. This possibility should be considered and taken into account in clinical practice since ibuprofen is a very commonly used over-the-counter drug, taken every day by several million people without medical control.

In conclusion, these agents should be consumed with caution by athletes, as they can attenuate the repolarization reserve and, together with the cardiac structural-electrophysiological changes that can result from long-term vigorous training, may lead to life-threatening arrhythmias.

ACKNOWLEDGEMENT

This work was carried out at the Department of Pharmacology and Pharmacotherapy, Szent- Györgyi Albert Medical School, University of Szeged. I respectfully thank Professor István Baczkó MD, Ph.D., the Head of the Department for ensuring the opportunity to do scientific research as a PhD student at the Department. I would like to express my thanks to Professor László Dux MD, Ph.D., DSc, the Head of the Doctoral School of Multidisciplinary Medical Sciences for allowing me to conduct doctoral studies at the University.

Most importantly, I would like to express my sincere gratitude to my all-time Ph.D. supervisors, Professor András Varró MD, Ph.D., DSc and Professor Norbert Jost Ph.D., DSc for their guidance, continuous support of my work and for introducing me to the fascinating world of cardiac cellular electrophysiology. And most importantly, I am thankful to them for teaching me the professional skills and critical thinking I need at scientific work. Their stimulating enthusiasm, kindness, and continuous support guided me through my doctoral studies. I am grateful to Professor András Varró MD, Ph.D., DSc for inspiring discussions and lots of excellent advice. I am thankful to László Virág Ph.D., since he thought me how to critically analyze the experiments.

I am also grateful for my closest colleagues and friends at the same time, Alexandra Polyák MD, Jenő Pintér MD, Noémi Tóth MD, Ph.D., and Mária Kosztka for their support, help, and work throughout the years. I believe that without their expertise, perennial curiosity, and perseverance, the scientific work presented above would have been poorer.

I wish to thank my senior collages Zsófia Nagy, Ph.D., Norbert Nagy Ph.D., and student collages Gergő Bitay, Gábor Mohácsi, Noémi Tóth, MD, Mohammed Aiman Saleh Abdullah, and Muhammad Naveed Khan, Ph.D. for their continuous support and help in my work, and for creating a cheerful and social milieu in the laboratory.

I am thankful to all my colleagues at the Department. I would like to say special thanks to Rea Fritz, Anikó Kőrös, Gábor Girst, Gábor Dobai, Zsolt Tóth, Róbert Motzwickler for their excellent administrative and technical support.

Above all, I would like to express my heartfelt gratitude to my family and friends. I wish to thank my mother, Éva, my grandfather, István, my aunt, Erika, and my ever-smiling cousin, Balázs, for their endless love, trust, and support which has meant so much to me all these years.

I am grateful to my partner, Máté, since his unconditional love, all-time support, encouragement, and optimistic attitude always helped and inspired me. Without my family and partner, none of these works would indeed have been possible.

FOUNDINGS

The work of the small animal model of the athlete's heart was supported by the National Research, Development, and Innovation Office (NKHIF K-119992 to A. V., NKHIF K-128851 to I. B., NKHIF K- 135464, NKFIH PD-125402, FK-129117, GINOP-2.3.2–15-2016–00047, and TKP2021-EGA-32), Hungarian National Scientific Research Fund (OTKAFK-138223 to P., B) the Ministry of Human Capacities of Hungary (20391–3/2018/FEKUSTRAT and EFOP3.6.2–16-2017–00006), from the Eötvös Loránd Research Network, from theUNKP-20–5-SZTE-165, ÚNKP-21–5-SZTE-543 from the János Bolyai Research Scholarship of the Hungarian Academy of Sciences to N. N., and by the Albert Szent-Györgyi Medical School institutional grant (SZTE ÁOK-KKA 2021 to L. V.).

The work of the cellular electrophysiological effects of cannabidiol was supported by the Economic Development and Innovation Operative Programme GINOP-2.3.2-15-2016-00012, the National Research Development and Innovation Office (NKFIH K 119992, NKFIH K 135464, and NKFIH K 128851), the Ministry of Human Capacities Hungary (20391- 3/2018/FEKUSTRAT and EFOP-3.6.2-16-2017-00006), and from the Eötvös Loránd Research Network are gratefully acknowledged. Open-access funding is provided by the University of Szeged.

The work of the cellular electrophysiological effects of ibuprofen was funded by the János Bolyai Research Scholarship of the Hungarian Academy of Sciences (for István Koncz, No. BO/00581/17) and the ÚNKP-18-4 and 19-4 (Bolyai+) New National Excellence Program of the Ministry for Innovation and Technology (for István Koncz) and the National Research, Development and Innovation Office – NKFIH PD-116011 (for István Koncz), K-119992 (for András Varró), FK-129117 (for Norbert Nagy), and the Hungarian Government-Ministry of Human Resources (grant EFOP-3.6.2-16-2017-00006, LIVE LONGER and EFOP 3.6.3-VEKOP-16-2017-00009 for TÁ-L), GINOP-2.3.2.-15-2016-00048), the Ministry of Human Capacities Hungary (20391-3/2018/FEKUSTRAT), and János Bolyai Research Scholarship of the Hungarian Academy of Sciences (for Norbert Nagy). The GINOP and EFOP projects are co-financed by the European Union and the European Regional Development Fund.

REFERENCES

1. Adel, N. (2017). Overview of chemotherapy-induced nausea and vomiting and evidence-based therapies. *Am J Manag Care*, *23*(14 Suppl), S259-S265. https://www.ncbi.nlm.nih.gov/pubmed/28978206
2. Akar, F. G., Wu, R. C., Juang, G. J., Tian, Y., Burysek, M., Disilvestre, D., Xiong, W., Armoundas, A. A., & Tomaselli, G. F. (2005). Molecular mechanisms underlying K+ current downregulation in canine tachycardia-induced heart failure. *Am J Physiol Heart Circ Physiol*, *288*(6), H2887-2896. https://doi.org/10.1152/ajpheart.00320.2004
3. Antzelevitch, C., Sicouri, S., Litovsky, S. H., Lukas, A., Krishnan, S. C., Di Diego, J. M., Gintant, G. A., & Liu, D. W. (1991). Heterogeneity within the ventricular wall. Electrophysiology and pharmacology of epicardial, endocardial, and M cells. *Circ Res*, *69*(6), 1427-1449. https://doi.org/10.1161/01.res.69.6.1427
4. Arpadffy-Lovas, T., Mohammed, A. S. A., Naveed, M., Koncz, I., Balati, B., Bitay, M., Jost, N., Nagy, N., Baczko, I., Virag, L., & Varro, A. (2022). Species-dependent differences in the inhibition of various potassium currents and in their effects on repolarization in cardiac ventricular muscle. *Can J Physiol Pharmacol*, *100*(9), 880-889. https://doi.org/10.1139/cjpp-2022-0028
5. Aschar-Sobbi, R., Izaddoustdar, F., Korogyi, A. S., Wang, Q., Farman, G. P., Yang, F., Yang, W., Dorian, D., Simpson, J. A., Tuomi, J. M., Jones, D. L., Nanthakumar, K., Cox, B., Wehrens, X. H., Dorian, P., & Backx, P. H. (2015). Increased atrial arrhythmia susceptibility induced by intense endurance exercise in mice requires TNFalpha. *Nat Commun*, *6*, 6018. https://doi.org/10.1038/ncomms7018
6. Asif, I. M., Rao, A. L., & Drezner, J. A. (2013). Sudden cardiac death in young athletes: what is the role of screening? *Curr Opin Cardiol*, *28*(1), 55-62. https://doi.org/10.1097/HCO.0b013e32835b0ab9
7. Azevedo, L. F., Perlingeiro, P. S., Hachul, D. T., Gomes-Santos, I. L., Brum, P. C., Allison, T. G., Negrao, C. E., & De Matos, L. D. (2014). Sport modality affects bradycardia level and its mechanisms of control in professional athletes. *Int J Sports Med*, *35*(11), 954-959. https://doi.org/10.1055/s-0033-1364024
8. Baczko, I., Jost, N., Virag, L., Bosze, Z., & Varro, A. (2016). Rabbit models as tools for preclinical cardiac electrophysiological safety testing: Importance of repolarization reserve. *Prog Biophys Mol Biol*, *121*(2), 157-168. https://doi.org/10.1016/j.pbiomolbio.2016.05.002
9. Bartos, D. C., Grandi, E., & Ripplinger, C. M. (2015). Ion Channels in the Heart. *Compr Physiol*, *5*(3), 1423-1464. https://doi.org/10.1002/cphy.c140069
10. Beaudry, R., Haykowsky, M. J., Baggish, A., & La Gerche, A. (2016). A Modern Definition of the Athlete's Heart-for Research and the Clinic. *Cardiol Clin*, *34*(4), 507-514. https://doi.org/10.1016/j.ccl.2016.06.001
11. Bell, R. M., Mocanu, M. M., & Yellon, D. M. (2011). Retrograde heart perfusion: the Langendorff technique of isolated heart perfusion. *J Mol Cell Cardiol*, *50*(6), 940-950. https://doi.org/10.1016/j.yjmcc.2011.02.018
12. Benito, B., Gay-Jordi, G., Serrano-Mollar, A., Guasch, E., Shi, Y., Tardif, J. C., Brugada, J., Nattel, S., & Mont, L. (2011). Cardiac arrhythmogenic remodeling in a rat

model of long-term intensive exercise training. *Circulation*, *123*(1), 13-22. https://doi.org/10.1161/CIRCULATIONAHA.110.938282

13. Bohm, P., Kastner, A., & Meyer, T. (2013). Sudden cardiac death in football. *J Sports Sci*, *31*(13), 1451-1459. https://doi.org/10.1080/02640414.2013.796064
14. Boyett, M. R., D'Souza, A., Zhang, H., Morris, G. M., Dobrzynski, H., & Monfredi, O. (2013). Viewpoint: is the resting bradycardia in athletes the result of remodeling of the sinoatrial node rather than high vagal tone? *J Appl Physiol (1985)*, *114*(9), 1351-1355. https://doi.org/10.1152/japplphysiol.01126.2012
15. Buchheit, M. (2014). Monitoring training status with HR measures: do all roads lead to Rome? *Front Physiol*, *5*, 73. https://doi.org/10.3389/fphys.2014.00073
16. Bushra, R., & Aslam, N. (2010). An overview of clinical pharmacology of Ibuprofen. *Oman Med J*, *25*(3), 155-1661. https://doi.org/10.5001/omj.2010.49
17. Chapman, J. H. (1982). Profound sinus bradycardia in the athletic heart syndrome. *J Sports Med Phys Fitness*, *22*(1), 45-48. https://www.ncbi.nlm.nih.gov/pubmed/7132315
18. Crescenzi, C., Zorzi, A., Vessella, T., Martino, A., Panattoni, G., Cipriani, A., De Lazzari, M., Perazzolo Marra, M., Fusco, A., Sciarra, L., Sperandii, F., Guerra, E., Tranchita, E., Fossati, C., Pigozzi, F., Sarto, P., Calo, L., & Corrado, D. (2021). Predictors of Left Ventricular Scar Using Cardiac Magnetic Resonance in Athletes With Apparently Idiopathic Ventricular Arrhythmias. *J Am Heart Assoc*, *10*(1), e018206. https://doi.org/10.1161/JAHA.120.018206
19. Crossmon, G. 1937. A modification of Mallory's connective tissue stain with a discussion of the principles involved. Anat. Rec. 69: 33–38. doi:10.1002/ar.1090690105.
20. Czegeny, Z., Nagy, G., Babinszki, B., Bajtel, A., Sebestyen, Z., Kiss, T., Csupor-Loffler, B., Toth, B., & Csupor, D. (2021). CBD, a precursor of THC in e-cigarettes. *Sci Rep*, *11*(1), 8951. https://doi.org/10.1038/s41598-021-88389-z
21. D'Andrea, A., Cocchia, R., Riegler, L., Scarafile, R., Salerno, G., Gravino, R., Golia, E., Pezzullo, E., Citro, R., Limongelli, G., Pacileo, G., Cuomo, S., Caso, P., Russo, M. G., Bossone, E., & Calabro, R. (2010). Left ventricular myocardial velocities and deformation indexes in top-level athletes. *J Am Soc Echocardiogr*, *23*(12), 1281-1288. https://doi.org/10.1016/j.echo.2010.09.020
22. D'Souza, A., Bucchi, A., Johnsen, A. B., Logantha, S. J., Monfredi, O., Yanni, J., Prehar, S., Hart, G., Cartwright, E., Wisloff, U., Dobryznski, H., DiFrancesco, D., Morris, G. M., & Boyett, M. R. (2014). Exercise training reduces resting heart rate via downregulation of the funny channel HCN4. *Nat Commun*, *5*, 3775. https://doi.org/10.1038/ncomms4775
23. Da Silva, E., Pinto, R. S., Cadore, E. L., & Kruel, L. F. (2015). Nonsteroidal anti-inflammatory drug use and endurance during running in male long-distance runners. *J Athl Train*, *50*(3), 295-302. https://doi.org/10.4085/1062-6050-49.5.04
24. Dello Russo, A., Compagnucci, P., Casella, M., Gasperetti, A., Riva, S., Dessanai, M. A., Pizzamiglio, F., Catto, V., Guerra, F., Stronati, G., Andreini, D., Pontone, G., Bonomi, A., Rizzo, S., Di Biase, L., Capucci, A., Natale, A., Basso, C., Fiorentini, C., . . . Tondo, C. (2022). Ventricular arrhythmias in athletes: Role of a comprehensive diagnostic workup. *Heart Rhythm*, *19*(1), 90-99. https://doi.org/10.1016/j.hrthm.2021.09.013
25. Deo, R., & Albert, C. M. (2012). Epidemiology and genetics of sudden cardiac death. *Circulation*, *125*(4), 620-637. https://doi.org/10.1161/CIRCULATIONAHA.111.023838

26. Docter, S., Khan, M., Gohal, C., Ravi, B., Bhandari, M., Gandhi, R., & Leroux, T. (2020). Cannabis Use and Sport: A Systematic Review. *Sports Health*, *12*(2), 189-199. https://doi.org/10.1177/1941738120901670
27. Dong, M., Sun, X., Prinz, A. A., & Wang, H. S. (2006). Effect of simulated I(to) on guinea pig and canine ventricular action potential morphology. *Am J Physiol Heart Circ Physiol*, *291*(2), H631-637. https://doi.org/10.1152/ajpheart.00084.2006
28. Eijsvogels, T. M. H., Thompson, P. D., & Franklin, B. A. (2018). The "Extreme Exercise Hypothesis": Recent Findings and Cardiovascular Health Implications. *Curr Treat Options Cardiovasc Med*, *20*(10), 84. https://doi.org/10.1007/s11936-018-0674-3
29. Farraj, A. K., Hazari, M. S., & Cascio, W. E. (2011). The utility of the small rodent electrocardiogram in toxicology. *Toxicol Sci*, *121*(1), 11-30. https://doi.org/10.1093/toxsci/kfr021
30. Ferdinandy, P., Baczko, I., Bencsik, P., Giricz, Z., Gorbe, A., Pacher, P., Varga, Z. V., Varro, A., & Schulz, R. (2019). Definition of hidden drug cardiotoxicity: paradigm change in cardiac safety testing and its clinical implications. *Eur Heart J*, *40*(22), 1771-1777. https://doi.org/10.1093/eurheartj/ehy365
31. Fraguas-Sanchez, A. I., & Torres-Suarez, A. I. (2018). Medical Use of Cannabinoids. *Drugs*, *78*(16), 1665-1703. https://doi.org/10.1007/s40265-018-0996-1
32. Grant, A. O. (2009). Cardiac ion channels. *Circ Arrhythm Electrophysiol*, *2*(2), 185-194. https://doi.org/10.1161/CIRCEP.108.789081
33. Gillon D (2006) Could common painkillers because of so many players' deaths? Herald Scotland, Friday 22 September 2006, Accessed 4th January, 2012.
34. Han, W., Bao, W., Wang, Z., & Nattel, S. (2002). Comparison of ion-channel subunit expression in canine cardiac Purkinje fibers and ventricular muscle. *Circ Res*, *91*(9), 790-797. https://doi.org/10.1161/01.res.0000039534.18114.d9
35. Harle, C. A., Danielson, E. C., Derman, W., Stuart, M., Dvorak, J., Smith, L., & Hainline, B. (2018). Analgesic Management of Pain in Elite Athletes: A Systematic Review. *Clin J Sport Med*, *28*(5), 417-426. https://doi.org/10.1097/JSM.0000000000000604
36. Hinterseer, M., Beckmann, B. M., Thomsen, M. B., Pfeufer, A., Dalla Pozza, R., Loeff, M., Netz, H., Steinbeck, G., Vos, M. A., & Kaab, S. (2009). Relation of increased short-term variability of QT interval to congenital long-QT syndrome. *Am J Cardiol*, *103*(9), 1244-1248. https://doi.org/10.1016/j.amjcard.2009.01.011
37. Hinterseer, M., Beckmann, B. M., Thomsen, M. B., Pfeufer, A., Ulbrich, M., Sinner, M. F., Perz, S., Wichmann, H. E., Lengyel, C., Schimpf, R., Maier, S. K., Varro, A., Vos, M. A., Steinbeck, G., & Kaab, S. (2010). Usefulness of short-term variability of QT intervals as a predictor for electrical remodeling and proarrhythmia in patients with nonischemic heart failure. *Am J Cardiol*, *106*(2), 216-220. https://doi.org/10.1016/j.amjcard.2010.02.033
38. Hobai, I. A., Khananshvili, D., & Levi, A. J. (1997). The peptide "FRCRCFa", dialysed intracellularly, inhibits the Na/Ca exchange in rabbit ventricular myocytes with high affinity. *Pflugers Arch*, *433*(4), 455-463. https://doi.org/10.1007/s004240050300
39. Holubek, W., Stolbach, A., Nurok, S., Lopez, O., Wetter, A., & Nelson, L. (2007). A report of two deaths from massive ibuprofen ingestion. *J Med Toxicol*, *3*(2), 52-55. https://doi.org/10.1007/BF03160908

40. Holly, R. G., Shaffrath, J. D., & Amsterdam, E. A. (1998). Electrocardiographic alterations associated with the hearts of athletes. *Sports Med*, *25*(3), 139-148. https://doi.org/10.2165/00007256-199825030-00001
41. Iffland, K., & Grotenhermen, F. (2017). An Update on Safety and Side Effects of Cannabidiol: A Review of Clinical Data and Relevant Animal Studies. *Cannabis Cannabinoid Res*, *2*(1), 139-154. https://doi.org/10.1089/can.2016.0034
42. Isaev, D., Shabbir, W., Dinc, E. Y., Lorke, D. E., Petroianu, G., & Oz, M. (2022). Cannabidiol Inhibits Multiple Ion Channels in Rabbit Ventricular Cardiomyocytes. *Front Pharmacol*, *13*, 821758. https://doi.org/10.3389/fphar.2022.821758
43. Janssen, P. M., & Periasamy, M. (2007). Determinants of frequency-dependent contraction and relaxation of mammalian myocardium. *J Mol Cell Cardiol*, *43*(5), 523-531. https://doi.org/10.1016/j.yjmcc.2007.08.012
44. Jensen-Urstad, K., Saltin, B., Ericson, M., Storck, N., & Jensen-Urstad, M. (1997). Pronounced resting bradycardia in male elite runners is associated with high heart rate variability. *Scand J Med Sci Sports*, *7*(5), 274-278. https://doi.org/10.1111/j.1600-0838.1997.tb00152.x
45. Johnson, E. K., Springer, S. J., Wang, W., Dranoff, E. J., Zhang, Y., Kanter, E. M., Yamada, K. A., & Nerbonne, J. M. (2018). Differential Expression and Remodeling of Transient Outward Potassium Currents in Human Left Ventricles. *Circ Arrhythm Electrophysiol*, *11*(1), e005914. https://doi.org/10.1161/CIRCEP.117.005914
46. Jost, N., Nagy, N., Corici, C., Kohajda, Z., Horvath, A., Acsai, K., Biliczki, P., Levijoki, J., Pollesello, P., Koskelainen, T., Otsomaa, L., Toth, A., Papp, J. G., Varro, A., & Virag, L. (2013). ORM-10103, a novel specific inhibitor of the Na+/Ca2+ exchanger, decreases early and delayed afterdepolarizations in the canine heart. *Br J Pharmacol*, *170*(4), 768-778. https://doi.org/10.1111/bph.12228
47. Jost, N., Virag, L., Bitay, M., Takacs, J., Lengyel, C., Biliczki, P., Nagy, Z., Bogats, G., Lathrop, D. A., Papp, J. G., & Varro, A. (2005). Restricting excessive cardiac action potential and QT prolongation: a vital role for IKs in human ventricular muscle. *Circulation*, *112*(10), 1392-1399. https://doi.org/10.1161/CIRCULATIONAHA.105.550111
48. Jost, N., Virag, L., Comtois, P., Ordog, B., Szuts, V., Seprenyi, G., Bitay, M., Kohajda, Z., Koncz, I., Nagy, N., Szel, T., Magyar, J., Kovacs, M., Puskas, L. G., Lengyel, C., Wettwer, E., Ravens, U., Nanasi, P. P., Papp, J. G., . . . Nattel, S. (2013). Ionic mechanisms limiting cardiac repolarization reserve in humans compared to dogs. *J Physiol*, *591*(17), 4189-4206. https://doi.org/10.1113/jphysiol.2013.261198
49. Joukar, S. (2021). A comparative review on heart ion channels, action potentials and electrocardiogram in rodents and human: extrapolation of experimental insights to clinic. *Lab Anim Res*, *37*(1), 25. https://doi.org/10.1186/s42826-021-00102-3
50. Kalla, A., Krishnamoorthy, P. M., Gopalakrishnan, A., & Figueredo, V. M. (2018). Cannabis use predicts risks of heart failure and cerebrovascular accidents: results from the National Inpatient Sample. *J Cardiovasc Med (Hagerstown)*, *19*(9), 480-484. https://doi.org/10.2459/JCM.0000000000000681
51. Karbassi, E., Fenix, A., Marchiano, S., Muraoka, N., Nakamura, K., Yang, X., & Murry, C. E. (2020). Cardiomyocyte maturation: advances in knowledge and implications for

regenerative medicine. *Nat Rev Cardiol*, *17*(6), 341-359. https://doi.org/10.1038/s41569-019-0331-x

52. Katona, P. G., McLean, M., Dighton, D. H., & Guz, A. (1982). Sympathetic and parasympathetic cardiac control in athletes and nonathletes at rest. *J Appl Physiol Respir Environ Exerc Physiol*, *52*(6), 1652-1657. https://doi.org/10.1152/jappl.1982.52.6.1652
53. Kohajda, Z., Virag, L., Hornyik, T., Husti, Z., Sztojkov-Ivanov, A., Nagy, N., Horvath, A., Varga, R., Prorok, J., Szlovak, J., Toth, N., Gazdag, P., Topal, L., Naveed, M., Arpadffy-Lovas, T., Paszti, B., Magyar, T., Koncz, I., Deri, S., . . . Varro, A. (2022). In vivo and cellular antiarrhythmic and cardiac electrophysiological effects of desethylamiodarone in dog cardiac preparations. *Br J Pharmacol*, *179*(13), 3382-3402. https://doi.org/10.1111/bph.15812
54. Kristof, A., Husti, Z., Koncz, I., Kohajda, Z., Szel, T., Juhasz, V., Biliczki, P., Jost, N., Baczko, I., Papp, J. G., Varro, A., & Virag, L. (2012). Diclofenac prolongs repolarization in ventricular muscle with impaired repolarization reserve. *PLoS One*, *7*(12), e53255. https://doi.org/10.1371/journal.pone.0053255
55. Kui, P., Orosz, S., Takacs, H., Sarusi, A., Csik, N., Rarosi, F., Cseko, C., Varro, A., Papp, J. G., Forster, T., Farkas, A. S., & Farkas, A. (2016). New in vitro model for proarrhythmia safety screening: IKs inhibition potentiates the QTc prolonging effect of IKr inhibitors in isolated guinea pig hearts. *J Pharmacol Toxicol Methods*, *80*, 26-34. https://doi.org/10.1016/j.vascn.2016.04.005
56. Kui, P., Polyak, A., Morvay, N., Tiszlavicz, L., Nagy, N., Ordog, B., Takacs, H., Lepran, I., Farkas, A., Papp, J. G., Jost, N., Varro, A., Baczko, I., & Farkas, A. S. (2021). Long-Term Endurance Exercise Training Alters Repolarization in a New Rabbit Athlete's Heart Model. *Front Physiol*, *12*, 741317. https://doi.org/10.3389/fphys.2021.741317
57. La Fountaine, M. F., Gossett, J. D., De Meersman, R. E., & Bauman, W. A. (2011). Increased QT interval variability in 3 recently concussed athletes: an exploratory observation. *J Athl Train*, *46*(3), 230-233. https://doi.org/10.4085/1062-6050-46.3.230
58. Lachenmeier, D. W., & Diel, P. (2019). A Warning against the Negligent Use of Cannabidiol in Professional and Amateur Athletes. *Sports (Basel)*, *7*(12). https://doi.org/10.3390/sports7120251
59. Lengyel, C., Orosz, A., Hegyi, P., Komka, Z., Udvardy, A., Bosnyak, E., Trajer, E., Pavlik, G., Toth, M., Wittmann, T., Papp, J. G., Varro, A., & Baczko, I. (2011). Increased short-term variability of the QT interval in professional soccer players: possible implications for arrhythmia prediction. *PLoS One*, *6*(4), e18751. https://doi.org/10.1371/journal.pone.0018751
60. Lengyel, C., Varro, A., Tabori, K., Papp, J. G., & Baczko, I. (2007). Combined pharmacological block of I(Kr) and I(Ks) increases short-term QT interval variability and provokes torsades de pointes. *Br J Pharmacol*, *151*(7), 941-951. https://doi.org/10.1038/sj.bjp.0707297
61. Lima, F. D., Stamm, D. N., Della Pace, I. D., Ribeiro, L. R., Rambo, L. M., Bresciani, G., Ferreira, J., Rossato, M. F., Silva, M. A., Pereira, M. E., Ineu, R. P., Santos, A. R., Bobinski, F., Fighera, M. R., & Royes, L. F. (2016). Ibuprofen intake increases exercise time to exhaustion: A possible role for preventing exercise-induced fatigue. *Scand J Med Sci Sports*, *26*(10), 1160-1170. https://doi.org/10.1111/sms.12549

62. Lindsay, M. M., & Dunn, F. G. (2007). Biochemical evidence of myocardial fibrosis in veteran endurance athletes. *Br J Sports Med*, *41*(7), 447-452. https://doi.org/10.1136/bjsm.2006.031534
63. Link, M. S., & Estes, N. A. (2010). Athletes and arrhythmias. *J Cardiovasc Electrophysiol*, *21*(10), 1184-1189. https://doi.org/10.1111/j.1540-8167.2010.01808.x
64. Lippi, G., Franchini, M., Guidi, G. C., & Kean, W. F. (2006). Non-steroidal anti-inflammatory drugs in athletes. *Br J Sports Med*, *40*(8), 661-662; discussion 662-663. https://doi.org/10.1136/bjsm.2006.027342
65. Lundberg, T. R., & Howatson, G. (2018). Analgesic and anti-inflammatory drugs in sports: Implications for exercise performance and training adaptations. *Scand J Med Sci Sports*, *28*(11), 2252-2262. https://doi.org/10.1111/sms.13275
66. Lundy, S. D., Zhu, W. Z., Regnier, M., & Laflamme, M. A. (2013). Structural and functional maturation of cardiomyocytes derived from human pluripotent stem cells. *Stem Cells Dev*, *22*(14), 1991-2002. https://doi.org/10.1089/scd.2012.0490
67. Macor, F., Fagard, R., & Amery, A. (1996). Power spectral analysis of RR interval and blood pressure short-term variability at rest and during dynamic exercise: comparison between cyclists and controls. *Int J Sports Med*, *17*(3), 175-181. https://doi.org/10.1055/s-2007-972828
68. Mahindru, A., Patil, P., & Agrawal, V. (2023). Role of Physical Activity on Mental Health and Well-Being: A Review. *Cureus*, *15*(1), e33475. https://doi.org/10.7759/cureus.33475
69. Malek, L. A., & Bucciarelli-Ducci, C. (2020). Myocardial fibrosis in athletes-Current perspective. *Clin Cardiol*, *43*(8), 882-888. https://doi.org/10.1002/clc.23360
70. Manolis, T. A., Manolis, A. A., & Manolis, A. S. (2019). Cannabis Associated "High" Cardiovascular Morbidity and Mortality: Marijuana Smoke Like Tobacco Smoke? A Deja Vu/Deja Vecu Story? *Mini Rev Med Chem*, *19*(11), 870-879. https://doi.org/10.2174/1389557518666181114113947
71. Manoukian, M. A. C., Migdal, C. W., Tembhekar, A. R., Harris, J. A., & DeMesa, C. (2017). Topical Administration of Ibuprofen for Injured Athletes: Considerations, Formulations, and Comparison to Oral Delivery. *Sports Med Open*, *3*(1), 36. https://doi.org/10.1186/s40798-017-0103-2
72. Maron, B. J. (2007). Hypertrophic cardiomyopathy and other causes of sudden cardiac death in young competitive athletes, with considerations for preparticipation screening and criteria for disqualification. *Cardiol Clin*, *25*(3), 399-414, vi. https://doi.org/10.1016/j.ccl.2007.07.006
73. Mazaleuskaya, L. L., Theken, K. N., Gong, L., Thorn, C. F., FitzGerald, G. A., Altman, R. B., & Klein, T. E. (2015). PharmGKB summary: ibuprofen pathways. *Pharmacogenet Genomics*, *25*(2), 96-106. https://doi.org/10.1097/FPC.0000000000000113
74. McCartney, D., Benson, M. J., Desbrow, B., Irwin, C., Suraev, A., & McGregor, I. S. (2020). Cannabidiol and Sports Performance: a Narrative Review of Relevant Evidence and Recommendations for Future Research. *Sports Med Open*, *6*(1), 27. https://doi.org/10.1186/s40798-020-00251-0

75. Merghani, A., Malhotra, A., & Sharma, S. (2016). The U-shaped relationship between exercise and cardiac morbidity. *Trends Cardiovasc Med*, *26*(3), 232-240. https://doi.org/10.1016/j.tcm.2015.06.005
76. Milani-Nejad, N., & Janssen, P. M. (2014). Small and large animal models in cardiac contraction research: advantages and disadvantages. *Pharmacol Ther*, *141*(3), 235-249. https://doi.org/10.1016/j.pharmthera.2013.10.007
77. Millar, S. A., Stone, N. L., Yates, A. S., & O'Sullivan, S. E. (2018). A Systematic Review on the Pharmacokinetics of Cannabidiol in Humans. *Front Pharmacol*, *9*, 1365. https://doi.org/10.3389/fphar.2018.01365
78. Mitchell, J. H., Haskell, W., Snell, P., & Van Camp, S. P. (2005). Task Force 8: classification of sports. *J Am Coll Cardiol*, *45*(8), 1364-1367. https://doi.org/10.1016/j.jacc.2005.02.015
79. Morganroth, J., Maron, B. J., Henry, W. L., & Epstein, S. E. (1975). Comparative left ventricular dimensions in trained athletes. *Ann Intern Med*, *82*(4), 521-524. https://doi.org/10.7326/0003-4819-82-4-521
80. Nanasi, P. P., Horvath, B., Tar, F., Almassy, J., Szentandrassy, N., Jost, N., Baczko, I., Banyasz, T., & Varro, A. (2021). Canine Myocytes Represent a Good Model for Human Ventricular Cells Regarding Their Electrophysiological Properties. *Pharmaceuticals (Basel)*, *14*(8). https://doi.org/10.3390/ph14080748
81. Nerbonne, J. M., & Guo, W. (2002). Heterogeneous expression of voltage-gated potassium channels in the heart: roles in normal excitation and arrhythmias. *J Cardiovasc Electrophysiol*, *13*(4), 406-409. https://doi.org/10.1046/j.1540-8167.2002.00406.x
82. Nerbonne, J. M., & Kass, R. S. (2005). Molecular physiology of cardiac repolarization. *Physiol Rev*, *85*(4), 1205-1253. https://doi.org/10.1152/physrev.00002.2005
83. Nguyen, T. P., Qu, Z., & Weiss, J. N. (2014). Cardiac fibrosis and arrhythmogenesis: the road to repair is paved with perils. *J Mol Cell Cardiol*, *70*, 83-91. https://doi.org/10.1016/j.yjmcc.2013.10.018
84. Nieman, D. C., Henson, D. A., Dumke, C. L., Oley, K., McAnulty, S. R., Davis, J. M., Murphy, E. A., Utter, A. C., Lind, R. H., McAnulty, L. S., & Morrow, J. D. (2006). Ibuprofen use, endotoxemia, inflammation, and plasma cytokines during ultramarathon competition. *Brain Behav Immun*, *20*(6), 578-584. https://doi.org/10.1016/j.bbi.2006.02.001
85. Niwa, N., & Nerbonne, J. M. (2010). Molecular determinants of cardiac transient outward potassium current (I(to)) expression and regulation. *J Mol Cell Cardiol*, *48*(1), 12-25. https://doi.org/10.1016/j.yjmcc.2009.07.013
86. O'Hara, T., & Rudy, Y. (2012). Quantitative comparison of cardiac ventricular myocyte electrophysiology and response to drugs in human and nonhuman species. *Am J Physiol Heart Circ Physiol*, *302*(5), H1023-1030. https://doi.org/10.1152/ajpheart.00785.2011
87. Odening, K. E., Gomez, A. M., Dobrev, D., Fabritz, L., Heinzel, F. R., Mangoni, M. E., Molina, C. E., Sacconi, L., Smith, G., Stengl, M., Thomas, D., Zaza, A., Remme, C. A., & Heijman, J. (2021). ESC working group on cardiac cellular electrophysiology position paper: relevance, opportunities, and limitations of experimental models for cardiac electrophysiology research. *Europace*, *23*(11), 1795-1814. https://doi.org/10.1093/europace/euab142

88. Oh, Y., Yang, S., Liu, X., Jana, S., Izaddoustdar, F., Gao, X., Debi, R., Kim, D. K., Kim, K. H., Yang, P., Kassiri, Z., Lakin, R., & Backx, P. H. (2020). Transcriptomic Bioinformatic Analyses of Atria Uncover Involvement of Pathways Related to Strain and Post-translational Modification of Collagen in Increased Atrial Fibrillation Vulnerability in Intensely Exercised Mice. *Front Physiol*, *11*, 605671. https://doi.org/10.3389/fphys.2020.605671
89. Orvos, P., Paszti, B., Topal, L., Gazdag, P., Prorok, J., Polyak, A., Kiss, T., Toth-Molnar, E., Csupor-Loffler, B., Bajtel, A., Varro, A., Hohmann, J., Virag, L., & Csupor, D. (2020). The electrophysiological effect of cannabidiol on hERG current and in guinea-pig and rabbit cardiac preparations. *Sci Rep*, *10*(1), 16079. https://doi.org/10.1038/s41598-020-73165-2
90. Ozturk, H. M., Yetkin, E., & Ozturk, S. (2019). Synthetic Cannabinoids and Cardiac Arrhythmia Risk: Review of the Literature. *Cardiovasc Toxicol*, *19*(3), 191-197. https://doi.org/10.1007/s12012-019-09522-z
91. Palatini, P., Maraglino, G., Sperti, G., Calzavara, A., Libardoni, M., Pessina, A. C., & Dal Palu, C. (1985). Prevalence and possible mechanisms of ventricular arrhythmias in athletes. *Am Heart J*, *110*(3), 560-567. https://doi.org/10.1016/0002-8703(85)90075-4
92. Panchal, N. K., & Prince Sabina, E. (2023). Non-steroidal anti-inflammatory drugs (NSAIDs): A current insight into its molecular mechanism eliciting organ toxicities. *Food Chem Toxicol*, *172*, 113598. https://doi.org/10.1016/j.fct.2022.113598
93. Paszti, B., Prorok, J., Magyar, T., Arpadffy-Lovas, T., Gyore, B., Topal, L., Gazdag, P., Szlovak, J., Naveed, M., Jost, N., Nagy, N., Varro, A., Virag, L., & Koncz, I. (2021). Cardiac electrophysiological effects of ibuprofen in dog and rabbit ventricular preparations: possible implication to enhanced proarrhythmic risk. *Can J Physiol Pharmacol*, *99*(1), 102-109. https://doi.org/10.1139/cjpp-2020-0386
94. Pelliccia, A., Di Paolo, F. M., & Maron, B. J. (2002). The athlete's heart: remodeling, electrocardiogram and preparticipation screening. *Cardiol Rev*, *10*(2), 85-90. https://doi.org/10.1097/00045415-200203000-00006
95. Peritz, D. C., Catino, A. B., Csecs, I., Kaur, G., Kheirkhahan, M., Loveless, B., Wasmund, S., Kholmovski, E., Morris, A., & Marrouche, N. F. (2020). High-intensity endurance training is associated with left atrial fibrosis. *Am Heart J*, *226*, 206-213. https://doi.org/10.1016/j.ahj.2020.05.015
96. Pigozzi, F., & Rizzo, M. (2008). Sudden death in competitive athletes. *Clin Sports Med*, *27*(1), 153-181, ix. https://doi.org/10.1016/j.csm.2007.09.004
97. Piktel, J. S., & Wilson, L. D. (2019). Translational Models of Arrhythmia Mechanisms and Susceptibility: Success and Challenges of Modeling Human Disease. *Front Cardiovasc Med*, *6*, 135. https://doi.org/10.3389/fcvm.2019.00135
98. Pluim, B. M., Zwinderman, A. H., van der Laarse, A., & van der Wall, E. E. (2000). The athlete's heart. A meta-analysis of cardiac structure and function. *Circulation*, *101*(3), 336-344. https://doi.org/10.1161/01.cir.101.3.336
99. Polyak, A., Kui, P., Morvay, N., Lepran, I., Agoston, G., Varga, A., Nagy, N., Baczko, I., Farkas, A., Papp, J. G., Varro, A., & Farkas, A. S. (2018). Long-term endurance training-induced cardiac adaptation in new rabbit and dog animal models of the human athlete's heart. *Rev Cardiovasc Med*, *19*(4), 135-142. https://doi.org/10.31083/j.rcm.2018.04.4161

100. Polyak, A., Topal, L., Zombori-Toth, N., Toth, N., Prorok, J., Kohajda, Z., Deri, S., Demeter-Haludka, V., Hegyi, P., Venglovecz, V., Agoston, G., Husti, Z., Gazdag, P., Szlovak, J., Arpadffy-Lovas, T., Naveed, M., Sarusi, A., Jost, N., Virag, L., . . . Varro, A. (2023). Cardiac electrophysiological remodeling associated with enhanced arrhythmia susceptibility in a canine model of elite exercise. *Elife*, *12*. https://doi.org/10.7554/eLife.80710
101. Pratt, C. M., Hertz, R. P., Ellis, B. E., Crowell, S. P., Louv, W., & Moye, L. (1994). Risk of developing life-threatening ventricular arrhythmia associated with tefenadine in comparison with over-the-counter antihistamines, ibuprofen and clemastine. *Am J Cardiol*, *73*(5), 346-352. https://doi.org/10.1016/0002-9149(94)90006-x
102. Rainsford, K. D. (2009). Ibuprofen: pharmacology, efficacy and safety. *Inflammopharmacology*, *17*(6), 275-342. https://doi.org/10.1007/s10787-009-0016-x
103. Rajanayagam, J., & Alsabri, M. (2021). Intense Endurance Exercise: A Potential Risk Factor in the Development of Heart Disease. *Cureus*, *13*(1), e12608. https://doi.org/10.7759/cureus.12608
104. Rapin, L., Gamaoun, R., El Hage, C., Arboleda, M. F., & Prosk, E. (2021). Cannabidiol use and effectiveness: real-world evidence from a Canadian medical cannabis clinic. *J Cannabis Res*, *3*(1), 19. https://doi.org/10.1186/s42238-021-00078-w
105. Ratliff, N. B., Harris, K. M., Smith, S. A., Tankh-Johnson, M., Gornick, C. C., & Maron, B. J. (2002). Cardiac arrest in a young marathon runner. *Lancet*, *360*(9332), 542. https://doi.org/10.1016/S0140-6736(02)09744-1
106. Redfern, W. S., Carlsson, L., Davis, A. S., Lynch, W. G., MacKenzie, I., Palethorpe, S., Siegl, P. K., Strang, I., Sullivan, A. T., Wallis, R., Camm, A. J., & Hammond, T. G. (2003). Relationships between preclinical cardiac electrophysiology, clinical QT interval prolongation and torsade de pointes for a broad range of drugs: evidence for a provisional safety margin in drug development. *Cardiovasc Res*, *58*(1), 32-45. https://doi.org/10.1016/s0008-6363(02)00846-5
107. Robyns, T., Lu, H. R., Gallacher, D. J., Garweg, C., Ector, J., Willems, R., Janssens, S., & Nuyens, D. (2016). Evaluation of Index of Cardio-Electrophysiological Balance (iCEB) as a New Biomarker for the Identification of Patients at Increased Arrhythmic Risk. *Ann Noninvasive Electrocardiol*, *21*(3), 294-304. https://doi.org/10.1111/anec.12309
108. Roden, D. M. (2004). Human genomics and its impact on arrhythmias. *Trends Cardiovasc Med*, *14*(3), 112-116. https://doi.org/10.1016/j.tcm.2004.01.001
109. Roden, D. M. (2006). Long QT syndrome: reduced repolarization reserve and the genetic link. *J Intern Med*, *259*(1), 59-69. https://doi.org/10.1111/j.1365-2796.2005.01589.x
110. Roden, D. M. (2008). Repolarization reserve: a moving target. *Circulation*, *118*(10), 981-982. https://doi.org/10.1161/CIRCULATIONAHA.108.798918
111. Rojas-Valverde, D. (2021). Potential Role of Cannabidiol on Sports Recovery: A Narrative Review. *Front Physiol*, *12*, 722550. https://doi.org/10.3389/fphys.2021.722550
112. Rosenbloom, C. J., Morley, F. L., Ahmed, I., & Cox, A. R. (2020). Oral non-steroidal anti-inflammatory drug use in recreational runners participating in Parkrun UK: Prevalence of use and awareness of risk. *Int J Pharm Pract*, *28*(6), 561-568. https://doi.org/10.1111/ijpp.12646

113. Ruegsegger, G. N., & Booth, F. W. (2018). Health Benefits of Exercise. *Cold Spring Harb Perspect Med*, *8*(7). https://doi.org/10.1101/cshperspect.a029694
114. Schouten, E. G., Dekker, J. M., Meppelink, P., Kok, F. J., Vandenbroucke, J. P., & Pool, J. (1991). QT interval prolongation predicts cardiovascular mortality in an apparently healthy population. *Circulation*, *84*(4), 1516-1523. https://doi.org/10.1161/01.cir.84.4.1516
115. Sellers, E. M., Schoedel, K., Bartlett, C., Romach, M., Russo, E. B., Stott, C. G., Wright, S., White, L., Duncombe, P., & Chen, C. F. (2013). A Multiple-Dose, Randomized, Double-Blind, Placebo-Controlled, Parallel-Group QT/QTc Study to Evaluate the Electrophysiologic Effects of THC/CBD Spray. *Clin Pharmacol Drug Dev*, *2*(3), 285-294. https://doi.org/10.1002/cpdd.36
116. Serpell, M. G., Notcutt, W., & Collin, C. (2013). Sativex long-term use: an open-label trial in patients with spasticity due to multiple sclerosis. *J Neurol*, *260*(1), 285-295. https://doi.org/10.1007/s00415-012-6634-z
117. Sondergaard, K. B., & Gislason, G. (2017). NSAIDs and cardiac arrest: Non-steroidal anti-inflammatory drug use is associated with increased risk of Out-of-hospital Cardiac Arrest: A nationwide Case-Time-Control study. *Eur Heart J*, *38*(23), 1788-1789. https://doi.org/10.1093/eurheartj/ehx267
118. Sondergaard, K. B., Weeke, P., Wissenberg, M., Schjerning Olsen, A. M., Fosbol, E. L., Lippert, F. K., Torp-Pedersen, C., Gislason, G. H., & Folke, F. (2017). Non-steroidal anti-inflammatory drug use is associated with increased risk of out-of-hospital cardiac arrest: a nationwide case-time-control study. *Eur Heart J Cardiovasc Pharmacother*, *3*(2), 100-107. https://doi.org/10.1093/ehjcvp/pvw041
119. Stampanoni Bassi, M., Sancesario, A., Morace, R., Centonze, D., & Iezzi, E. (2017). Cannabinoids in Parkinson's Disease. *Cannabis Cannabinoid Res*, *2*(1), 21-29. https://doi.org/10.1089/can.2017.0002
120. Sutherland, F. J., & Hearse, D. J. (2000). The isolated blood and perfusion fluid perfused heart. *Pharmacol Res*, *41*(6), 613-627. https://doi.org/10.1006/phrs.1999.0653
121. Thomas, B. L., & Viljoen, M. (2019). Heart Rate Variability and Academic Performance of First-Year University Students. *Neuropsychobiology*, *78*(4), 175-181. https://doi.org/10.1159/000500613
122. Topal, L., Naveed, M., Orvos, P., Paszti, B., Prorok, J., Bajtel, A., Kiss, T., Csupor-Loffler, B., Csupor, D., Baczko, I., Varro, A., Virag, L., & Jost, N. (2021). The electrophysiological effects of cannabidiol on action potentials and transmembrane potassium currents in rabbit and dog cardiac ventricular preparations. *Arch Toxicol*, *95*(7), 2497-2505. https://doi.org/10.1007/s00204-021-03086-0
123. Topal, L., Polyak, A., Toth, N., Agoston, G., Bencsik, P., Kohajda, Z., Prorok, J., Deri, S., Nagy, N., Jost, N., Virag, L., Farkas, A. S., Varro, A., & Baczko, I. (2022). Endurance training-induced cardiac remodeling in a guinea pig athlete's heart model. *Can J Physiol Pharmacol*, *100*(10), 993-1004. https://doi.org/10.1139/cjpp-2022-0073
124. Van Wijck, K., Lenaerts, K., Van Bijnen, A. A., Boonen, B., Van Loon, L. J., Dejong, C. H., & Buurman, W. A. (2012). Aggravation of exercise-induced intestinal injury by Ibuprofen in athletes. *Med Sci Sports Exerc*, *44*(12), 2257-2262. https://doi.org/10.1249/MSS.0b013e318265dd3d

125. Varro, A., & Baczko, I. (2010). Possible mechanisms of sudden cardiac death in top athletes: a basic cardiac electrophysiological point of view. *Pflugers Arch*, *460*(1), 31-40. https://doi.org/10.1007/s00424-010-0798-0
126. Varro, A., & Baczko, I. (2011). Cardiac ventricular repolarization reserve: a principle for understanding drug-related proarrhythmic risk. *Br J Pharmacol*, *164*(1), 14-36. https://doi.org/10.1111/j.1476-5381.2011.01367.x
127. Varro, A., Balati, B., Iost, N., Takacs, J., Virag, L., Lathrop, D. A., Csaba, L., Talosi, L., & Papp, J. G. (2000). The role of the delayed rectifier component IKs in dog ventricular muscle and Purkinje fibre repolarization. *J Physiol*, *523 Pt 1*(Pt 1), 67-81. https://doi.org/10.1111/j.1469-7793.2000.00067.x
128. Varro, A., Tomek, J., Nagy, N., Virag, L., Passini, E., Rodriguez, B., & Baczko, I. (2021). Cardiac transmembrane ion channels and action potentials: cellular physiology and arrhythmogenic behavior. *Physiol Rev*, *101*(3), 1083-1176. https://doi.org/10.1152/physrev.00024.2019
129. Virag, L., Jost, N., Papp, R., Koncz, I., Kristof, A., Kohajda, Z., Harmati, G., Carbonell-Pascual, B., Ferrero, J. M., Jr., Papp, J. G., Nanasi, P. P., & Varro, A. (2011). Analysis of the contribution of I(to) to repolarization in canine ventricular myocardium. *Br J Pharmacol*, *164*(1), 93-105. https://doi.org/10.1111/j.1476-5381.2011.01331.x
130. Wang, Y., & Ashokan, K. (2021). Physical Exercise: An Overview of Benefits From Psychological Level to Genetics and Beyond. *Front Physiol*, *12*, 731858. https://doi.org/10.3389/fphys.2021.731858
131. Wang, Z., Feng, J., Shi, H., Pond, A., Nerbonne, J. M., & Nattel, S. (1999). Potential molecular basis of different physiological properties of the transient outward K+ current in rabbit and human atrial myocytes. *Circ Res*, *84*(5), 551-561. https://doi.org/10.1161/01.res.84.5.551
132. Warden, S. J. (2010). Prophylactic use of NSAIDs by athletes: a risk/benefit assessment. *Phys Sportsmed*, *38*(1), 132-138. https://doi.org/10.3810/psm.2010.04.1770
133. Warner, D. C., Schnepf, G., Barrett, M. S., Dian, D., & Swigonski, N. L. (2002). Prevalence, attitudes, and behaviors related to the use of nonsteroidal anti-inflammatory drugs (NSAIDs) in student athletes. *J Adolesc Health*, *30*(3), 150-153. https://doi.org/10.1016/s1054-139x(01)00325-1
134. Wilson, M., O'Hanlon, R., Prasad, S., Deighan, A., Macmillan, P., Oxborough, D., Godfrey, R., Smith, G., Maceira, A., Sharma, S., George, K., & Whyte, G. (2011). Diverse patterns of myocardial fibrosis in lifelong, veteran endurance athletes. *J Appl Physiol (1985)*, *110*(6), 1622-1626. https://doi.org/10.1152/japplphysiol.01280.2010
135. Wisniowska, B., Tylutki, Z., Wyszogrodzka, G., & Polak, S. (2016). Drug-drug interactions and QT prolongation as a commonly assessed cardiac effect - comprehensive overview of clinical trials. *BMC Pharmacol Toxicol*, *17*, 12. https://doi.org/10.1186/s40360-016-0053-1
136. Wolfes, J., Ellermann, C., Baumer, S., Fehr, M., Willy, K., Wegner, F., Leitz, P. R., Eckardt, L., & Frommeyer, G. (2022). Experimental evidence for proarrhythmic effects of nonsteroidal anti-inflammatory drugs in a sensitive whole-heart model. *Basic Clin Pharmacol Toxicol*, *130*(1), 103-109. https://doi.org/10.1111/bcpt.13671

137. Yang, Z. F., Wang, H. W., Zheng, Y. Q., Zhang, Y., Liu, Y. M., & Li, C. Z. (2008). Possible arrhythmiogenic mechanism produced by ibuprofen. *Acta Pharmacol Sin*, *29*(4), 421-429. https://doi.org/10.1111/j.1745-7254.2008.00754.x
138. Yarishkin, O. V., Hwang, E. M., Kim, D., Yoo, J. C., Kang, S. S., Kim, D. R., Shin, J. H., Chung, H. J., Jeong, H. S., Kang, D., Han, J., Park, J. Y., & Hong, S. G. (2009). Diclofenac, a Non-steroidal Anti-inflammatory Drug, Inhibits L-type Ca Channels in Neonatal Rat Ventricular Cardiomyocytes. *Korean J Physiol Pharmacol*, *13*(6), 437-442. https://doi.org/10.4196/kjpp.2009.13.6.437
139. Yun, J., Yoon, K. S., Lee, T. H., Lee, H., Gu, S. M., Song, Y. J., Cha, H. J., Han, K. M., Seo, H., Shin, J., Park, H. K., Kim, H. S., & Kim, Y. H. (2016). Synthetic cannabinoid, JWH-030, induces QT prolongation through hERG channel inhibition. *Toxicol Res (Camb)*, *5*(6), 1663-1671. https://doi.org/10.1039/c6tx00259e
140. Zgair, A., Wong, J. C., Lee, J. B., Mistry, J., Sivak, O., Wasan, K. M., Hennig, I. M., Barrett, D. A., Constantinescu, C. S., Fischer, P. M., & Gershkovich, P. (2016). Dietary fats and pharmaceutical lipid excipients increase systemic exposure to orally administered cannabis and cannabis-based medicines. *Am J Transl Res*, *8*(8), 3448-3459. https://www.ncbi.nlm.nih.gov/pubmed/27648135
141. Zhang, C. D., Xu, S. L., Wang, X. Y., Tao, L. Y., Zhao, W., & Gao, W. (2020). Prevalence of Myocardial Fibrosis in Intensive Endurance Training Athletes: A Systematic Review and Meta-Analysis. *Front Cardiovasc Med*, *7*, 585692. https://doi.org/10.3389/fcvm.2020.585692
142. Zicha, S., Moss, I., Allen, B., Varro, A., Papp, J., Dumaine, R., Antzelevich, C., & Nattel, S. (2003). Molecular basis of species-specific expression of repolarizing K+ currents in the heart. *Am J Physiol Heart Circ Physiol*, *285*(4), H1641-1649. https://doi.org/10.1152/ajpheart.00346.2003
143. Zicha, S., Xiao, L., Stafford, S., Cha, T. J., Han, W., Varro, A., & Nattel, S. (2004). Transmural expression of transient outward potassium current subunits in normal and failing canine and human hearts. *J Physiol*, *561*(Pt 3), 735-748. https://doi.org/10.1113/jphysiol.2004.075861
144. Ziltener, J. L., Leal, S., & Fournier, P. E. (2010). Non-steroidal anti-inflammatory drugs for athletes: an update. *Ann Phys Rehabil Med*, *53*(4), 278-282, 282-278. https://doi.org/10.1016/j.rehab.2010.03.001
145. Zorzi, A., Vio, R., Bettella, N., & Corrado, D. (2020). Criteria for interpretation of the athlete's ECG: A critical appraisal. *Pacing Clin Electrophysiol*, *43*(8), 882-890. https://doi.org/10.1111/pace.14001

I.

Canadian Journal of Physiology and Pharmacology

Article

Endurance training-induced cardiac remodeling in a guinea pig athlete's heart model

L. Topal[a], **A. Polyák**[a,b], **N. Tóth**[a], **G. Ágoston**[c], **P. Bencsik**[a], **Zs. Kohajda**[d], **J. Prorok**[a,d], **Sz. Déri**[a], **N. Nagy**[a,d], **N. Jost**[a,d,e], **L. Virág**[a,e], **A.S. Farkas**[f], **A. Varró**[a,d,e], **and I. Baczkó**[a,e]

[a]Department of Pharmacology and Pharmacotherapy, University of Szeged, Szeged, 6720, Hungary; [b]Department of Pediatrics and Pediatric Health Center, University of Szeged, Szeged, 6725, Hungary; [c]Institute of Family Medicine, University of Szeged, Szeged, 6720, Hungary; [d]ELKH-SZTE Research Group of Cardiovascular Pharmacology, Szeged, Hungary; [e]Department of Pharmacology and Pharmacotherapy, Interdisciplinary Excellence Centre, University of Szeged, Szeged, 6720, Hungary; [f]Department of Internal Medicine, Cardiology, University of Szeged, Szeged, 6725, Hungary

Corresponding author: **András Varró** (email: varro.andras@med.u-szeged.hu)

Abstract

Besides the health benefits of regular exercise, high-level training—above an optimal level—may have adverse effects. In this study, we investigated the effects of long-term vigorous training and its potentially detrimental structural–functional changes in a small animal athlete's heart model. Thirty-eight 4-month-old male guinea pigs were randomized into sedentary and exercised groups. The latter underwent a 15-week-long endurance-training program. To investigate the effects of the intense long-term exercise, in vivo (echocardiography, electrocardiography), ex vivo, and in vitro (histopathology, patch-clamp) measurements were performed. Following the training protocol, the exercised animals exhibited structural left ventricular enlargement and a significantly higher degree of myocardial fibrosis. Furthermore, resting bradycardia accompanied by elevated heart rate variability occurred, representing increased parasympathetic activity in the exercised hearts. The observed prolonged QTc intervals and increased repolarization variability parameters may raise the risk of electrical instability in exercised animals. Complex arrhythmias did not occur in either group, and there were no differences between the groups in ex vivo or cellular electrophysiological experiments. Accordingly, the high parasympathetic activity may promote impaired repolarization in conscious exercised animals. The detected structural–functional changes share similarities with the human athlete's heart; therefore, this model might be useful for investigations on cardiac remodeling.

Key words: long-term endurance training, cardiac remodeling, echocardiography, electrocardiography, histology

Résumé

En dehors des bienfaits pour la santé qu'apporte l'exercice physique régulier, l'entraînement de haut niveau – au-delà d'un degré optimal – pourrait avoir des effets indésirables. Cette étude portait sur les effets de l'entraînement vigoureux à long terme de même que sur des variations structurelles ou fonctionnelles potentiellement délétères dans un modèle de cœur d'athlète chez un petit animal. Nous avons réparti aléatoirement 38 cobayes mâles âgés de 4 mois dans des groupes de sédentarité et d'exercice physique. Les animaux de ce dernier groupe ont suivi un programme d'entraînement en endurance sur 15 semaines. Nous avons procédé à des épreuves in vivo (échocardiographie, électrocardiographie), ex vivo et in vitro (histopathologie, « patch-clamp ») en vue d'étudier les effets de l'exercice intense à long terme. À la suite du protocole, les animaux entraînés ont présenté une augmentation structurelle de la taille du ventricule gauche et une augmentation marquée du degré de fibrose myocardique. En outre, nous avons observé une bradycardie au repos accompagnée d'une augmentation de la variabilité de la fréquence cardiaque chez les animaux entraînés, ce qui représente une augmentation de l'activité parasympathique cardiaque dans leur cas. La prolongation des intervalles QTc et la hausse des paramètres de la variabilité de la repolarisation pourraient entraîner un accroissement du risque d'instabilité électrique chez les animaux entraînés. Nous n'avons pas observé d'arythmies complexes dans l'un ou l'autre groupe, ni de différence entre eux quant aux mesures ex vivo ou dans le cadre des expériences d'électrophysiologie cellulaire. Conséquemment, l'augmentation de l'activité parasympathique à des degrés élevés pourrait favoriser l'apparition d'anomalies de la repolarisation chez les animaux entraînés

conscients. Les variations structurelles et fonctionnelles que nous avons décelées présentent des points communs avec le cœur d'athlète chez l'humain. Par conséquent, ce modèle pourrait être utile en vue d'étudier le remodelage cardiaque. [Traduit par la Rédaction]

Mots-clés : entraînement en endurance à long terme, remodelage cardiaque, échocardiographie, électrocardiographie, histologie

Introduction

The positive impact of regular exercise on a healthy and fulfilling lifestyle is undoubted (Deslandes et al. 2009; Lavie et al. 2019). Therefore, active athletes are considered the healthiest members of our society. Regular and intense long-term training can elicit reversible structural and functional adaptation of the heart, called the "athlete's heart". Despite its beneficial impacts, there is an increasing amount of evidence that long-term high-intensity sporting activity may also have adverse effects beyond an "optimal dose" (Eijsvogels et al. 2018). As pointed out previously by Maron (2007), sudden cardiac death (SCD) occurs more frequently among active athletes who participate in sporting activities with high dynamic and low isometric intensity like football and basketball players. Recently, an increasing number of studies have investigated the presence of fibrosis in human endurance racers (Malek and Bucciarelli-Ducci 2020; Zhang et al. 2020; Rajanayagam and Alsabri 2021). In addition, the long-term heavy training-induced heart adaptation can also be associated with other pathological conditions (e.g., hypertrophic cardiomyopathy, arrhythmogenic right ventricular cardiomyopathy, or congenital coronary artery anomaly), which in turn, increase the incidence of cardiac arrhythmias and even SCD (Corrado et al. 2003; Alpert et al. 2015). Although SCD is rare in young top athletes, it occurs approximately two to four times more often than in the age-matched control population (Marijon et al. 2011). Furthermore, in a significant number of cases, the cause of malignant arrhythmias and even SCD cannot be verified satisfactorily. Although many screening strategies are known, the early detection of increased susceptibility for these unexpected events in apparently healthy individuals is challenging. In addition, in a number of cases, autopsy findings remain negative (Asif et al. 2013), suggesting that there must be uninvestigated and still unknown causes behind these tragic events that claim deeper examination. It is hypothesized that altered cardiac morphology and impaired cardiac repolarization can be arrhythmogenic substrates that may underline the development of malignant ventricular arrhythmias following long-term heavy training, although the exact mechanisms are still unclear (Varro and Baczko 2010).

The underlying mechanisms responsible for the development of malignant arrhythmias in the athlete's heart are still unclear; therefore, there is a critical need to investigate cardiac remodeling in animal models with a significant translational value for the human heart. The goals of this study were to develop an animal model that was relevant to the human athlete's heart and to assess mechanisms underlying cardiac structural–electrical changes due to long-term endurance training.

Materials and methods

Ethical issues

The experiments were carried out in compliance with the *Guide for the Care and Use of Laboratory Animals* (USA NIH publication No. 85-23, revised 1996) and conformed to Directive 2010/63/EU of the European Parliament. The protocols have been approved by the Ethical Committee for the Protection of Animals in Research of the University of Szeged, Szeged, Hungary, and by the Department of Animal Health and Food Control of the Ministry of Agriculture and Rural Development (authority approval number XIII/2163/2019).

Experimental protocol

Male albino Dunkin–Hartley guinea pigs with initial weights of 300–350 g were randomly assigned to exercised ("EXE", $n = 19$) and sedentary ("SED", $n = 19$) groups. The guinea pigs from both groups were 4-month-old at the beginning of the training protocol.

Running sessions were performed on a special rodent treadmill system (Treadmill for rats, Elunit Group/Elunit Medical Equipment, Belgrade, Serbia) with four separated corridors for the animals and controllable gradient and speed intensity. The exercised group underwent a 15-week-long training session, while the sedentary animals did not participate in the training. However, they were subjected to the same handling procedure as the exercised animals (including placement on the treadmill) to avoid differences originating from different animal handling. The protocol started with a 2-week-long warm-up period (to get accustomed to handling, non-invasive in vivo ECG measurements, and treadmill running); thereafter, the exercised group underwent a progressive endurance-training program combined with interval training sessions. The animals were trained five times a week with 60–90 min daily running sessions. To enhance the strain, the speed and the grade of the treadmill were increased progressively every week until reaching 0.6–1.92 km/h and 14% inclination. The training protocol was tested in preliminary experiments and set to the maximum level that could be performed without significant distress to the animals.

Electrocardiography

In conscious guinea pigs, ECGs were recorded using precordial leads at the 15th week without any pain or stress. The ECGs were recorded with National Instruments data acquisition hardware (PC card, National Instruments, Austin, TX., USA) and SPEL Advanced Haemosys software (version 3.26, MDE Heidelberg GmbH, Heidelberg, Germany). The records were digitalized and stored on a computer for later analysis.

RR, PQ, QRS, and QT intervals were measured by manual positioning of screen markers of 40 consecutive sinus beats at the 10th minute after initiation of the recording, then mean values were calculated. As QT interval is influenced by the heart rate, baseline data for ventricular heart rates and QT intervals were used to determine the relationship between the RR interval and the consecutive QT interval in sinus rhythm as described previously (Polyak et al. 2018). These data were obtained from 38 guinea pigs in vivo. Forty consecutive QT intervals were measured together with the corresponding RR intervals. Simple linear regression revealed a positive correlation between QT and RR intervals in guinea pigs (QT = 0.55 × RR + 9.31). The equation was rearranged to allow the calculation of the rate-corrected QT interval in guinea pigs at an RR interval of 182 ms using the formula $QT_{cx} = QT_x - 0.55 \times (RR_{(x-1)} - 182)$. With these equations, plotting QT_c against the corresponding RR interval produces a regression line with a slope of zero, indicating that these corrections remove the influence of the heart rate.

Measurement of the beat-to-beat variability and instability of the ECG intervals

Beat-to-beat variability and instability parameters of the RR and QT intervals (e.g., the "root mean square of the successive differences", the "standard deviation of the successive differences", the "short-term variability", "long-term variability", "long-term instability", and "instability" of the ECG intervals) were derived and calculated from 60 consecutive sinus beats as described previously (Polyak et al. 2018).

Echocardiography

Transthoracic echocardiographic examination was performed at the 15th week of the training protocol in conscious animals. M-mode parasternal long axis view was applied using 11.5 MHz transducer (GE 10S-RS, GE Healthcare, Chicago, IL, USA), connected to an echocardiographic imaging unit (Vivid S5, GE Healthcare, Chicago, IL, USA). All parameters were analyzed by an expert cardiologist in a randomized and blinded manner. Left ventricular internal diameter during systole (LVIDs) and diastole (LVIDd), thickness of the left ventricular posterior wall at systole (LVPWs), interventricular septum (IVS), and end ejection fraction (EF) were measured in M-mode images. The wall thickness and diameter parameters were corrected with the animal's body weight. Fractional shortening (FS) was calculated as FS = [(LVIDd − LVIDs)/LVIDd] × 100].

Ex vivo electrophysiological measurements in isolated Langendorff perfused guinea pig hearts and in vitro histopathology

Of 38 guinea pigs, 12 were used for ex vivo Langendorff measurements and thereafter for in vitro histopathological experiments ("EXE" $n = 6$, "SED" $n = 6$). The method of Langendorff perfusion we used was described in detail (Kui et al. 2016). The animals were anticoagulated with sodium heparin (1000 international units) injected intraperitoneally and were over-anesthetized with thiopental-sodium (80 mg/kg intraperitoneally), then their hearts were excised and attached to a vertical Langendorff apparatus. Throughout the experiments, Krebs–Henseleit buffer solution was used containing (in mM): NaCl 118.5, glucose 11.1, $MgSO_4$ 0.5, NaH_2PO_4 1.2, KCl 4.3, $NaHCO_3$ 25.0, and $CaCl_2$ 1.8. The experimental protocol started with a 20-min equilibration period. This was followed by a 30-min-long period when the ECG recordings were performed.

Subsequently, the hearts were removed from the apparatus and cardiac tissue samples were fixed using a formaldehyde solution. Samples were taken from the subendocardial region of the atria, septal, and ventricular free wall for histological studies. Paraffin sections of the hearts were subjected to Crossmon's trichrome staining (Crossmon 1937) to identify collagen deposition. Semi-quantitative analysis was performed by an external pathologist in a blinded manner to assess the degree of the interstitial fibrosis by evaluating the samples on a semiquantitative scoring scale: 0 = no fibrosis, 1 = moderate fibrosis, 2 = severe fibrosis.

Isolation of single myocardial myocytes

Twenty-six guinea pig hearts ("EXE" $n = 13$, "SED" $n = 13$) were used for in vitro cellular electrophysiological experiments. The termination of the animals is described in detail above. Hearts were excised rapidly and immersed in a cold (4 °C) Ca^{2+}-containing isolation solution composed of (in mM) $CaCl_2$ 0.75, NaCl 135, KCl 4.7, KH_2PO_4 1.2, $MgSO_4$ 1.2, HEPES 10 glucose 10, Taurine 35, sodium pyruvate 5, and pH adjusted to 7.4 with NaOH. Thereafter, each heart was cannulated and retrogradely perfused via the aorta on a Langendorff apparatus with a Ca^{2+}-containing isolation solution at the constant temperature of 37 °C for 10 min with a composition described above. The hearts then were perfused with Ca^{2+}-free isolation solution for a period of 8–10 min. Finally, the perfusion was completed with a solution containing 0.8 g/L collagenase (type II, Worthington), 0.1 g/L proteinase (type XIV, Sigma–Aldrich), 100 μm $CaCl_2$, and the heart was perfused for a further 10–15 min with this solution. At the end of the enzymatic dissociation process, the left ventricular myocardium was minced and gently agitated. Freshly isolated cells were placed in a storage solution with a high concentration of potassium, containing (in mM): L-glutamic acid monohydrate 203.2, Taurine 125.15, KCl 74.55, KH_2PO_4 136.09, HEPES 238.3, $MgCl_2$ 203.31, glucose 180.16, EGTA 380.35, pH adjusted to 7.3 with KOH before use.

Voltage-clamp measurements

The full methodology of transmembrane ionic current measurements using the whole-cell configuration was described in detail in our previously published studies. Manual patch-clamp recordings of transmembrane currents were undertaken using rectangular command pulses for slow delayed rectifier potassium current (I_{Ks}) (Topal et al. 2021), late sodium current (I_{NaL}) (Hezso et al. 2021) measurements, and voltage ramp for the Na^+/Ca^{2+} exchanger current (I_{NCX}) (Hobai et al. 1997; Otsomaa et al. 2020). Experiments were carried out at 37 °C.

Fig. 1. Echocardiographic cardiac dimensions in conscious guinea pigs following 15-week-long endurance training. The wall thicknesses and diameter parameters were corrected with the animal's body weight. LVIDd, end-diastolic left ventricular internal diameter (A); IVSd, end-diastolic interventricular septal wall thickness (B); LVPWs, end-systolic left ventricular posterior wall thickness (C). All values are means ± SEM. $^{*}P < 0.05$, unpaired *t*-test, "EXE" versus "SED" guinea pig.

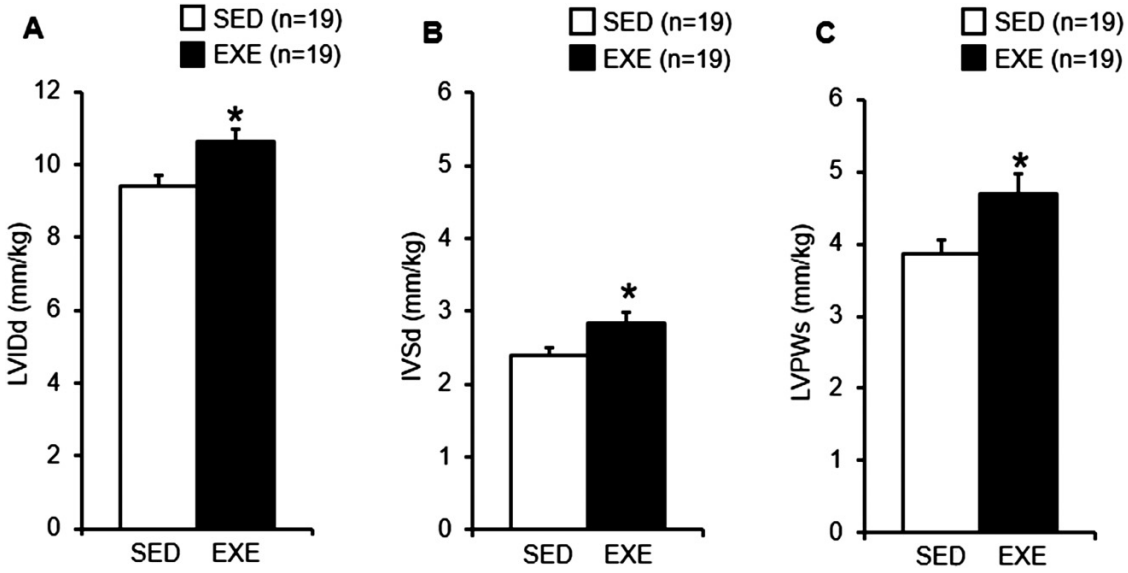

Measurements of single cell action potentials

The perforated patch-clamp technique was used to measure action potentials from isolated left ventricular myocytes from both exercised and sedentary animals. The membrane potential was recorded in the current-clamp configuration. The myocytes were paced with a rapid rectangular pulse (from 0 to 180 mV, 5 ms) at a frequency of 1 Hz to elicit the action potential. A HEPES- Tyrode solution was used as the extracellular solution (composition in mM: NaCl 144, NaH_2PO_4 0.4, KCl 4.0, $CaCl_2$ 1.8, $MgSO_4$ 0.53, glucose 5.5 and HEPES 5.0, at pH of 7.4) served as normal superfusate. The patch pipette solution contained (in mM): 120 K-gluconate, 2.5 NaCl, 2.5 MgATP, 2.5 Na_2ATP, 5 HEPES, 20 KCl, titrated to pH 7.2 with KOH. 50 μM β-escin was added to the pipette solution to achieve the membrane patch perforation. Membrane voltage was obtained by using an Axoclamp 1-D amplifier (Molecular Devices, Sunnyvale, CA, USA) connected to a Digidata 1440 A (Molecular Devices, Sunnyvale, CA, USA) analog-digital converter. The membrane voltage was recorded by Clampex 10.0 (Molecular Devices, Sunnyvale, CA, USA). At least 60 beats were recorded, and the action potential duration was measured at 90% of repolarization (APD_{90}). The short-term APD (STV-APD) variability was calculated by analyzing 30 consecutive action potentials described above.

Statistical analysis

IBM SPSS Statistics V25 software package was used for statistical analysis. Continuous data were expressed as mean ± standard error of the mean (SEM). Unpaired Student's *t*-test was applied to whether there was a statistically significant difference between the means in independent groups, respectively. Data were considered statistically significant when $p < 0.05$.

Results

Structural echocardiographic parameters

The 15-week-long high-intensity endurance-training program resulted in the following significantly greater echocardiographic parameters at diastole (corrected for body weight): the internal dimension of the left ventricle (LVIDd) (Fig. 1A) and the interventricular septum thickness (IVSd) (Fig. 1B). In addition, a significant increase was also observed in the LVPWs in exercised guinea pigs (Fig. 1C). An increased tendency was detected in the left ventricular end-systolic dimension (LVIDs) in the exercised group compared to the sedentary animals, although it did not reach statistical significance ("EXE" vs. "SED": 5.1 ± 0.4 vs. 4.3 ± 0.3, $p > 0.05$). The EF and the FS were not different between the two groups (EF: "EXE" vs. "SED": 86.1 ± 1.9 vs. 87.4 ± 2.2, $p > 0.05$, FS: "EXE" vs. "SED": 52.9 ± 2.5 vs. 54.9 ± 2.7, $p > 0.05$). The structural changes detected by echocardiography are shown in Fig. 1.

Long-term endurance training-induced fibrosis

A significantly higher degree of fibrosis manifested in the subendocardial region of the right atria, the right ventricle, and in the septal wall of the hearts in the exercised group compared to sedentary animals and, in addition, enhanced fibrosis was also present in the left ventricle, although it did not reach statistical significance (Fig. 2).

Effects of endurance training on heart rate and PQ and QRS intervals of the ECG

In conscious animals, the 15-week long-term endurance-training program resulted in significantly lengthened RR intervals in the exercised group (Fig. 3A), representing training-induced bradycardia. However, after sympathetic

Fig. 2. Enhanced myocardial fibrosis in the exercised guinea pig hearts. Upper panels (A, B, C), representative histological images using Crossmon's trichrome staining taken from sedentary control (A, fibrosis score 0) and exercised guinea pigs (B, fibrosis score 1 and C, fibrosis score 2). The estimation of the amount of scarring via fibrosis scoring (D) and bar charts showing the presence of fibrosis within the groups, expressed as the percentage of the total number of animals, irrespective of the degree of fibrosis (E) in sedentary and exercised guinea pigs. Semi-quantitative analysis was performed to score the degree of the interstitial fibrosis with the following criteria: 0 = no fibrosis; 1 = moderate fibrosis; 2 = severe fibrosis. $^{*}P < 0.05$, unpaired *t*-test; "EXE" versus "SED" guinea pig.

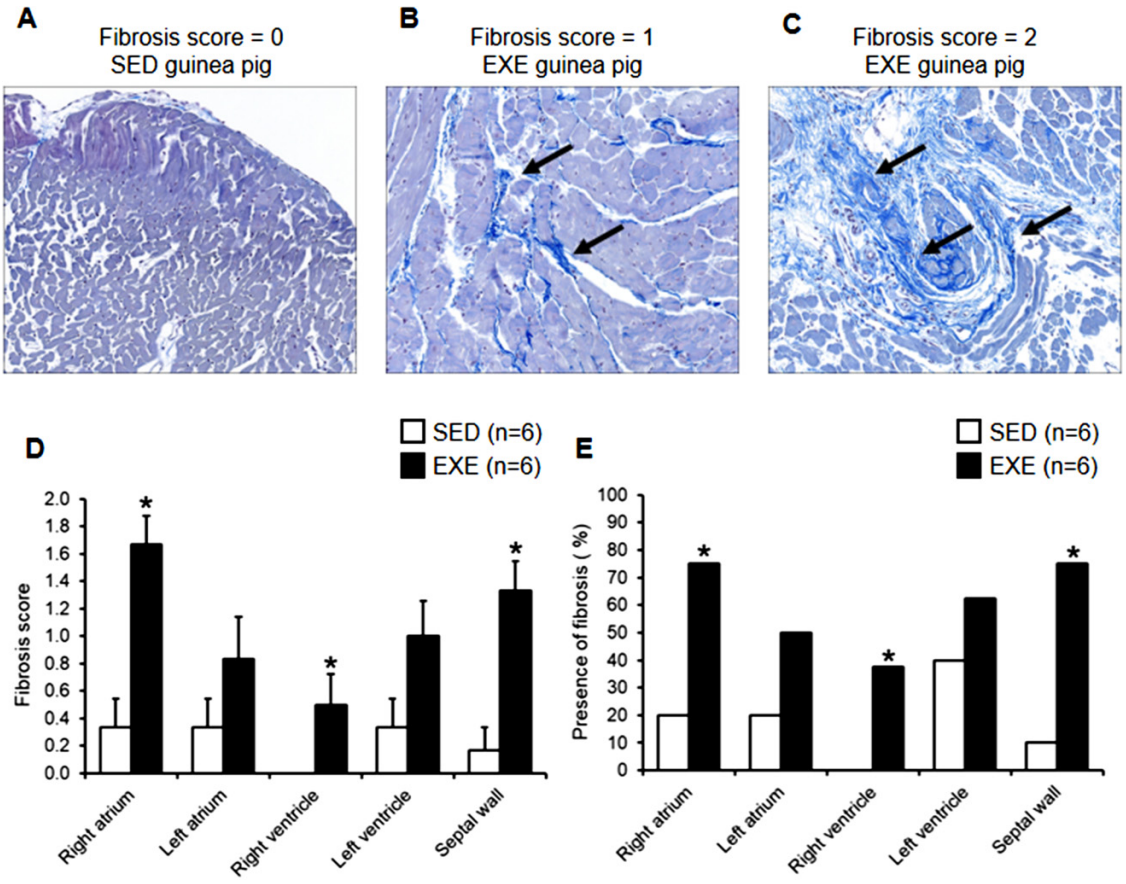

and parasympathetic denervation, the RR intervals did not differ significantly between the groups during ex vivo Langendorff experiments (Fig. 3B), which support the prominent influence of the parasympathetic nervous system on training-induced resting bradycardia.

The beat-to-beat variabilities, including root mean square of the successive differences (rmsSD) (Fig. 3C) and standard deviation of successive differences (sdSD) of the RR intervals in exercised animals significantly increased compared to the sedentary group (Fig. 3D), representing the influence of the increased parasympathetic tone.

There was no statistically significant difference during in vivo ECG measurements in PQ intervals ("EXE" vs. "SED": 55.0 ± 1.5 vs. 51.9 ± 1.2 ms, $p > 0.05$), but the QRS interval was significantly widened in the exercised group compared to sedentary animals by the end of the training protocol ("EXE" vs. "SED": 51.8 ± 1.5 vs. 45.6 ± 1.0 ms, $p < 0.05$). The PQ and QRS intervals were not different between the two groups in ex vivo Langendorff experiments. (PQ: "EXE" vs. "SED": 54.0 ± 2.0 vs. 59.4 ± 2.3 ms, $p > 0.05$, QRS: "EXE" vs. "SED": 30.9 ± 1.02 vs. 29.7 ± 1.2 ms, $p > 0.05$).

Effects of endurance exercise on ECG repolarization parameters and their beat-to-beat variabilities

In in vivo measurements, significantly prolonged QT intervals were detected in the exercised group compared to sedentary animals at the 15th week (Fig. 4A). Since the heart rate influences the length of the QT interval, the heart rate-corrected QT interval (QTc) was calculated as described above. The QTc of the exercised animals was significantly longer compared to untrained animals at rest (Fig. 4B). The short-term beat-to-beat variability of the QT interval (STV-QT) that characterizes the instability of cardiac ventricular repolarization was elevated in the exercised group; however, it did not reach statistically significant difference (Fig. 4C). Other beat-to-beat variability parameters of repolarization were calculated (including long-term variability (LTV), long-term instability (LTI), instability (I)), and an increased tendency was observed in these parameters, but none reached a statistically significant difference (LTV-QT: "EXE" vs. "SED": 3.2 ± 0.2 vs. 2.7 ± 0.2 ms, $p > 0.05$, LTI-QT: "EXE" vs. "SED": 2.8 ± 0.2 vs.

Fig. 3. The effect of long-term endurance training on RR intervals and their beat-to-beat variabilities in conscious guinea pigs and in ex vivo Langendorff experiments. The mean RR intervals in conscious guinea pigs (A) and the mean RR intervals in ex vivo Langendorff experiments (B). The RR variability parameters in conscious guinea pigs (C, D). All values were derived and calculated from 60 consecutive ventricular complexes during sinus rhythm at the 15th week. rmsSD, root mean square of successive differences; sdSD, the standard deviation of successive differences of the RR intervals. Representative figures of beat-to-beat heart rate in conscious sedentary (E) and exercised (F) guinea pigs at the end of the endurance training program. All values are means ± SEM. $^{*}P < 0.05$, unpaired *t*-test; "EXE" versus "SED" guinea pig.

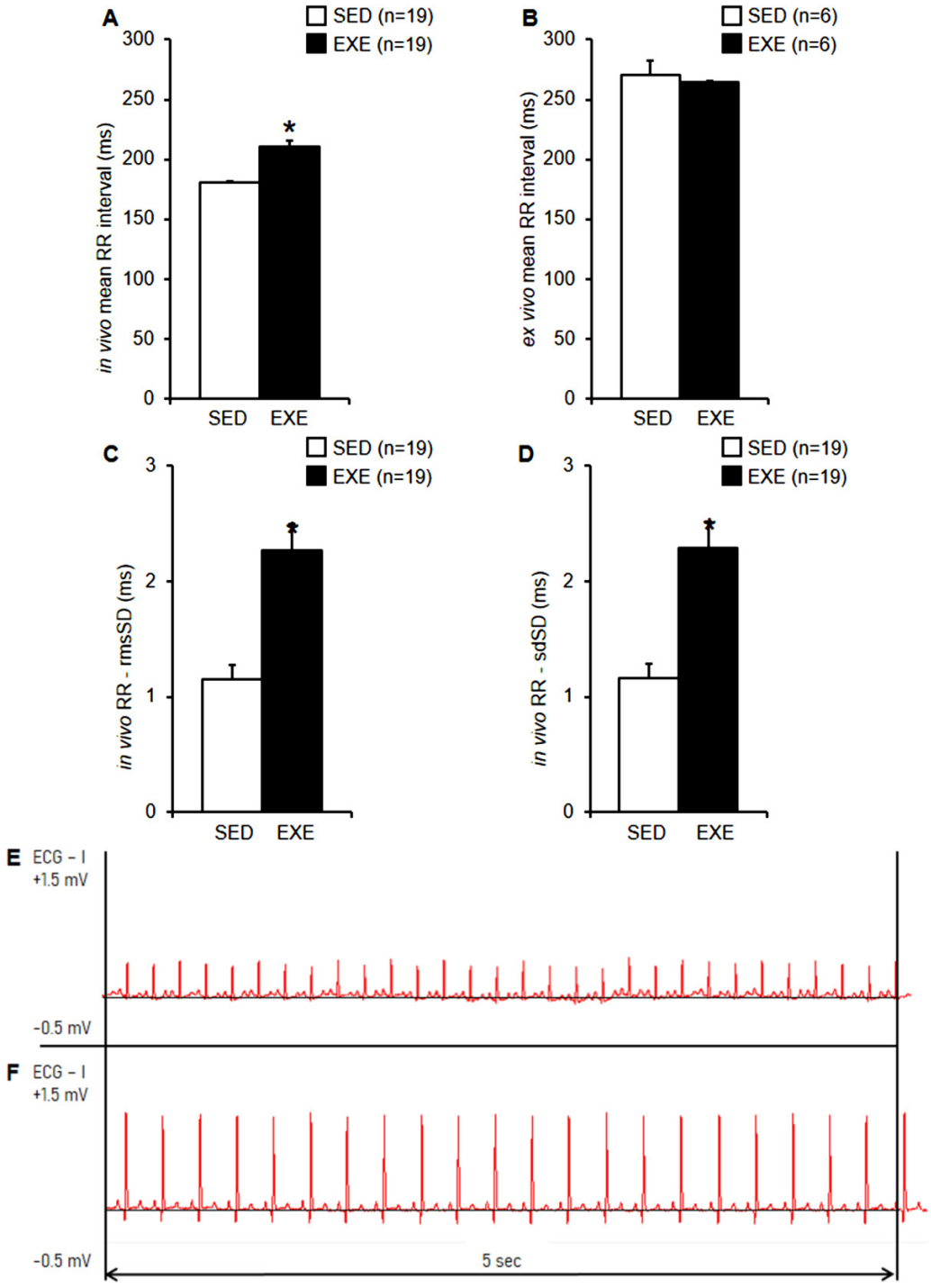

2.4 ± 0.2 ms, $p > 0.05$, I-QT: "EXE" vs. "SED": 4.8 ± 0.3 vs. 4.3 ± 0.3 ms, $p > 0.05$).

Similar to unchanged RR intervals, there were no substantial differences in QT intervals between the groups in ex vivo Langendorff experiments ("EXE" vs. "SED": 133.1 ± 2.2 vs. 131.7 ± 2.6 ms, $p > 0.05$).

No cardiac arrhythmias were observed during in vivo ECG recordings in either group. Although a few ventricular

Fig. 4. Effect of sustained training on the ECG QT interval and its beat-to-beat variability parameters as markers of repolarization inhomogeneity. The QT interval (A), the heart rate corrected QT interval (QTc) (B), and short-term variability of QT interval (STV-QT) of the ECG (C) in conscious guinea pigs at the 15th week. All values were derived and calculated from 40 consecutive ventricular complexes during sinus rhythm. Representative figures of the length of QT interval in conscious sedentary (E) and exercised (F) guinea pigs at the end of the endurance training program. All values are means ± SEM. *$P < 0.05$, unpaired *t*-test; "EXE" versus "SED" guinea pig.

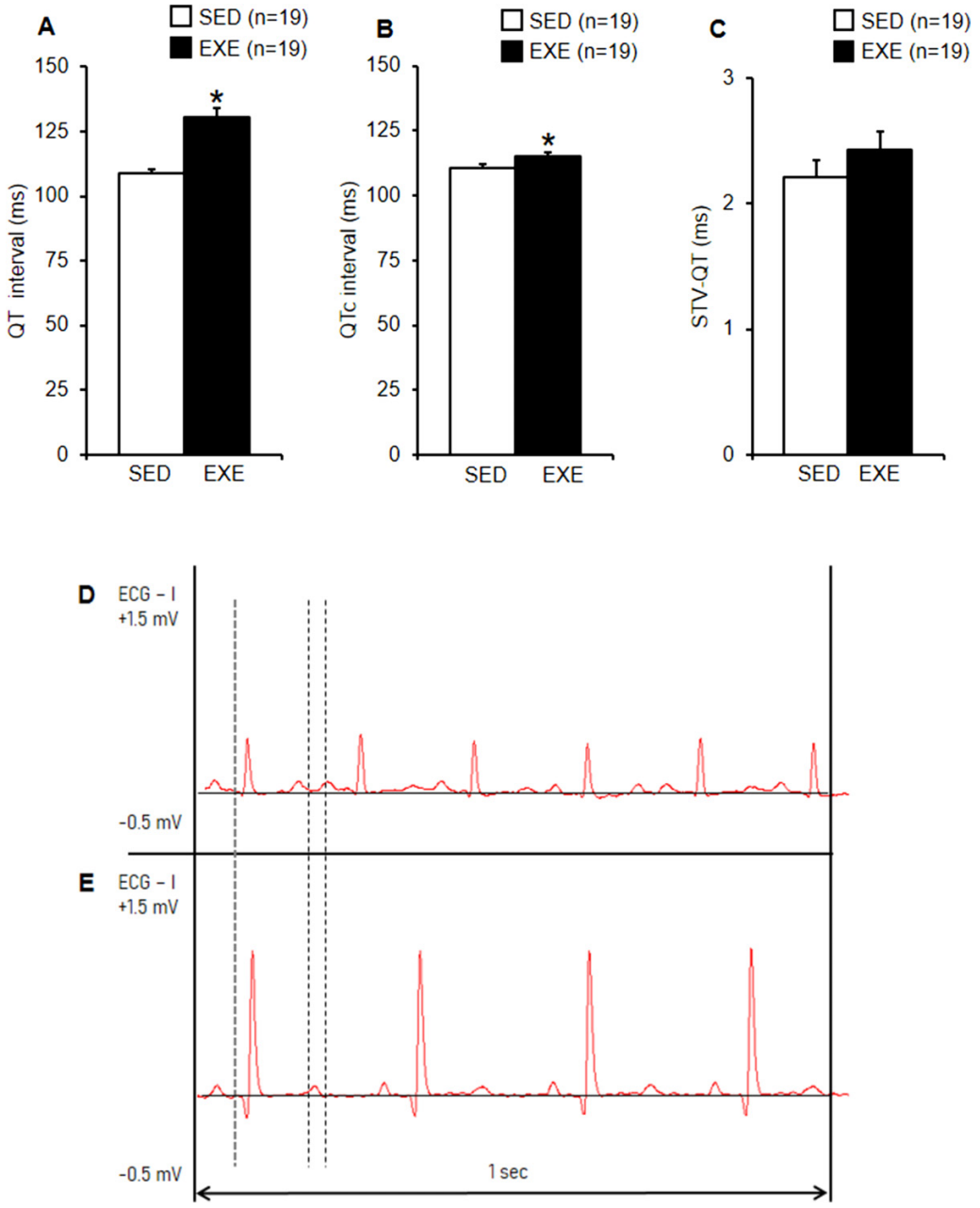

arrhythmias were detected in both groups during ex vivo Langendorff experiments, there were no differences in numbers and complexity of these arrhythmias between the groups (data not shown).

Cellular electrophysiological properties in exercised and in sedentary guinea pig hearts

Under the current exercise training protocol and experimental measuring conditions, the magnitudes of I_{Ks}, I_{NaL}, and I_{NCX} in native guinea pig ventricular myocytes showed no significant differences between the exercised and sedentary groups (I_{Ks} at + 50 mV: "EXE" vs. "SED": 2.1 ± 0.2 pA/pF vs. 1.8 ± 0.2 pA/pF $p > 0.05$, I_{NaL}: "EXE" vs. "SED": 0.4 ± 0.02 pA/pF vs. 0.5 ± 0.03 pA/pF $p > 0.05$, I_{NCX} at + 20 mV: 1.4 ± 0.1 pA/pF vs. 1.4 ± 0.1 pA/pF, $I_{NCX,}$ at − 80 mV: −0.9 ± 0.1 pA/pF vs. −1.0 ± 0.1 pA/pF $p > 0.05$).

In agreement with these data, there was no significant difference in APD_{90} length in myocytes isolated from the left ventricle of the exercised group compared to the sedentary

group ("EXE" vs. "SED": 347.0 ± 10.6 ms vs. 337.2 ± 13.3 ms, $p > 0.05$). The short-term variability of action potential duration did not differ significantly between the groups (STV-APD: "EXE" vs. "SED" 8.6 ± 0.7 ms vs. 8,4 ± 0.7 ms, $p > 0.05$).

Discussion

This study investigated the effect of 15-week-long endurance training on a newly developed guinea pig model that has similar baseline cardiac electrophysiological properties as the human heart, unlike commonly used rodent models (e.g., rat and mouse) with a lack of action potential plateau phase and have several other electrophysiological differences.

On the basis of echocardiographic and histological findings, the present training protocol led to structural cardiac remodeling, including increased left ventricular dimensions and incipient myocardium enlargement. In addition, a higher degree of fibrosis developed that may impart heart vulnerability to adverse events like malignant cardiac arrhythmias. Significant resting bradycardia and increased heart rate variabilities were observed in consciously exercised guinea pigs. On the contrary, however, the heart rate parameters showed no differences between the examined groups in ex vivo experiments. These findings support the idea that the observed changes may relate to the increased vagal tone due to intense training. The significantly prolonged QT and QTc intervals and the elevated variability parameters of the repolarization (including short-term variability, long-term variability, long-term-instability, and instability) represent impaired repolarization and higher repolarization instability (Thomsen et al. 2004; Lengyel et al. 2007) in conscious exercised animals; however, there were no signs of these changes in ex vivo Langendorff experiments. Moreover, in the case of in vitro cellular electrophysiological experiments, neither the measured transmembrane ionic currents nor the isolated cellular action potential durations and the variability of cellular action potential durations showed significant differences between the groups.

These in vivo and in vitro electrophysiological findings suggest that the observed changes may relate to the enhanced parasympathetic tone following the currently used endurance-training protocol.

Animal models of the human heart

To our knowledge, this is the first study on exercised guinea pigs that evaluates detailed structural and functional cardiac alterations following long-term endurance training.

Rodents are widely used laboratory animals because of their several advantages, including low maintenance cost, easy housing, and handling (Milani-Nejad and Janssen 2014). There are a variety of mouse and rat athlete's heart models in the literature (Chu et al. 2000; Benito et al. 2011; Radovits et al. 2013), but their translational values to humans must be interpreted with caution. The heart rate of small rodents is much higher than those in larger animals and humans; thus both the systolic and diastolic phases of the myocardium are faster to maintain cardiac output (Janssen and Periasamy 2007). As a consequence, there are marked electrophysiological differences at the cellular level, e.g., shorter action potential duration, a rapid repolarization time, and the lack of plateau phase (Farraj et al. 2011).

Guinea pigs are widely used small animals in the field of cardiovascular research that shares the same logistical and financial benefits as rats and mice, however, with additional advantages. This has its origin in the average conscious resting heart rate is lower in guinea pigs, and ventricular action potentials exhibit a distinct plateau phase unlike in smaller rodents (Farraj et al. 2011). Also, ionic currents and QT interval characteristics are similar to those of larger non-rodent laboratory animals (e.g., rabbit, dog) with a significant translational value to the human heart (Jost et al. 2013; Baczko et al. 2016; Nanasi et al. 2021). In addition, the primary repolarizing ionic currents in guinea pig hearts are I_{Ks} and I_{Kr} (Farraj et al. 2011; O'Hara and Rudy 2012) and which have an uncertain role in rats or mice; however, the main repolarizing transmembrane ionic currents in the human myocardium that are thought to be damaged because of heavy long-term exercise. These similarities of the guinea pig to the human myocardium make the model a closer representation of the human heart.

Structural cardiac changes after long-term heavy endurance training

The frequency of training and the specific nature of each sporting activity have a great impact on the physiological cardiac response and adaptation (Morganroth et al. 1975). The regular isotonic exercises associated with endurance sports (e.g., long-distance running, swimming, road cycling) usually result in cardiac enlargement (increased left ventricular cavity dimension); however, obvious cardiac hypertrophy (increase in left ventricular wall thickness) is not present in every case (D'Andrea et al., 2010; Morganroth et al. 1975; Mitchell et al. 2005, 2010). Our structural and hemodynamic echocardiographic results correspond to previously observed long-term high dynamic demand training-induced cardiac adaptation in human athlete's heart. This study found that the left ventricular muscle began to dilate and enlarge after long-term endurance training, similar to the result of Polyak et al. (2018). With respect to cardiac function, the EF and FS remained unchanged in our exercised guinea pigs compared to sedentary animals, similar to findings in studies among elite athletes (Pluim et al. 2000).

The effect of long-term intensive endurance exercise on the development of myocardial fibrosis, as a potentially dangerous myocardial arrhythmia substrate, has been previously investigated in several human studies and exercise-trained animal models. La Gerche et al. (2012) showed that cardiac septal fibrosis was found in endurance athletes. Wilson et al. (2011) reported that significant myocardial fibrosis was associated with the increased number of years of endurance training and the number of completed endurance races. Thirdly, Crescenzi et al. (2021) investigated the presence of myocardial fibrosis and scars via high sensitivity cardiac magnetic resonance imaging among 251 competitive athletes. Finally, Benito et al. (2011) clearly detected the presence of fibrosis

after several weeks of endurance training in rats, which seemed to be right chamber-specific. Our histopathological findings are in agreement with these studies that myocardial fibrosis occurs due to long-term intense endurance training. A significantly higher level of fibrosis was documented both in the left and right atrial, septal, and right ventricular regions of the heart, and a near significant similar trend was observed in the left ventricle. Although this structural abnormality is electrocardiographically and echocardiographically silent in most cases, myocardial fibrosis has a great impact because it may modulate the onset and maintenance of re-entry ventricular arrhythmias which can lead to SCD (Balaban et al. 2018; Schelbert 2019).

There may be an association between the structural changes of exercised hearts and significantly prolonged QRS durations in the present study that may create a potential risk for the development of arrhythmias (arrhythmia substrate). However, this hypothesis needs further investigation.

Long-term endurance training-induced vagal tone enhancement

Resting bradycardia due to regular high-intensity exercise is a frequent finding among elite athletes and is considered well-proven in many studies. As highlighted previously, endurance training leads to a lower heart rate at rest due to enhanced vagal activity (Macor et al. 1996; Jensen-Urstad et al. 1997). On the other hand, recently published studies questioned the exclusive role of enhanced vagal activity on exercise-induced resting bradycardia. Accordingly, it was suggested that morphological and electrical remodeling of the sinus node had as a great impact on the resting bradycardia as the changes in vagal tone (Katona et al. 1982; Boyett et al. 2013).

Our findings suggested that this type of training protocol at the applied frequency and intensity did not induce intrinsic remodeling of the sinus node. However, it cannot be ruled out that after more intense and longer endurance training, accompanied by more pronounced bradycardia, the intrinsic remodeling would also have a role. Heart rate variability parameters are widely used as non-invasive markers that mimic the function and responsiveness of the heart and are considered markers of parasympathetic tone (Thomas et al. 2019). Furthermore, these parameters correlate well with physical fitness levels in elite athletes (Buchheit 2014). In the present study, significantly increased in vivo heart rate variability parameters were observed suggesting the effectiveness of the applied training protocol. In addition, overall, these finding supports the idea that the resting bradycardia, accompanied by the increased heart rate variability parameters, was related to the higher parasympathetic activity due to endurance training.

The effect of long-term endurance training on cardiac repolarization

A number of studies suggested a possible link between disease-induced cardiac remodeling (e.g., hypertrophic cardiomyopathy or heart failure) and increased electrical inhomogeneity. For example, similar to the athlete's heart, the failing heart exhibits marked hypertrophy accompanied by prolongation and inhomogeneity of repolarization and impairment of repolarization reserve, and therefore, increased arrhythmia susceptibility (Wang and Hill 2010; Husti et al. 2021). The possible electrophysiological similarities between the abovementioned pathophysiological conditions and the athlete's heart, which is considered as a result of normal physiological adaptation in general, are still unclear.

In our study, the short-term beat-to-beat variability of the QT intervals (STV-QT) was elevated in the conscious exercised animals compared to the sedentary group. As highlighted previously, the STV-QT was significantly increased in elite soccer players (Lengyel et al. 2011). The STV-QT characterizes the instability of cardiac ventricular repolarization and has been shown to predict severe ventricular arrhythmias both in animal experimental (Thomsen et al. 2004; Lengyel et al. 2007) and clinical (Hinterseer et al. 2009, 2010; Varkevisser et al. 2012) settings.

In our present study, increased duration and inhomogeneity of cardiac repolarization were observed in exercised animals at the end of the training program. The observed prolongation in QT intervals can be attributed to increased vagal tone. In guinea pig left ventricular myocytes, the major rate-dependent current is the I_{Ks}, which plays a key role in repolarization (O'Hara and Rudy 2012). Our results suggested an association between the significant resting bradycardia and prolonged QT intervals with the enhanced vagal tone that can influence I_{Ks}. It is well-established that I_{Ks} strongly depends on the intracellular cAMP level and phosphorylation of ionic channels (Gallacher et al. 2007; Thompson et al. 2017). Therefore, an increased parasympathetic tone would decrease intracellular cAMP via G_i-protein and phosphorylation of I_{Ks} channels, resulting in smaller I_{Ks} magnitude and consequent with repolarization prolongation in conscious exercised animals. Moreover, this mechanism does not play a role in Langendorff experiments or in isolated single cells. This can serve as an explanation for the lack of effect on QT interval in ex vivo and on APD_{90} and I_{Ks} magnitude in in vitro settings in the present study.

Limitations

As mild repolarization changes are seen in top athletes and the incidence of malignant arrhythmias is rare, it makes it almost impossible to model it properly in animal experiments. However, this guinea pig model is economical and allows a relatively large sample size. Although there is no native transient outward potassium current (I_{to}) in the guinea pig heart, it has several additional electrophysiological benefits that make this model useful for further investigations of long-term endurance training-induced cardiac remodeling. In our study, mild structural and functional cardiac remodeling occurred following the applied training program. The application of a longer and greater intensity training protocol is warranted in further studies to thoroughly examine the effect of long-term high-intensity endurance training, especially at cellular and molecular levels.

Conclusion

In the present study, a novel guinea pig exercise-induced athlete's heart model was introduced. In our model, similar to the endurance-trained human athlete's heart, a long-term endurance training led to increased left ventricular end-diastolic diameter and moderate enlargement of cardiac muscle due to increased volume load. In addition, mild fibrosis was also present that may also occur in human athlete's heart according to recently published studies. The widened QRS in conscious exercised animals may be associated with structural and functional cardiac remodeling. The in vivo resting bradycardia and increased heart rate variability parameters together with unchanged ex vivo results indicated a higher resting vagal tone in exercised animals. The increased parasympathetic activity led to prolonged QT interval. The increased in vivo QT variability parameters may indicate impaired repolarization and higher repolarization instability in exercised guinea pigs. These findings, after further investigations, may explain the higher risk of developing arrhythmias in human athletes.

Acknowledgements

This work was supported by the National Research, Development and Innovation Office (NKHIF K-119992 to A. V., NKHIF K-128851 to I. B., NKHIF K- 135464, NKFIH PD-125402, FK-129117, GINOP-2.3.2–15-2016–00047, and TKP2021-EGA-32), Hungarian National Scientific Research Fund (OTKA-FK-138223 to P., B) the Ministry of Human Capacities of Hungary (20391–3/2018/FEKUSTRAT and EFOP3.6.2–16-2017–00006), from the Eötvös Loránd Research Network, from the UNKP-20–5-SZTE-165, ÚNKP-21–5-SZTE-543 from the János Bolyai Research Scholarship of the Hungarian Academy of Sciences to N. N., and by the Albert Szent-Györgyi Medical School institutional grant (SZTE ÁOK-KKA 2021 to L. V.).

Article information

History dates

Received: 6 February 2022
Accepted: 9 May 2022
Accepted manuscript online: 14 July 2022
Version of record online: 14 September 2022

Notes

This paper is part of a Collection of selected papers from the IACS European and North American Sections - Banja Luka, Bosnia, and Herzegovina: "Cardiprotection and cardiometabolic diseases: from bench to bedside".

Copyright

Author information

Author ORCIDs

L. Topal https://orcid.org/0000-0003-0663-6352

Author notes

L. Topal and A. Polyák shared the first authorship.

Competing interests

There is no conflict of interest between the authors.

References

Alpert, C., Day, S.M., and Saberi, S. 2015. Sports and exercise in athletes with hypertrophic cardiomyopathy. Clin. Sports Med. **34**: 489–505. doi:10.1016/j.csm.2015.03.005. PMID: 26100424.

Asif, I.M., Rao, A.L., and Drezner, J.A. 2013. Sudden cardiac death in young athletes: what is the role of screening? Curr. Opin. Cardiol. **28**: 55–62. doi:10.1097/HCO.0b013e32835b0ab9. PMID: 23196775.

Baczko, I., Jost, N., Virag, L., Bosze, Z., and Varro, A. 2016. Rabbit models as tools for preclinical cardiac electrophysiological safety testing: importance of repolarization reserve. Prog. Biophys. Mol. Biol. **121**: 157–168. doi:10.1016/j.pbiomolbio.2016.05.002. PMID: 27208697.

Balaban, G., Halliday, B.P., Mendonca Costa, C., Bai, W., Porter, B. Rinaldi, C.A., et al. 2018. Fibrosis microstructure modulates reentry in non-ischemic dilated cardiomyopathy: insights from imaged guided 2D computational modeling. Front Physiol. **9**: 1832. doi:10.3389/fphys.2018.01832. PMID: 30618838.

Benito, B., Gay-Jordi, G., Serrano-Mollar, A., Guasch, E., Shi, Y. Tardif, J. C., et al. 2011. Cardiac arrhythmogenic remodeling in a rat model of long-term intensive exercise training. Circulation, **123**: 13–22. doi:10.1161/CIRCULATIONAHA.110.938282. PMID: 21173356.

Boyett, M.R., D'Souza, A., Zhang, H., Morris, G.M., Dobrzynski, H., and Monfredi, O. 2013. Viewpoint: Is the resting bradycardia in athletes the result of remodeling of the sinoatrial node rather than high vagal tone? J. Appl. Physiol. (1985). **114**: 1351–1355. doi:10.1152/japplphysiol.01126.2012. PMID: 23288551.

Buchheit, M. 2014. Monitoring training status with HR measures: Do all roads lead to Rome? Front. Physiol. **5**: 73. doi:10.3389/fphys.2014.00073. PMID: 24578692.

Chu, T.F., Huang, T.Y., Jen, C.J., and Chen, H.I. 2000. Effects of chronic exercise on calcium signaling in rat vascular endothelium. Am. J. Physiol. Heart Circ. Physiol. **279**: H1441–H1446. doi:10.1152/ajpheart.2000.279.4.H1441. PMID: 11009427.

Corrado, D., Basso, C., Rizzoli, G., Schiavon, M., and Thiene, G. 2003. Does sports activity enhance the risk of sudden death in adolescents and young adults? J. Am. Coll. Cardiol. **42**: 1959–1963. doi:10.1016/j.jacc.2003.03.002. PMID: 14662259.

Crescenzi, C., Zorzi, A., Vessella, T., Martino, A., Panattoni, G. Cipriani, A., et al. 2021. Predictors of left ventricular scar using cardiac magnetic resonance in athletes with apparently idiopathic ventricular arrhythmias. J. Am. Heart Assoc. **10**: e018206. doi:10.1161/JAHA.120.018206. PMID: 33381977.

Crossmon, G. 1937. A modification of Mallory's connective tissue stain with a discussion of the principles involved. Anat. Rec. **69**: 33–38. doi:10.1002/ar.1090690105.

D'Andrea, A., Cocchia, R., Riegler, L., Scarafile, R., Salerno, G. Gravino, R., et al. 2010. Left ventricular myocardial velocities and deformation indexes in top-level athletes. J. Am. Soc. Echocardiogr. **23**: 1281–1288. doi:10.1016/j.echo.2010.09.020. PMID: 21111925.

Deslandes, A., Moraes, H., Ferreira, C., Veiga, H., Silveira, H. Mouta, R., et al. 2009. Exercise and mental health: many reasons to move. Neuropsychobiology, **59**: 191–198. doi:10.1159/000223730. PMID: 19521110.

Eijsvogels, T.M.H., Thompson, P.D., and Franklin, B.A. 2018. The "extreme exercise hypothesis": recent findings and cardiovascular health implications. Curr. Treat. Options Cardiovasc. Med. **20**: 84. doi:10.1007/s11936-018-0674-3. PMID: 30155804.

Farraj, A.K., Hazari, M.S., and Cascio, W.E. 2011. The utility of the small rodent electrocardiogram in toxicology. Toxicol. Sci. **121**: 11–30. doi:10.1093/toxsci/kfr021. PMID: 21278051.

Gallacher, D.J., Van de Water, A., Van der Linde, H., Hermans, A.N., Lu, H.R., Towart, R., and Volders, P.G. 2007. In vivo mechanisms precipitating torsades de pointes in a canine model of drug-induced

long-QT1 syndrome. Cardiovasc. Res. **76**: 247–256. doi:10.1016/j.cardiores.2007.06.019. PMID: 17669388.

Hezso, T., Naveed, M., Dienes, C., Kiss, D., Prorok, J. Arpadffy-Lovas, T., et al. 2021. Mexiletine-like cellular electrophysiological effects of GS967 in canine ventricular myocardium. Sci. Rep. **11**: 9565. doi:10.1038/s41598-021-88903-3. PMID: 33953276.

Hinterseer, M., Beckmann, B.M., Thomsen, M.B., Pfeufer, A., Dalla Pozza, R. Loeff, M., et al. 2009. Relation of increased short-term variability of QT interval to congenital long-QT syndrome. Am. J. Cardiol. **103**: 1244–1248. doi:10.1016/j.amjcard.2009.01.011. PMID: 19406266.

Hinterseer, M., Beckmann, B.M., Thomsen, M.B., Pfeufer, A., Ulbrich, M. Sinner, M.F., et al. 2010. Usefulness of short-term variability of QT intervals as a predictor for electrical remodeling and proarrhythmia in patients with nonischemic heart failure. Am. J. Cardiol. **106**: 216–220. doi:10.1016/j.amjcard.2010.02.033. PMID: 20599006.

Hobai, I.A., Khananshvili, D., and Levi, A.J. 1997. The peptide "FRCRCFa," dialysed intracellularly, inhibits the Na/Ca exchange in rabbit ventricular myocytes with high affinity. Pflugers Arch. **433**: 455–463. doi:10.1007/s004240050300. PMID: 9000424.

Husti, Z., Varro, A., and Baczko, I. 2021. Arrhythmogenic remodeling in the failing heart. Cells, 10. doi:10.3390/cells10113203.

Janssen, P.M., and Periasamy, M. 2007. Determinants of frequency-dependent contraction and relaxation of mammalian myocardium. J. Mol. Cell Cardiol. **43**: 523–531. doi:10.1016/j.yjmcc.2007.08.012. PMID: 17919652.

Jensen-Urstad, K., Saltin, B., Ericson, M., Storck, N., and Jensen-Urstad, M. 1997. Pronounced resting bradycardia in male elite runners is associated with high heart rate variability. Scand. J. Med. Sci. Sports. **7**: 274–278. doi:10.1111/j.1600-0838.1997.tb00152.x. PMID: 9338944.

Jost, N., Virag, L., Comtois, P., Ordog, B., Szuts, V. Seprenyi, G., et al. 2013. Ionic mechanisms limiting cardiac repolarization reserve in humans compared to dogs. J. Physiol. **591**: 4189–4206. doi:10.1113/jphysiol.2013.261198. PMID: 23878377.

Katona, P.G., Mclean, M., Dighton, D.H., and Guz, A. 1982. Sympathetic and parasympathetic cardiac control in athletes and nonathletes at rest. J. Appl. Physiol. Respir. Environ. Exerc. Physiol. **52**: 1652–1657. doi:10.1152/jappl.1982.52.6.1652. PMID: 7107476.

Kui, P., Orosz, S., Takacs, H., Sarusi, A., Csik, N. Rarosi, F., et al. 2016. New in vitro model for proarrhythmia safety screening: IKs inhibition potentiates the QTc prolonging effect of IKr inhibitors in isolated guinea pig hearts. J. Pharmacol. Toxicol. Methods. **80**: 26–34. doi:10.1016/j.vascn.2016.04.005. PMID: 27063345.

La Gerche, A., Burns, A.T., Mooney, D.J., Inder, W.J., Taylor, A.J. Bogaert, J., et al. 2012. Exercise-induced right ventricular dysfunction and structural remodelling in endurance athletes. Eur. Heart J. **33**: 998–1006. doi:10.1093/eurheartj/ehr397. PMID: 22160404.

Lavie, C., Ozemek, C., Carbone, S., Katzmarzyk, P.T., and Blair, S.N. 2019. Sedentary behavior, exercise, and cardiovascular health. Circ. Res. **124**: 799–815. doi:10.1161/CIRCRESAHA.118.312669. PMID: 30817262.

Lengyel, C., Varro, A., Tabori, K., Papp, J.G., and Baczko, I. 2007. Combined pharmacological block of I(Kr) and I(Ks) increases short-term QT interval variability and provokes torsades de pointes. Br. J. Pharmacol. **151**: 941–951. doi:10.1038/sj.bjp.0707297. PMID: 17533421.

Lengyel, C., Orosz, A., Hegyi, P., Komka, Z., Udvardy, A. Bosnyak, E., et al. 2011. Increased short-term variability of the QT interval in professional soccer players: possible implications for arrhythmia prediction. PLoS One, **6**: e18751. doi:10.1371/journal.pone.0018751. PMID: 21526208.

Macor, F., Fagard, R., and Amery, A. 1996. Power spectral analysis of RR interval and blood pressure short-term variability at rest and during dynamic exercise: comparison between cyclists and controls. Int. J. Sports. Med. **17**: 175–181. doi:10.1055/s-2007-972828. PMID: 8739570.

Malek, L.A., and Bucciarelli-Ducci, C. 2020. Myocardial fibrosis in athletes—current perspective. Clin. Cardiol. **43**: 882–888. doi:10.1002/clc.23360. PMID: 32189357.

Marijon, E., Tafflet, M., Celermajer, D.S., Dumas, F., Perier, M.C. Mustafic, H., et al. 2011. Sports-related sudden death in the general population. Circulation, **124**: 672–681. doi:10.1161/CIRCULATIONAHA.110.008979. PMID: 21788587.

Maron, B.J. 2007. Hypertrophic cardiomyopathy and other causes of sudden cardiac death in young competitive athletes, with considerations for preparticipation screening and criteria for disqualification. Cardiol. Clin. **25**: 399–414, vi. doi:10.1016/j.ccl.2007.07.006. PMID: 17961794.

Milani-Nejad, N., and Janssen, P.M. 2014. Small and large animal models in cardiac contraction research: advantages and disadvantages. Pharmacol. Ther. **141**: 235–249. doi:10.1016/j.pharmthera.2013.10.007. PMID: 24140081.

Mitchell, J.H., Haskell, W., Snell, P., and Van Camp, S.P. 2005. Task force 8: classification of sports. J. Am. Coll. Cardiol. **45**: 1364–1367. doi:10.1016/j.jacc.2005.02.015. PMID: 15837288.

Morganroth, J., Maron, B., Henry, W.L., and Epstein, S.E. 1975. Comparative left ventricular dimensions in trained athletes. Ann. Intern. Med. **82**: 521–524. doi:10.7326/0003-4819-82-4-521. PMID: 1119766.

Nanasi, P.P., Horvath, B., Tar, F., Almassy, J., Szentandrassy, N. Jost, N., et al. 2021. Canine myocytes represent a good model for human ventricular cells regarding their electrophysiological properties. Pharmaceuticals (Basel), **14**: 748. doi:10.3390/ph14080748. PMID: 35056069.

O'Hara, T., and Rudy, Y. 2012. Quantitative comparison of cardiac ventricular myocyte electrophysiology and response to drugs in human and nonhuman species. Am. J. Physiol. Heart Circ. Physiol. **302**: H1023–H1030. doi:10.1152/ajpheart.00785.2011. PMID: 22159993.

Otsomaa, L., Levijoki, J., Wohlfahrt, G., Chapman, H., Koivisto, A.P. Syrjanen, K., et al. 2020. Discovery and characterization of ORM-11372, a novel inhibitor of the sodium-calcium exchanger with positive inotropic activity. Br. J. Pharmacol. **177**: 5534–5554. doi:10.1111/bph.15257. PMID: 32959887.

Pluim, B.M., Zwinderman, A.H., Van der Laarse, A., and Van der Wall, E.E. 2000. The athlete's heart. A meta-analysis of cardiac structure and function. Circulation, **101**: 336–344. doi:10.1161/01.cir.101.3.336. PMID: 10645932.

Polyak, A., Kui, P., Morvay, N., Lepran, I., Agoston, G. Varga, A., et al. 2018. Long-term endurance training-induced cardiac adaptation in new rabbit and dog animal models of the human athlete's heart. Rev. Cardiovasc. Med. **19**: 135–142. doi:10.31083/j.rcm.2018.04.4161. PMID: 31064165.

Radovits, T., Olah, A., Lux, A., Nemeth, B.T., Hidi, L. Birtalan, E., et al. 2013. Rat model of exercise-induced cardiac hypertrophy: hemodynamic characterization using left ventricular pressure-volume analysis. Am. J. Physiol. Heart Circ. Physiol. **305**: H124–H134. doi:10.1152/ajpheart.00108.2013. PMID: 23645462.

Rajanayagam, J., and Alsabri, M. 2021. Intense endurance exercise: a potential risk factor in the development of heart disease. Cureus, **13**: e12608. doi:10.7759/cureus.12608. PMID: 33585098.

Schelbert, E.B. 2019. Myocardial scar and fibrosis: the ultimate mediator of outcomes? Heart Fail. Clin. **15**: 179–189. doi:10.1016/j.hfc.2018.12.009. PMID: 30832810.

Thomas, B.L., Claassen, N., Becker, P., and Viljoen, M. 2019. Validity of commonly used heart rate variability markers of autonomic nervous system function. Neuropsychobiology, **78**: 14–26. doi:10.1159/000495519. PMID: 30721903.

Thompson, E., Eldstrom, J., Westhoff, M., Mcafee, D., Balse, E., and Fedida, D. 2017. cAMP-dependent regulation of IKs single-channel kinetics. J. Gen. Physiol. **149**: 781–798. doi:10.1085/jgp.201611734. PMID: 28687606.

Thomsen, M.B., Verduyn, S.C., Stengl, M., Beekman, J.D., De Pater, G. Van Opstal, J., et al. 2004. Increased short-term variability of repolarization predicts d-sotalol-induced torsades de pointes in dogs. Circulation, **110**: 2453–2459. doi:10.1161/01.CIR.0000145162.64183.C8. PMID: 15477402.

Topal, L., Naveed, M., Orvos, P., Paszti, B., Prorok, J. Bajtel, A., et al. 2021. The electrophysiological effects of cannabidiol on action potentials and transmembrane potassium currents in rabbit and dog cardiac ventricular preparations. Arch. Toxicol. **95**: 2497–2505. doi:10.1007/s00204-021-03086-0. PMID: 34031697.

Varkevisser, R., Wijers, S.C., Van der Heyden, M.A., Beekman, J.D., Meine, M., and Vos, M.A. 2012. Beat-to-beat variability of repolarization as a new biomarker for proarrhythmia in vivo. Heart Rhythm, **9**: 1718–1726. doi:10.1016/j.hrthm.2012.05.016. PMID: 22609158.

Varro, A., and Baczko, I. 2010. Possible mechanisms of sudden cardiac death in top athletes: a basic cardiac electrophysiological point of view. Pflugers Arch. **460**: 31–40. doi:10.1007/s00424-010-0798-0. PMID: 20186549.

Wang, Y., and Hill, J.A. 2010. Electrophysiological remodeling in heart failure. J. Mol. Cell Cardiol. **48**: 619–632. doi:10.1016/j.yjmcc.2010.01.009. PMID: 20096285.

Wilson, M., O'Hanlon, R., Prasad, S., Deighan, A., Macmillan, P. Oxborough, D., et al. 2011. Diverse patterns of myocardial fibrosis in lifelong, veteran endurance athletes. J. Appl. Physiol. (1985). **110**: 1622–1626. doi:10.1152/japplphysiol.01280.2010. PMID: 21330616.

Zhang, C.D., Xu, S.L., Wang, X.Y., Tao, L.Y., Zhao, W., and Gao, W. 2020. Prevalence of myocardial fibrosis in intensive endurance training athletes: a systematic review and meta-analysis. Front. Cardiovasc. Med. **7**: 585692. doi:10.3389/fcvm.2020.585692. PMID: 33102537.

II.

Archives of Toxicology (2021) 95:2497–2505
https://doi.org/10.1007/s00204-021-03086-0

ORGAN TOXICITY AND MECHANISMS

The electrophysiological effects of cannabidiol on action potentials and transmembrane potassium currents in rabbit and dog cardiac ventricular preparations

Leila Topal[1] · Muhammad Naveed[1] · Péter Orvos[1] · Bence Pászti[1] · János Prorok[2] · Ákos Bajtel[3] · Tivadar Kiss[3] · Boglárka Csupor-Löffler[4] · Dezső Csupor[3,4] · István Baczkó[1,5] · András Varró[1,2,5] · László Virág[1,5] · Norbert Jost[1,2]

Received: 7 April 2021 / Accepted: 17 May 2021 / Published online: 24 May 2021

Abstract

Cannabis use is associated with known cardiovascular side effects such as cardiac arrhythmias or even sudden cardiac death. The mechanisms behind these adverse effects are unknown. The aim of the present work was to study the cellular cardiac electrophysiological effects of cannabidiol (CBD) on action potentials and several transmembrane potassium currents, such as the rapid (I_{Kr}) and slow (I_{Ks}) delayed rectifier, the transient outward (I_{to}) and inward rectifier (I_{K1}) potassium currents in rabbit and dog cardiac preparations. CBD increased action potential duration (APD) significantly in both rabbit (from 211.7 ± 11.2. to 224.6 ± 11.4 ms, $n = 8$) and dog (from 215.2 ± 9.0 to 231.7 ± 4.7 ms, $n = 6$) ventricular papillary muscle at 5 µM concentration. CBD decreased I_{Kr}, I_{Ks} and I_{to} (only in dog) significantly with corresponding estimated EC_{50} values of 4.9, 3.1 and 5 µM, respectively, without changing I_{K1}. Although the EC_{50} value of CBD was found to be higher than literary C_{max} values after CBD smoking and oral intake, our results raise the possibility that potassium channel inhibition by lengthening cardiac repolarization might have a role in the possible proarrhythmic side effects of cannabinoids in situations where CBD metabolism and/or the repolarization reserve is impaired.

Keywords Cannabidiol · Electrophysiology · Action potential · Potassium currents · Rabbit · Dog

Introduction

Cannabis has been one of the most abused hallucinogenic drugs since ancient times with an estimated 150 million consumers worldwide (Kalla et al. 2018). Moreover, the increasingly widespread use of e-cigarettes, the number of people inhaling cannabinoids might even be higher. In addition, the use of cannabis products for medicinal purposes is increasing globally. The enhanced general interest for the use of cannabis and cannabis-derived products was facilitated following the discovery of the cannabinoid system in humans (Sierra et al. 2018). The subsequent new findings on biological actions of cannabinoids on the central nervous system and immune functions attracted further attention. At present, there are cannabis-based drugs on the market with well-defined indications, including treatment of nausea and vomiting following chemotherapy, anorexia, pain related to cancer, spasticity and pain associated with multiple sclerosis, and Dravet and Lennox-Gastaut syndromes (Fraguas-Sánchez and Torres-Suárez 2018). These drugs contain known amounts of CBD and/or THC in pure form or as

Leila Topal and Muhammad Naveed are contributed equally to this manuscript, both considered to be first author.

László Virág and Norbert Jost shared senior authorship.

✉ Norbert Jost
jost.norbert@med.u-szeged.hu

1 Department of Pharmacology and Pharmacotherapy, Faculty of Medicine, University of Szeged, Dóm tér 12, 6720 Szeged, Hungary

2 ELKH-SZTE Research Group for Cardiovascular Pharmacology, Eötvös Loránd Research Network, Szeged, Hungary

3 Department of Pharmacognosy, Faculty of Pharmacy, University of Szeged, Szeged, Hungary

4 Institute for Translational Medicine, Medical School, University of Pécs, Pécs, Hungary

5 Department of Pharmacology and Pharmacotherapy, Interdisciplinary Excellence Centre, University of Szeged, 6720 Szeged, Hungary

herbal extract (Fraguas-Sánchez and Torres-Suárez 2018). In addition to the use of CBD-containing products, CBD oil is very common with several, clinically unsupported indications. The consumption of cannabinoids, particularly CBD, which is enriched in numerous products, can be higher in case of the intake of CBD oils than in case of smoking cannabis. The consumption of cannabinoids, particularly CBD, which is enriched in numerous products, can be higher in case of the intake of CBD oils than in case of smoking cannabis. At high temperature, the majority of CBD is broken down (Czégény et al. 2021), whilst from CBD oils (in fact CBD dissolved in vegetable oils) containing up to 20% CBD, a significant amount of CBD is absorbed.

The possible cardiovascular side effects of cannabinoid use have been indicated in several reports, ranging from arrhythmias to myocardial infarction and even sudden cardiac death (Pacher et al. 2018). According to a cohort study, marijuana smokers can have a 4.8-fold increase of risk developing acute myocardial infarction following the first hour of cannabinoid exposure (Mittleman et al. 2001). On the other hand, other reports do not support the link between cannabis use and cardiovascular events (Singh et al. 2019). Accordingly, an important comprehensive study assessed data for 316,397 cannabis users and 20,499,215 non-users found that cannabis use was an independent predictor of heart failure (Kalla et al. 2018). Although the mechanisms explaining these observations are poorly understood, the effects of cannabinoids exerted via the G protein-coupled cannabinoid receptors are suspected to play key roles. In addition, numerous studies reported proarrhythmic properties of cannabinoids including ventricular arrhythmias and even sudden cardiac death (Courts et al. 2016; Ozturk et al. 2019; Manolis et al. 2019). However, the mechanism of these arrhythmias remains unclear (Ozturk et al. 2019). It was reported earlier and also recently that certain voltage-gated ion channels like cardiac sodium, calcium (Al Kury et al. 2014), hERG and Kv4.3 channels (Amoros et al. 2010) might be also related to the reported cardiac effects of cannabinoids, but the possible effects of CBD on various cardiac potassium currents which play a crucial role in cardiac repolarization have not been studied yet in detail. Such transmembrane ion currents in cardiac ventricular muscle are the rapid (I_{Kr}) and slow (I_{Ks}) delayed rectifier potassium currents, the transient outward (I_{to}) and inward rectifier (I_{K1}) potassium currents, all important for cardiac repolarization. Several cardiac and non-cardiac drugs are known to inhibit I_{Kr} (also called hERG ion channel) and consequently they prolong cardiac QT interval and enhance dispersion of repolarization. The latter has been associated with the development of life-threatening arrhythmias. Therefore, the official drug development procedure requires an early screening of whether a potential drug candidate has any activities on the hERG channels (Sanguinetti and Tristani-Firouzi 2006). However, drug effects on cardiac repolarization cannot be accurately estimated by measuring hERG channel and currents (Orvos et al. 2019), since drugs can also affect cardiac repolarization and action potential by acting on different currents other than hERG or I_{Kr}.

Therefore, in the present study the aim was to investigate the effect of CBD, a major cannabinoid, on cardiac ventricular action potential and on several cardiac transmembrane currents to provide further experimental data for the elucidation of the possible mechanisms of its adverse cardiac electrophysiological effects.

Methods

Animals and materials

All experiments were carried out in compliance with the Guide for the Care and Use of Laboratory Animals (USA NIH publication NO 85-23, revised 1996) and conformed to the Directive 2010/63/EU of the European Parliament. The protocols have been approved by the Ethical Committee for the Protection of Animals in Research of the University of Szeged, Szeged, Hungary (approval numbers: I-74-15-2017 and I-74-24-2017) and by the Department of Animal Health and Food Control of the Ministry of Agriculture and Rural Development (authority approval numbers XIII/3330/2017 and XIII/3331/2017).

Conventional microelectrode technique

Action potentials were recorded in right ventricular trabecular or papillary muscle preparations obtained from dog or rabbit hearts using conventional microelectrode techniques as described earlier in detail (Jost et al. 2013; Orvos et al. 2019).

Preparations were individually mounted in a tissue chamber with a volume of 50 ml. During experiments modified Locke's solution was used, containing (in mM): NaCl 128.3, KCl 4, $CaCl_2$ 1.8, $MgCl_2$ 0.42, $NaHCO_3$ 21.4 and glucose 10. The pH of this solution was set between 7.35 and 7.4 when gassed with the mixture of 95% O_2 and 5% CO_2 at 37 °C. Each preparation was stimulated through a pair of platinum electrodes in contact with the preparation using rectangular current pulses of 1–3 ms duration at twice of the threshold strength at a constant basic cycle length of 1000 ms for ventricular preparations. These stimuli were delivered for at least 60 min allowing the preparation to equilibrate before the measurements were initiated. Transmembrane potentials were recorded using conventional glass microelectrodes, filled with 3 M KCl and having tip resistances of 5–20 MΩ, connected to the input of a high

impedance electrometer (Experimetria, type 309, Budapest, Hungary) which was coupled to a dual beam oscilloscope.

The resting potential (RP), action potential amplitude (APA), maximum upstroke velocity (V_{max}) and APD measured at 50% and 90% of repolarization (APD_{50} and APD_{90}, respectively) were determined off-line using an in-house developed software (APES) running on a computer equipped with an ADA 3300 analogue-to-digital data acquisition board (Real Time Devices, Inc., State College, Pennsylvania) having a maximum sampling frequency of 40 kHz.

Attempts were made to maintain the same impalement throughout each experiment. In case an impalement became dislodged, adjustment was attempted, and if the action potential characteristics of the re-established impalement deviated by less than 5% from the previous measurement, the experiment continued.

Voltage-clamp measurements

Ventricular myocytes were enzymatically dissociated from canine or rabbit hearts as described earlier in detail (Jost et al. 2013; Orvos et al. 2019). One drop of cell suspension was placed in a transparent recording chamber mounted on the stage of an inverted microscope (Olympus IX51, Olympus, Tokyo, Japan), and individual myocytes were allowed to settle and adhere to the chamber bottom for at least 5–10 min before superfusion was initiated and maintained by gravity. Only rod-shaped cells with clear striations were used. HEPES-buffered Tyrode's solution (composition in mM: NaCl 144, NaH_2PO_4 0.4, KCl 4.0, $CaCl_2$ 1.8, $MgSO_4$ 0.53, glucose 5.5 and HEPES 5.0, at pH of 7.4) served as the normal superfusate.

Micropipettes were fabricated from borosilicate glass capillaries (Science Products GmbH, Hofheim, Germany), using a P-97 Flaming/Brown micropipette puller (Sutter Co, Novato, CA, USA), and had a resistance of 1.5–2.5 MOhm when filled with pipette solution. The membrane currents were recorded with Axopatch-200B amplifiers (Molecular Devices, Sunnyvale, CA, USA) by means of the whole-cell configuration of the patch-clamp technique. The membrane currents were digitized with 250 kHz analogue-to-digital converters (Digidata 1440A, Molecular Devices, Sunnyvale, CA, USA) under software control (pClamp 10, Molecular Devices, Sunnyvale, CA, USA). Experiments were carried out at 37 °C.

Measurement of potassium currents

The inward rectifier (I_{K1}), transient outward (I_{to}), rapid (I_{Kr}) and slow (I_{Ks}) delayed rectifier potassium currents were recorded in HEPES-buffered Tyrode's solution. The composition of the pipette solution (in mM) was the following: KOH 110, KCl 40, K_2ATP 5, $MgCl_2$ 5, EGTA 5 and HEPES 10 (pH was adjusted to 7.2 by aspartic acid). 1 µM nisoldipine was added to the bath solution to block I_{CaL}. When I_{Kr} was recorded I_{Ks} was inhibited using the selective I_{Ks} blocker HMR 1556 (0.5 µM). During I_{Ks} measurements (a transmembrane current strongly depending from cAMP and protein kinase A, PKA; Christian et al. 2011), I_{Kr} was blocked by 0.5 µM dofetilide and the bath solution contained 0.1 µM forskolin.

Data analysis

All data are expressed as means ± SEM. The "*n*" number refers to the number of experiments (*i.e.* the number of cells in case of patch-clamp and the number of ventricular muscle preparations—papillary or trabecular muscle—in case of action potential measurements). Statistical analysis was performed with Student's *t* test for paired data. The results were considered statistically significant when $P < 0.05$.

Results

The cardiac cellular electrophysiological effect of CBD was studied on various transmembrane ionic currents by the whole-cell configuration of the patch-clamp technique in native rabbit and dog ventricular myocytes and on action potentials in rabbit and dog ventricular papillary muscles by the conventional microelectrode technique. Figure 1 and Table 1 show that CBD lengthens action potential duration (APD_{90}) significantly at the concentration of 5 µM without changing other action potential parameters significantly.

Whole-cell patch-clamp experiments in rabbit cardiac ventricular myocytes revealed significant inhibition of the rapid delayed rectifier potassium current (I_{Kr}) (Figs. 2A and 3) with an estimated EC_{50} value of 4.9 µM. I_{Kr} was activated by 1000 ms long depolarizing voltage pulses with pulse frequency of 0.05 Hz to the potentials ranging from − 30 mV to 50 mV and then the cell was repolarized to − 40 mV. The deactivating tail current at − 40 mV after the test pulse was assessed as I_{Kr}. The holding potential was − 80 mV.

In similar experiments in rabbit myocytes CBD depressed the slow delayed rectifier potassium current (I_{Ks}, Fig. 2B) with an estimated EC_{50} value of 3.1 µM (Fig. 4), after 20 mV 5 s long test pulse measured at − 40 mV. I_{Ks} was recorded similarly to I_{Kr}. After 5 s long depolarizing voltage pulses to various test potentials with pulse frequency of 0.1 Hz the cell was repolarized to − 40 mV and the tail current amplitude was measured.

CBD even in the high concentration of 10 µM concentration did not influence the transient outward potassium current (I_{to}) in rabbit (Fig. 5A) but decreased it significantly in dog (Fig. 5B) ventricular myocytes with an estimated EC_{50} value of 5 µM (Fig. 6). I_{to} was activated by 300 ms long depolarizing

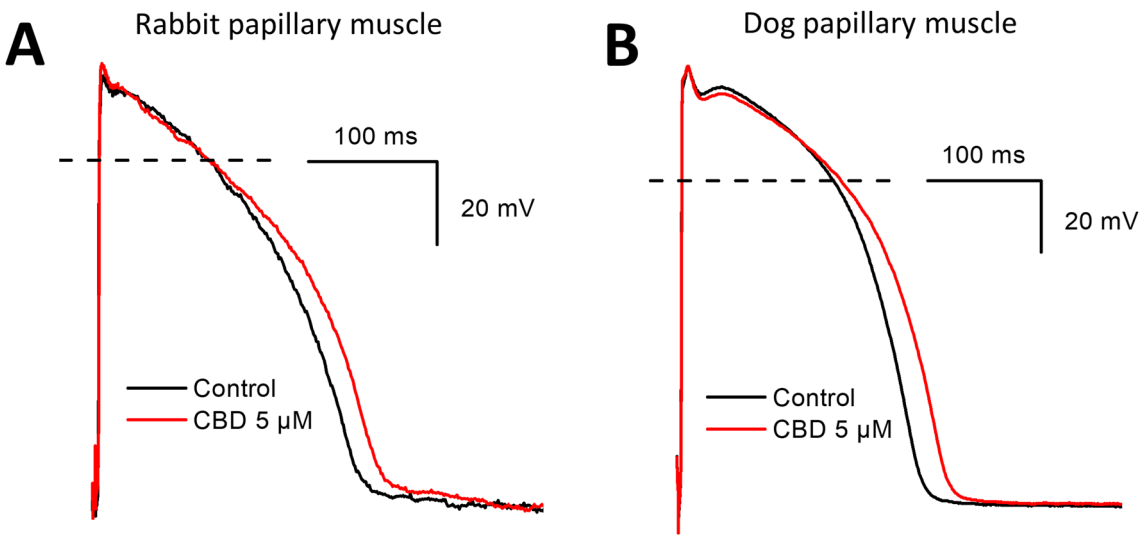

Fig. 1 Effect of CBD on the action potentials recorded from rabbit (panel **A**) and dog (panel **B**) papillary muscles. Dashed lines indicate zero mV levels

Table 1 Effect of acute exposure to CBD on the action potential parameters in rabbit and dog right ventricular papillary muscle preparations

Parameters	Rabbit ventricular muscle ($n=8$)		Dog ventricular muscle ($n=6$)	
	Control	CBD 5 µM	Control	CBD 5 µM
RP (mV)	− 84.1 ± 2.2	− 82.7 ± 1.7	− 84.7 ± 1.7	− 84.7 ± 2.3
APA (mV)	105.2 ± 3.0	106.4 ± 3.0	118.4 ± 3.3	120.4 ± 2.2
V_{max} (V/s)	120.3 ± 20.6	113.0 ± 17.1	186.4 ± 21.7	201.0 ± 25.2
APD_{50} (ms)	171.8 ± 13.6	**183.0 ± 12.8**	178.3 ± 8.2	193.1 ± 4.5
APD_{90} (ms)	211.7 ± 11.2	**224.6 ± 11.4**	215.2 ± 9.0	**231.7 ± 4.7**

Bold values are considered to be statistically significant ($P < 0.05$ versus control)

$P < 0.05$ versus control

RP resting membrane potential, *APA* action potential amplitude, V_{max} maximum upstroke velocity

APD_{50} and APD_{90} action potential duration measured at 50 and 90% of repolarization

voltage pulses arising from the holding potential of − 90 mV to test potentials gradually increasing up to 50 mV. The pulse frequency was 0.33 Hz.

As Fig. 7 indicates, CBD did not significantly change the inward rectifier potassium current (I_{K1}) even at the high, 10 µM concentration. I_{K1} current was measured as the steady-state current level at the end of the 300 ms long voltage pulse in the voltage range of − 100 to 0 mV with a pulse frequency of 0.33 Hz. The holding potential was − 90 mV.

Discussion

The main result of this study is that 5 µM CBD prolongs repolarization. This effect on repolarization in rabbit and dog papillary muscle can be best explained by the multiple effects CBD exerts on various potassium channels. Accordingly, as our previous results (Orvos et al. 2020) indicated, CBD administration at lower concentrations (1, 2.5 and 5 µM) resulted in hERG/I_{Kr} depression and a consequent lengthening of APD_{90}, but this effect was counterbalanced by the inhibition of inward Ca^{2+} and Na^{+} currents following CBD application at the high concentration of 10 µM. Similar effects were reported earlier with quinidine, an antiarrhythmic drug, with established proarrhythmic properties (Roden and Hoffman 1985; Varro et al. 1985).

A few previous studies with cannabinoids showed effects on various transmembrane ion channels such as inward sodium, (Al Kury et al. 2014; Ghovanloo et al. 2018; Orvos et al. 2020) inward calcium (Al Kury et al. 2014; Orvos et al. 2020), outward transient current (Li et al. 2012) and human Kv1.5 and Kv4.3 channels (Barana et al. 2010). In addition, in previous studies (Orvos et al. 2020) hERG/I_{Kr} channel inhibition and QT prolongation were also reported in anaesthetized rats (Yun et al. 2016) and guinea pig (Orvos et al. 2020) by a synthetic cannabinoid compound (JWH-030) and CBD. This synthetic cannabinoid compound structurally differs from CBDs and inhibited hERG channels with a relatively high EC_{50}

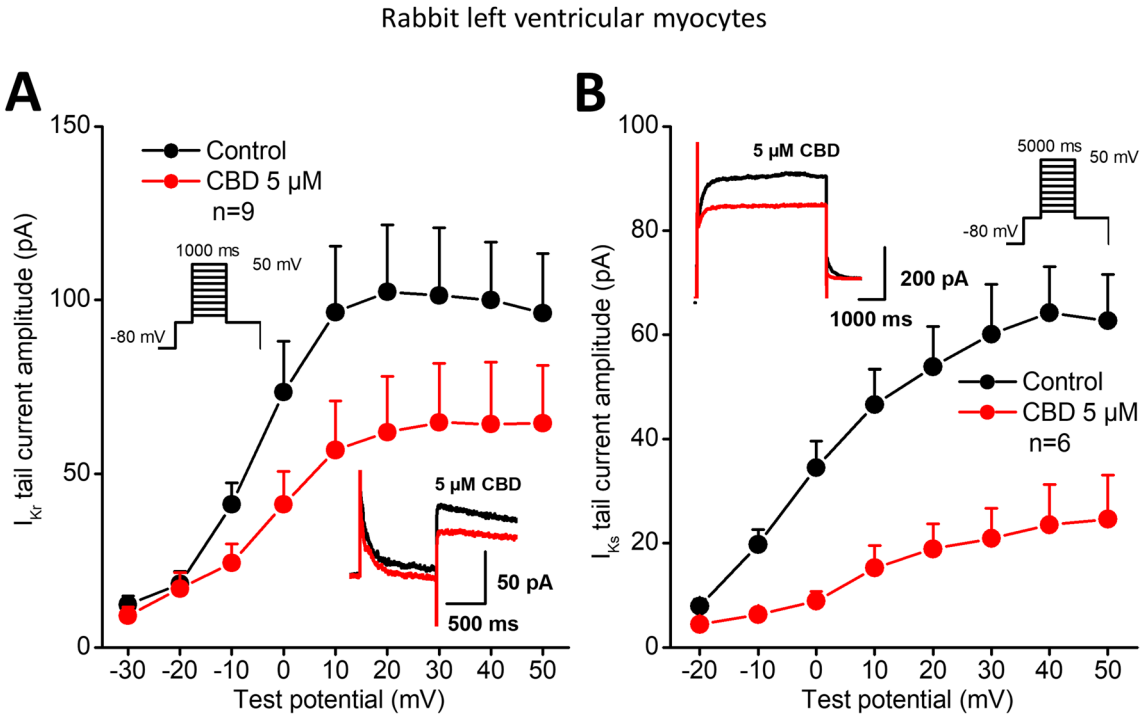

Fig. 2 Effect of CBD on the rapid (I_{Kr}) and slow (I_{Ks}) delayed rectifier potassium currents. Panels show current–voltage curves for I_{Kr} (panel **A**) and for I_{Ks} (panel **B**) in control conditions and after application of 5 µM CBD. Insets indicate the voltage protocols and original I_{Kr} and I_{KS} current records in control and in the presence of CBD. Data are expressed as means ± SEM

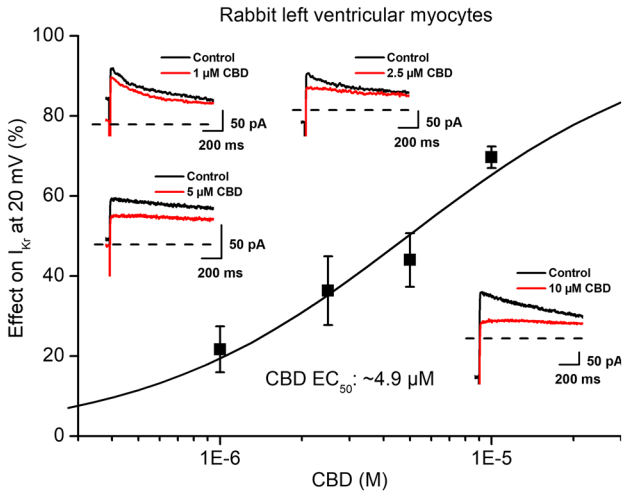

Fig. 3 Effect of CBD on the rapid (I_{Kr}) delayed rectifier potassium currents. The panel displays CBD concentration–response curve indicating an estimated EC_{50} value of 4.9 µM for I_{Kr} blockade. The insets show the tail current section of original I_{Kr} current traces in control conditions and in the presence of 1 µM, 2.5 µM, 5 µM and 10 µM CBD recorded from rabbit left ventricular myocytes after a 1 s long pulse to 20 mV test potential with pulsing cycle length of 20 s. I_{Kr} deactivating tail current was measured at -40 mV. The dashed lines refer to the baseline for I_{Kr} tail current level after the test pulse at − 40 mV. Data are expressed as means ± SEM

(88.36 µM). Also, in rat ventricle hERG/I_{Kr} seems not as important for controlling repolarization as Kv4.2 and Kv1.5 channels. Therefore, the cannabinoid-evoked QT changes in rat most likely can be attributed to Kv1.5 and Kv4.2 rather than hERG channel inhibition. The finding of the present study that CBD inhibits I_{to} in dog but not in rabbit ventricular myocytes are in good agreement with the previously mentioned rat study, since in dog I_{to} is conducted Kv 4.3 (Han et al. 2002) but in rabbit by Kv 1.4 channels (Wang et al. 1999). Since the APD measurements in the present study were taken in subendocardial preparations, the latter effect on I_{to} may result in more pronounced repolarization dispersion in dog and human ventricle where in midmyocardial cells I_{to} is greater than in the subendocardium (Zicha et al. 2004).

According to human pharmacokinetic data, the C_{max} values for CBD can reach 0.35 µM and 0.58 µM during CBD smoking (19.2 mg) or following oral administration (400 mg), respectively (Millar et al. 2018). In the present experiments, CBD had inhibitory potency on both the hERG channel and I_{Kr} activity, with an EC_{50} value higher than literary C_{max} values in patients. This suggests small or negligible proarrhythmic risk in physiological conditions in healthy individuals. This is indeed in good agreement

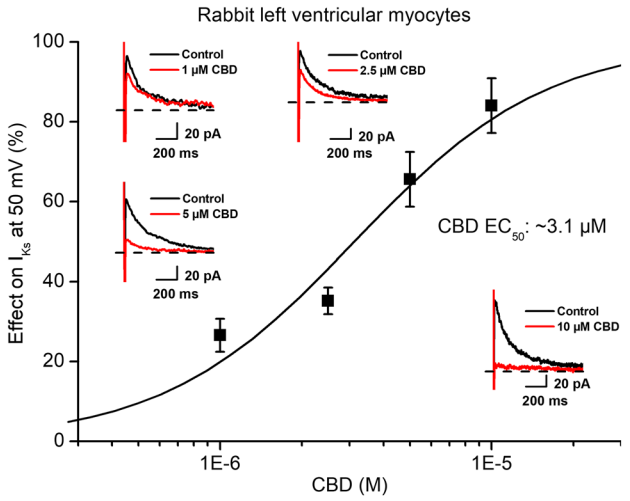

Fig. 4 Effect of CBD on the slow (I_{Ks}) delayed rectifier potassium currents. The panel displays CBD concentration–response curve indicating an estimated EC_{50} value of 3.1 µM for I_{Ks} blockade. The insets show the tail current section of original I_{Ks} current traces in control conditions and in the presence of 1 µM, 2.5 µM, 5 µM and 10 µM CBD recorded from rabbit left ventricular myocytes after a 5 s long pulse to 50 mV test potential with pulsing cycle length of 10 s. I_{Ks} deactivating tail current was measured at -40 mV. The dashed lines refer to the baseline for I_{Ks} tail current level after the test pulse at − 40 mV. Data are expressed as means ± SEM

with clinical reports showing no significant QT_c prolongation in patients after CBD administration (Sellers et al. 2013). Also, in another clinical study, it was found that long term Sativex (THC + CBD) treatment evoked T wave changes in only 1 out of 146 patients (Serpell et al. 2013). Therefore, it is likely that in case of inhalation or oral use of cannabis-derived products, CBD itself may not represent a significant proarrhythmic risk. Based on the comparison of hERG or I_{Kr} activity, cardiac action potential duration, and QT prolongation against QT effects and reports of arrhythmogenic (torsade de pointes) potential of 100 drugs, a margin of 30-fold between hERG EC_{50} and C_{max} was proposed to be an acceptable degree of safety regarding arrhythmogenesis (Redfern et al. 2003). Taking into account the EC_{50} values for I_{Kr}, I_{Ks} and I_{to} inhibition in our experiments (4.9, 3.1 and 5 µM, respectively), the ratios of EC_{50} and C_{max} values are in the range of about 8–9, which refers to moderately increased risk of arrhythmia. However, in patients who have considerably slower drug elimination due to certain concomitant diseases or in case of concurrent use of other drugs that inhibit the metabolism of CBD, higher C_{max} values can develop (Iffland and Grotenhermen

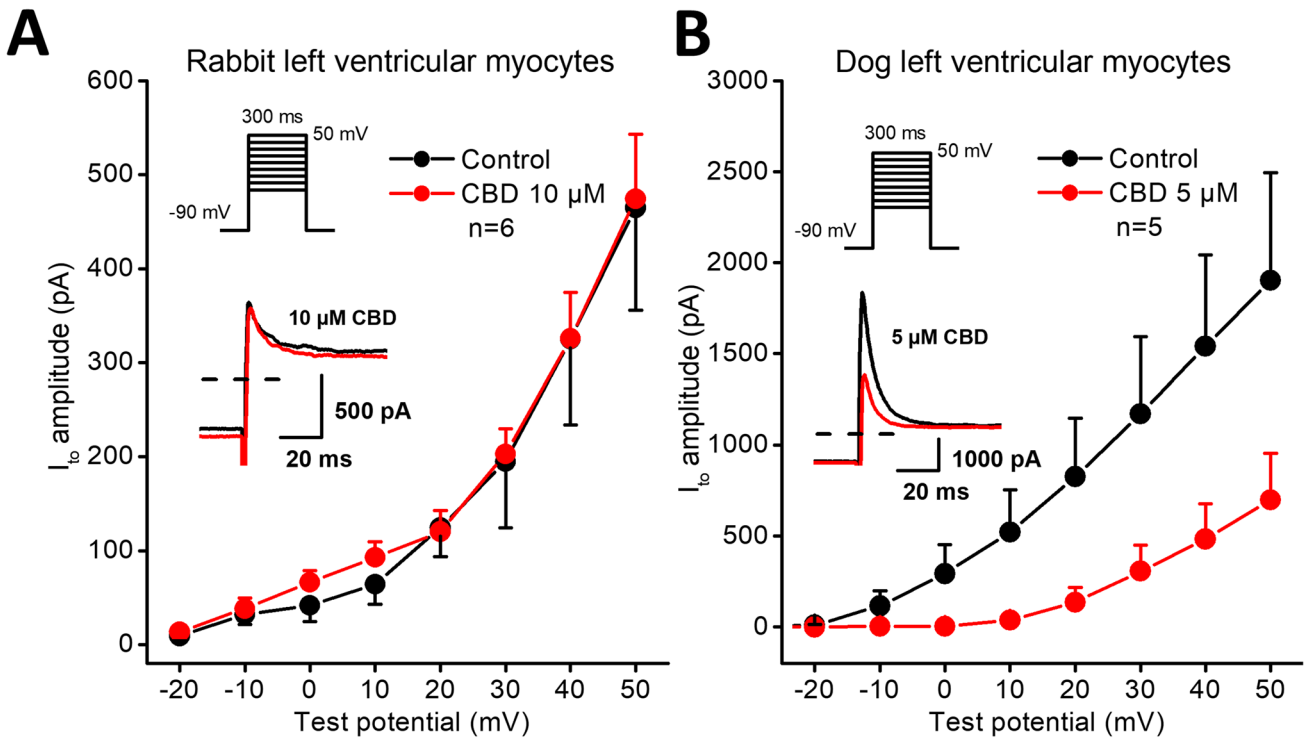

Fig. 5 Effect of CBD on the transient outward potassium current (I_{to}) in rabbit and dog ventricular myocytes. Panels show current–voltage curves for I_{to} in control conditions and after application of CBD in rabbit (panel **A**) and in dog (panel **B**) ventricular myocytes. Insets indicate the voltage protocols and original I_{to} current records in control and in the presence of CBD. Dashed lines indicate zero current levels. Data are expressed as means ± SEM

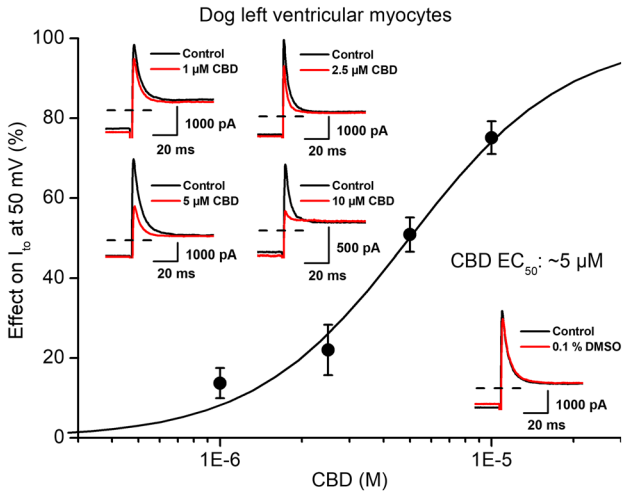

Fig. 6 Effect of CBD on the transient outward potassium current (I_{to}) in dog ventricular myocytes. The panel displays CBD concentration–response curve indicating an estimated EC_{50} value of 5 μM for I_{to} blockade. Insets show original I_{to} current traces in control conditions and in the presence of 1 μM, 2.5 μM, 5 μM and 10 μM CBD recorded from dog left ventricular myocytes after a 300 ms long pulse to 50 mV test potential with pulsing cycle length of 3 s. The inset on right-bottom displays original I_{to} current traces in control conditions and in the presence of the solvent (0.1% DMSO). Dashed lines indicate zero current levels. Data are expressed as means ± SEM

2017), and this may further increase the risk for arrhythmia development.

Moreover, when CBD intake is combined with pharmacological agents affecting cardiac repolarization, as well as in certain pathophysiological situations such as hypokalemia, or diseases like LQT syndrome, diabetes mellitus, HCM or heart failure where cardiac repolarization reserve (Varró and Baczkó 2011) or drug metabolism is impaired, CBD can have an additive effect, further increasing the proarrhythmic risk and the possible incidence of sudden cardiac death. Such additive interactions were reported both in animal experimental (Lengyel et al. 2007) and clinical settings (Wisniowska et al. 2016). The cardiovascular effects of CBD may only partly be attributed to its effects on transmembrane ion channels, the cardiovascular safety of this compound may be influenced by its activities on other targets, and by the presence of myocardial ischemia (Ferdinandy et al. 2019) as well. Therefore, further studies are needed to assess the unwanted cardiovascular effects of CBD and other cannabinoids both in vivo and in vitro studies, with special focus on the benefit-risk assessment of products with different cannabinoid content.

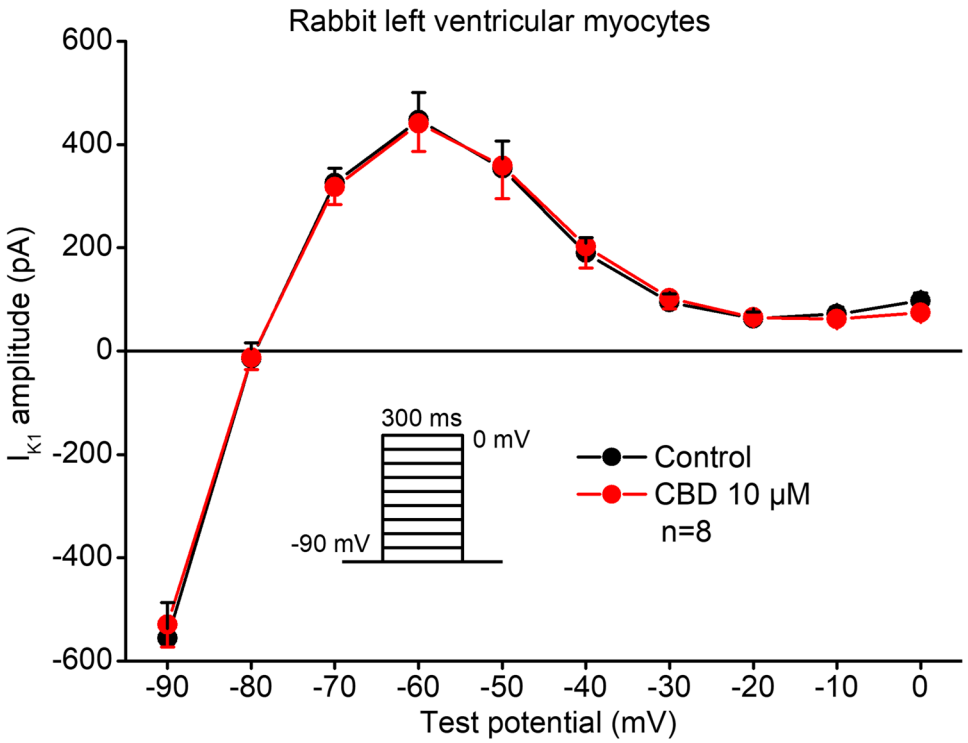

Fig. 7 Lack of effect of CBD on the inward rectifier potassium current in rabbit left ventricular myocytes. The panel shows steady-state current–voltage curves for I_{K1} in control conditions and after application of 10 μM CBD in rabbit left ventricular myocytes. Inset indicates the voltage protocol. Data are expressed as means ± SEM

Author contributions DC, LV, IB, NJ and AV conceived the experiment, LT, MN, PO, BP, JP, BC-L, TK and AB conducted the experiment(s), LT, MN, PO, BP, JP, BC-L, TK, AB and LV analysed the results, DC, LV, IB, NJ and AV, prepared the manuscript. All authors reviewed the manuscript.

Funding Open access funding provided by University of Szeged. Financial support from the Economic Development and Innovation Operative Programme GINOP-2.3.2-15-2016-00012, the National Research Development and Innovation Office (NKFIH K 135464 and NKFIH K 128851), the Ministry of Human Capacities Hungary (20391-3/2018/FEKUSTRAT and EFOP-3.6.2-16-2017-00006), and from the Eötvös Loránd Research Network are gratefully acknowledged.

Data availability The data underlying this article will be shared on reasonable request to the corresponding author.

Declarations

Conflict of interest The authors declare that they have no conflict of interest.

Ethical approval All experiments were carried out in compliance with the Guide for the Care and Use of Laboratory Animals (USA NIH publication NO 85-23, revised 1996) and conformed to the Directive 2010/63/EU of the European Parliament. The protocols have been approved by the Ethical Committee for the Protection of Animals in Research of the University of Szeged, Szeged, Hungary (approval numbers: I-74-15-2017 and I-74-24-2017) and by the Department of Animal Health and Food Control of the Ministry of Agriculture and Rural Development (authority approval numbers XIII/3330/2017 and XIII/3331/2017).

References

Al Kury LT, Voitychuk OI, Yang KH, Thayyullathil FT, Doroshenko P, Ramez AM et al (2014) Effects of the endogenous cannabinoid anandamide on voltage-dependent sodium and calcium channels in rat ventricular myocytes. Br J Pharmacol 171:3485–3498

Amoros I, Barana A, Caballero R, Gómez R, Osuna L, Lillo MP et al (2010) Endocannabinoids and cannabinoid analogues block human cardiac Kv4.3 channels in a receptor-independent manner. J Mol Cell Cardiol 48:201–210

Barana A, Amoros I, Caballero R, Gómez R, Osuna L, Lillo MP et al (2010) Endocannabinoids and cannabinoid analogues block cardiac hKv1.5 channels in a cannabinoid receptor-independent manner. Cardiovasc Res 85:56–67

Christian F, Szaszák M, Friedl S, Drewianka S, Lorenz D, Goncalves A et al (2011) Small molecule AKAP-protein kinase A (PKA) interaction disruptors that activate PKA interfere with compartmentalized cAMP signaling in cardiac myocytes. J Biol Chem 286(11):9079–9096. https://doi.org/10.1074/jbc.M110.160614

Courts J, Maskill V, Gray A, Glue P (2016) Signs and symptoms associated with synthetic cannabinoid toxicity: systematic review. Australas Psychiatry 24:598–601

Czégény Z, Nagy G, Babinszki B, Bajtel Á, Sebestyén Z, Kiss T, Csupor-Löffler B, Tóth B, Csupor D (2021) CBD, a precursor of THC in e-cigarettes. Sci Rep 11(1):8951. https://doi.org/10.1038/s41598-021-88389-z

Ferdinandy P, Baczkó I, Bencsik P, Giricz Z, Görbe A, Pacher P et al (2019) Definition of hidden drug cardiotoxicity: paradigm change in cardiac safety testing and its clinical implications. Eur Heart J 40(22):1771–1777. https://doi.org/10.1093/eurheartj/ehy365

Fraguas-Sánche AI, Torres-Suárez AI (2018) Medical use of cannabinoids. Drugs 78(16):1665–1703. https://doi.org/10.1007/s40265-018-0996-1

Ghovanloo MR, Shuart NG, Mezeyova J, Dean RA, Ruben PC, Goodchild SJ (2018) Inhibitory effects of cannabidiol on voltage-dependent sodium currents. J Biol Chem 293:16546–16558

Han W, Bao W, Wang Z, Nattel S (2002) Comparison of ion-channel subunit expression in canine cardiac Purkinje fibers and ventricular muscle. Circ Res 91(9):790–797. https://doi.org/10.1161/01.res.0000039534.18114.d9

Iffland K, Grotenhermen F (2017) An update on safety and side effects of cannabidiol: a review of clinical data and relevant animal studies. Cannabis Cannabinoid Res 2:139–154

Jost N, Nagy N, Corici C, Kohajda Z, Horváth A, Acsai K et al (2013) ORM-10103, a novel specific inhibitor of the Na^+/Ca^{2+} exchanger, decreases early and delayed after depolarizations in the canine heart. Br J Pharmacol 170(4):768–778. https://doi.org/10.1111/bph.12228

Kalla A, Krishnamoorthy PM, Gopalakrishnan A, Figueredo VM (2018) Cannabis use predicts risks of heart failure and cerebrovascular accidents: results from the National Inpatient Sample. J Cardiovasc Med (hagerstown) 19:480–484

Lengyel C, Varro A, Tabori K, Papp JG, Baczko I (2007) Combined pharmacological block of I(Kr) and I(Ks) increases short-term QT interval variability and provokes torsades de pointes. Br J Pharmacol 151:941–951

Li Q, Ma HJ, Song SL, Shi M, Ma HJ, Li DP, Zhang Y (2012) Effects of anandamide on potassium channels in rat ventricular myocytes: a suppression of I(to) and augmentation of K(ATP) channels. Am J Physiol Cell Physiol 302:C924–C930

Manolis TA, Manolis AA, Manolis AS (2019) Cannabis associated 'high' cardiovascular morbidity and mortality: marijuana smoke like tobacco smoke? A deja vu/deja vecu story? Mini Rev Med Chem 19:870–879

Millar SA, Stone NL, Yates AS, O'Sullivan SE (2018) A Systematic review on the pharmacokinetics of cannabidiol in humans. Front Pharmacol 9:1365

Mittleman MA, Lewis RA, Maclure M, Sherwood JB, Muller JE (2001) Triggering myocardial infarction by marijuana. Circulation 103:2805–2809

Orvos P, Kohajda Z, Szlovák J, Gazdag P, Árpádffy-Lovas T, Tóth D et al (2019) Evaluation of possible proarrhythmic potency: comparison of the effect of dofetilide, cisapride, sotalol, terfenadine, and verapamil on hERG and native IKr currents and on cardiac action potential. Toxicol Sci 168(2):365–380. https://doi.org/10.1093/toxsci/kfy299

Orvos P, Pászti B, Topal L, Gazdag P, Prorok J, Polyák A et al (2020) The electrophysiological effect of cannabidiol on hERG current and in guinea-pig and rabbit cardiac preparations. Sci Rep 10(1):16079. https://doi.org/10.1038/s41598-020-73165-2

Ozturk HM, Yetkin E, Ozturk S (2019) Synthetic cannabinoids and cardiac arrhythmia risk: review of the literature. Cardiovasc Toxicol 19:191–197

Pacher P, Steffens S, Hasko G, Schindler TH, Kunos G (2018) Cardiovascular effects of marijuana and synthetic cannabinoids: the good, the bad, and the ugly. Nat Rev Cardiol 15:151–166

Redfern W, Carlsson L, Davis AS, Lynch WG, MacKenzie I, Palethorpe S et al (2003) Relationships between preclinical cardiac electrophysiology, clinical QT interval prolongation and torsade de pointes for a broad range of drugs: evidence for a provisional safety margin in drug development. Cardiovasc Res 58:32–45

Roden DM, Hoffman BF (1985) Action potential prolongation and induction of abnormal automaticity by low quinidine concentrations in canine Purkinje fibers. Relationship to potassium and cycle length. Circ Res 56:857–867

Sanguinetti MC, Tristani-Firouzi M (2006) hERG potassium channels and cardiac arrhythmia. Nature 440:463–469

Sellers EM, Schoedel K, Bartlett C, Romach M, Russo EB, Stott CG et al (2013) A multiple-dose, randomized, double-blind, placebo-controlled, parallel-group QT/QTc study to evaluate the electrophysiologic effects of THC/CBD spray. Clin Pharmacol Drug Dev 2:285–294

Serpell MG, Notcutt W, Collin C (2013) Sativex long-term use: an open-label trial in patients with spasticity due to multiple sclerosis. J Neurol 260:285–295

Sierra S, Luquin N, Navarro-Otano J (2018) The endocannabinoid system in cardiovascular function: novel insights and clinical implications. Clin Auton Res 28(1):35–52. https://doi.org/10.1007/s10286-017-0488-5

Singh SM, Koh M, Fang J, Ko DT (2019) The risk of cardiovascular events on cannabis' highest day. Can J Cardiol 35:1589–1591

Varro A, Elharrar V, Surawicz B (1985) Effect of antiarrhythmic drugs on the premature action potential duration in canine cardiac Purkinje fibers. J Pharmacol Exp Ther 233:304–311

Varró A, Baczkó I (2011) Cardiac ventricular repolarization reserve: a principle for understanding drug-related proarrhythmic risk. Br J Pharmacol 164(1):14–36. https://doi.org/10.1111/j.1476-5381.2011.01367.x

Wang Z, Feng J, Shi H, Pond A, Nerbonne JM, Nattel S (1999) Potential molecular basis of different physiological properties of the transient outward K+ current in rabbit and human atrial myocytes. Circ Res 84(5):551–561. https://doi.org/10.1161/01.res.84.5.551

Wisniowska B, Tylutki Z, Wyszogrodzka G, Polak S (2016) Drug-drug interactions and QT prolongation as a commonly assessed cardiac effect - comprehensive overview of clinical trials. BMC Pharmacol Toxicol 17:12

Yun J, Yoon KS, Lee TH, Lee H, Gu SM, Song YJ et al (2016) Synthetic cannabinoid, JWH-030, induces QT prolongation through hERG channel inhibition. Toxicol Res (camb) 5:1663–1671

Zicha S, Xiao L, Stafford S, Cha TJ, Han W, Varro A, Nattel S (2004) Transmural expression of transient outward potassium current subunits in normal and failing canine and human hearts. J Physiol 561(Pt 3):735–748. https://doi.org/10.1113/jphysiol.2004.075861

III.

SCIENTIFIC REPORTS
nature research

Check for updates

OPEN

The electrophysiological effect of cannabidiol on hERG current and in guinea-pig and rabbit cardiac preparations

Péter Orvos[1,7], Bence Pászti[2,7], Leila Topal[2], Péter Gazdag[2], János Prorok[3], Alexandra Polyák[2,3], Tivadar Kiss[4], Edit Tóth-Molnár[1], Boglárka Csupor-Löffler[5], Ákos Bajtel[4], András Varró[2,3,6], Judit Hohmann[4], László Virág[2,6,8] & Dezső Csupor[4,8]✉

Cannabis use is associated with cardiovascular adverse effects ranging from arrhythmias to sudden cardiac death. The exact mechanism of action behind these activities is unknown. The aim of our work was to study the effect of cannabidiol (CBD), tetrahydrocannabinol and 11-nor-9-carboxy-tetrahydrocannabinol on cellular cardiac electrophysiological properties including ECG parameters, action potentials, hERG and I_{Kr} ion channels in HEK cell line and in rabbit and guinea pig cardiac preparations. CBD increased action potential duration in rabbit and guinea pig right ventricular papillary muscle at lower concentrations (1 µM, 2.5 µM and 5 µM) but did not significantly change it at 10 µM. CBD at high concentration (10 µM) decreased inward late sodium and L-type calcium currents as well. CBD inhibited hERG potassium channels with an IC_{50} value of 2.07 µM at room temperature and delayed rectifier potassium current with 6.5 µM at 37 °C, respectively. The frequency corrected QT interval (QT_c) was significantly lengthened in anaesthetized guinea pig without significantly changing other ECG parameters. Although the IC_{50} value of CBD was higher than literary C_{max} values after CBD smoking and oral intake, our results raise the possibility that hERG and potassium channel inhibition might have a role in the possible proarrhythmic adverse effects of cannabinoids in situations where metabolism of CBD impaired and/or the repolarization reserve is weakened.

Cannabis is the most abused hallucinogenic drug, with an estimated of 150 million consumers worldwide[1]. With the increasingly widespread use of e-cigarettes, the number of people inhaling cannabinoids might even be higher. Moreover, the use of cannabis products for medicinal purposes is increasing globally. The interest for the use of cannabis and cannabis-derived products started following the discovery of the cannabinoid system in the human brain and body and the subsequent reports on new findings on biological activities of cannabinoids on central nervous system and immune functioning. Currently, there are cannabis-based medicines on the market with well-defined medicinal indications, including treatment of nausea and vomiting associated with chemotherapy, anorexia, pain related to cancer, spasticity and pain associated with multiple sclerosis, Dravet and Lennox-Gastaut syndromes. These medicines contain known amounts of CBD and/or THC in pure form or as standardized herbal extract[2]. Besides, the use of CBD-containing products (CBD oil) is very widespread with several, clinically unsupported indications. The intake of cannabinoids, especially CBD, which is enriched in several products, may be higher in case of the consumption of CBD oils than in case of smoking cannabis.

[1]Department of Ophthalmology, Faculty of Medicine, Albert Szent-Györgyi Clinical Center, University of Szeged, Szeged, Hungary. [2]Department of Pharmacology and Pharmacotherapy, University of Szeged, Szeged, Hungary. [3]MTA-SZTE Research Group for Cardiovascular Pharmacology, Hungarian Academy of Sciences, Szeged, Hungary. [4]Department of Pharmacognosy, Faculty of Pharmacy, University of Szeged, Eötvös u. 6, Szeged 672, Hungary. [5]Institute for Translational Medicine, Medical School, University of Pécs, Pecs, Hungary. [6]Department of Pharmacology and Pharmacotherapy, Interdisciplinary Excellence Centre, University of Szeged, Szeged 6720, Hungary. [7]These authors contributed equally: Péter Orvos and Bence Pászti. [8]These authors jointly supervised this work: László Virág and Dezső Csupor. ✉email: csupor.dezso@pharmacognosy.hu

The cardiovascular adverse effects of cannabinoid use have been reported in several case reports, and range from arrhythmias to myocardial infarction and sudden death[3]. According to the results of a cohort study, marijuana smokers have a 4.8-fold increased risk of developing acute myocardial infarction during the first hour of exposure[4]. However, other data do not support the association between cannabis use and cardiovascular events[5]. The most comprehensive study assessed data for 316,397 cannabis users and 20,499,215 non-users, and found that cannabis use is an independent predictor of heart failure[1]. Although the exact mechanisms explaining these observations are unknown, the activities of cannabinoids exerted via the G protein-coupled cannabinoid receptors are supposed to be of key importance. In addition, several studies described the proarrhythmic potency of cannabinoids ranging from ventricular arrhythmias to sudden cardiac death[6–8]. However, the exact association and mechanism of these arrhythmias remain unknown[7]. Besides, certain voltage-gated ion channels like cardiac sodium, calcium[9] and Kv4.3 channels[10] might also be related to the reported cardiovascular effects of cannabinoids, but the exact role of these channels has not been studied yet in detail. One of the most important ion channels in cardiac repolarization is the rapid delayed rectifier potassium channel (I_{Kr}), which plays a critical role in cardiac repolarization, having a pore-forming subunit encoded by the *hERG* (the human Ether-à-go-go-Related Gene) gene. Inhibitors of I_{Kr} (also called hERG ion channel) are known to lengthen the QT interval, and hence might induce life-threatening arrhythmias. Therefore, formal drug development requires an early screening of whether the potential drug candidates bear any activities on the hERG channels[11]. However, drug effects on cardiac repolarization cannot be accurately estimated by measuring hERG channel currents alone[12], since drug responses on native I_{Kr} channel and action potential can be different from those measured in hERG.

In the present study cannabidiol (CBD), tetrahydrocannabinol (THC) and 11-nor-9-carboxy-tetrahydrocannabinol (11-nor-9-carboxy-THC), the main metabolite of THC was assessed for their effects on the hERG channels in an in vitro assay. CBD and THC are the major components of cannabis products for medicinal and recreational use, respectively, and since the latter is quickly metabolized to 11-nor-9-carboxy-THC, these three compounds were chosen to be tested in vitro.

Therefore, the aim of our work was to study the in vitro and in vivo effects of CBD a major cannabinoid on cardiac ventricular action potential, on ECG parameters, on the hERG and on other native cardiac transmembrane channels to provide experimental data for the elucidation of their possible adverse cardiac electrophysiological effects.

Results

As our first test shown in Fig. 1, CBD was found to be an inhibitor of the hERG potassium channel with intermediate potency represented by IC_{50} values of 2.07 ± 0.12 μM (n = 6) at room temperature. The IC_{50} values for the inhibition elicited by THC were higher (10.30 ± 0.55 μM, n = 6 at room temperature). 11-Nor-9-carboxy-THC exhibited only a marginal effect ($IC_{50} = 65.40 \pm 3.82$ μM, n = 4 at room temperature).

The cardiac cellular electrophysiological effect of the most potent cannabis compound CBD was further studied on various transmembrane ionic currents by the whole-cell configuration of the patch clamp technique in native rabbit ventricular myocytes and on action potentials in rabbit and guinea pig right ventricular papillary muscle by the conventional microelectrode technique and on in vivo ECG studies in anaesthetized guinea pigs. Figure 2 shows that CBD lengthens action potential duration (APD_{90}) slightly but significantly at 1 μM and at 2.5 μM. This latter effect depended on the stimulation frequency and vanished at slow pacing rate. At high 10 μM concentration CBD exerted variable effect on repolarization including minimal or no change, shortening and lengthening of APD_{90} resulting statistically not significant alteration of APD. At 1 and 2.5 μM CBD caused triangulation in some experiments but not in others reflected as not significant change in APD_{90}–APD_{25}. Similar results were obtained in guinea pig papillary muscles where 2.5 and 5 μM CBD increased APD_{90} from 186.2 ± 6.1 ms and 179.9 ± 6.0 ms to 192.2 ± 6.8 and to 191.5 ± 8.9 ms, respectively ($p < 0.05$, n = 5).

In anaesthetized in vivo guinea-pig experiments intravenous administration of 0.3 mg/kg and 1 mg/kg CBD lengthened QTc and QRS intervals in a statistically significant manner without significantly changing other ECG parameter (Fig. 3).

Whole-cell patch clamp experiments on rabbit native cardiac ventricular myocytes revealed significant and voltage-dependent inhibition of the rapid delayed rectifier potassium current (I_{Kr}) (Figs. 4a,c) with an estimated IC_{50} value of 6.5 μM after a 20 mV 1 s long test pulse and measured at −40 mV as deactivating tail current (Fig. 4b).

The observation that high (10 μM) concentration of CBD did not further lengthened APD prompted us to study the possible effect of CBD on inward L-type Ca^{2+} (I_{CaL}) and late inward Na^{+} (I_{NaL}) currents. As Fig. 5a,b show, 10 μM CBD decreased I_{CaL} significantly and in a frequency-dependent manner. In addition, 10 μM CBD also significantly inhibited I_{NaL} by 41.5% at −20 mV (Fig. 5c,d).

Discussion

The main result of our study is that CBD lengthens repolarization at low and does not change it statistically significant manner at higher concentrations. This effect on repolarization in rabbit papillary muscle can be best explained by the multiple ion channel effects of CBD. Accordingly, at lower concentrations (1, 2.5 and 5 μM) I_{Kr} depression results in lengthening of APD_{90}, which is counterbalanced by inward Ca^{2+} and Na^{+} currents inhibition at 10 μM. Similar effect was earlier described by quinidine, an antiarrhythmic drug, with reported proarrhythmic property[13,14]. The I_{Kr} inhibition by CBD, which is consistent with the hERG blockade, is most probably a direct effect on the channel but the effect of CBD on I_{NaL} and on I_{CaL} can be either direct or receptor mediated, as well. It needs more research to be established.

The higher IC_{50} values of THC and 11-nor-9-carboxy-THC than that of CBD in hERG current measurement in our study does not necessarily mean that CBD is more potent in other type of experiments since potency can

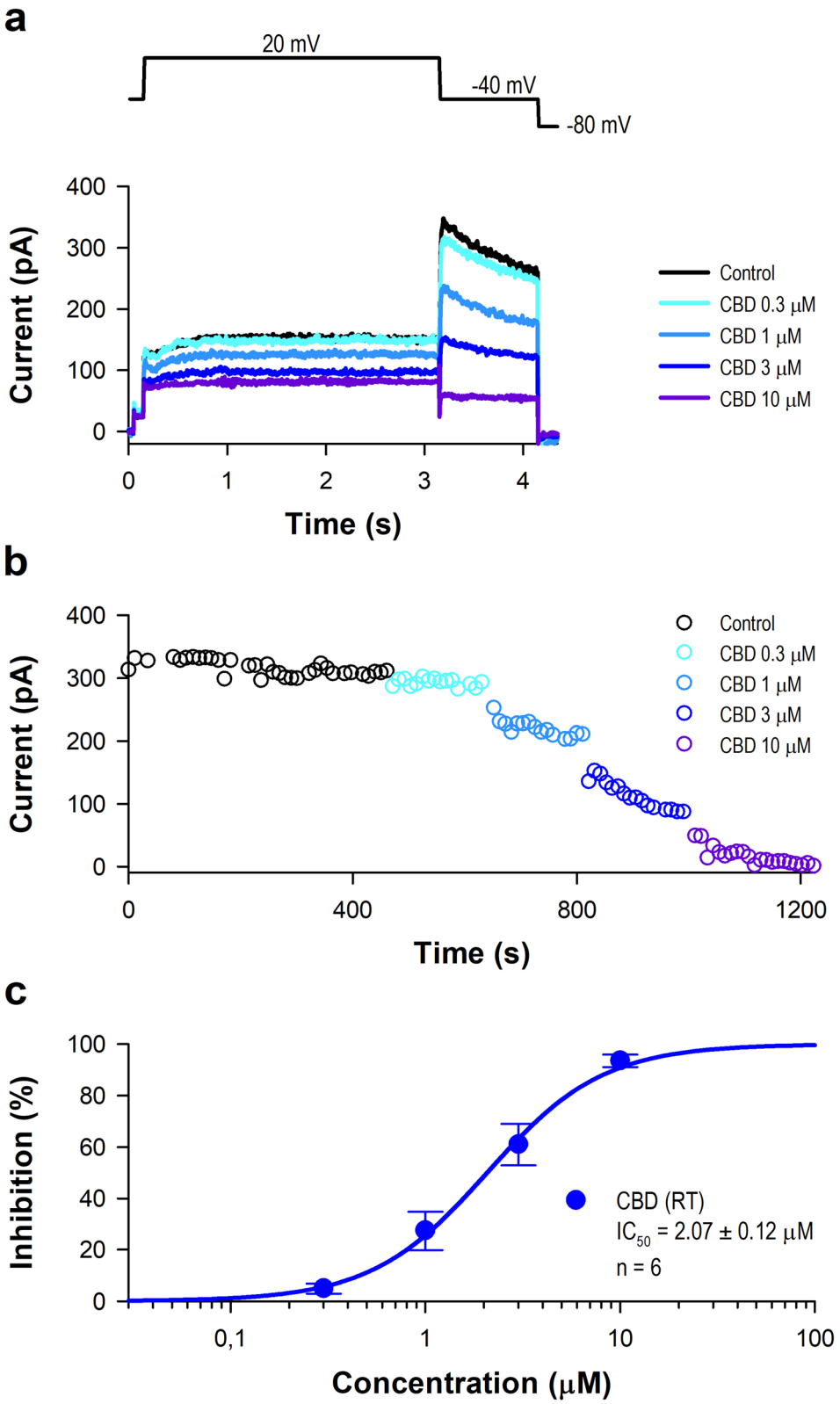

Figure 1. Effect of CBD on hERG current at room temperature. (**a**) Representative current curves obtained from HEK-hERG cells treated with 0.3, 1, 3, and 10 μM CBD. The currents were recorded using the voltage protocol shown at the top of the panel after 3–5 min acute superfusion of the drugs without washout. (**b**) Time-course of the hERG peak tail current amplitude upon the application of different concentrations of CBD. (**c**) Dose–response curves of CBD's inhibitory activity on the hERG channel.

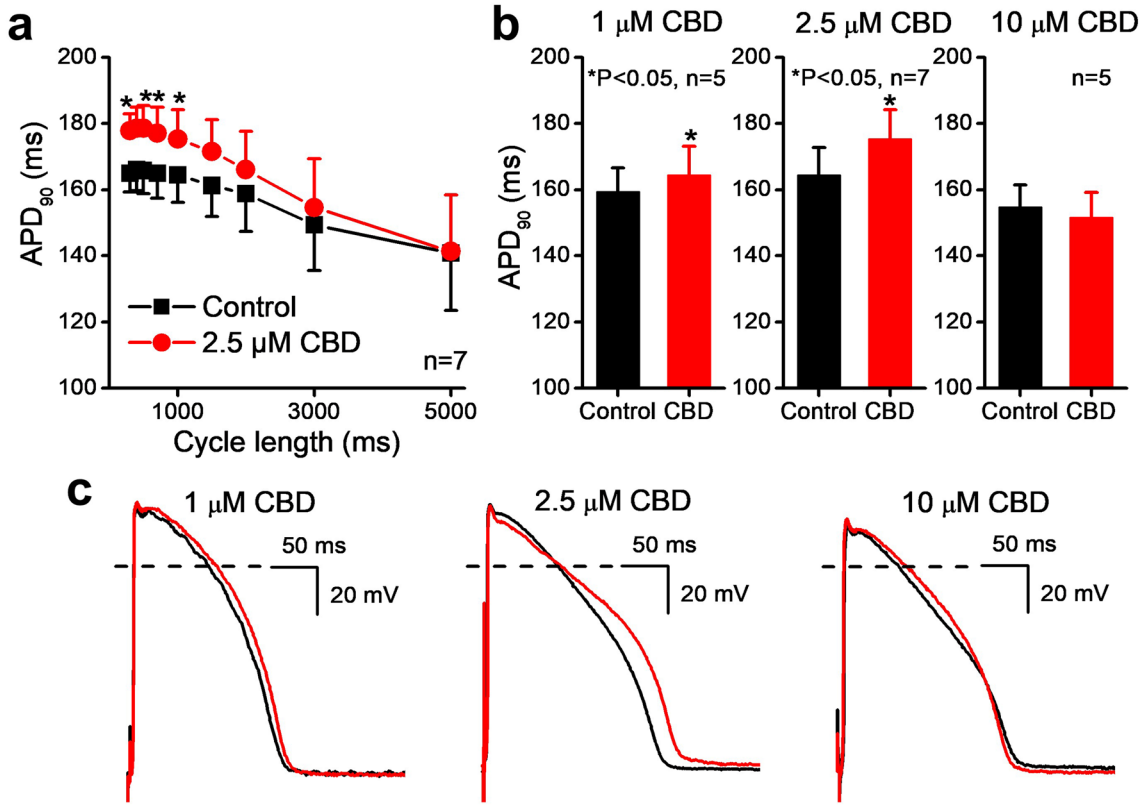

Figure 2. Effect of CBD after 30–50 min acute superfusion of the drug without washout on action potentials recorded from rabbit right ventricular papillary muscle at 37 °C. (**a**) The cycle length-dependent effect of 2.5 μM CBD on the duration of action potentials (APD_{90}). Bar diagrams (**b**) indicates the effects of 1 μM, 2.5 μM and 10 μM CBD on the action potential duration during steady-state at 1000 ms cycle length. Original action potential traces are shown on (**c**) recorded at 1000 ms cycle length in control conditions and in the presence of 1 μM, 2.5 μM and 10 μM CBD.

differ from a target to another[12]. However, in our study due to technical limitations we focused our investigations to examine the effects of CBD in more depth.

Some previous study with cannabinoids showed effects on various transmembrane ion channels such as inward sodium[9,15], inward calcium[9], outward transient current[16] and human Kv1.5 and Kv4.3 channels[10,17]. Our results in rabbit ventricular myocytes are in good agreement with those reported by Al Kury et al. on inward calcium and sodium currents in rat ventricular myocytes[9]. In a previous study hERG channel inhibition and QT lengthening were also reported in anaesthetized rats[18] by a synthetic cannabinoid compound (JWH-030). This synthetic cannabinoid compound differs from those investigated by us and inhibited hERG channel with a relatively high IC_{50} (88.36 μM). In addition, in rat ventricle hERG/I_{Kr} seems not so important to control repolarization than Kv4.2 and Kv1.5 channels. Therefore, the cannabinoid-evoked QT changes in rat most likely can be attributed to Kv1.5 and Kv4.2 rather than hERG channel inhibition. It is worth to note that in the same study[18] a cannabinoid derivate JWH-030 did not change APD in low but shortened it at high (30 μM) concentration. Therefore, the results of our study is in partial agreement with these earlier reports and the differences are best explained by different preparations, chemical differences of the studied compounds and experimental conditions.

The IC_{50} values reported here together with the C_{max} values of CBD allow the assessment of cardiovascular risks of this compound. Based on the comparison of hERG or I_{Kr} activity, cardiac action potential duration, and QT prolongation against QT effects and reports of arrhythmogenic (torsade de pointes) potential of 100 drugs, a margin of at least 30-fold between hERG IC_{50} and C_{max} was proposed to an acceptable degree of safety from arrhythmogenesis[19]. According to human pharmacokinetic data, the C_{max} values for CBD might reach 0.35 μM and 0.58 μM after CBD smoking (19.2 mg) and oral intake (400 mg), respectively[20]. In our experiments CBD had an inhibitory effect on both the hERG channel and I_{Kr} activity, with an IC_{50} value higher than literary C_{max} values in patients. Considering the IC_{50} values for I_{kr} and hERG channel inhibition in our experiments (6.5 and 2.07 μM, respectively), the ratios of IC_{50} and C_{max} values are in the range of 3.57–18.57. This safety margin (below 30) suggests a potential proarrhythmic risk in human setting. However, previous clinical reports documented no significant QT and QT_c prolongation in patients after CBD administration[21]. Also, in another study it was found that long term Sativex (CBD + THC) treatment evoked T wave changes only 1 out of 146 patients[22]. This might be explained by the effects of CBD on other ion channels than hERG and I_{Kr} (eg. I_{CaL} and I_{NaL}). However, in patients who have slower drug elimination due to certain diseases or in case of concurrent use of medicines inhibiting the metabolism of CBD, higher C_{max} values may develop and the risk of arrhythmia might be increased[23]. Moreover, when co-administered with pharmacological agents affecting cardiac repolarization, as well as in certain

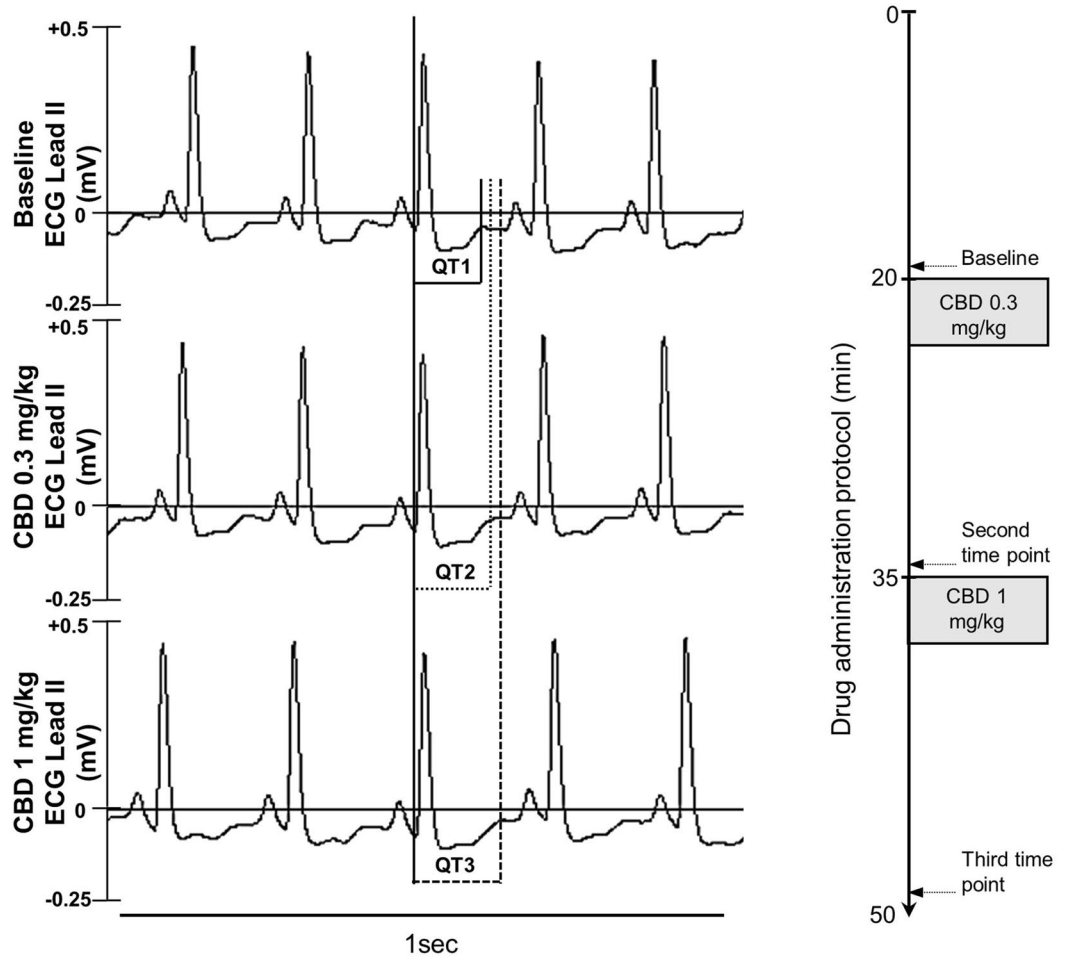

(n=5)	RR (ms)	HR (bpm)	QT (ms)	QTc (ms)	QRS (ms)
1. Baseline	212.8±12.2	285.5±14.0	130.6±8.2	145.8±3.9	47.6±2.9
2. CBD 0.3 mg/kg	211.2±6.7	286.5±8.0	135.1±5.6	150.9±3.0*	48.1±2.4
3. CBD 1 mg/kg	204.9±5.6	295.7±7.1	139.4±5.3	157.8±3.1*	50.1±1.9*

Figure 3. The volume conducted electrocardiogram (ECG lead II) signals in regular sinus rhythm in a pentobarbital anaesthetized (30 mg/kg i.p. bolus injection) guinea pig at three different time points indicated with dashed arrows: **1.** drug-free baseline, value determined from 40 consecutive beats before drug administration; **2.** value determined from 40 consecutive beats 15 min after the 0.3 mg/kg intravenously (iv) administered cannabidiol (CBD) by 2 min bolus; **3.** value determined from 40 consecutive beats 15 min after the 1 mg/kg iv administered CBD by 2 min bolus. RR interval: the time elapsed between two successive R-waves of the QRS signal on the ECG. *HR* heart rate, *QT interval* the time from the start of the Q wave to the end of the T wave, *QTc interval* heart rate corrected QT interval, calculated with a correction method described earlier[27,28], *QRS interval* the time from the onset to the end of the QRS complex. Table shows the mean ± SE values of the ECG intervals at three different time points. Changes in mean scores over three time points were compared using the repeated measures ANOVA with Bonferroni correction. *$p < 0.05$ was taken as indicative of a statistically significant difference between values.

pathophysiological conditions such as hypokalaemia, or diseases like LQT syndrome, HCM, diabetes mellitus or heart failure where cardiac repolarization reserve or drug metabolism is impaired, CBD may have an additive effect, further increasing the proarrhythmic risk and the possibility of sudden cardiac death. Such additive

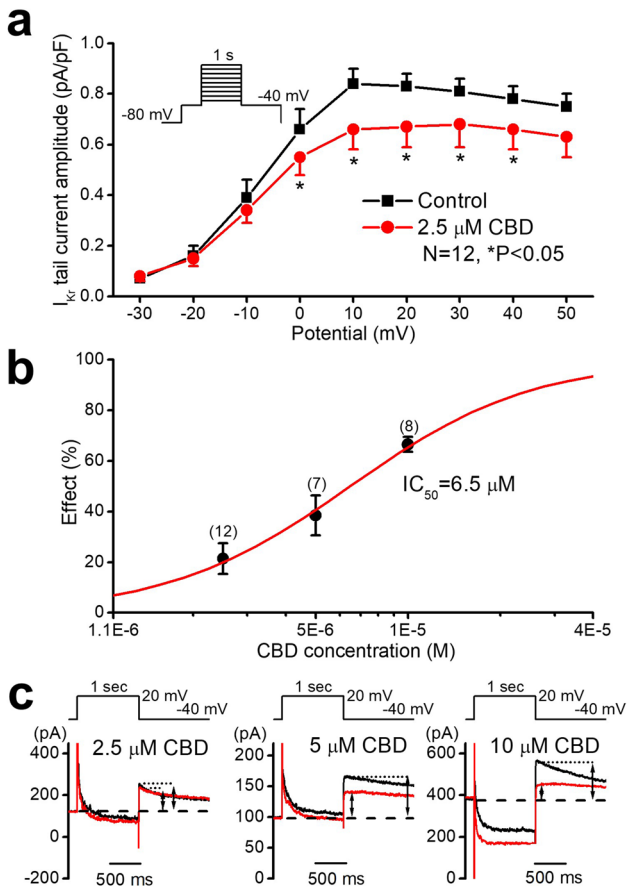

Figure 4. Effect of CBD after 3–5 min acute superfusion of the drug without washout on the rapid delayed rectifier potassium current (I_{Kr}) in rabbit left ventricular myocytes at 37 °C. Current–voltage curves show the inhibition of I_{Kr} by 2.5 μM CBD (**a**). (**b**) Displays CBD concentration–response curve indicating an estimated IC_{50} value of 6.5 μM for I_{Kr} blockade. Original I_{Kr} current traces are shown on (**c**) in control conditions and in the presence of 2.5 μM, 5 μM and 10 μM CBD recorded from rabbit left ventricular myocytes after a 1 s long pulse to 20 mV test potential with pulsing cycle length of 20 s. I_{Kr} deactivating tail current was measured at −40 mV. The vertical axis on the left side of the panels shows the absolute current level. The dashed lines refer to the baseline for I_{Kr} tail current level after the test pulse at −40 mV. The arrows indicate the amplitudes of the I_{Kr} tail currents.

effect was reported in both in experiments[24] and in patients[25]. The cardiovascular effects of CBD may only partly be interpreted on its effects on hERG and I_{Kr} ion channels, the cardiovascular safety of this compound may be influenced by its activities on other ion channels. Further studies are needed to assess the effects of other cannabinoids as well, and the in vivo relevance of these results, with special focus on the benefit-risk assessment of products with different cannabinoid content.

Methods

The hERG channel current was measured by planar technology in HEK 293 cell line by the whole-cell configuration using an automated patch clamp system (Patchliner, Nanion Technologies GmbH., Munich, Germany) at room temperature as described previously[12]. The following solutions were used during automated patch-clamp recording (compositions in mM): internal solution: KCl 50, NaCl 10, KF 60, EGTA 20, HEPES 10, pH 7.2 (KOH); external solution: NaCl 140, KCl 4, glucose-monohydrate 5, $MgCl_2$ 1, $CaCl_2$ 3, HEPES 10, pH 7.4 (NaOH). The voltage protocol for hERG ion channel started with a short (100 ms) −40 mV step to establish the baseline region. A depolarizing step was applied to the test potential of 20 mV for 3 s, and then the cell was repolarized to −40 mV (1 s) to evoke outward tail current. The peak tail current was corrected the leak current defined during the first period to −40 mV. Holding potential was −80 mV. The pulse frequency was approximately 0.1 Hz. Recording started in external solution. After this control period, increasing concentrations of the test compound were applied, in order to record a complete concentration–response curve.

The action potential measurements were carried out in rabbit and guinea pig right ventricular papillary muscles by the conventional microelectrode techniques at 37 °C as described in detail earlier[12,26]. Isolated muscle preparations obtained from the right ventricle were individually mounted in a tissue chamber while superfused with oxygenated modified Locke's solution containing (in mM): NaCl 128.3, KCl 4, $CaCl_2$ 1.8, $MgCl_2$ 0.42,

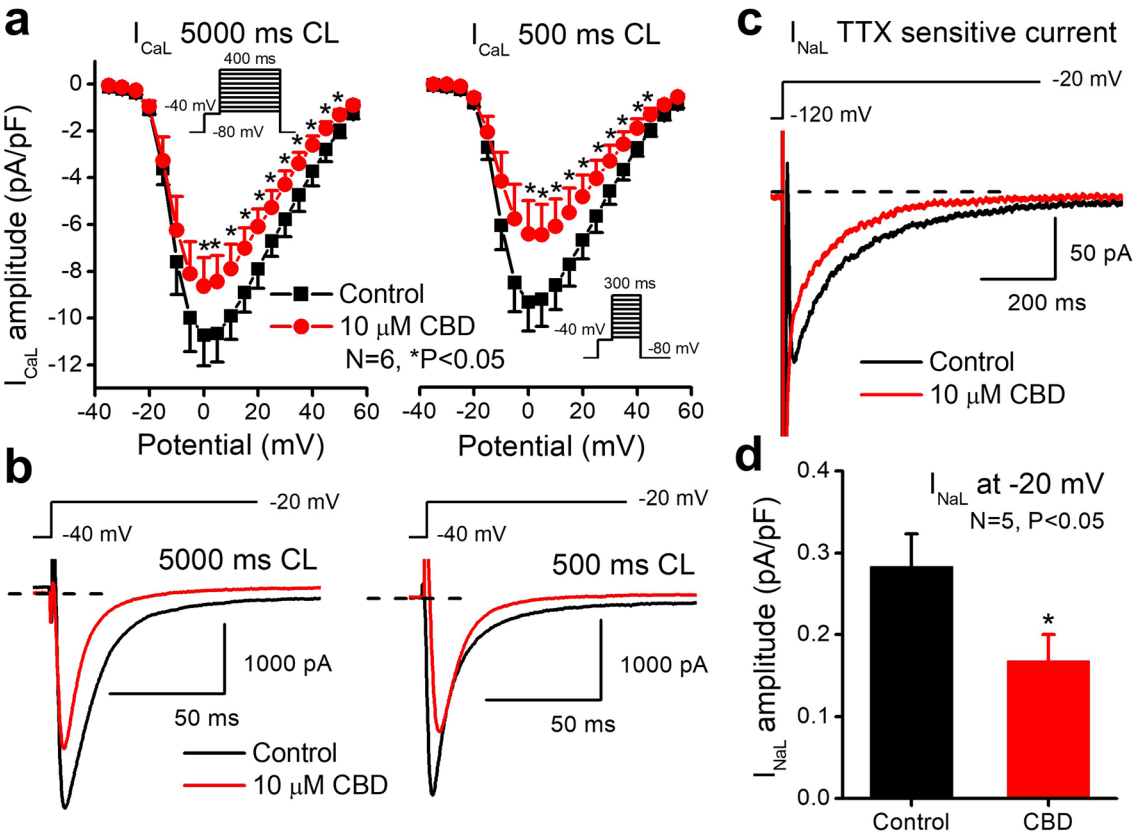

Figure 5. Effect of CBD after 3–5 min acute superfusion of the drug without washout on L-type calcium (I_{CaL}) and on the late sodium (I_{NaL}) currents in rabbit left ventricular myocytes at 37 °C. On (**a**) current–voltage curves show the inhibition of I_{CaL} by 10 μM CBD at 5000 ms (left) and at 500 ms (right) cycle lengths. Original I_{CaL} current traces are shown on (**b**) in control conditions and in the presence of 10 μM CBD recorded from rabbit left ventricular myocytes at 5000 ms (left) and at 500 ms (right) cycle lengths at 0 mV test potential. TTX sensitive current (I_{NaL}) traces (**c**) and a bar diagram (**d**) show the inhibition of I_{NaL} by 10 μM CBD measured at −20 mV in rabbit left ventricular myocytes.

$NaHCO_3$ 21.4 and glucose 10 (pH 7.35–7.4) and stimulated through a pair of platinum electrodes with constant cycle length of 1000 ms. In case of cycle length-dependent measurements stimulation with different constant cycle lengths ranging from 300 to 5000 ms were also applied. Transmembrane potentials were recorded using conventional glass microelectrodes, filled with 3 M KCl and having tip resistances of 5–20 MΩ, connected to the input of a high impedance electrometer (Experimetria, type 309, Budapest, Hungary). The analog action potential signals were digitized with analogue-to-digital converters (ADA 3300, Real Time Devices Inc., State College, PA, USA) under software control (APES home-made software).

Transmembrane ion currents in native rabbit ventricular myocytes were measured by the whole-cell configuration of the patch clamp technique at 37 °C (Axopatch 200B, Molecular Devices Inc., Sunnyvale, CA, USA) as described in detail earlier[12]. Rapid delayed rectifier potassium current (I_{Kr}), was recorded in HEPES-buffered Tyrode's solution containing (in mM) NaCl 144, NaH_2PO_4 0.33, KCl 4.0, $CaCl_2$ 1.8, $MgCl_2$ 0.53, glucose 5.5 and HEPES 5.0, at pH of 7.4. The composition of the pipette solution (in mM) was the following: KOH 110, KCl 40, K_2ATP 5, $MgCl_2$ 5, EGTA 5, and HEPES 10 (pH was adjusted to 7.2 by aspartic acid). 1 μM nisoldipine and 0.5 μM HMR-1556 (the selective blocker of the slow delayed rectifier K^+ current—I_{Ks}) were added to the external solution to eliminate I_{CaL} and I_{Ks}, respectively. I_{Kr} was determined as tail current at −40 mV after the end of 1 s long depolarizing pulses ranging from −30 to +50 mV with pulsing cycle length of 20 s. The L-type calcium current (I_{CaL}) was recorded in HEPES-buffered Tyrode's solution supplemented with 3 mM 4-aminopyridine. A special solution was used to fill the micropipettes (composition in mM: CsCl 125, TEACl 20, MgATP 5, EGTA 10, HEPES 10, pH was adjusted to 7.2 by CsOH). I_{CaL} current was evoked by 400 ms long depolarizing voltage pulses to various test potentials ranging from −35 to +55 mV with pulsing cycle length of 5 s. The holding potential was −80 mV. A short prepulse to −40 mV served to inactivate Na^+ current. The sodium current was activated by 2 s long depolarizing voltage pulses to −20 mV from the holding potential of −120 mV with pulsing cycle length of 5 s. After 5–7 min incubation with CBD the external solution was replaced by that containing 20 μM TTX. TTX at this concentration completely blocks the late sodium current (I_{NaL}). The external solution was HEPES-buffered Tyrode's solution supplemented with 1 μM nisoldipine, 0.5 μM HMR-1556 and 0.1 μM dofetilide in order to block I_{CaL}, I_{Ks} and I_{Kr} currents. The composition of the pipette solution (in mM) was: KOH 110, KCl 40, K_2ATP 5, $MgCl_2$ 5, EGTA 5, HEPES 10 (pH was adjusted to 7.2 by aspartic acid).

ECG recordings were taken from adult guinea-pigs of both sexes (600–800 g) anaesthetized by intraperitoneal 30 mg/kg pentobarbital and I–III leads were recorded after 15 min of cumulative intravenous administration of CBD into the jugular vein[27].

Statistics. All data are expressed as means ± SEM. Statistical analysis was performed with Student's *t* test for paired data. The results were considered statistically significant when p was < 0.05.

Animal ethics statement. All experiments performed in rabbit and guinea pig ventricular preparations were carried out in compliance with the Guide for the Care and Use of Laboratory Animals (USA NIH publication NO 85-23, revised 1996) and conformed to the Directive 2010/63/EU of the European Parliament. The protocols have been approved by the Ethical Committee for the Protection of Animals in Research of the University of Szeged, Szeged, Hungary (approval number: I-74-24-2017) and by the Department of Animal Health and Food Control of the Ministry of Agriculture and Rural Development (authority approval number XIII/3331/2017).

Received: 5 February 2020; Accepted: 10 September 2020
Published online: 30 September 2020

References

1. Kalla, A., Krishnamoorthy, P. M., Gopalakrishnan, A. & Figueredo, V. M. Cannabis use predicts risks of heart failure and cerebrovascular accidents: Results from the National Inpatient Sample. *J. Cardiovasc. Med. (Hagerstown)* **19**, 480–484 (2018).
2. Fraguas-Sánchez, A. I. & Torres-Suárez, A. I. Medical use of cannabinoids. *Drugs* **78**, 1665–1703 (2018).
3. Pacher, P., Steffens, S., Hasko, G., Schindler, T. H. & Kunos, G. Cardiovascular effects of marijuana and synthetic cannabinoids: The good, the bad, and the ugly. *Nat. Rev. Cardiol.* **15**, 151–166 (2018).
4. Mittleman, M. A., Lewis, R. A., Maclure, M., Sherwood, J. B. & Muller, J. E. Triggering myocardial infarction by marijuana. *Circulation* **103**, 2805–2809 (2001).
5. Singh, S. M., Koh, M., Fang, J. & Ko, D. T. The risk of cardiovascular events on cannabis' highest day. *Can. J. Cardiol.* **35**, 1589–1591 (2019).
6. Courts, J., Maskill, V., Gray, A. & Glue, P. Signs and symptoms associated with synthetic cannabinoid toxicity: Systematic review. *Australas. Psychiatry* **24**, 598–601 (2016).
7. Ozturk, H. M., Yetkin, E. & Ozturk, S. Synthetic cannabinoids and cardiac arrhythmia risk: Review of the literature. *Cardiovasc. Toxicol.* **19**, 191–197 (2019).
8. Manolis, T. A., Manolis, A. A. & Manolis, A. S. Cannabis associated 'high' cardiovascular morbidity and mortality: Marijuana smoke like tobacco smoke? A Deja Vu/Deja Vecu Story?. *Mini Rev. Med. Chem.* **19**, 870–879 (2019).
9. Al Kury, L. T. *et al.* Effects of the endogenous cannabinoid anandamide on voltage-dependent sodium and calcium channels in rat ventricular myocytes. *Br. J. Pharmacol.* **171**, 3485–3498 (2014).
10. Amoros, I. *et al.* Endocannabinoids and cannabinoid analogues block human cardiac Kv4.3 channels in a receptor-independent manner. *J. Mol. Cell. Cardiol.* **48**, 201–210 (2010).
11. Sanguinetti, M. C. & Tristani-Firouzi, M. hERG potassium channels and cardiac arrhythmia. *Nature* **440**, 463–469 (2006).
12. Orvos, P. *et al.* Evaluation of possible proarrhythmic potency: Comparison of the effect of dofetilide, cisapride, sotalol, terfenadine, and verapamil on hERG and native IKr currents and on cardiac action potential. *Toxicol. Sci.* **168**, 365–380 (2019).
13. Roden, D. M. & Hoffman, B. F. Action potential prolongation and induction of abnormal automaticity by low quinidine concentrations in canine Purkinje fibers. Relationship to potassium and cycle length. *Circ. Res.* **56**, 857–867 (1985).
14. Varro, A., Elharrar, V. & Surawicz, B. Effect of antiarrhythmic drugs on the premature action potential duration in canine cardiac Purkinje fibers. *J. Pharmacol. Exp. Ther.* **233**, 304–311 (1985).
15. Ghovanloo, M.-R. *et al.* Inhibitory effects of cannabidiol on voltage-dependent sodium currents. *J. Biol. Chem.* **293**, 16546–16558 (2018).
16. Li, Q. *et al.* Effects of anandamide on potassium channels in rat ventricular myocytes: A suppression of I(to) and augmentation of K(ATP) channels. *Am. J. Physiol. Cell Physiol.* **302**, C924–C930 (2012).
17. Barana, A. *et al.* Endocannabinoids and cannabinoid analogues block cardiac hKv1.5 channels in a cannabinoid receptor-independent manner. *Cardiovasc. Res.* **85**, 56–67 (2010).
18. Yun, J. *et al.* Synthetic cannabinoid, JWH-030, induces QT prolongation through hERG channel inhibition. *Toxicol. Res. (Camb)* **5**, 1663–1671 (2016).
19. Redfern, W. *et al.* Relationships between preclinical cardiac electrophysiology, clinical QT interval prolongation and torsade de pointes for a broad range of drugs: Evidence for a provisional safety margin in drug development. *Cardiovasc. Res.* **58**, 32–45 (2003).
20. Millar, S. A., Stone, N. L., Yates, A. S. & O'Sullivan, S. E. A systematic review on the pharmacokinetics of cannabidiol in humans. *Front. Pharmacol.* **9**, 1365 (2018).
21. Sellers, E. M. *et al.* A multiple-dose, randomized, double-blind, placebo-controlled, parallel-group QT/QTc study to evaluate the electrophysiologic effects of THC/CBD spray. *Clin. Pharmacol. Drug Dev.* **2**, 285–294 (2013).
22. Serpell, M. G., Notcutt, W. & Collin, C. Sativex long-term use: An open-label trial in patients with spasticity due to multiple sclerosis. *J. Neurol.* **260**, 285–295 (2013).
23. Iffland, K. & Grotenhermen, F. An update on safety and side effects of cannabidiol: A review of clinical data and relevant animal studies. *Cannabis Cannabinoid Res.* **2**, 139–154 (2017).
24. Lengyel, C., Varro, A., Tabori, K., Papp, J. G. & Baczko, I. Combined pharmacological block of I(Kr) and I(Ks) increases short-term QT interval variability and provokes torsades de pointes. *Br. J. Pharmacol.* **151**, 941–951 (2007).
25. Wisniowska, B., Tylutki, Z., Wyszogrodzka, G. & Polak, S. Drug-drug interactions and QT prolongation as a commonly assessed cardiac effect—comprehensive overview of clinical trials. *BMC Pharmacol. Toxicol.* **17**, 12 (2016).
26. Lengyel, C. *et al.* Pharmacological block of the slow component of the outward delayed rectifier current (I(Ks)) fails to lengthen rabbit ventricular muscle QT(c) and action potential duration. *Br. J. Pharmacol.* **132**, 101–110 (2001).
27. Farkas, A. S. *et al.* The role of the Na^+/Ca^{2+} exchanger, I Na and I CaL in the genesis of dofetilide-induced torsades de pointes in isolated, AV-blocked rabbit hearts. *Br. J. Pharmacol.* **156**, 920–932 (2009).
28. Carlsson, L., Abrahamsson, C., Andersson, B., Duker, G. & Schiller-Linhardt, G. Proarrhythmic effects of the class III agent almokalant: Importance of infusion rate, QT dispersion, and early afterdepolarisations. *Cardiovasc. Res.* **27**, 2186–2193 (1993).

Acknowledgements
The authors thank Dora Bokor, PharmD, for proofreading the manuscript. Financial support from the Economic Development and Innovation Operative Programme GINOP-2.3.2-15-2016-00012, the National Research Development and Innovation Office (NKFIH K 119992), the Ministry of Human Capacities Hungary (20391 3/2018/FEKUSTRAT and EFOP-3.6.2-16-2017-00006), and from the Hungarian Academy of Sciences are gratefully acknowledged.

Author contributions
D.C., B.C.-L., L.V. and A.V. conceived the experiment, P.O., B.P., L.T., A.P., Á.B., P.G., J.P. and E.T.-M. conducted the experiment(s), P.O., L.V. and A.V. analysed the results, D.C., T.K., J.H., L.V. and A.V. prepared the manuscript. All authors reviewed the manuscript.

Competing interests
The authors declare no competing interests.

Additional information
Correspondence and requests for materials should be addressed to D.C.

Reprints and permissions information is available at www.nature.com/reprints.

Publisher's note Springer Nature remains neutral with regard to jurisdictional claims in published maps and institutional affiliations.

IV.

Cardiac electrophysiological effects of ibuprofen in dog and rabbit ventricular preparations: Possible implication to enhanced proarrhythmic risk

Bence Pászti[a,§], János Prorok[a,c,§], Tibor Magyar[a,], Tamás Árpádffy-Lovas[a,], Balázs Györe[d], Leila Topál[a], Péter Gazdag[a], Jozefina Szlovák[a], Muhammad Naveed[a], Norbert Jost[a,b,c], Norbert Nagy[a,c], András Varró[a,b,c,+], László Virág[a,b,c,*], István Koncz[a,*]

[a]Department of Pharmacology and Pharmacotherapy, Faculty of Medicine, University of Szeged, Szeged, Hungary;
[b]Department of Pharmacology and Pharmacotherapy, Interdisciplinary Excellence Centre, University of Szeged, Szeged, Hungary
[c]MTA-SZTE Research Group of Cardiovascular Pharmacology, Szeged, Hungary
[d] Department of Oral Surgery, Faculty of Dentistry, University of Szeged, Hungary

[§] Shared first authorship
[*] Shared senior authorship
[+] Corresponding author

Author for correspondence at:
Andras Varró MD, PhD
Department of Pharmacology & Pharmacotherapy
Faculty of Medicine
University of Szeged
Dóm tér 12,
H-6721 Szeged, Hungary

Telephone: +36 62 545 682
Fax: +36 62 545 680
E-mail: varro.andras@med.u-szeged.hu

Abstract

Ibuprofen is a widely used non-steroidal anti-inflammatory drug, which has recently been associated with increased cardiovascular risk, but its electrophysiological effects have not yet been properly studied in isolated cardiac preparations. We studied the effects of ibuprofen on action potential characteristics and several transmembrane ionic currents using the conventional microelectrode technique and the whole-cell configuration of the patch-clamp technique on cardiac preparations and enzymatically isolated ventricular myocytes. In dog (200 μM; n=6) and rabbit (100 μM; n=7) papillary muscles, ibuprofen moderately but significantly prolonged repolarization at 1 Hz stimulation frequency. In dog Purkinje fibers, repolarization was abbreviated, and maximal rate of depolarization was depressed in a frequency-dependent manner. Levofloxacin (40 μM) alone did not alter repolarization, but augmented the ibuprofen-evoked repolarization lengthening in rabbit preparations (n=7). In dog myocytes, ibuprofen (250 μM) did not significantly influence I_{K1}, but decreased the amplitude of I_{to} and I_{Kr} potassium currents by 28.2% (60 mV) and 15.2% (20 mV) respectively. Ibuprofen also depressed I_{NaL} and I_{Ca} currents by 19.9% and 16.4%. We conclude that ibuprofen seems to be free from effects on AP parameters at lower concentrations. However, at higher concentrations it may alter repolarization reserve, contributing to the observed proarrhythmic risk in patients.

Keyword: ibuprofen , levofloxacin , repolarization reserve

List of abbreviations

APA: Action potential amplitude

APD_{50}: Action potential duration at 50% of repolarization

APD_{90}: Action potential duration at 90% of repolarization

I_{Ca}: Voltage-dependent calcium current

I_{K1}: Inward rectifier potassium current

I_{Kr}: Rapidly activating delayed rectifier potassium current

I_{Ks}: Slowly activating delayed rectifier potassium current

I_{NaL}: Late sodium current

I_{to}: Transient outward potassium current

RMP: Resting membrane potential

TdP: Torsades de pointes ventricular tachycardia

SEM: Standard error of the mean

V_{max}: Maximal rate of the action potential upstroke

Introduction

Ibuprofen is one of the most widely used non-steroidal anti-inflammatory drugs (NSAIDs) (Rainsford et al., 2009). However, a recent Danish, nationwide case–time–control study (Sondergaard et al., 2017) found that short term therapy with ibuprofen was associated with an increased risk of cardiac arrest. It is important to mention that this study also concluded that there was an increased risk of out-of-hospital cardiac arrest in diclofenac users. In an observational, historical cohort evaluation (Pratt et al., 1994) it was found that the ibuprofen cohort had a significantly higher arrhythmic event rate. A case report outlined a probable relationship between standard ibuprofen dosing and palpitations (Douglas, 2010). Surprisingly, very little is known about the cardiac electrophysiological effect of ibuprofen, and the cellular cardiac electrophysiological effects of ibuprofen have been investigated only in one study on guinea pig papillary muscle and sinoatrial node (Yang et al., 2008). In these preparations ibuprofen dose-dependently shortened action potential duration and decreased the maximal rate of depolarization (V_{max}) at therapeutically relevant and at high concentrations. The effects of ibuprofen on the action potential parameters and the underlying transmembrane currents have not yet been reported in other cardiac preparations, including those obtained from larger animals (e.g. rabbit or dog), closer to human in heart size, in spontaneous frequency, and in basic electrophysiological properties. Repolarization prolonging properties have also been reported among fluoroquinolone antibiotic agents (Chiba et al., 2000; Garnett & Johannesen, 2016; Komatsu et al., 2019), and combination of such antibiotics and NSAIDs is a common practice in the treatment of infections. Therefore, the purpose of our work was to further characterize the cellular electrophysiological effects of ibuprofen and levofloxacin using preparations obtained from the hearts of large animals, namely dogs and rabbits. We found that 50 μM ibuprofen did not influence the action potential parameters including action potential duration (APD) in dog and rabbit ventricular muscle preparations but at higher concentrations (100-200 μM), especially when repolarization reserve (Varró et al., 2000; Roden, 2006; Varró & Baczkó, 2011) had been previously attenuated, some repolarization lengthening occurred. Therefore, although at low therapeutic concentrations the drug could be considered safe regarding its cardiac electrophysiological effects, it is important to further improve our understanding concerning the possible unfavorable association between ibuprofen and increased cardiovascular risk reported in clinical studies.

Methods

Conventional microelectrode technique

All experiments were conducted in compliance with the Guide for the Care and Use of Laboratory Animals (USA NIH publication No 85-23, revised 1996) and conformed to Directive 2010/63/EU of the European Parliament. The protocols were approved by the Review Board of the Department of Animal Health and Food Control of the Ministry of Agriculture and Rural Development, Hungary (XIII./1211/2012). Ventricular (papillary) muscles were obtained from the right ventricle of rabbits and dogs. Free-running (false tendons of) Purkinje fibers were isolated from both ventricles of dog hearts removed through a right lateral thoracotomy. Male New Zealand rabbits (2–3 kg) were terminated by rapid cervical dislocation, and Beagle dogs (10–15 kg) of both sexes were anesthetized and sacrificed using high dose sodium pentobarbital (60 mg/kg iv). The preparations were placed in a tissue bath and allowed to equilibrate for at least 2 hours while superfused (flow rate 4-5 ml/min) with Locke's solution containing (in mM): NaCl 120, KCl 4, $CaCl_2$ 1.8, $MgCl_2$ 1, $NaHCO_3$ 22, and glucose 11. The pH of this solution was 7.35 to 7.40 when gassed with 95% O_2 and 5% CO_2 at 37 °C. During the equilibration period, the ventricular muscle tissues were stimulated at a basic cycle length of 1000 ms, Purkinje fibers were stimulated at a basic cycle length of 500 ms. Electrical pulses of 0.5–2 ms in duration and twice diastolic threshold in intensity (S_1) were delivered to the preparations through bipolar platinum electrodes. Transmembrane potentials were recorded with the use of glass capillary microelectrodes filled with 3 M KCl (tip resistance: 5 to 15 MΩ). The microelectrodes were coupled through an Ag-AgCl junction to the input of a high-impedance, capacitance-neutralizing amplifier (Experimetria 2011). Intracellular recordings were displayed on a storage oscilloscope (Hitachi V-555) and led to a computer system (APES) designed for on-line determination of the following parameters: resting membrane potential (RMP), action potential amplitude (APA), action potential duration at 50% (APD_{50}) and 90% (APD_{90}) repolarization and the maximum rate of rise of the action potential upstroke (V_{max}). The following types of stimulation were applied in the course of the experiments: stimulation with a constant cycle length of 1000 ms (ventricular muscles); stimulation with a constant cycle length of 500 ms (Purkinje fibers). In case of Purkinje fibers, stimulation with different constant cycle lengths ranging from 300 to 1000 ms were also applied. Control recordings were obtained after equilibration period. The effects of ibuprofen and DMSO not exceeding 18.8% were determined at the given concentrations, after the addition of each compound until 30 minutes

elapsed, in a cumulative manner. Compounds were purchased from Sigma/Merck for all experiments.

Whole cell configuration of the patch clamp technique

Untreated adult beagle dogs of either sex (body weights 8-15 kg) were used for the study. All experiments were conducted in compliance with the *Guide for the Care and Use of Laboratory Animals* (USA NIH publication No 85-23, revised 1985). The protocols were approved by the review board of Committee on Animal Research (CAR) of the Albert Szent-Györgyi Medical University (54/1999 OEj).

The isolation and preparation of dog ventricular myocytes were described earlier in detail (Varró et al, 2000). One drop of cell suspension was placed in a transparent recording chamber mounted on the stage of an inverted microscope. The myocytes were allowed to settle and adhere to the bottom for at least 5-10 minutes before superfusion was initiated with Tyrode solution containing (in mM): NaCl 144, NaH_2PO_4 0.4, KCl 4.0, $CaCl_2$ 1.8, $MgSO_4$ 0.53, glucose 5.5 and HEPES 5.0 (pH 7.4, NaOH). Temperature was set to 37°C. Only rod shaped cells with clear cross-striations were used. Patch-clamp micropipettes were fabricated from borosilicate glass capillaries using a micropipette puller (Flaming/Brown, type P-97, Sutter Co., Novato, CA, USA). These electrodes had resistances between 1.5 and 2.5 MΩ. Membrane currents were recorded with Axopatch 200B patch-clamp amplifiers (Molecular Devices Inc., Sunnyvale, CA, USA) using the whole-cell configuration of the patch-clamp technique. After establishing a high resistance (1-10 GΩ) seal by gentle suction, the cell membrane beneath the tip of the electrode was disrupted by suction or application of short electrical pulses. Membrane currents were digitized after low-pass filtering at 1 kHz using analog-to-digital converters (Digidata 1440A, Molecular Devices Inc., Sunnyvale, CA, USA) under software control (pClamp 10, Molecular Devices Inc., Sunnyvale, CA, USA). The various ion currents were measured as described earlier in detail (Kohajda et al., 2016). The same software was used for off-line analysis.

Statistical analysis

Results are expressed as mean ± S.E.M. Normality of distributions was verified using Shapiro-Wilk test, and homogeneity of variances was verified using Bartlett's test in each treatment group. Statistical comparisons were made using Student's t-test for Tables 1, 2A, and 2B. Variance analysis (ANOVA) for repeated measurements was performed, followed by Bonferroni's post-hoc test for Table 2C. Differences were considered significant when $p < 0.05$.

3. Results

Effects of ibuprofen on transmembrane action potentials

We have investigated the effects of ibuprofen on cardiac action potentials in the concentration range of 50–200 μM (10.3–41.2 μg/ml) in rabbit and dog right ventricular papillary muscle using the conventional microelectrode technique. As Table 1B and 1C, and Figures 1A and 2C show, ibuprofen in dog right ventricular papillary muscle at 50 and 200 μM and at 1 Hz stimulation frequency did not change the resting membrane potential (RMP), the action potential amplitude (APA), or the maximal rate of depolarization (V_{max}), but at 200 μM it moderately lengthened the action potential duration measured at 50 and 90% levels (APD_{50} and APD_{90}). The solvent DMSO at the applied concentration did not affect any of the measured action potential parameters (Table 1A and Figures 1E).

In dog Purkinje fibers, action potentials were studied at a 500 ms constant cycle length (Table 1D), and also at various stimulation cycle lengths, ranging from 300–1000 ms (Figure 2A). At constant cycle length stimulation, ibuprofen at 200 μM concentration elicited significant abbreviation of the action potential duration (APD_{90}), while all other characteristics, including the RP, APA and V_{max}, remained unchanged. As Figure 2B indicates, in Purkinje fibers V_{max} was decreased and APD was shortened in a frequency dependent manner. The decrease in APD_{90} was more pronounced at slower cycle lengths, being significant from 500 ms to 1000 ms. V_{max} depression was observed only at high stimulation rate corresponding to 300 ms cycle length. DMSO elicited no changes in the action potential characteristics of the Purkinje fibers at any cycle length (Table 1A, Figures 1E, 2C and 2D).

The widely known antibiotic, levofloxacin at 40 μM did not change action potential parameters, including APD_{90} in rabbit papillary muscles at 1 Hz stimulation rate (Table 2B

and Figure 3A). However, when levofloxacin was applied in combination with 100 μM ibuprofen, the extent of APD lengthening evoked by levofloxacin was greater than that observed without the application of ibuprofen (Table 2C and Figure 3B).

In order to elucidate the mechanism of the changes induced by ibuprofen in the action potential, the effects of ibuprofen on the transmembrane ionic currents were investigated by the whole cell configuration of the patch clamp technique in dog ventricular myocytes at 250 μM (51.5 μg/ml). The solvent DMSO at the applied concentration did not influence the amplitude or kinetics of the measured transmembrane ionic currents (Figures 4–5). In dog ventricular myocytes, 250 μM ibuprofen did not significantly alter the inward rectifier (I_{K1}) potassium (Figure 4A) and moderately but significantly decreased the transient outward (I_{to}, Figure 4B and 4D) and rapid delayed rectifier (I_{Kr}, Figure 4C and 4E) potassium currents.

Since cardiac repolarization is determined not only by outward potassium currents but also by late inward sodium (I_{NaL}) and L-type inward calcium (I_{Ca}) currents, the effect of ibuprofen was also studied on I_{NaL} and I_{Ca} in dog ventricular myocytes. As Figure 5 indicates, 250 μM ibuprofen moderately, but in a statistically significant manner decreased the amplitude of both I_{NaL} and I_{Ca}.

4. Discussion

The most important message of the present study is to show that ibuprofen in normal situations and therapeutically relevant concentrations exerts none or only moderate repolarization lengthening in ventricular muscle preparations, but in a situation where repolarization reserve has been attenuated, the degree of repolarization lengthening was further increased. This raises the possibility that under such conditions it may enhance proarrhythmic risk and consequent sudden cardiac death.

The paucity of reports regarding the cardiac electrophysiological effects of ibuprofen is surprising in spite of its worldwide use and the two decades of concerns regarding increased risk associated with NSAID drugs in general (Bombardier et al., 2000; Huang, Hsiao, Tsai, et al., 2006; Huang, Hsiao, Wen, et al., 2006). In addition, in a recent meta-analysis it has been reported that two NSAID drugs, diclofenac and ibuprofen, increase out-of-hospital cardiac arrest and consequent sudden deaths (Sondergaard et al., 2017). Although the mechanism of these observations is not clear and can be linked to causes other than direct ion channel

modulation, the possibility of direct effect of ibuprofen on transmembrane ion channels should be also considered. This argument is further strengthened by the previous experimental study (Kristóf et al., 2012), which indicated that diclofenac decreased repolarisation reserve by inhibiting I_{Ks} and I_{Kr} in dog heart. In this paper it has also been shown that diclofenac also facilitated TdP-like arrhythmia in *in vivo* rabbit experiments (Kristóf et al., 2012).

The applied concentrations in the present study were similar to those of the work of Yang et al. (Yang et al., 2008), and fall into the range of low and high therapeutic plasma levels (10–50 μg/ml) observed in patients (Holubek et al., 2007). It is also worth mentioning that in certain situations, including high age, altered metabolism caused by disease or drug interactions, plasma levels may rise beyond normal. In addition, much higher (260 and 352 μg/ml) plasma levels have also been reported after drug intoxication (Holubek et al., 2007).

In guinea pig ventricle it has been previously shown (Yang et al., 2008) that ibuprofen in the concentration range of 10–80 μg/ml shortened APD and depressed V_{max} in a frequency dependent manner. In addition, ibuprofen also depressed slow response action potentials and sinus nodal frequency both indicative of I_{Ca} inhibition (Yang et al., 2008) with concomitant increase of PP and QRS intervals in the ECG, but with a shorter QTc (Yang et al., 2008). Our present results are in partial agreement with the ones reported by Yang et al. (Yang et al., 2008). In the present study, we could confirm the frequency-dependent V_{max} and I_{Ca} inhibition reported by Yang et al. (2008), and we also found inhibition of I_{NaL}. All these effects would lead to shortening in repolarization. However, contrary to the findings reported by Yang et al. (2008), in our experiments moderate but statistically significant repolarization lengthening was observed in ventricular muscle, but not in Purkinje fibers. Also, Yarishkin et al. (2009) reported that diclofenac but not ibuprofen decreased I_{NaL} and I_{Ca} in rat ventricular myocytes. These dissimilarities are most likely due to the difference in the species (neonatal rat vs rabbit), in the experimental conditions (room temperature vs. 37 °C), and in the preparations (1 day cultured trabecules vs isolated papillary muscles) used. Unlike rabbit and dog, guinea pig ventricle lacks I_{to} (Zicha et al., 2003), and expresses very strong I_{Ks} (Bartos et al., 2015). Consequently, in guinea pig ventricle I_{to} and I_{Kr} inhibition have less impact on repolarization when compared to that in rabbit or dog. Therefore, in guinea pig ventricle the ibuprofen-evoked I_{Ca} and I_{NaL} inhibition would change the balance of inward and outward currents, favoring relative augmentation of outward currents, with an overall result of

shortened repolarization. Similar effect should be expected in dog Purkinje fibers, in which relatively strong I_{NaL} exists. The opposite effect is expected in rabbit and dog ventricle, where the density of I_{Ks} is weaker than in the guinea pig, therefore I_{Kr} should have a stronger contribution to repolarization (Jost et al., 2013). In addition, ibuprofen inhibits I_{to}, which also plays an important role in the repolarization reserve (Virág et al., 2011). It should be mentioned that NSAIDs, including ibuprofen, are often used in patients with fever. Therefore, it would be worthwhile to study the effect of ibuprofen and other NSAIDs under hyperthermic conditions as well.

It is well known that fluoroquinolone antibiotics have some repolarization prolonging and proarrhythmic potency (Chiba et al., 2000; Garnett & Johannesen, 2016; Komatsu et al., 2019). To test potential interaction between ibuprofen and these antibiotics, we chose to study levofloxacin, which has been reported to possess relatively low proarrhythmic risk (Chiba et al., 2000; Milberg et al., 2007), due to its unpronounced repolarization lengthening (Hagiwara et al., 2001) and hERG channel inhibiting (Kang et al., 2001) properties compared to others, especially sparfloxacin (Chiba et al., 2000; Hagiwara et al., 2001). In our experiments, in good agreement with the results of Hagiwara et al., levofloxacin did not evoke significant changes when applied alone. However, when levofloxacin was applied in combination with ibuprofen, noteworthy APD prolongation was observed. Ibuprofen alone elicited a moderate prolongation of APD, and this was increased even further by levofloxacin. It should be emphasized that the observed APD prolongation by ibuprofen, with or without levofloxacin, is not marked, and it is far from being excessive. Nevertheless, this effect should draw attention to the possibility that the combined effect of two drugs with low or even minimal effect on repolarization, and seemingly marginal potassium channel blocking properties may still be additive by collectively decreasing the repolarization reserve. Therefore, in certain situations where repolarization reserve is already attenuated (Varró & Baczkó, 2011), e.g., in specific genetic disorders, heart failure, hypertophic cardiomyopathy, low serum potassium concentrations or ischemic heart disease, this may lead to marked repolarization defects. This may ultimately contribute to enhanced proarrhythmic risk and consequent sudden cardiac death.

In conclusion, it seems that ibuprofen in normal situations, at least regarding its cardiac electrophysiological properties, is a relatively safe drug. However, in certain conditions characterized by attenuated repolarization reserve, ibuprofen may enhance proarrhythmic risk,

and may even contribute to the incidence of sudden cardiac death observed in clinical studies. This possibility should be considered and taken into account in clinical practice, since ibuprofen is a very commonly used over-the-counter drug, taken every day by several million people without medical control.

Acknowledgments

This work was funded by the János Bolyai Research Scholarship of the Hungarian Academy of Sciences (for István Koncz, No. BO/00581/17) and the ÚNKP-18-4 and 19-4 (Bolyai+) New National Excellence Program of the Ministry for Innovation and Technology (for IK) and the National Research, Development and Innovation Office – NKFIH PD-116011 (for IK), K-119992 (for AV), FK-129117 (for NN), and the Hungarian Government-Ministry of Human Resources (grant EFOP-3.6.2-16-2017-00006, LIVE LONGER and EFOP 3.6.3-VEKOP-16-2017-00009 for TÁ-L), GINOP-2.3.2.-15-2016-00048), the Ministry of Human Capacities Hungary (20391-3/2018/FEKUSTRAT), and János Bolyai Research Scholarship of the Hungarian Academy of Sciences (for NN). The GINOP and EFOP projects are co-financed by the European Union and the European Regional Development Fund.

References

Bartos, D. C., Grandi, E., & Ripplinger, C. M. (2015). Ion Channels in the Heart. *Comprehensive Physiology*, *5*(3), 1423–1464. https://doi.org/10.1002/cphy.c140069

Bombardier, C., Laine, L., Reicin, A., Shapiro, D., Burgos-Vargas, R., Davis, B., Day, R., Ferraz, M. B., Hawkey, C. J., Hochberg, M. C., Kvien, T. K., Schnitzer, T. J., & VIGOR Study Group. (2000). Comparison of upper gastrointestinal toxicity of rofecoxib and naproxen in patients with rheumatoid arthritis. VIGOR Study Group. *The New England Journal of Medicine*, *343*(21), 1520–1528, 2 p following 1528. https://doi.org/10.1056/NEJM200011233432103

Chiba, K., Sugiyama, A., Satoh, Y., Shiina, H., & Hashimoto, K. (2000). Proarrhythmic effects of fluoroquinolone antibacterial agents: in vivo effects as physiologic substrate for torsades. *Toxicology and Applied Pharmacology*, *169*(1), 8–16. https://doi.org/10.1006/taap.2000.9041

Douglas, R. J. (2010). Palpitations following regular ibuprofen dosing in a 13-year-old girl: a case report. *Journal of Medical Case Reports*, *4*, 76. https://doi.org/10.1186/1752-1947-4-76

Garnett, C., & Johannesen, L. (2016). Commentary on: "Levofloxacin-Induced QTc Prolongation Depends on the Time of Drug Administration." *CPT: Pharmacometrics & Systems Pharmacology*, *5*(9), 452–454. https://doi.org/10.1002/psp4.12128

Hagiwara, T., Satoh, S., Kasai, Y., & Takasuna, K. (2001). A comparative study of the fluoroquinolone antibacterial agents on the action potential duration in guinea pig ventricular myocardia. *Japanese Journal of Pharmacology*, *87*(3), 231–234. https://doi.org/10.1254/jjp.87.231

Holubek, W., Stolbach, A., Nurok, S., Lopez, O., Wetter, A., & Nelson, L. (2007b). A report of two deaths from massive ibuprofen ingestion. *Journal of Medical Toxicology: Official Journal of the American College of Medical Toxicology*, *3*(2), 52–55. https://doi.org/10.1007/BF03160908

Huang, W.-F., Hsiao, F.-Y., Tsai, Y.-W., Wen, Y.-W., & Shih, Y.-T. (2006). Cardiovascular events associated with long-term use of celecoxib, rofecoxib and meloxicam in Taiwan: an observational study. *Drug Safety*, *29*(3), 261–272. https://doi.org/10.2165/00002018-200629030-00009

Huang, W.-F., Hsiao, F.-Y., Wen, Y.-W., & Tsai, Y.-W. (2006). Cardiovascular events associated with the use of four nonselective NSAIDs (etodolac, nabumetone, ibuprofen, or naproxen) versus a cyclooxygenase-2 inhibitor (celecoxib): a population-based analysis in Taiwanese adults. *Clinical Therapeutics*, *28*(11), 1827–1836. https://doi.org/10.1016/j.clinthera.2006.11.009

Jost, N., Virág, L., Comtois, P., Ordög, B., Szuts, V., Seprényi, G., Bitay, M., Kohajda, Z., Koncz, I., Nagy, N., Szél, T., Magyar, J., Kovács, M., Puskás, L. G., Lengyel, C., Wettwer, E., Ravens, U., Nánási, P. P., Papp, J. G., … Nattel, S. (2013). Ionic mechanisms limiting cardiac repolarization reserve in humans compared to dogs. *The Journal of Physiology*, *591*(17), 4189–4206. https://doi.org/10.1113/jphysiol.2013.261198

Kang, J., Wang, L., Chen, X. L., Triggle, D. J., & Rampe, D. (2001). Interactions of a series of fluoroquinolone antibacterial drugs with the human cardiac K+ channel HERG. *Molecular Pharmacology*, *59*(1), 122–126. https://doi.org/10.1124/mol.59.1.122

Kohajda, Z., Farkas-Morvay, N., Jost, N., Nagy, N., Geramipour, A., Horváth, A., Varga, R. S., Hornyik, T., Corici, C., Acsai, K., Horváth, B., Prorok, J., Ördög, B., Déri, S., Tóth, D., Levijoki, J., Pollesello, P., Koskelainen, T., Otsomaa, L., … Virág, L. (2016). The Effect of a Novel Highly Selective Inhibitor of the Sodium/Calcium Exchanger (NCX) on Cardiac Arrhythmias in In Vitro and In Vivo Experiments. *PloS One*, *11*(11), e0166041. https://doi.org/10.1371/journal.pone.0166041

Komatsu, R., Mizuno, H., Ishizaka, T., Ito, A., Jikuzono, T., Kakoi, T., Bando, M., Koga, T., Handa, J., Takahashi, Y., Kanno, A., Ozaki, H., Chiba, K., & Japan activity for Improvement of Cardiovascular Evaluation by Telemetry system (J-ICET). (2019). Exposure-response analysis of drug-induced QT interval prolongation in telemetered monkeys for translational prediction to human. *Journal of Pharmacological and Toxicological Methods*, *99*, 106606. https://doi.org/10.1016/j.vascn.2019.106606

Kristóf, A., Husti, Z., Koncz, I., Kohajda, Z., Szél, T., Juhász, V., Biliczki, P., Jost, N., Baczkó, I., Papp, J. G., Varró, A., & Virág, L. (2012). Diclofenac prolongs repolarization in ventricular muscle with impaired repolarization reserve. *PloS One*, *7*(12), e53255. https://doi.org/10.1371/journal.pone.0053255

Mäkelä, A. L., Lempiäinen, M., & Ylijoki, H. (1981). Ibuprofen levels in serum and synovial fluid. Scandinavian Journal of Rheumatology. Supplement, 39, 15–17. https://doi.org/10.3109/03009748109095329

Milberg, P., Hilker, E., Ramtin, S., Cakir, Y., Stypmann, J., Engelen, M. A., Mönnig, G., Osada, N., Breithardt, G., Haverkamp, W., & Eckardt, L. (2007). Proarrhythmia as a class effect of quinolones: increased dispersion of repolarization and triangulation of action potential predict torsades de pointes. *Journal of Cardiovascular Electrophysiology*, *18*(6), 647–654. https://doi.org/10.1111/j.1540-8167.2007.00793.x

Pratt, C. M., Hertz, R. P., Ellis, B. E., Crowell, S. P., Louv, W., & Moyé, L. (1994). Risk of developing life-threatening ventricular arrhythmia associated with tefenadine in comparison with over-the-counter antihistamines, ibuprofen and clemastine. *The American Journal of Cardiology*, *73*(5), 346–352. https://doi.org/10.1016/0002-9149(94)90006-x

Rainsford, K. D. (2009). Ibuprofen: pharmacology, efficacy and safety. *Inflammopharmacology*, *17*(6), 275–342. https://doi.org/10.1007/s10787-009-0016-x

Roden, D. M. (2006). Long QT syndrome: reduced repolarization reserve and the genetic link. *Journal of Internal Medicine*, *259*(1), 59–69. https://doi.org/10.1111/j.1365-2796.2005.01589.x

Sondergaard, K. B., Weeke, P., Wissenberg, M., Schjerning Olsen, A.-M., Fosbol, E. L., Lippert, F. K., Torp-Pedersen, C., Gislason, G. H., & Folke, F. (2017). Non-steroidal anti-inflammatory drug use is associated with increased risk of out-of-hospital cardiac arrest: a nationwide case-time-control study. *European Heart Journal. Cardiovascular Pharmacotherapy*, *3*(2), 100–107. https://doi.org/10.1093/ehjcvp/pvw041

Varró, A., & Baczkó, I. (2011). Cardiac ventricular repolarization reserve: a principle for understanding drug-related proarrhythmic risk. *British Journal of Pharmacology*, *164*(1), 14–36. https://doi.org/10.1111/j.1476-5381.2011.01367.x

Varró, A., Baláti, B., Iost, N., Takács, J., Virág, L., Lathrop, D. A., Csaba, L., Tálosi, L., & Papp, J. G. (2000). The role of the delayed rectifier component IKs in dog ventricular muscle and Purkinje fiber repolarization. *The Journal of Physiology*, *523 Pt 1*, 67–81. https://doi.org/10.1111/j.1469-7793.2000.00067.x

Virág, L., Jost, N., Papp, R., Koncz, I., Kristóf, A., Kohajda, Z., Harmati, G., Carbonell-Pascual, B., Ferrero, J. M., Papp, J. G., Nánási, P. P., & Varró, A. (2011). Analysis of the contribution of I(to) to repolarization in canine ventricular myocardium. *British Journal of Pharmacology*, *164*(1), 93–105. https://doi.org/10.1111/j.1476-5381.2011.01331.x

Yang, Z., Wang, H., Zheng, Y., Zhang, Y., Liu, Y., & Li, C. (2008). Possible arrhythmiogenic mechanism produced by ibuprofen. *Acta Pharmacologica Sinica*, *29*(4), 421–429. https://doi.org/10.1111/j.1745-7254.2008.00754.x

Yarishkin, O. V., Hwang, E. M., Kim, D., Yoo, J. C., Kang, S. S., Kim, D. R., Shin, J.-H.-J., Chung, H.-J., Jeong, H.-S., Kang, D., Han, J., Park, J.-Y., & Hong, S.-G. (2009). Diclofenac, a Non-steroidal Anti-inflammatory Drug, Inhibits L-type Ca Channels in Neonatal Rat Ventricular Cardiomyocytes. *The Korean Journal of Physiology & Pharmacology: Official Journal of the Korean Physiological Society and the Korean Society of Pharmacology*, *13*(6), 437–442. https://doi.org/10.4196/kjpp.2009.13.6.437

Zicha, S., Moss, I., Allen, B., Varro, A., Papp, J., Dumaine, R., Antzelevich, C., & Nattel, S. (2003). Molecular basis of species-specific expression of repolarizing K+ currents in the heart. *American Journal of Physiology. Heart and Circulatory Physiology*, *285*(4), H1641-1649. https://doi.org/10.1152/ajpheart.00346.2003

Figure 1. The effects of ibuprofen and DMSO on action potentials recorded from different cardiac preparations. Original action potential records show that ibuprofen (at 100 μM) slightly but significantly lengthened the action potential duration in rabbit ventricular muscle (panel A) and in dog ventricular muscle (at 200 μM, panel B) at a basic cycle length of 1000 ms. However, in dog Purkinje fiber (panel C) the drug significantly shortened the action potential repolarization at a basic cycle length of 500 ms. DMSO at 2.2‰ did not alter action potential duration in any of the preparations at the same cycle lengths (panels D–F).

Figure 2. Cycle length dependent changes in action potential duration (APD_{90}, panels A and C) and in maximal rate of depolarization (V_{max}, panels B and D) measured under control conditions and in the presence of 200 μM ibuprofen and DMSO at 2.2‰ in dog Purkinje fiber preparations. Values are means ± SEM, asterisks indicate significant changes.

Figure 3. The effects of levofloxacin alone (panel A) and in combination with 100 μM ibuprofen (panel B) on action potentials recorded from rabbit ventricular muscle preparation. Original action potential records indicate that 40 μM levofloxacin did not influence the ventricular repolarization in rabbit (panel A), however, in combination with 100 μM ibuprofen levofloxacin significantly lengthened the action potential duration (panel B).

Figure 4. Panels A–C show the effects of the solvent DMSO at 1‰ and ibuprofen at 250 μM on the potassium currents I_{K1}, I_{to}, and I_{Kr} respectively in ventricular myocytes; the insets show the applied voltage protocols. Legend: control, black lines and empty boxes; DMSO, green lines and green boxes; ibuprofen; red lines and circles. Values are means ± SEM, asterisks indicate $p<0.05$, ANOVA for repeated measurements followed by Bonferroni's post-hoc test. Panels D and E show original current traces of the I_{to} and I_{Kr} currents respectively, recorded in control conditions and in the presence of DMSO and after the application of 250 μM ibuprofen. In panel E, the dotted arrows indicate the amplitude of I_{Kr} tail currents at -40 mV.

Figure 5. Panels A and B show the effects of the solvent DMSO at 1‰ and ibuprofen at 250 μM on the L-type calcium current (I_{Ca}) and the late sodium current (I_{NaL}) respectively in ventricular myocytes; the insets show the applied voltage protocols. Values are means ± SEM, asterisks indicate $p<0.05$, ANOVA for repeated measurements followed by Bonferroni's post-hoc test (A), Student's t-test (B). Upper panels show original current traces of the I_{NaL} and I_{Ca} currents respectively, recorded in control conditions and in the presence of DMSO and after the application of 250 μM ibuprofen. I_{NaL} was defined as TTX sensitive current by subtracting current traces recorded in the presence of 20 μM TTX from traces of control, DMSO and ibuprofen recordings.

Table 1. The electrophysiological effects of DMSO (2.2‰) and ibuprofen (50 μM and 200 μM) in canine right ventricular papillary muscle preparations (VM; A, B and C), at basic cycle length of 1000 ms; and ibuprofen (200 μM) in canine Purkinje fibers (PF; D) at basic cycle length of 500 ms; RP, resting potential; APA, action potential amplitude; V_{max}, maximum rate of depolarization; APD_{50} and APD_{90}, action potential durations at 50% and 90% of repolarization. Results are expressed as means ± SEM; *p<0.05, Student's t-test for paired data.

A	Sample	RP (mV)	APA (mV)	V_{max} (V/s)	APD_{50} (ms)	APD_{90} (ms)	APD_{90} (%)
Control	Canine VM (6)	-83.3 ± 2.3	106.7 ± 1.5	136.7 ± 14.2	157.8 ± 11.6	203.6 ± 7.6	
DMSO (2.2‰)	Canine VM (6)	-85.8 ± 1.7	105.3 ± 1.4	123.3 ± 17.0	153.8 ± 11.5	201.6 ± 8.0	-1.0 ± 1.2

B	Sample	RP (mV)	APA (mV)	V_{max} (V/s)	APD_{50} (ms)	APD_{90} (ms)	APD_{90} (%)
Control	Canine VM (8)	-83.2 ± 1.6	108.1 ± 1.0	175.2 ± 22.3	187.0 ± 9.3	227.5 ± 9.7	
Ibuprofen (50 μM)	Canine VM (8)	-85.3 ± 2.1	106.7 ± 1.9	172.4 ± 29.9	187.7 ± 9.7	225.9 ± 8.9	-0.6 ± 1.0

C	Sample	RP (mV)	APA (mV)	V_{max} (V/s)	APD_{50} (ms)	APD_{90} (ms)	APD_{90} (%)
Control	Canine VM (6)	-89.0 ± 1.8	110.6 ± 2.4	174.6 ± 20.3	173.8 ± 8	214.1 ± 5.9	
Ibuprofen (200 μM)	Canine VM (6)	-89.1 ± 3.2	113.4 ± 3.0	192.9 ± 27.1	181.6 ± 6.3	223.0 ± 4.9*	4.3 ± 1.0

D	Sample	RP (mV)	APA (mV)	V_{max} (V/s)	APD_{50} (ms)	APD_{90} (ms)	APD_{90} (%)
Control	Canine PF	-89.7	133.5	580.7	163.9	253.4	

	(7)	± 0.7	± 3.3	± 36.0	± 10.9	± 14.2	
Ibuprofen	Canine PF	-87.3	135.9	621.5	163.7	242.0	-4.5
(200 μM)	(7)	± 1.0	± 3.4	± 93.5	± 11.2	± 13.7*	± 0.7

Table 2. The electrophysiological effects of DMSO (2.2‰), levofloxacin (40 μM) and ibuprofen (100 μM) in rabbit right ventricular papillary muscle preparations at a basic cycle length of 1000 ms; APA, action potential amplitude; V_{max}, maximum rate of depolarization; APD_{50} and APD_{90}, action potential durations at 50% and 90% of repolarization. Results are expressed as means ± SEM; *p<0.05, Student's t-test for paired data (Tables 2A and 2B), ANOVA for repeated measurements followed by Bonferroni's post-hoc test (Table 2C).

A	Sample	RP (mV)	APA (mV)	V_{max} (V/s)	APD_{50} (ms)	APD_{90} (ms)	APD_{90} (%)
Control	Rabbit VM (6)	-81.7 ± 1.9	119.1 ± 2.3	222.0 ± 21.9	123.8 ± 7.9	158.7 ± 7.7	
DMSO (2.2‰)	Rabbit VM (6)	-81.6 ± 2.6	115.8 ± 4.7	181.9 ± 20.5	123.0 ± 7.2	159.3 ± 7.1	0.7 ± 1.9

B	Sample	RP (mV)	APA (mV)	V_{max} (V/s)	APD_{50} (ms)	APD_{90} (ms)	APD_{90} (%)
Control	Rabbit VM (7)	-86.9 ± 1.3	109.0 ± 2.6	127.6 ± 7.5	149.6 ± 9.6	163.8 ± 6.6	
Levofloxacin (40 μM)	Rabbit VM (7)	-85.8 ± 2.0	111.3 ± 4.0	128.0 ± 8.0	156.9 ± 26.0	164.1 ± 7.0	0.1 ± 0.8

C	Sample	RP (mV)	APA (mV)	V_{max} (V/s)	APD_{50} (ms)	APD_{90} (ms)	APD_{90} (%)
Control	Rabbit VM (9)	-86.5 ± 1.6	108.0 ± 3.7	147.7 ± 21.2	121.8 ± 7.1	164.7 ± 8.7	
Ibuprofen (100 μM)	Rabbit VM (9)	-85.6 ± 2.7	107.3 ± 2.3	145.2 ± 19.3	123.3 ± 7.5	169.3 ± 8.7*	2.9 ± 0.9
Levofloxacin (40 μM)	Rabbit VM (9)	87.4 ± 2.2	111.0 ± 3.7	148.5 ± 19.4	138.2 ± 13.1	183.2 ± 12.5*	7.6 ± 1.9

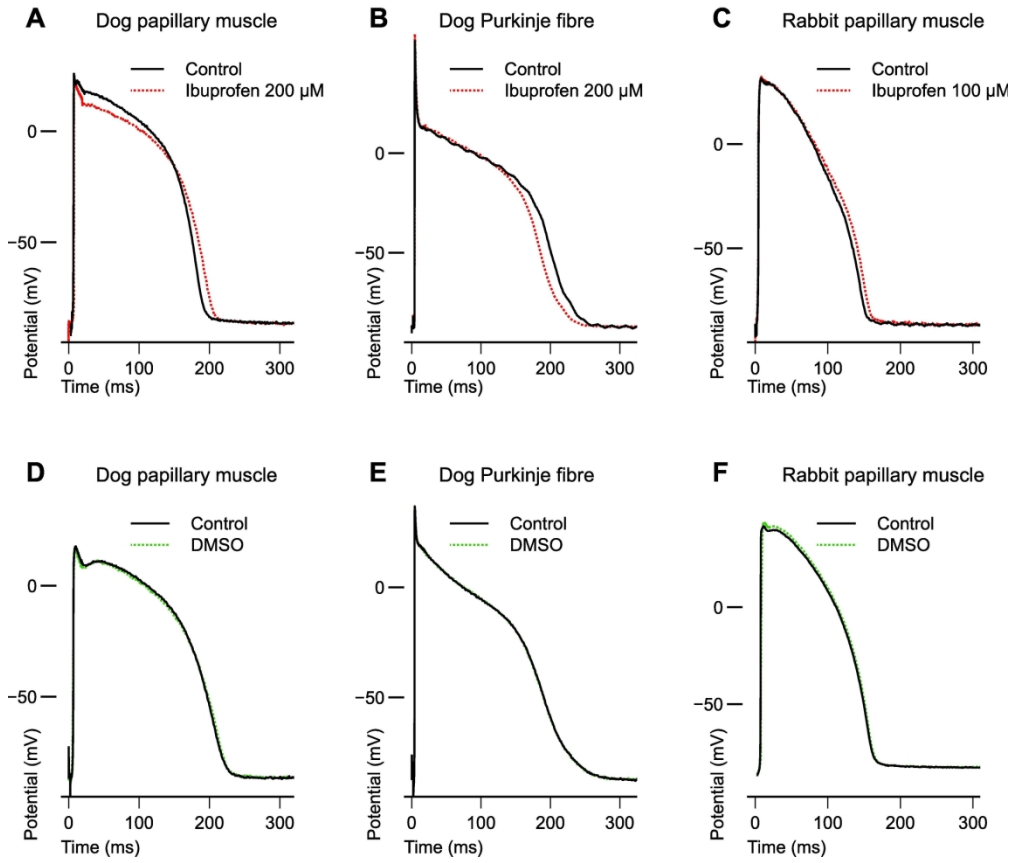

Figure 1. The effects of ibuprofen and DMSO on action potentials recorded from different cardiac preparations. Original action potential records show that ibuprofen (at 100 µM) slightly but significantly lengthened the action potential duration in rabbit ventricular muscle (panel A) and in dog ventricular muscle (at 200 µM, panel C) at a basic cycle length of 1000 ms. However, in dog Purkinje fiber (panel B) the drug significantly shortened the action potential repolarization at a basic cycle length of 500 ms. DMSO at 2.2‰ did not alter action potential duration in any of the preparations at the same cycle lengths (panels D–F).

181x155mm (300 x 300 DPI)

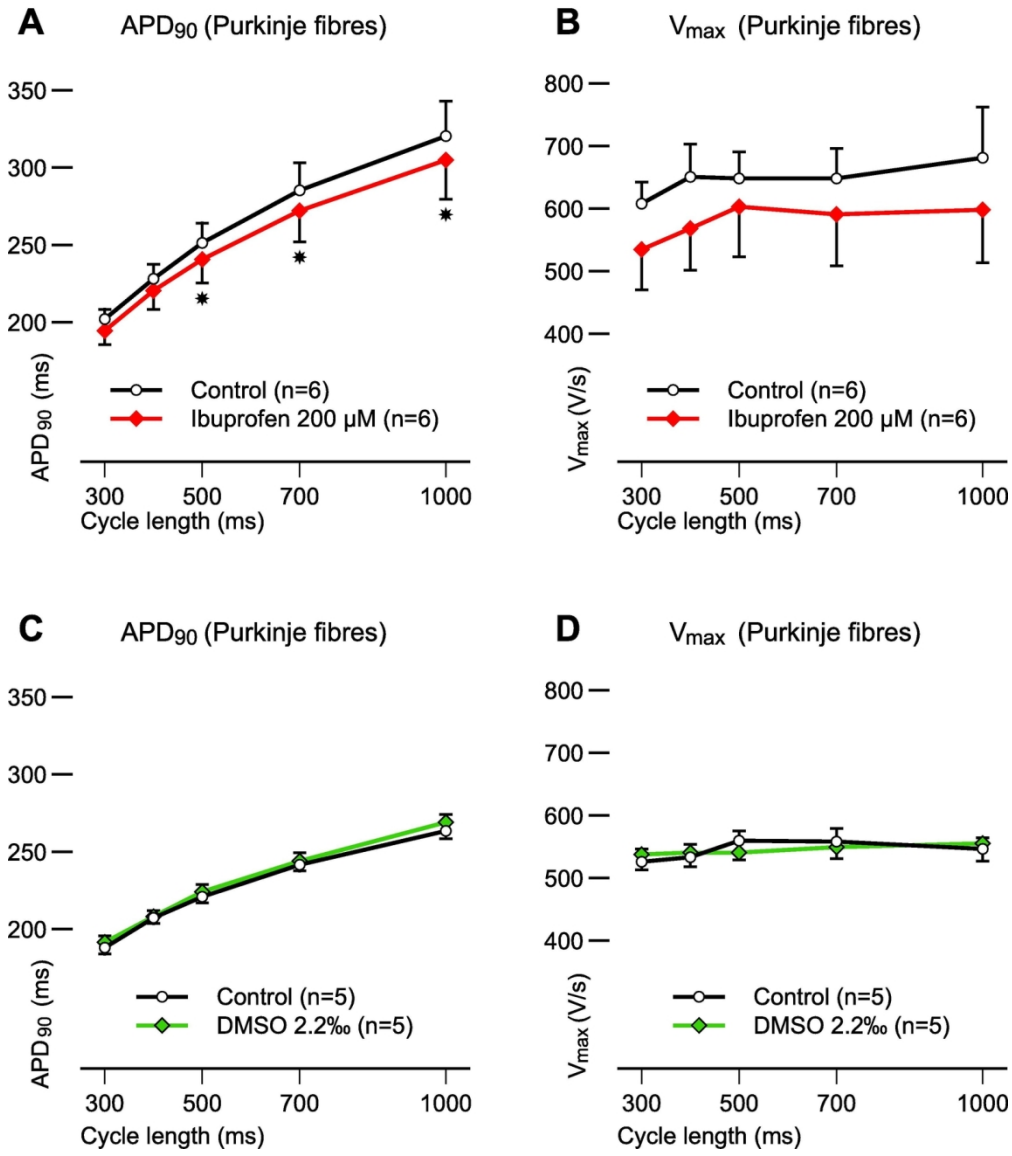

Figure 2. Cycle length dependent changes in action potential duration (APD90, panels A and C) and in maximal rate of depolarization (Vmax, panels B and D) measured under control conditions and in the presence of 200 µM ibuprofen and DMSO at 2.2‰ in dog Purkinje fiber preparations. Values are means ± SEM, asterisks indicate significant changes.

135x155mm (300 x 300 DPI)

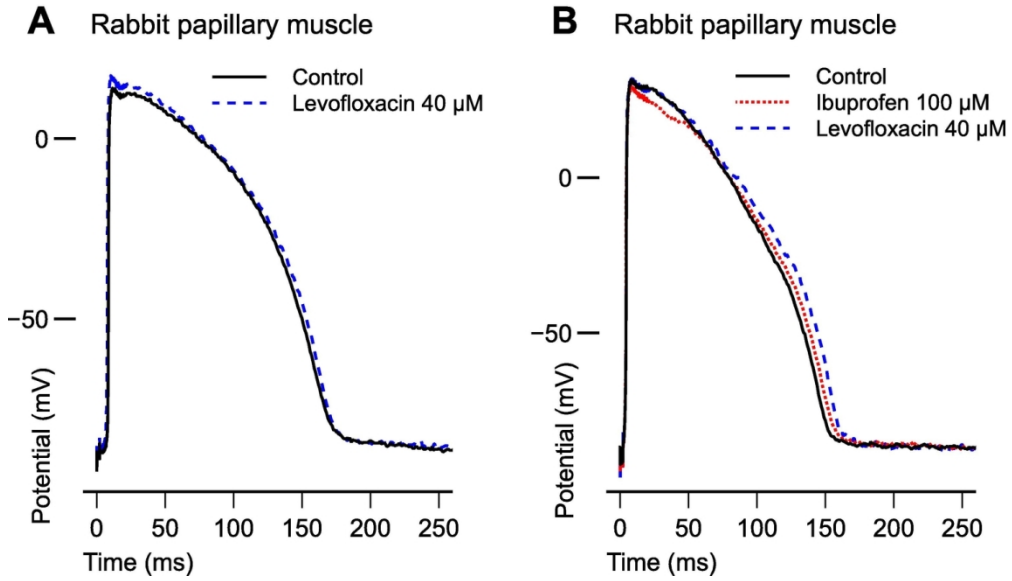

Figure 3. The effects of levofloxacin alone (panel A) and in combination with 100 μM ibuprofen (panel B) on action potentials recorded from rabbit ventricular muscle preparation. Original action potential records indicate that 40 μM levofloxacin did not influence the ventricular repolarization in rabbit (panel A), however, in combination with 100 μM ibuprofen levofloxacin significantly lengthened the action potential duration (panel B).

129x75mm (300 x 300 DPI)

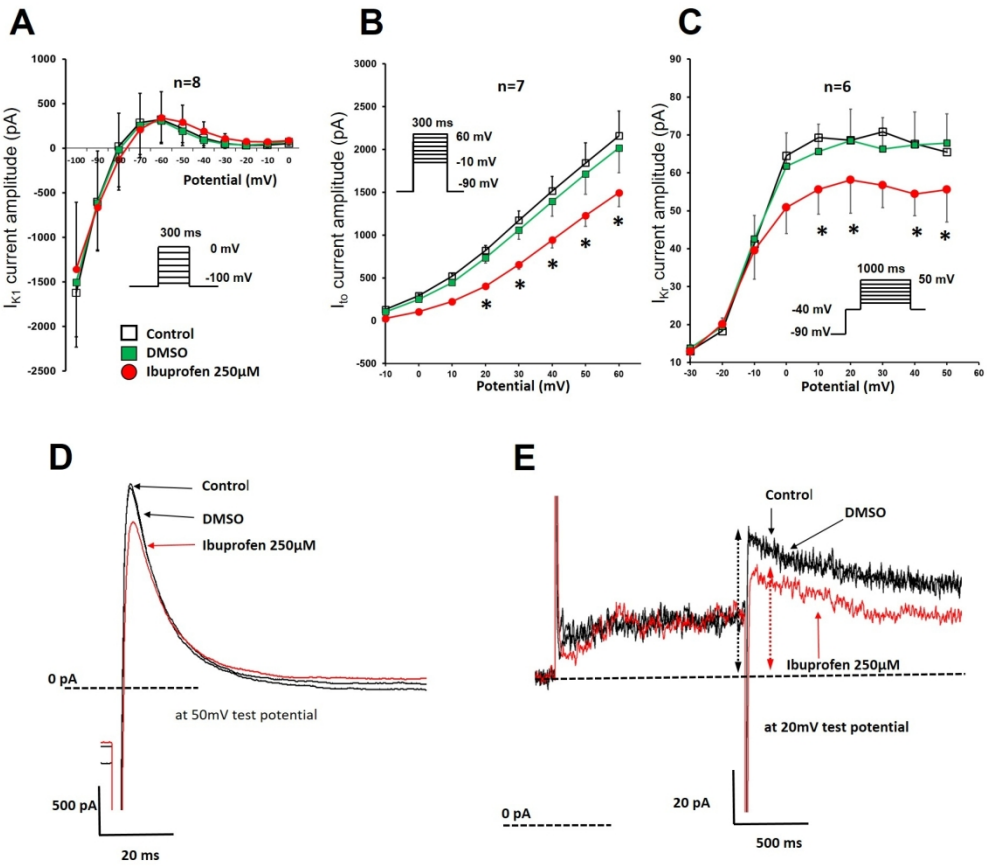

Figure 4. Panels A–C show the effects of the solvent DMSO at 1‰ and ibuprofen at 250 µM on the potassium currents IK1, Ito, and IKr respectively in ventricular myocytes; the insets show the applied voltage protocols. Legend: control, black lines and empty boxes; DMSO, green lines and green boxes; ibuprofen; red lines and circles. Values are means ± SEM, asterisks indicate $p<0.05$, ANOVA for repeated measurements followed by Bonferroni's post-hoc test. Panels D and E show original current traces of the Ito and IKr currents respectively, recorded in control conditions and in the presence of DMSO and after the application of 250 µM ibuprofen. In panel E, the dotted arrows indicate the amplitude of IKr tail currents at -40 mV.

315x279mm (150 x 150 DPI)

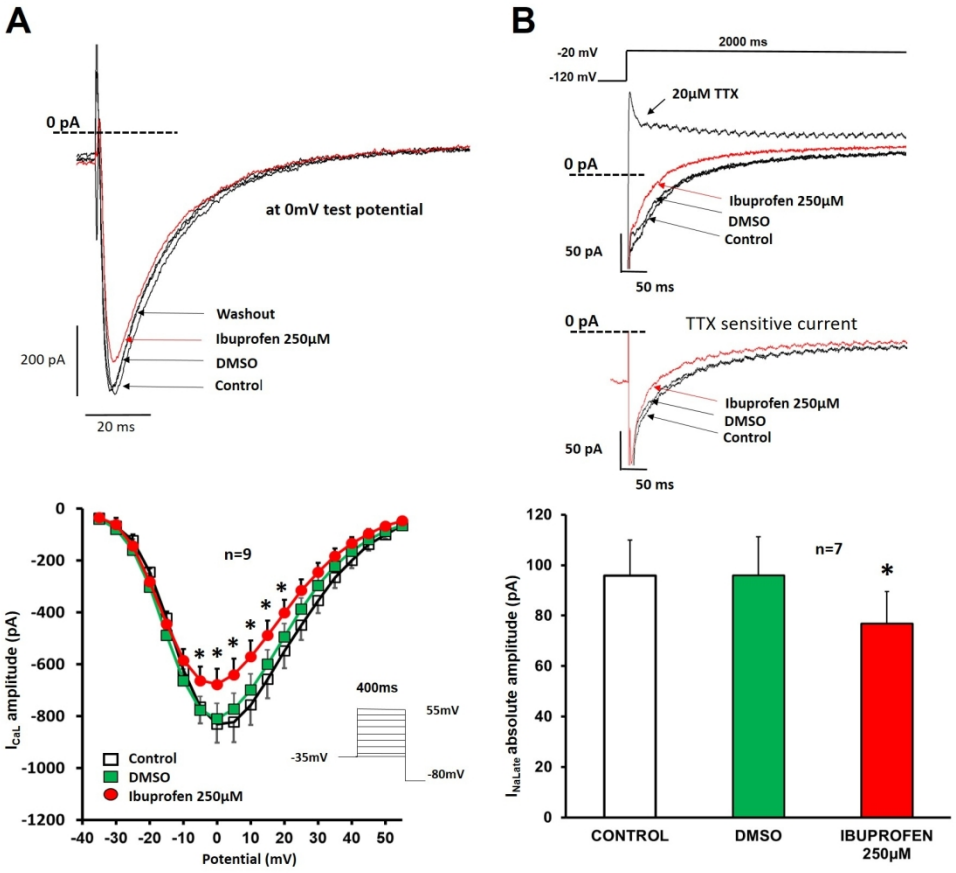

Figure 5. Panels A and B show the effects of the solvent DMSO at 1‰ and ibuprofen at 250 µM on the L-type calcium current (ICa) and the late sodium current (INaL) respectively in ventricular myocytes; the insets show the applied voltage protocols. Values are means ± SEM, asterisks indicate $p<0.05$, ANOVA for repeated measurements followed by Bonferroni's post-hoc test (A), Student's t-test (B). Upper panels show original current traces of the INaL and ICa currents respectively, recorded in control conditions and in the presence of DMSO and after the application of 250 µM ibuprofen. INaL was defined as TTX sensitive current by subtracting current traces recorded in the presence of 20 µM TTX from traces of control, DMSO and ibuprofen recordings.

313x278mm (150 x 150 DPI)

Szegedi Tudományegyetem Szent-Györgyi Albert
Orvostudományi Kar
Farmakológiai és Farmakoterápiai Intézet
Igazgató: Prof. Dr. Baczkó István
6720 Szeged, Dóm tér 12.
Tel.: (62) 545-682
e-mail: baczko.istvan@med.u-szeged.hu

NYILATKOZAT

Alulírott Prof. Dr. Varró András levelező szerző nyilatkozom, hogy az alábbi közleményben:

Topal Leila; Polyák Alexandra Júlia; Tóth Noémi; Ágoston Gergely; Bencsik Péter; Kohajda Zsófia; Prorok János; Déri Szilvia; Nagy Norbert; Jost Norbert László; Virág László; Farkas Attila; Varró András; Baczkó István

Endurance training-induced cardiac remodeling in a guinea pig athlete's heart model

CANADIAN JOURNAL OF PHYSIOLOGY AND PHARMACOLOGY 100:10pp. 993-1004., 12 p. (2022)

Dr. Topal Leila a Ph.D. disszertációjában a közlemény egészéhez tartozó kísérleteket használja fel. Ezek az eredmények későbbi Ph.D. disszertációban nem kerülnek felhasználásra.

Prof. Dr. Varró András
SZTE SZAOK Farmakológiai és Farmakoterápiai Intézet

Szeged, 2022. március 30.

Szegedi Tudományegyetem Szent-Györgyi Albert Orvostudományi Kar
Farmakológiai és Farmakoterápiai Intézet
Igazgató: Prof. Dr. Baczkó István
6720 Szeged, Dóm tér 12.
Tel.: (62) 545-682
e-mail: baczko.istvan@med.u-szeged.hu

NYILATKOZAT

Alulírottak Prof. Dr. Varró András témavezető, Prof. Dr. Jost Norbert László levelező szerző és társtémavezető nyilatkozzuk, hogy az alábbi közleményben:

Topal Leila; Naveed Muhammad; Orvos Péter; Pászti Bence József; Prorok János; Bajtel Ákos; Kiss Tivadar; Csupor-Löffler Boglárka; Csupor Dezső; Baczkó István; Varró András; Virág László; Jost Norbert László

The electrophysiological effects of cannabidiol on action potentials and transmembrane potassium currents in rabbit and dog cardiac ventricular preparations

ARCHIVES OF TOXICOLOGY, 95 (7). pp. 2497-2505. ISSN 0340-5761 (2021)

Dr. Topal Leila a Ph.D. disszertációjában a patch-clamp kísérleteket, vagyis a 2., 3., 4., 5., 6. és 7. ábrákhoz tartozó kísérleteket használja fel. Ezek az eredmények későbbi Ph.D. disszertációban nem kerülnek felhasználásra.

Prof. Dr. Jost Norbert László
SZTE SZAOK Farmakológiai és Farmakoterápiai Intézet

Prof. Dr. Varró András
SZTE SZAOK Farmakológiai és Farmakoterápiai Intézet

Szeged, 2022. március 30.

Szegedi Tudományegyetem Szent-Györgyi Albert Orvostudományi Kar
Farmakológiai és Farmakoterápiai Intézet
Igazgató: Prof. Dr. Baczkó István
6720 Szeged, Dóm tér 12.
Tel.: (62) 545-682
e-mail: baczko.istvan@med.u-szeged.hu

NYILATKOZAT

Alulírottak Prof. Dr. Varró András témavezető és Dr. Csupor Dezső levelező szerző nyilatkozzuk, hogy az alábbi közleményben:

Orvos Péter; Pászti Bence; Topal Leila; Gazdag Péter; Prorok János; Polyák Alexandra Júlia; Kiss Tivadar; Tóth-Molnár Edit; Csupor-Löffler Boglárka; Bajtel Ákos; Varró András; Hohmann Judit; Virág László; Csupor Dezső

The electrophysiological effect of cannabidiol on hERG current and in guinea-pig and rabbit cardiac preparations

SCIENTIFIC REPORTS (2045-2322 2045-2322): 10 1 Paper 16079. 9 p. (2020

Dr. Topal Leila a Ph.D. disszertációjában a patch-clamp kísérleteket, vagyis a 4. és 5. ábrákhoz tartozó kísérleteket használja fel. Ezek az eredmények későbbi Ph.D. disszertációban nem kerülnek felhasználásra.

Dr. Csupor Dezső
SZTE Gyógyszerésztudományi Kar

Prof. Dr. Varró András
SZTE SZAOK Farmakológiai és Farmakoterápiai Intézet

Szeged, 2022. március 30.

Szegedi Tudományegyetem Szent-Györgyi Albert Orvostudományi Kar
Farmakológiai és Farmakoterápiai Intézet
Igazgató: Prof. Dr. Baczkó István
6720 Szeged, Dóm tér 12.
Tel.: (62) 545-682
e-mail: baczko.istvan@med.u-szeged.hu

NYILATKOZAT

Alulírott Prof. Dr. Varró András levelező szerző és témavezető nyilatkozom, hogy az alábbi közleményben:

Pászti Bence József; Prorok János; Magyar Tibor; Árpádffy-Lovas Tamás; Györe Balázs; Topal Leila; Gazdag Péter; Szlovák Jozefina; Naveed Muhammad; Jost Norbert László; Nagy Norbert; Varró András; Virág László; Koncz Istvan

Th Cardiac electrophysiological effects of ibuprofen in dog and rabbit ventricular preparations: Possible implication to enhanced proarrhythmic risk

CANADIAN JOURNAL OF PHYSIOLOGY AND PHARMACOLOGY, 99 (1). pp. 102-109. ISSN 0008-4212 (2021)

Dr. Topal Leila a Ph.D. disszertációjában a patch-clamp kísérleteket, vagyis a 4A, 4B, 4D, illetve az 5. ábrákhoz tartozó kísérleteket használja fel. Ezek az eredmények későbbi Ph.D. disszertációban nem kerülnek felhasználásra.

Prof. Dr. Varró András
SZTE SZAOK Farmakológiai és Farmakoterápiai Intézet

Szeged, 2022. március 30.